

TECHNISCHE UNIVERSITÄT MÜNCHEN
Lehrstuhl für Bauchemie

**The Phenomenon of Cement Ageing on Moist Air:
Surface Chemistry, Mechanisms and Effects on
Admixture Performance**

Elina Dubina

Vollständiger Abdruck der von der Fakultät für Chemie der Technischen Universität München
zur Erlangung des akademischen Grades eines

Doktors der Naturwissenschaften (Dr. rer. nat.)

genehmigten Dissertation.

Vorsitzender: Univ.-Prof. Dr. Klaus Köhler

Prüfer der Dissertation: 1. Univ.-Prof. Dr. Johann P. Plank
2. Univ.-Prof. Dr. Cordt Zollfrank

Die Dissertation wurde am 26.11.2012 bei der Technischen Universität München eingereicht
und durch die Fakultät für Chemie am 04.02.2013 angenommen.

To complete a PhD project is a lot like to train for a marathon –
they are both endurance events, they require a consistent
and carefully calculated amount of effort
to complete them and not burn out.

But after you cross the
finish line you are the
happiest person
in the world.



ACKNOWLEDGMENT

Looking back, I am very grateful for all I have received throughout these years. It has certainly shaped me as a person and has led me to where I am now. Several people contributed to the successful completion of this thesis, to whom I am grateful and indebted:

I would like to express my deep gratitude to **Professor Johann Plank** for being a great doctor father and offering me a wonderful subject for research. I always enjoyed being a Ph.D. student at the Chair for Construction Chemicals. I am also grateful for his encouragement to present my work at international scientific conferences and thus, he gave me the possibility to improve my presentation skills.

I would like to thank my project co-supervisor **Dr. Leon Black**, Leeds University, for his invaluable assistance with x-ray photoelectron spectroscopy and guidance throughout this work, especially during my stays at Leeds University in July 2010 and from July to August 2011. His enthusiasm contributed much to the completion of this work.

I also would like to address special thanks to **Professor Lars Wadsö**, Lund University, for his scientific input and fruitful discussions during my stay at Lund University from May to July 2009.

My industrial advisors, **Dr. Holger König** and **Dr. Maciej Zajac**, both from HeidelbergCement/Germany, are acknowledged for their stimulating discussions and guidance during this work.

Furthermore, I want to thank **Dr. Roland Sieber** for introducing me to the x-ray diffraction and for his contribution to this work.

Nanocem, a research network of European cement producers and academic institutions, is thanked for funding most of this work and for giving me the opportunity to present and discuss the results at several consortium meetings as well as at international conferences.

Special thanks go to the members of Nanocem for valuable discussions and helpful critics during the preparation of publications.

I would like to thank **Marie-Alix Dalang-Secrétan** at Nanocem for her always so kind help in the administration of this project.

Special thanks also go to the **secretary at the Chair for Construction Chemicals** for the help to cope with bureaucracy and administration.

I would like to express my gratitude to **Mark Whittaker**, Leeds and **Lidija Korat**, Ljubljana for their pleasant collaboration on the project.

I am thankful to **Johanna de Reese, Hang Bian, Helena Keller, Fatima Dugonjić-Bilić, Ahmad Habbaba and Tobias Kornprobst** for their friendship and the friendly conversations which always made me feel positive.

My special thanks go to **Dr. Oksana Storcheva**, who kindly invited me to write this thesis in her office and always gave me a cup of ginger tea when I most needed it.

My particular thanks go to our computer expert **Tom Pavlitschek** for his support during submission of graphics, illustrations and images to journals.

For help in laboratory experiments, my thanks go to **Dagmar Lettrich** and **Richard Beiderbeck**.

I am grateful to my senior colleagues **Sebastian Wistuba, Markus Gretz, Mirko Gruber, Christof Schröfl, Bernhard Sachsenhauser, Friedrich von Hoessle, Vera Nilles, Helena Keller, Nils Recalde Lummer and Nadia Zouaoui** for their support, especially at the beginning of my doctorate studies.

I also thank colleagues who joined the group after me - **Daniel Bülchen, Nan Zou, Salami Oyewole Taye, Michael Glanzer-Heinrich, Constantin Tiemeyer, Alex Lange, Markus Meier, Stefan Baueregger, Yu Jin, Julia Pickelmann, Maike Müller, Timon Echt, Somruedee Klaithong and Lei Lei** for the collegial atmosphere. I wish them all the best for their future.

*Thousand thanks to my friends who supported me ever since and made my life more enjoyable during some stormy times in my Ph.D. and especially to **Serina Ng** for her deep friendship and for sharing the glory and sadness of conference deadlines and day-to-day research.*

*Finally, I am forever indebted to **my parents** for their love, understanding, endless patience and encouragement when it was most required.*

CHEMICAL NOTATION

In this work, the chemical formula of many cement compounds is expressed as a sum of oxides. In accordance to a special notation established by cement chemists, these oxides are abbreviated as follows:

A	Al ₂ O ₃
C	CaO
F	Fe ₂ O ₃
H	H ₂ O
K	K ₂ O
M	MgO
N	Na ₂ O
S	SiO ₂
\bar{S}	SO ₃
\bar{C}	CO ₂

Cement notation	Chemical formula	Mineral name
AF _t or C ₆ A \bar{S} ₃ H ₃₂	[Ca ₃ Al(OH) ₆] ₂ · (SO ₄) ₃ · 26 H ₂ O	Calcium trisulfoaluminate hydrate, ettringite, AF _t
AF _m or C ₄ A \bar{S} H ₁₂	[Ca ₂ Al(OH) ₆] ₂ · SO ₄ · 6 H ₂ O	Calcium monosulfoaluminate hydrate, monosulfate, AF _m
C ₄ A \bar{C} H ₁₁	[Ca ₂ Al(OH) ₆] ₂ · CO ₃ · 5 H ₂ O	Tetracalcium monocarboaluminate hydrate, monocarboaluminate
C ₃ A	c, Ca ₉ Al ₆ O ₁₈ o, Ca _{8,5} NaAl ₆ O ₁₈	c = cubic or o = orthorhombic tricalcium aluminate, aluminate
C-A-H	x CaO · y Al ₂ O ₃ · z H ₂ O	Calcium aluminate hydrate, C-A-H phases, AF _m
C ₄ AF or C ₂ (A,F)	Ca ₄ Al ₂ Fe ₂ O ₁₀	Tetracalcium aluminate ferrite, ferrite
CH	Ca(OH) ₂	Portlandite
C ₂ S	Ca ₂ SiO ₄	Dicalciumsilicate, belite
C ₃ S	Ca ₃ (SiO ₄)O	Tricalciumsilicate, alite
C-S-H	x CaO · y SiO ₂ · z H ₂ O	Calcium silicate hydrate, C-S-H phases
C \bar{S} H ₂	CaSO ₄ · 2 H ₂ O	Calcium sulfate dihydrate, gypsum
C \bar{S} H _{0,5}	CaSO ₄ · 0.5 H ₂ O	Calcium sulfate hemihydrate, hemihydrate
C \bar{S}	CaSO ₄	Calcium sulfate, anhydrite
KC \bar{S} ₂ H	K ₂ SO ₄ · CaSO ₄ · H ₂ O	Syngonite

ABBREVIATION

a(H ₂ O)	Water activity
BET	Brunauer, Emmet and Teller (BET)
bwoc	By weight of cement
BNS	β-naphthalene sulfonic acid formaldehyde condensate
c	Cubic
CAC	Calcium Aluminate Cement
d	Days
(E)SEM	(Environmental) Scanning Electron Microscope
EDX	Energy Dispersive X-ray analysis
FTIR-ATR	Fourier Transform Infrared - Attenuated Total Reflectance
h	Hours
LOI	Loss of Ignition
m	Monoclinic
min	Minutes
nm	Nanometer
o	Orthorhombic
OPC	Ordinary Portland Cement
rel. Int.	Relative Intensity
RH	Relative Humidity
s	Seconds
SLU	Self Levelling Underlayment
T	Temperature
t	Time
TGA	Thermogravimetric analysis
TOF-SIMS	Time-of-flight secondary ion mass spectrometry
TOC	Total Organic Carbon
w/b	Water-to-binder ratio
w/c	Water-to-cement ratio
wt. %	Weight percentage
XRD	X-ray diffraction
XRF	X-ray fluorescence
XPS	X-ray photoelectron spectroscopy
μ	Micro
μ(H ₂ O)	Chemical potential of water

ABSTRACT

Prehydration is the reaction of anhydrous cement with water vapour in air, leading to partial hydration and carbonation on the surface of the cement. Industrial cements can undergo some prehydration during their manufacturing process or during transportation and storage. Alteration of the cement properties during storage resulting from prehydration is highly undesirable, but has been repeatedly noticed by users. Early investigations on this subject have shown that cement which was stored for longer periods in humid air may fail in the field. Thus, cement prehydration can result in additional cost for both the cement and admixture industry. Therefore, the subject of cement prehydration is highly interesting for manufacturers as well as applicators.

In this thesis, the general phenomenon of cement prehydration was scientifically investigated under laboratory conditions. The main objectives of this work were:

1. Identify key cement phases which are most affected by prehydration
2. Identify and develop tools and analytical methods for surface characterisation of nano-scale layers of cement hydrates
3. Study mechanisms of very early cement hydration and carbonation for individual clinker phases
4. Describe scientifically the impact of prehydration and carbonation on cement hydration and interaction with chemical admixtures

First, the effects of water sorption on the surfaces of individual cement constituents were investigated using a dynamic water vapour balance instrument. The amount of water sorbed chemically and/or physically per unit of surface area of the powders and the relative humidity at which water sorption starts to occur on the phases were determined. The experiments demonstrated the uptake of water by the various cement clinker phases starts at very different relative humidities (RHs): free lime and orthorhombic C_3A begin to sorb large amounts of water at 14 % and 55 % RHs. They are followed by β - $CaSO_4 \cdot \frac{1}{2} H_2O$ and cubic C_3A . While C_4AF , gypsum and anhydrite sorb very low amounts of water. Surprisingly, the silicates C_3S and C_2S sorb almost no water at all which is an indication of their low reactivity compared to other clinker phases.

Secondly, several analytical methods were utilised to provide information on the composition and speciation of the prehydrated surface. X-ray photoelectron spectroscopy was identified as a very useful analytical technique, which allowed to detect only a few nanometer thin layers of cement hydrates. Prehydration is essentially a surface reaction, hence common bulk analysis methods such as x-ray diffraction can be applied only at a later stage of prehydration to detect hydration products when the crystallinity of the products is more pronounced. The study also confirmed the potential of micro-Raman spectroscopy for monitoring the prehydration behaviour of minor cement constituents, particularly when amorphous products are involved in the reaction processes.

Next, it was shown that prehydration of cement is far more complex than the sum of each individual prehydration reactions. The study of individual cement constituents does not account for interactions between different phases which can take place in actual cements. Therefore, further studies were conducted utilising binary mixtures. ESEM imaging revealed that in a moist atmosphere, a liquid water film condenses on the surfaces of the phases as a consequence of capillary condensation between the particles. In such water films, the individual cement constituents dissolve partially and can then react with each other. In the presence of C_3A and calcium sulphate hemihydrate, ettringite (AF_t phase) was observed as the predominant prehydration product of both C_3A modifications. This signifies that ion transport had occurred between the C_3A and sulphate. From this, it was concluded that prehydration of cement powder is mainly facilitated through capillary condensation and less through surface interaction with gaseous water molecules.

Furthermore, the mechanism of carbonation in moist air was studied by x-ray photoelectron spectroscopy for cubic and orthorhombic C_3A . The results demonstrated that the presence of sodium ions strongly impacts the carbonation behaviour of orthorhombic C_3A , thus causing its higher sensitivity towards humidity and atmospheric carbon dioxide.

Finally, the impact of prehydration and carbonation on cement hydration and on interaction with chemical admixtures was investigated. The results showed that the uptake of moisture and carbonation can cause a significant change in the flow, water retention and set behaviour patterns. As a result of partial surface hydration both the specific surface area and the surface charge of cement are changed. This results in substantial effects on the interaction with admixtures. Generally, effectiveness of superplasticizers is decreased with prehydrated cement whereby polycarboxylates and polycondensates (BNS) are very strongly affected

while casein suffers much less from prehydration. In water-retention, effectiveness of methyl cellulose is enhanced in aged cement while cement accelerators experienced a significant loss in their performance. Thus, the effects of partial surface hydration of cement can be both positive and negative with respect to the performance of admixture, with detrimental effects being more prevalent than benefits.

This thesis highlights the practical relevance of prehydration and aims to provide a broader view of the influence of prehydration on cement properties and its subsequent behaviour in the absence and presence of chemical admixtures.

ZUSAMMENFASSUNG

Der Begriff Vorhydratation (im Englischen *prehydration*) beschreibt die Gesamtheit aller Prozesse und Effekte, die während der Lagerung von Zement an dessen Oberfläche mit Wasserdampf oder atmosphärischem Kohlenstoffdioxid stattfinden können. Industrielle Zemente können unter dem Einfluss von Feuchtigkeit während der Herstellung, bei der anschließenden Lagerung im Silo und beim Transport in Kontakt mit Luftfeuchtigkeit kommen und geringfügig vorhydratisieren. Eine Veränderung der Verarbeitungseigenschaften von länger gelagerten Zementen ist unerwünscht, wurde aber von Anwendern häufig beobachtet. Frühe Untersuchungen zeigten dass Zemente, die längere Zeit lagern und dabei der Einwirkung feuchter Luft ausgesetzt sind, zu großen Problemen bei der Anwendung führen können. Diese negativen Folgen können sowohl für die Zement- als auch für die Zusatzmittelindustrie zusätzliche Kosten verursachen. Die Zementalterung stellt daher sowohl für Zement- und Zusatzmittelhersteller als auch für Anwender ein wichtiges Thema dar.

Ziel dieser Arbeit war es, die bei der Alterung von Portlandzement mit Luftfeuchtigkeit unter kontrollierten Bedingungen ablaufenden Prozesse zu untersuchen und die Auswirkungen auf die Zementeigenschaften aufzuklären. Im Rahmen dieser Arbeit sollten folgende Punkte geklärt werden:

1. Welche der Zementbestandteile reagieren besonders stark mit Luftfeuchtigkeit?
2. Welche analytischen Methoden sind zur Charakterisierung von nur wenige Nanometer dünnen Zementhydratschichten geeignet?
3. Welche chemischen Reaktionen laufen bei der Vorhydratation und Carbonatisierung reiner Zementbestandteile ab?
4. Welche Folgen hat die Vorhydratation und Carbonatisierung von Zement für seine Verarbeitungseigenschaften und die Wechselwirkung mit Zusatzmitteln?

Als erstes wurde der Einfluss der Luftfeuchtigkeit auf einzelne Zementbestandteile mit Hilfe einer Wasserdampfsorptionswaage untersucht. Dabei wurde die pro Oberfläche chemisch und/oder physikalisch aufgenommene Menge an Wasser sowie die Schwellenwerte an Luftfeuchtigkeit, ab denen Wassersorption auftritt, für alle wichtigen Zementbestandteile einzeln ermittelt. Die Ergebnisse zeigten, dass im Multikomponentensystem Zement die einzelnen Phasen sehr unterschiedliches Verhalten gegenüber Luftfeuchtigkeit aufweisen.

Freikalk (CaO) und orthorhombisches C₃A nehmen die größten Mengen an Wasser auf, und zwar ab 14 % (CaO) bzw. 55 % rel. F. (C₃A₆). Darauf folgen β-CaSO₄ · ½ H₂O und kubisches C₃A. C₄AF, Gips und Anhydrit wiederum nehmen noch geringere Mengen an Wasserdampf auf. Die Silikate (C₃S und C₂S) besitzen die geringste Sensitivität gegenüber Luftfeuchtigkeit und nehmen nahezu kein Wasser auf, ein Indiz für ihre generell sehr langsame Anfangsreaktion mit Wasser.

Im nächsten Schritt wurde nach geeigneten analytischen Methoden gesucht, die zur Klärung der mechanistischen Abläufe an der Oberfläche während der Vorhydratation der Zementbestandteile beitragen können. Photoelektronenspektroskopie (XPS) wurde als eine hervorragende Methode zur Untersuchung von nur wenige Nanometer dünnen Oberflächenschichten bestätigt und erfolgreich zur Identifizierung der ersten Hydratschichten bereits während der ersten Stunden der Alterung angewendet. Bei der Vorhydratation handelt es sich überwiegend um eine Oberflächenreaktion, deswegen können konventionelle Methoden der Zementanalytik wie z. B. Röntgenbeugung (XRD) nur dann zur Identifizierung der Produkte herangezogen werden, wenn auf der untersuchten Partikeloberfläche bereits genügend dicke Schichten kristalliner Phasen entstanden sind. Die im Rahmen dieser Arbeit durchgeführten Untersuchungen bestätigten, dass Mikro-Raman Spektroskopie zuverlässig Aufschluss über die Entstehung amorpher Phasen während der Vorhydratation und Carbonatisierung liefern kann.

Die Vorhydratation von Zement stellt einen komplexen Vorgang dar, der sich nicht mit der Summe der Einzelreaktionen beschreiben lässt. Untersuchungen zu individuellen Klinkerphasen geben deshalb keinen Aufschluss über die Wechselwirkungen zwischen verschiedenen Zementbestandteilen, die während der Alterung des Multikomponentensystems Zement stattfinden können. Daher wurden weitere Experimente mit binären Mischungen durchgeführt. Mittels atmosphärischer Rasterelektronenmikroskopie (ESEM) konnten Wasserfilme, welche als Folge von Kapillarkondensation zwischen den Zementpartikeln entstanden waren, auf den Oberflächen der Phasen nachgewiesen werden. In den Wasserfilmen können die einzelnen Bestandteile in Lösung gehen und chemisch miteinander reagieren. In Gegenwart von Calciumsulfat-Halbhydrat wurde Ettringit als Haupthydratationsprodukt für beide C₃A-Modifikationen gefunden. Dieses Experiment lieferte somit einen klaren Nachweis für den Ionentransport zwischen C₃A und Sulfat-Ionen, der bei der Lagerung an feuchter Luft stattfindet. Folglich findet Vorhydratation überwiegend

über Kapillarkondensation von Wasser auf der Phasenoberfläche und nur zum geringen Teil in Form einer direkten Wechselwirkung zwischen Feststoffoberfläche und Wasserdampf statt.

Des Weiteren wurde die Carbonatisierung von orthorhombischem und kubischem C_3A an feuchter Luft in Abhängigkeit von der Expositionsdauer mittels Photoelektronenspektroskopie untersucht. Es wurde gefunden, dass sowohl der Hydratations- als auch Carbonisierungsgrad sowie die Art der Reaktionsprodukte mit der Dauer der Lagerung korrelieren und stark von der C_3A -Modifikation abhängen, wobei orthorhombisches C_3A deutlich stärker reagiert. Dieses Verhalten konnte auf die strukturellen Unterschiede zwischen beiden Modifikationen und vor allem auf die Dotierung des orthorhombischen C_3A mit Natriumionen zurückgeführt werden.

Im letzten Teil wurde die Wechselwirkung von gealtertem Zement mit bauchemischen Zusatzmitteln untersucht. Die Ergebnisse zeigten, dass Feuchteaufnahme und Carbonatisierung während der Zementalterung das Fließ-, Wasserretentions- und Abbindeverhalten deutlich verändern können. Infolge Oberflächenhydratation verändern sich sowohl die spezifische Oberfläche als auch die Oberflächenladung des Zements, was die Wechselwirkung mit Zusatzmitteln erheblich beeinflusst. Es wurde gefunden, dass die Wirkung von Fließmitteln mit feuchteexponiertem Zement generell schlechter ist als mit frischem. Polycarboxylate und Polykondensate (NSF) verlieren dabei besonders an Wirkung, während das Biopolymer Casein nur geringe Einbußen erleidet. Im Gegensatz zu diesem schädlichen Effekten nimmt die Wasserretentionswirkung von Methylcellulose in gealtertem Zement sogar zu. Andererseits verlieren Abbindebeschleuniger wie z. B. Calciumformiat und amorphes Al_2O_3 deutlich an Wirkung bzw. Konvertieren sogar zu Abbindeverzögerern. Die Effekte dieser Oberflächenhydratation können demnach sowohl positiv als auch negativ bezüglich der Wirkung der Zusatzmittel sein, wobei die schädlichen Auswirkungen überwiegen.

Diese Ergebnisse dieser Arbeit unterstreichen die Bedeutung der Zementalterung in der baupraktischen Anwendung. Gleichzeitig liefern sie einen Beitrag zur Klärung der Ursachen sowie Folgen für die hydraulischen Eigenschaften einzelner Zementklinker sowie Portlandzement in An- und Abwesenheit von Zusatzmitteln.

LIST OF PUBLICATIONS

This thesis includes the following publications:

SCI(E) journal papers:

(1) "A sorption balance study of water vapour sorption on anhydrous cement minerals and cement constituents"

E. Dubina, L. Wadsö, J. Plank,

Cement and Concrete Research 41 (11) (2011), 1196 – 1204.

Refereed Conference proceedings:

(2) "The effects of prehydration of a combination of cubic C₃A with β-hemihydrate on adsorption of BNS superplasticizer"

E. Dubina, J. Plank, L. Wadsö, L. Black,

Proceedings of the 13th ICCI International Congress on the Chemistry of Cement, Madrid/Spain, 2011, 250.

Manuscripts submitted to journals:

(3) "Interaction of environmental moisture with cubic and orthorhombic C₃A in the absence and presence of sulfates"

E. Dubina, J. Plank, L. Black, L. Wadsö,

submitted on 16/10/2012 to *Advances in Cement Research*.

(4) "Impact of water vapour and carbon dioxide on surface composition of C₃A polymorphs studied by x-ray photoelectron spectroscopy"

E. Dubina, L. Black, J. Plank,

to be submitted to *Cement and Concrete Research*.

(5) "Influence of water vapour and carbon dioxide on free lime during storage at 80 °C studied by Raman spectroscopy"

E. Dubina, L. Korat, L. Black, J. Strupi Šuput, J. Plank,

submitted on 9/11/2012 to Spectrochimica Acta Part A: Molecular and Biomolecular Spectroscopy.

Non-reviewed journal publications:

(6) "Influence of moisture- and CO₂-induced ageing in cement on the performance of admixtures used in construction chemistry"

E. Dubina, J. Plank,

ZKG International, 10 (2012), 60 – 68.

(7) "Investigation of the long-term stability during storage of drymix mortars, Part 2. Influence of Moisture Exposure on the Performance of Self-levelling mortars (SLUs)"

E. Dubina, J. Plank,

ALITinform, 4 – 5 (26) (2012), 86 – 99.

Further publications:

"Interaction of water vapour with anhydrous cement minerals"

E. Dubina, L. Black, R. Sieber, J. Plank,

Advances in Applied Ceramics 109 (5) (2010), 260 – 268.

"The effect of prehydration on the engineering properties of CEM I Portland cement"

M. Whittaker, **E. Dubina**, F. Al-Mutawa, L. Arkless, J. Plank and L. Black,

Advances in Cement Research 25 (1) (2013), 12 – 20.

"The Effects of Prehydration at Moderate Humidities on the Engineering Properties of Portland Cement"

F. Al-Mutawa, M. Whittaker, L. Arkless, **E. Dubina**, J. Plank, L. Black,

Cement and Concrete Science, London, 2011.

**"Investigation of the long-term stability during storage of cement in drymix mortars,
Part 1. Prehydration of clinker phases, free lime and sulfate phases under different
relative humidities"**

E. Dubina, J. Plank, L. Wadsö, L. Black, H. König,

ALITinform, 3 (20) (2011), 38 – 45.

**"Untersuchungen zur Vorhydratation von Zementklinkerphasen und Sulfatträgern
unter Einsatz einer Sorptionswaage"**

E. Dubina, J. Plank, L. Wadsö, L. Black, H. König,

GDCh monograph 42 (2010), 238 – 245.

"The Effects of Cement Prehydration on Engineering Properties"

M. Whittaker, **E. Dubina**, J. Plank, L. Black,

C. H. Fentiman, R. J. Mangabhai (Eds.),

Cement and Concrete Science, Birmingham (2010), 101 – 104.

**"Surface prehydration of cement clinker phases and industrial cements, caused by
water vapour"**

J. Plank, **E. Dubina**, L. Wadsö,

7th International Symposium on Cement and Concrete (ISCC), Jinan, China, (2010).

"Untersuchungen zur Vorhydratation von Zement"

E. Dubina, R. Sieber, J. Plank, L. Black,

GDCh monograph 39 (2008), 329 – 337.

**"Effects of pre-hydration on hydraulic properties on Portland cement and synthetic
clinker phases"**

E. Dubina, R. Sieber, J. Plank, L. Black,

C. H. Fentiman, R. J. Mangabhai (Eds.),

Cement and Concrete Science, Manchester (2008), 46 – 49.

CONTENT

1	INTRODUCTION	1
2	SCOPE OF THE WORK.....	3
3	STATE OF THE ART.....	5
3.1	Ordinary Portland Cement	5
3.2	Hydration of Portland Cement	7
3.3	Chemical admixtures.....	8
3.4	Prehydration of cement	10
3.5	Water vapour – solid interactions.....	13
3.5.1	Relative and absolute humidity.....	13
3.5.2	States of sorbed water.....	14
3.5.3	Chemical potential of water.....	16
4	EXPERIMENTAL	19
4.1	Materials.....	19
4.1.1	Pure clinker phases and other cementitious components.....	19
4.1.2	Admixtures and drymix mortar.....	21
4.2	Exposure of samples to relative humidity	21
4.2.1	Sorption balance instrument	22
4.2.2	Saturated salt solutions	24
4.2.3	Climate chamber.....	24
5	METHODS	27
5.1	Surface analysis.....	27
5.1.1	X-ray diffraction analysis	29
5.1.2	X-ray photoelectron spectroscopy	29
5.1.3	IR spectroscopy and Raman analysis	30
5.1.4	Time-of-flight secondary ion mass spectrometry (TOF-SIMS).....	31
5.1.5	Scanning electron microscopy	32

5.2	Bulk analysis	33
5.3	Interactions with admixtures	35
6	RESULTS AND DISCUSSIONS.....	37
6.1	Sorption balance study on anhydrous cement minerals - paper 1	37
6.2	X-ray photoelectron spectroscopic study on C ₃ A polymorphs - paper 2	40
6.3	Raman spectroscopic study on CaO - paper 3	43
6.4	Sorption balance study on binary mixtures - paper 4	45
6.5	The effects of prehydration on the adsorption of BNS superplasticizer - paper 5	47
6.6	The effects of prehydration on the performance of chemical admixtures - paper 6 ...	49
6.7	The effects of prehydration on the performance of drymix mortars - paper 7	50
6.8	Further preliminary results	53
6.8.1	An attempt to utilise SIMS technique in the analysis of cement prehydration.....	53
6.8.2	Study on the sorption kinetics applying a shrinking core model.....	56
6.8.3	Prehydration of different calcium sulphates at 80 % RH and 80 °C	63
6.8.4	CEM I prehydrated at 80 °C and 10 – 80 % RH	65
6.8.5	CEM II / A-LL prehydrated at 35 °C and 90 % RH.....	66
7	CONCLUSIONS AND OUTLOOK.....	71
7.1	Conclusions	71
7.2	Outlook.....	73
8	REFERENCES	75

1 INTRODUCTION

With an annual global production of 2.8 billion tonnes in 2010, Ordinary Portland Cement (OPC) is the most often applied binder material used in the world. This volume is expected to increase to some 4 billion tonnes per year in 2015 [1]. Major growth is expected in countries such as China and India as well as in regions like the Middle East and Latin America [2].

The most important physical properties of cement such as workability, setting behaviour, strength development and durability are related to the cement hydration process, in which the material quality plays a decisive role. In industrial use, cement may be stored for up to months or even a year before usage. For dry mixed mortars, for example, the usual shelf life guaranteed is 6 months to 1 year, as stated on the bags. Alteration of the workability properties during storage is highly undesirable, but has been repeatedly noticed by users [3, 4]. The principal consequences of this phenomenon, otherwise known as prehydration of cement, include increased setting time, decreased compressive strength and heat of hydration and altered rheological properties [5–7].

Prehydration of cement may start already during its production. There, a first contact with water can occur from the dehydration of gypsum which is interground with clinker in the ball mill at elevated temperature. Additionally, cement producers sometimes lower the milling temperature by spraying e.g. 2 % of water into the mill. Also, during storage in the silo the cement may change as a result of prehydration, as the temperature is still high, and water can be released from the interground gypsum as long as the temperature exceeds 42 °C. Therefore, cement may already be prehydrated before it is delivered to the customer. Further prehydration might occur during inappropriate storage on the building site as is shown in **Figure 1**.

It is known that cement prehydration can be one of the reasons for the occasionally reported poor response of admixtures with aged cement. There, even incompatibility between a particular chemical and a certain batch of the same otherwise compatible cement or cement based dry-mix formulation was observed, indicating that the nature of the problem is complex, and that it needs further understanding. Thus, cement prehydration can result in additional costs for both cement and admixture suppliers.



Figure 1: Photos of cement bags on a construction site, illustrating inappropriate storage conditions in summer (**left**) and winter (**right**)

Despite the widespread use of cement, a fundamental understanding is lacking with regard to its interaction with water vapour and atmospheric carbon dioxide. Furthermore, the knowledge of very early cement hydration and related analytical methods is still limited. Only a few methods such as x-ray photoelectron, FTIR-ATR and micro-Raman spectroscopy can be applied to investigate the surface reaction upon ageing. The presence of different phases in cement requires the use of complementary techniques to study the very early interactions of water vapour with cement.

In order to fill this gap of knowledge NANOCEM, a European consortium of industrial and academic partners concerned with fundamental cement and concrete research, initiated Core Project # 7 entitled “Fundamental mechanisms of cement prehydration”. This doctoral project was focused on the prehydration processes of cement components under laboratory conditions and subsequently the related consequences for its behaviour in the absence and presence of chemical admixtures.

2 SCOPE OF THE WORK

The current doctoral project was designed to add to the fundamental knowledge on the prehydration of cement. Based on a literature review and the findings from the candidate's Master Thesis, several topics in cement and concrete science concerning prehydration were identified which merited further investigation [8]. In particular, the targets as follows were set:

- Identify key cement phases which are most affected by prehydration, and develop a simple model of it
- Identify and develop tools and analytical methods for surface characterisation of nanometer scale layers of cement hydrates
- Study the mechanisms of very early cement hydration and carbonation for individual clinker phases
- Describe the impact of prehydration and carbonation on cement hydration and interaction with chemical admixtures

These research steps should allow to understand which parameters influence the ageing of cement, thus providing a scientific basis for the future development of cements possessing a longer shelf-life.

Beginning with less complex investigations on pure clinker phases and cement constituents, the work was carried forward on binary mixtures of C_3A and calcium sulphate hemihydrate, followed by an analysis of actual cements in absence and presence of admixtures.

Finally, some preliminary results on basic dry mix mortar formulations were developed. The wide selection of analytical methods employed as well as the diverse experimental conditions for cement materials tested provides a rather thorough understanding of the effects of water vapour and carbon dioxide on cement.

3 STATE OF THE ART

3.1 Ordinary Portland Cement

Ordinary Portland Cement (OPC) is a multi-mineral system. Its chemical composition is strongly dependent on the chemical composition of the raw materials, from which the clinker is sintered in a kiln at ~ 1450 °C. The main clinker phases are calcium silicates (Ca_3SiO_5 and Ca_2SiO_4), calcium aluminate ($\text{Ca}_3\text{Al}_2\text{O}_6$) and ferrite ($\text{Ca}_4\text{Al}_{4-x}\text{Fe}_x\text{O}_{10}$) which are commonly denominated as C_3S , C_2S , C_3A and C_4AF , respectively. Due to the industrial process, these phases are not pure, but contain variable amounts of foreign ions in their crystal lattice which may alter the crystal structure. A list of the characteristics of the four main cement phases is presented in **Table 1**.

Table 1: Main phases of Portland cement and their characteristics [9, 10]

Parameter	Clinker phase			
	C_3S	C_2S	C_3A	C_4AF
Technical name	alite phase	belite	aluminate phase	ferrite phase
Amount in CEM I [wt. %]	40 – 80 \varnothing 60	0 – 30 \varnothing 15	3 – 15 \varnothing 7	4 – 15 \varnothing 8
Foreign oxides	MgO, Al_2O_3 Fe_2O_3	K_2O , Na_2O Al_2O_3 , Fe_2O_3	K_2O , Na_2O Fe_2O_3 , MgO SiO_2	SiO_2 , MgO TiO_2
Number of modifications	7	5	3	1
Typical modifications in technical clinker	monoclinic (m_{II})	β -belite, monoclinic (rarely α - and α' -belite)	cubic, orthorhombic	orthorhombic
Reactivity	high	low	very high	low
Heat of hydration (J/g)	- 520	- 260	- 1160	- 420
Contribution to strength	high at early ages	high at late ages	high at very early ages	very low

Different calcium sulphates, generally in the form of dihydrate (gypsum, $\text{CaSO}_4 \cdot 2 \text{H}_2\text{O}$) and water-free calcium sulphate (anhydrite, CaSO_4) are added to the clinker in order to retard the initial hydration of the aluminate phase. Calcium sulphate hemihydrate (bassanite,

$\text{CaSO}_4 \cdot 0.5 \text{H}_2\text{O}$) is more soluble compared to the former phases and originates from the dehydration of gypsum during the grinding process of the clinker at temperatures above $42 \text{ }^\circ\text{C}$ [11]. As decomposition proceeds, soluble anhydrite (anhydrite II) may be formed in the mill at temperatures above $100 \text{ }^\circ\text{C}$. Soluble anhydrite is as soluble as hemihydrate [12, 13].

Due to the use of alternative fuels and the recovery of waste kiln dust, the content of alkalis in cement clinker increased. The alkali sulphates thus became an important sulphate source [14]. Sulphates present in fuels and raw materials preferentially form alkali sulphates. The solubility of alkali sulphates is generally higher than that of calcium sulphates, as is shown in **Table 2**. Thus, Portland cements may have the same total SO_3 content, but depending on the type of sulphate, the availability of sulphate ions can be completely different.

Table 2: Solubility of various sulphate sources in Portland cement at room temperature [15]

Sulphate compound	Solubility (g/L) at $25 \text{ }^\circ\text{C}$
Calcium sulphate dihydrate ($\text{CaSO}_4 \cdot 2 \text{H}_2\text{O}$)	2.1
Syngenite ($\text{CaSO}_4 \cdot \text{K}_2\text{SO}_4 \cdot \text{H}_2\text{O}$)	2.5
Natural calcium sulphate anhydrite (CaSO_4)	2.7
Calcium sulphate hemihydrate ($\text{CaSO}_4 \cdot 0.5 \text{H}_2\text{O}$)	6.2 – 8.2
Soluble calcium sulphate anhydrite (CaSO_4)	6.3
Calcium langbeinite ($2 \text{CaSO}_4 \cdot \text{K}_2\text{SO}_4$)	6.3
Arcanite (K_2SO_4)	120
Aphthitalite ($\text{Na}_2\text{SO}_4 \cdot 3 \text{K}_2\text{SO}_4$)	120

In addition, cement contains other minor compounds such as CaO or MgO. Since the reactions that involve clinker formation seldom go to completion during the clinkering process, usually small amounts (less than 1 % by mass) of uncombined calcium oxide (CaO referred to as “free lime”) are present in cement. An excess of free lime in cement can result in expansion leading to cracking and strength loss of concrete due to internal tension. MgO occurs in most raw materials and, when present above $\sim 2 \text{ } \%$ by mass, will crystallize as free MgO, which may also expand during the hydration of cement in a similar way as CaO.

3.2 Hydration of Portland Cement

The term “hydration” includes all chemical and physical processes occurring in the cement – water system. These processes can be obtained by measuring the heat flow as a function of time. **Figure 2** shows the typical heat evolution curve recorded for the 3 days of hydration of ordinary Portland cement when using an isothermal calorimeter. The curve can be divided into five stages. Their main characteristics are summarised in **Table 3**. Recently, the mechanisms governing these stages have been reviewed by BULLARD *et al.* [16].

One of the most discussed phenomenon in the literature is the reason behind the occurrence of an induction period. The first theory which explains the slowdown in the rate of reaction is based on the formation of a metastable barrier product on the surface of the reacting particle. Another theory explains the decreasing rate of cement dissolution by the build-up in concentration of ions in solution. Reasons for and against these theories are presented in [16]. Hydration stages 3 and 4 are generally accepted to be controlled by the nucleation and growth of the main hydrate phase C–S–H. As discussed [16, 17] and demonstrated [18] in the literature, there is evidence that diffusion through the C–S–H layer is not the rate controlling mechanism in stage 4, although it may become so during stage 5.

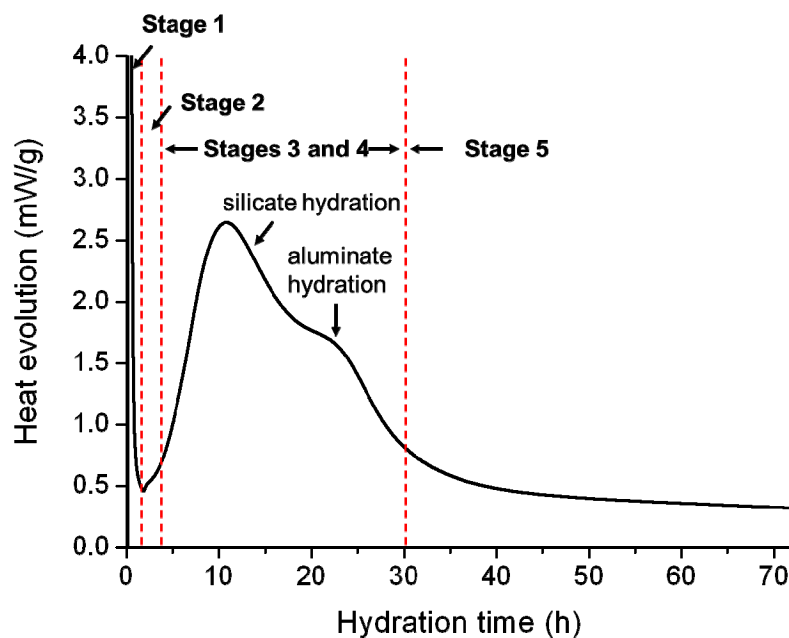


Figure 2: Typical heat evolution curve of Portland cement (CEM I 52.5 N, $w/c = 0.5$) within the first 72 hours

Table 3: Five stages of Portland cement hydration and their characteristics

Stage	Characteristics	Literature
1 Dissolution	During the first minutes, cement dissolves and ions are released into the pore solution, but the reaction rapidly slows to a low rate.	[19]
2 Induction	During the following hours, low activity and low heat evolution are observed.	[20]
3 Acceleration	The rate of heat evolution increases for several hours until it reaches a peak.	[21–24]
4 Deceleration	The rate of heat evolution decreases for a few hours.	[21–24]
5 Slow hydration	After the deceleration period, the hydration rate continues at a low decreasing level.	[21–24]

3.3 Chemical admixtures

Chemical admixtures are the ingredients in concrete other than Portland cement, water and aggregate, which are added to the mix immediately before or during the mixing process [25]. According to EN 934-2, concrete admixtures are materials that are added to the concrete in quantities not larger than 5 per cent by mass of cement in order to modify its properties in its fresh and hardened state [26]. Chemical admixtures are classified according to their function, e. g. for the entrainment of air, reduction of water or cement content, plastification of fresh concrete or mortar and the control of setting time. Such admixtures, in most cases organic compounds, can have a very strong impact on the hydration behaviour of cement. **Figure 3** illustrates the impact of the admixtures (accelerator and retarder) on the hydration evolution of a commercial Portland cement. Recently, an extensive review on the impact of the admixtures on the hydration kinetics has been published by CHEUNG *et al.* [27].

Superplasticizers are among the most widely used admixtures. In general, they can be applied in two ways. On one hand, for the same fluidity they allow to reduce the w/c ratio by up to ~ 30 % [28]. This implies a reduced pore volume and therefore an increased compressive strength. On the other hand they can be used as fluidifying agents, which means that the

fluidity of concrete is improved at a constant w/c ratio. The fundamental mechanisms of interaction between cements and superplasticizers were reviewed by YAMADA [29].

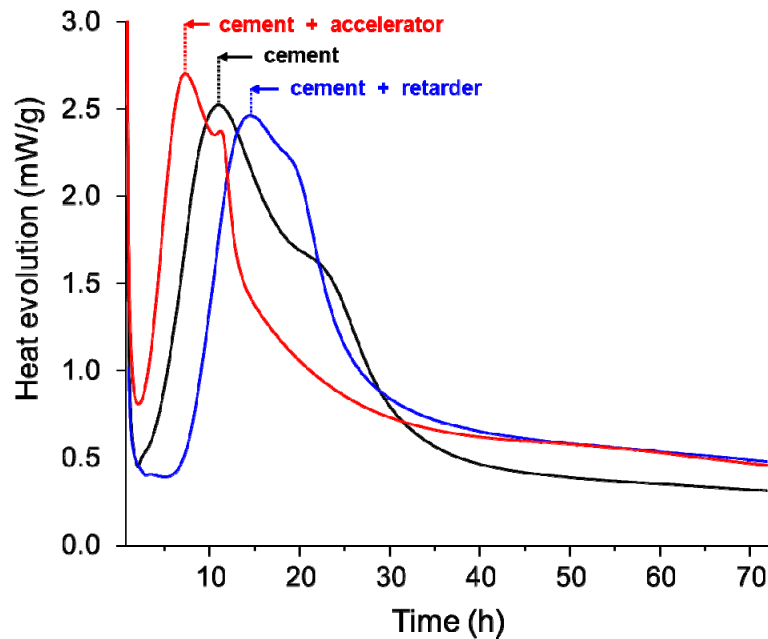


Figure 3: Typical heat evolution curve of Portland cement (CEM I 52.5 N, w/c = 0.5) in the presence of various chemical admixtures

Water-retention admixtures are used to improve the properties of mortars such as water retention, workability and the consistency of the slurry [30]. Among the most frequently used cellulose ethers are methyl hydroxyethyl cellulose (MHEC) and methyl hydroxypropyl cellulose (MHPC). The working mechanism of MHEC in cement was investigated and discussed by BÜLICHEN *et al.* [31].

Retarders slow the rate of cement hydration, preventing the cement from setting before it can be placed and compacted. This type of admixture is mainly used in hot climates or on very large pours. BISHOP and BARRON summarized all four proposed mechanisms of set retardation, which can be categorized as follows [32]:

- calcium complexation preventing precipitation of portlandite
- formation of a semipermeable layer which later is broken down by osmotic pressure gradients
- surface adsorption of retarders directly on anhydrous surface
- nucleation and growth poisoning of hydrates

The first two mechanisms are now considered to occur less often. In the first case, because very strong chelators can be moderate retarders while strong retarders can be poor chelators [33]. In the second case, because direct SEM observation reveals that during the induction period much of the C_3S surface shows no hydration product [20].

Accelerators are used to speed up the rate of early hydration of the cement. They can accelerate the setting or the early strength development. The most common accelerators are grouped as soluble inorganic salts such as calcium formate and soluble organic compounds. Using quasielastic neutron scattering (QENS) JUENGER *et al.* proposed that the relative effect of the accelerator anions and cations generally followed the HOFMEISTER series, and that the acceleration from $CaCl_2$ was due to its ability to flocculate hydrophilic colloids, so that the C–S–H layer that forms around the cement grains from the initial stage of hydration would be more permeable, hence it would allow a faster diffusion of ions and water [34, 35].

3.4 Prehydration of cement

From construction practice it is known that Portland cement is a hygroscopic material which can interact with surrounding water vapour present in the atmosphere. This can cause partial hydration on the surface of cement. In the literature this ageing phenomenon is often referred to as prehydration of cement.

The first studies on prehydration of cement under laboratory conditions were performed in the 1930. MEYERS found that prehydration of cement retarded the heat evolution. Also, the 3 and 7 day compressive strengths were considerably reduced [36]. WOODS *et al.* and DAVIS *et al.* found independently that prehydrated cement showed reduced heat of hydration and the loss of ignition was appreciably increased in such cements after storage [37, 38].

HORNIBROOK *et al.* proposed controlled prehydration as a way to produce low-heat, high-sulphate-resistant cement for use e. g. in dam construction instead of the coarse ground, low-alite and high-belite cements utilised during that time as low-heat cements [39]. In that study different commercial cements, including two low-heat Boulder dam, two high-early-strength and six standard Portland cements were studied, whereby prehydration increased the resistance to sulphate attack, with the exception of the cements high in tricalcium aluminate.

WEITHASE and HANSEN observed abnormal set when prehydrated Portland cement was used [40, 41]. KALOUSEK reported about formation of ettringite on the surface of prehydrated cement [42, 43]. The formation of syngenite was observed when alkali sulphates were present in moisture exposed cement [5].

Prehydration of cement may arise following prolonged storage when relative humidity is high. However, this phenomenon may be observed early on, where during grinding of the cement clinker temperatures are high enough to dehydrate gypsum to the more soluble calcium sulphates, bassanite or anhydrite, with the release of water [44, 45].

Additionally, cement producers sometimes lower the milling temperature which ideally should not exceed 115 °C by spraying e.g. 2 % of water into the mill [13, 46, 47]. Also, during storage in the silo, the cement may change as a result of prehydration, as the temperature is still at ~ 80 °C, and water can be released from the interground gypsum as long as the temperature exceeds 42 °C [11]. This may lead to the formation of agglomerates during storage first reported by MATOUSCHEK which, along with the hydration of the cement, leads to a phenomenon known as “silo set” described by THEISEN and JOHANSEN [48, 49].

The interaction of cement with water vapour has detrimental effects on its engineering properties [36, 48]. More recently, WHITTAKER *et al.* correlated changes in the engineering performance with changes in anhydrous cement speciation induced by prehydration under controlled conditions [50].

In addition to the influence mentioned above, factors affecting the degree of prehydration include the temperature, the relative humidity (RH), the time of exposure and the particle fineness, where smaller particles lead to smaller pore spaces thus resisting water vapour ingress through the cement bed as stated by RICHARTZ [51].

The alteration of cement due to prehydration also affects the properties of the mortars and concretes produced. Particularly when chemical admixtures and complex binder formulations such as drymix mortars are applied, a large influence of cement prehydration was found [3]. The influence of cement ageing on the performance of superplasticizers was recently described by WINNEFELD [3]. He found that cement prehydration influences the workability of pastes containing sulfonated naphthalene formaldehyde polycondensate more strongly than those with polycarboxylate ether.

SCHMIDT *et al.* reported that prehydration of cement in rapid hardening dry mix mortars caused an increased setting time and water demand [52]. ZURBRIGGEN and GOETZ-NEUHOEFFER published a case study on the impact of prehydration on mixed binders containing tartaric acid. They found that reducing the reactivity of the binders by ageing the drymix has the same effect as increasing the concentration of the tartaric acid [53].

However, in certain cases controlled prehydration might even be beneficial. MALTESE *et al.* noticed in a shotcrete system containing aluminium sulfate as accelerator a favorable decrease of setting time [4]. The authors used a Portland cement containing β -hemihydrate which was previously exposed to moisture. Such an effect seems to be related to the reduction of the β -hemihydrate dissolution rate.

Due to the complex nature of cement, it is challenging to identify the key processes occurring during prehydration on the surfaces of cement particles. To overcome this challenge several groups studied prehydration of individual cement clinker phases. Concerning the cement clinker phases, they found that it is mainly the C_3A phase that is sensitive to moisture [5, 48].

BREVAL studied the impact of water vapour on the morphology and composition of the hydration products of cubic C_3A [54]. She observed gel, hexagonal and cubic phases on the surface of the prehydrated cubic C_3A . In presence of gypsum cubic C_3A also reacted to ettringite [55].

JENSEN *et al.* assessed the reactivity of the clinker phases – C_3S , C_2S and cubic C_3A – by exposing them to different relative humidities for up to 1 year [56]. They observed thresholds below which the phases would not react with water vapour. C_3A prehydrated above 60 % RH, producing mostly C_3AH_6 , whilst the thresholds for C_3S and C_2S were much higher, at 85 % and 90 % respectively. Furthermore, the RH appeared to affect the nature of the C-S-H. At a very high RH (~ 99 %), silicate prehydration produced C-S-H with a C/S ratio of 1.7, a typical value for conventionally hydrated C_3S . While, at 83 % RH, the C/S ratio increased to 3 with little or no CH formation.

More recently, different analytical methods which allow to study the changes owed to prehydration were applied [57]. It was found, that XPS is a suitable technique to study very early hydration products on the surface of clinker minerals which are typically less crystalline, while XRD analysis is more reliable at a later stage of exposure to moisture, when the crystallinity of the products is more distinct and a larger amount of hydrates is present.

3.5 Water vapour – solid interactions

It is widely recognised that the presence of atmospheric moisture in anhydrous cementitious systems can lead to many significant changes in physical and chemical properties. Therefore, a detailed analysis of interactions at the “water vapour – solid” interface is required to understand the impact of prehydration. This chapter summarises the main terms and definitions used in the literature to describe the interactions between water vapour and solid material. It also provides an overview about states of sorbed water and discusses the chemical potential of water.

3.5.1 Relative and absolute humidity

Humidity is the quantity of water vapour present in air [58]. It can be expressed as absolute or in relative values. Relative humidity (φ ; RH) is defined as the ratio of the partial pressure of water vapour in a volume unit of air to the saturated vapour pressure of water vapour at a prescribed temperature:

$$\varphi = \frac{p}{p^0} \cdot 100 \% \quad \text{equation (1)}$$

Where:

φ : relative humidity

p : partial pressure of water vapour

p^0 : saturated vapour pressure of water vapour at the prescribed temperature

Absolute humidity ($\varphi_{\text{absolute}}$; AH) is the quantity of water in a particular volume of air. The most common units are grams per cubic meter (g/m^3). The absolute humidity changes as air pressure changes.

If ideal gas behaviour is assumed, the absolute humidity can be calculated as:

$$\varphi_{\text{absolute}} = C \cdot \left(\frac{p_w}{T}\right) \quad \text{equation (2)}$$

Where:

C : constant 2.16679 ($\text{g} \cdot \text{K}/\text{J}$)

p_w : vapour pressure in Pa

T : temperature in K

Warm air contains more water vapour (moisture) than cold air. **Figure 4** illustrates the values for both absolute and relative humidity at 20 °C and 40 °C. Generally, the water vapour pressure at saturation is a function of temperature. Consequently, the absolute water content occurring at a constant RH increases with temperature. At any RH level, at 40 °C there is about three times more water vapour present in the atmosphere than at 20 °C.

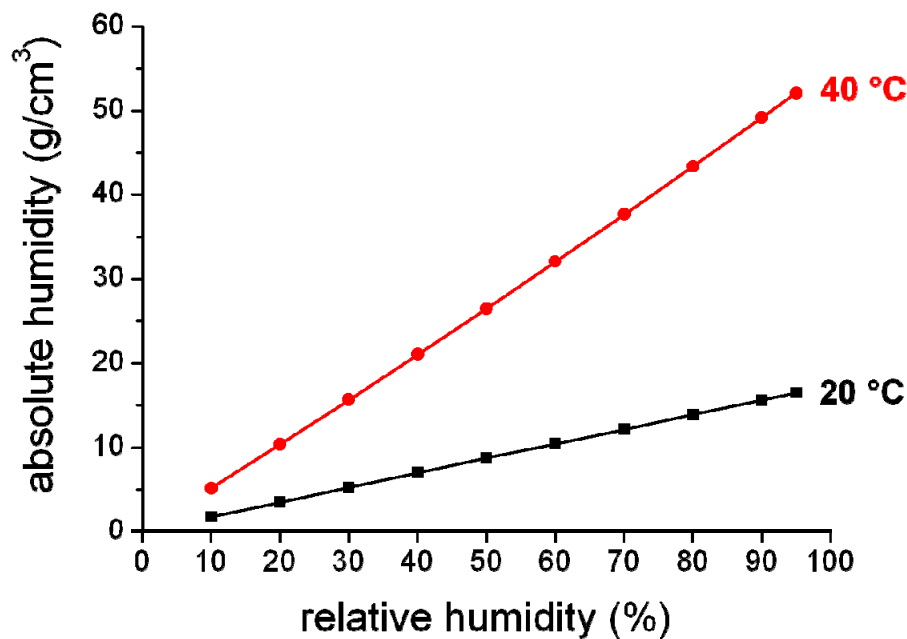


Figure 4: Calculated values for absolute humidity at 20 °C and 40 °C [59]

3.5.2 States of sorbed water

Anhydrous cement is hygroscopic and can sorb water vapour either physically or chemically, or in both ways. Water molecules can bind physically on the surfaces of cement grains via van der Waals forces (adsorption), forming mono or multilayers. At higher relative humidity, capillary condensation and capillary water uptake may occur. Both processes are physical by nature. When some inorganic salts such as K_2SO_4 are present in the system, dissolution may occur. Additionally, water can react chemically with clinker phases, yielding crystalline hydration products which may adsorb additional water molecules on their surfaces. When both adsorption and absorption occur, the term sorption is often used.

Figure 5 illustrates the different kinds of interactions between cement constituents and water vapour as described above.

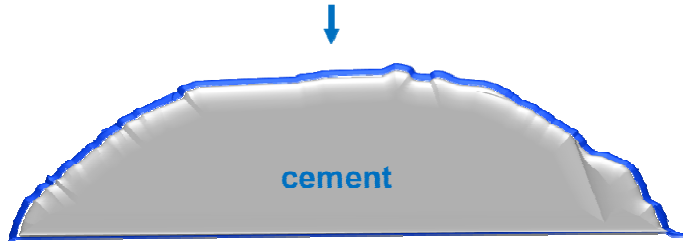
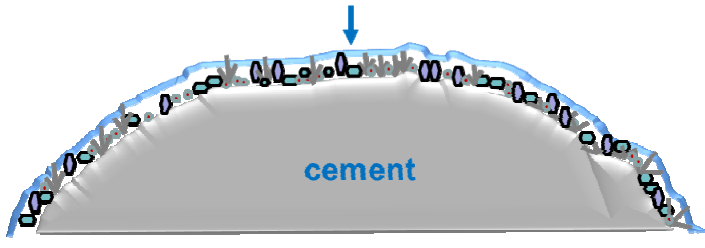
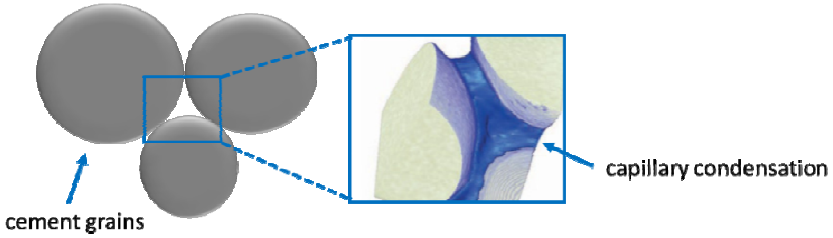
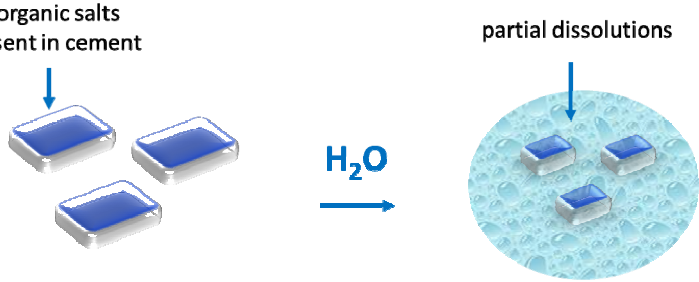
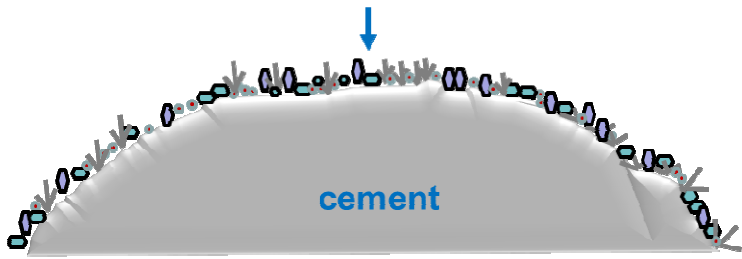
Surface interaction	Adsorption of water on anhydrous cement	<p>Adsorption of water on the surface of anhydrous particles</p> 
	Adsorption of water on hydration products	<p>Adsorption of water on the surface of cement hydrates</p> 
Condensed water	Capillary condensation	
	Dissolution	<p>Inorganic salts present in cement</p> 
Bulk interaction	Absorption of water and formation of hydrates	<p>formation of different cement hydrates (AF_m, AF_t, C-S-H)</p> 

Figure 5: Schematic illustration of potential water-solid interactions occurring in cementitious systems

The chemical incorporation of water into amorphous solids and the formation of early hydration products on the surface of cement particles can result in changes of the properties of cement powder. Generally, physically bound water will be reversibly desorbed when the water vapour pressure is decreased or the temperature is increased. In this case, the forces between the solid (adsorbent) surface and the vapour molecules (adsorbate) are weak. The forces involved in chemical reactions are much greater than those in physical adsorption.

The tendency to take up water vapour is best assessed by measuring sorption or desorption as a function of relative humidity at constant temperature and under conditions where sorption or desorption is essentially occurring independently of time, i.e., at equilibrium. Sorption is usually expressed as weight of water taken up per unit weight of solid and plotted versus relative humidity.

3.5.3 Chemical potential of water

Unlike in conventional hydration, the absence of excess water in which the cement components can dissolve during prehydration limits the ionic mobility and results in localised reactions. Furthermore, the water activity $a(\text{H}_2\text{O})$, and thus the chemical potential of water $\mu(\text{H}_2\text{O})$ is also affected by the water vapour pressure (RH) [60]. The water chemical potential is an important parameter which is related to the change in the Gibbs free energy of the system. In a recently published study, BAQUERIZO *et al.* showed that changes of the water chemical potential $\mu(\text{H}_2\text{O})$ impacts the interlayer/interchannel water content of sensitive cement hydrates, e. g. of AF_m and AF_t [61].

The water chemical potential under atmospheric conditions as a function of temperature can be defined as follows:

$$\mu(\text{H}_2\text{O})_{l,T} = \mu^0(\text{H}_2\text{O})_l + RT \ln(a(\text{H}_2\text{O})) \quad \text{equation (3)}$$

Where $\mu^0(\text{H}_2\text{O})_l$ is the standard chemical potential of liquid water at 298.15 K, R is the gas constant 8.314 J/(K mol), T is the temperature in K and $a(\text{H}_2\text{O})$ is the activity of water which can be linked to the relative humidity at a given water vapour pressure p and a known saturation vapour pressure of water p^0 according to Raoul's law [62]:

$$a(\text{H}_2\text{O}) = \frac{p}{p^0} = \frac{RH}{100} \quad \text{equation (4)}$$

There are 3 possibilities to change $\mu(\text{H}_2\text{O})$: by changing the $a(\text{H}_2\text{O})$ at a constant temperature, by adjusting the temperature at constant $a(\text{H}_2\text{O})$ and by decreasing the $a(\text{H}_2\text{O})$ and thus the $\mu(\text{H}_2\text{O})$ by dissolving ionic compounds.

The last case is particularly important when alkali ions are present in the system which cause high ionic strength, thus leading to precipitation of the hydrates with lower water content than that at high water activities [61].

4 EXPERIMENTAL

4.1 Materials

In this chapter the materials applied are presented. Additional details and related results can be found in the publications which are part of this thesis.

4.1.1 Pure clinker phases and other cementitious components

Cement clinker production involves the heating, calcining and sintering of ground raw materials. The cement clinker phases were synthesised according to [63] and further details are given in **paper 2**.

The minor cement component CaO was prepared by calcination of CaCO₃ obtained from Merck.

Grinding was performed for 10 minutes at 250 rpm at a temperature of 21 °C and an estimated relative humidity of 20 %. No grinding agent was added in the milling process.

As calcium sulfates, gypsum (purity 98 wt. %), β – hemihydrate (purity 97 wt. %) and anhydrite (purity 99 wt. %) from Sigma-Aldrich were used.

Figure 6 illustrates the steps of grinding (**Fig. 6 a**), the calcination at high temperature (**Fig. 6 b**) and it shows the C₃A and C₄AF powders obtained after the sintering (**Fig. 6 c and d**). In order to obtain flat surfaces for XPS analysis, the powdered C₃A and C₃S phases were pressed into pellets and sintered again (**Fig. 6 e and f**).

Precautions were taken to prevent reaction with atmospheric carbon dioxide and water vapour by storing the freshly ground samples in sealed 20 mL glass bottles placed in a vacuum desiccator containing silica gel as a drying agent.

Binary mixtures of individual cubic and orthorhombic C₃A respectively with calcium sulphate hemihydrate were prepared by manually blending the C₃A and calcium sulphate hemihydrate powders at a molar ratio of 1 : 1.

4 Experimental

An OPC type CEM I 52.5 N obtained from HeidelbergCement (Geseke plant, Germany) was used for prehydration experiments. Its clinker composition was determined through powder Q-XRD technique using *Rietveld* refinement. The amounts of gypsum ($\text{CaSO}_4 \cdot 2 \text{H}_2\text{O}$) and hemihydrate ($\text{CaSO}_4 \cdot 0.5 \text{H}_2\text{O}$) present in the cement sample were measured by thermogravimetry. The amount of free lime (CaO) was quantified following the extraction method established by FRANKE [64]. The exact cement composition is reported in **paper 6**.

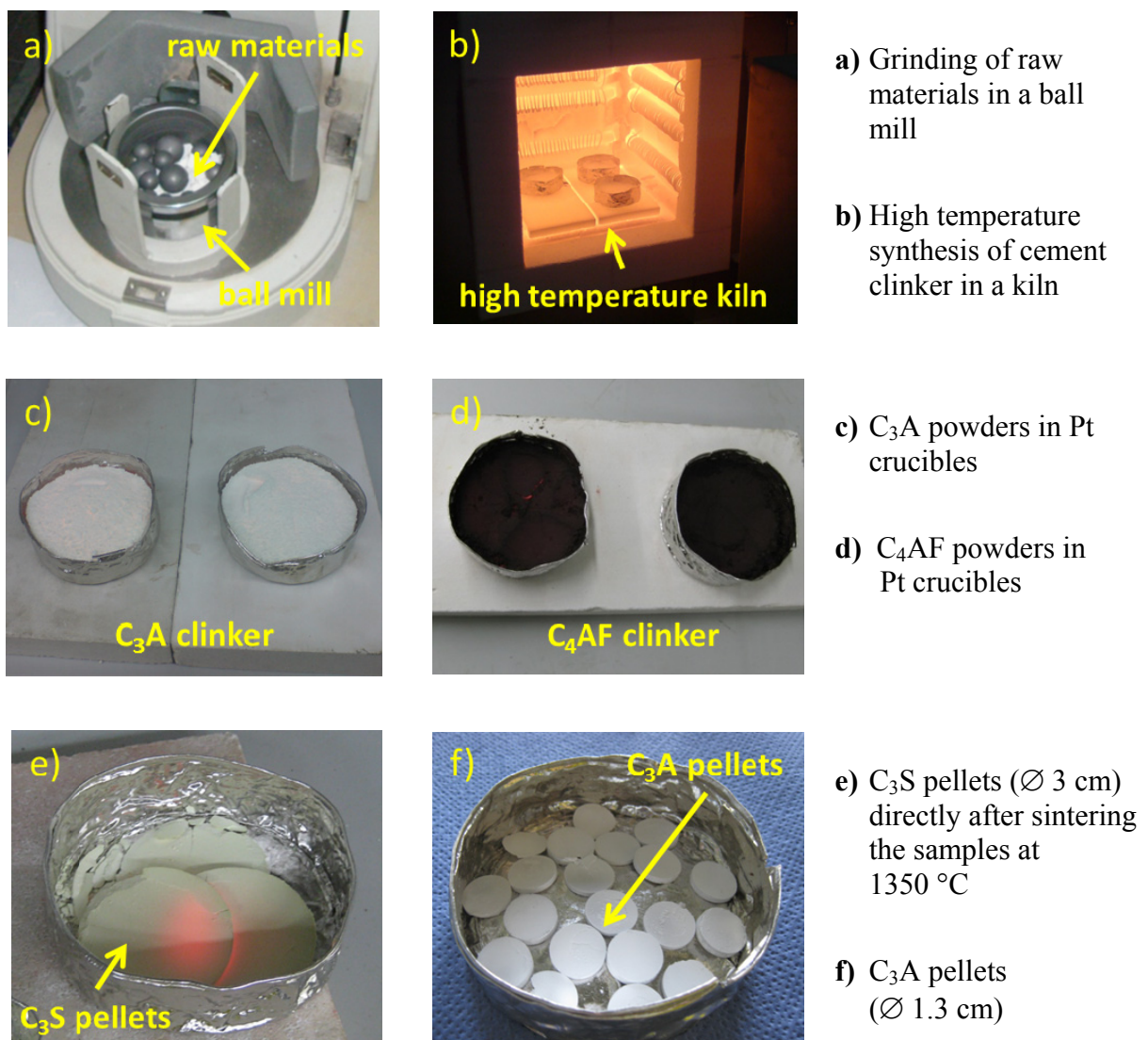


Figure 6: Preparation of different clinker phases as powders or pellets

4.1.2 Admixtures and drymix mortar

Different chemical admixtures (superplasticizers, accelerators and a water retention agent) were tested in this work. Their chemical structures and further conditions are reported in **paper 6**.

To simulate the prehydration of a drymix mortar, a basic formulation for a self-levelling compound (SLU) based on a ternary binder system (OPC/CAC/CaSO₄) with different admixtures (PCE, casein, retarders) was used. Details about these materials are reported in **paper 7**. **Figure 7** shows the individual anhydrous compounds used in the basic SLU formulation. The SLU mortar was prepared by dry-blending the components in an overhead shaker for 20 min to achieve a homogeneous mix.

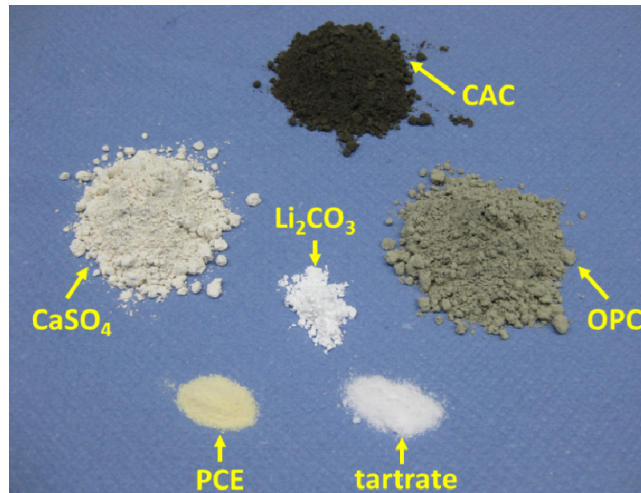


Figure 7: The individual compounds used in the basic SLU formulation

4.2 Exposure of samples to relative humidity

In order to study prehydration of cement and its components under different conditions, several methods of exposure to moisture were used. The main experiments were performed using a water sorption balance instrument and a climate chamber. The method must provide a certain amount of prehydrated material under given storage conditions. **Figure 8** demonstrates that when utilising a sorption balance instrument, only small amounts of prehydrated material (~ 5 to 150 mg) can be obtained, while a climate chamber allows to expose samples on a big scale of several kg.

To minimise the impact of preparation in some investigations such as x-ray diffraction or SEM analysis, samples were exposed directly to the moist environment in the specific sample holders (**Fig. 8**). For the ESEM investigations, samples were exposed *in-situ* to the relative humidity in the chamber of the instrument by adjusting the partial pressure of water vapour and temperature of the ESEM sample holder.

The different exposure methods, their advantages and disadvantages are summarised in the following sections.

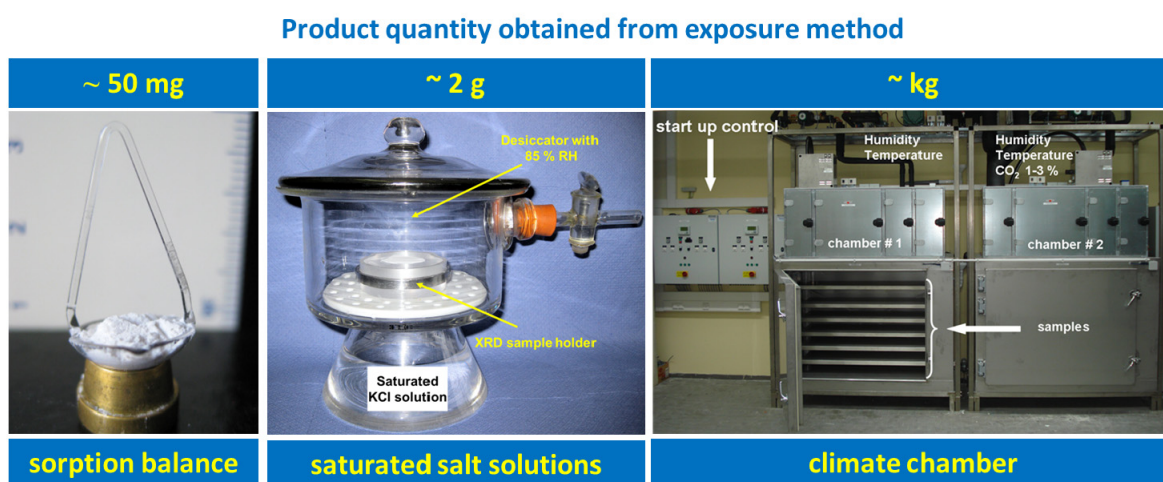


Figure 8: Prehydration of samples using different equipment: powder in the sample pan of a sorption balance instrument (**left**); XRD sample holder with material exposed to water vapour over saturated KCl solution (**middle**); climate chamber with powders stored on plexiglas boards (**right**)

4.2.1 Sorption balance instrument

The sorption balance instrument enables an automatic and relatively quick measurement of sorption and desorption of water vapour for small samples [65]. The moisture uptake can be investigated by different relative humidity programs constructed from RH-steps and RH-ramps [66]. Changes of temperature and relative humidity around a sample can be programmed separately. **Figure 9** illustrates the schematic set up of the instrument and shows images of the tubes with the sample pan in the instrument. Exposure conditions of the samples using the sorption balance instrument are reported in **papers 1 and 4**.

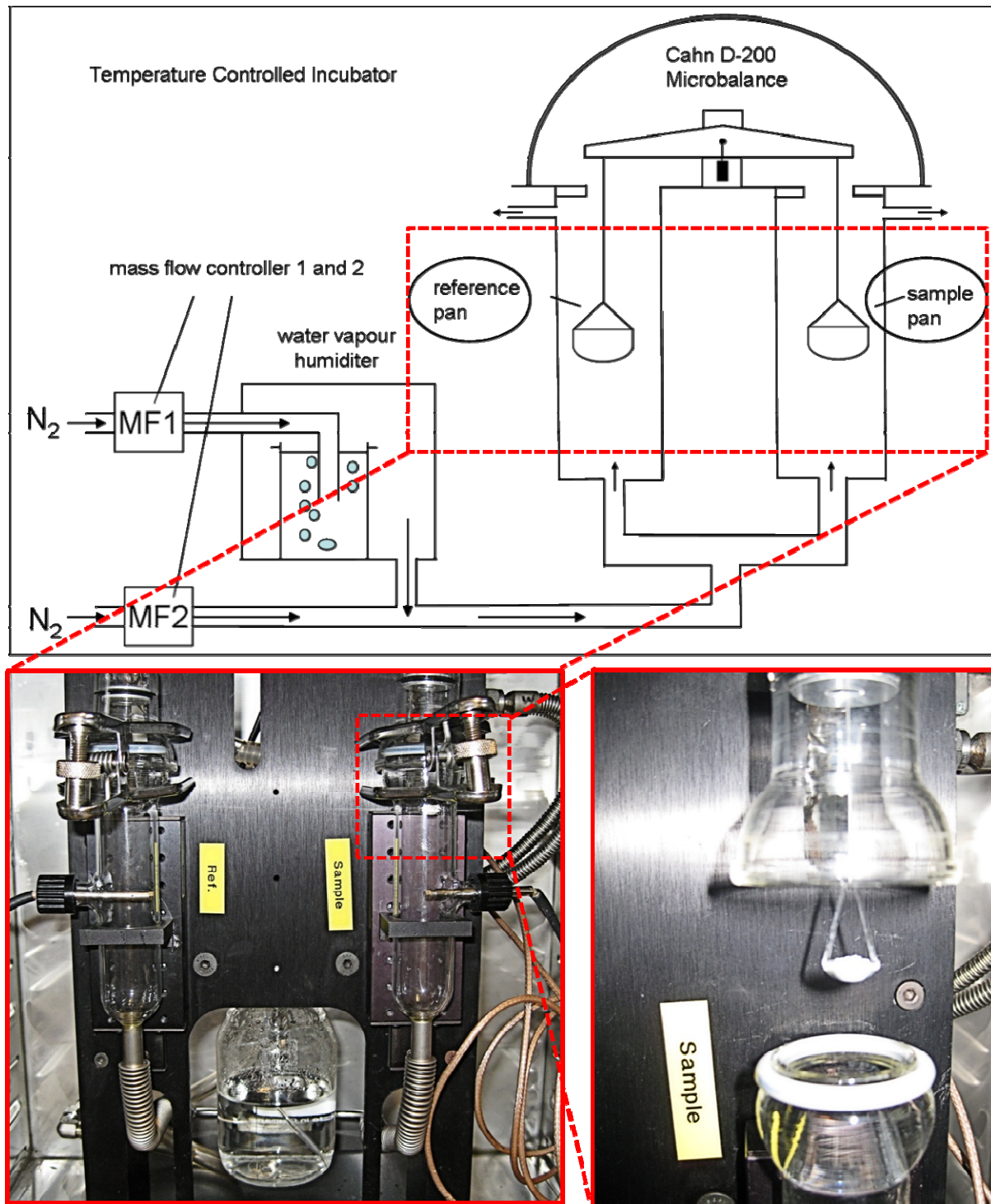


Figure 9: Schematic illustration of a sorption balance instrument (DVS)

A slow, steady flow of mixed dry and water vapour saturated gas passing the relatively small sample ensures that the relative humidity very near the sample surface and in the gas surrounding the sample holder will be almost the same. The flow rate of the moist nitrogen is

rather low, approximately 1 mm/s. This nitrogen flow helps to eliminate surface resistance to moisture leaving or entering the sample, which in turn results in the equilibrium being reached faster.

The sorption balance instrument has the additional advantage that also desorption of water can be studied by decreasing the relative humidity to 1 % only.

Furthermore, the impact of atmospheric CO₂ can be excluded by using nitrogen gas, thus evidencing only the impact of water vapour on the sample during storage.

The disadvantage of the method is that only small samples can be employed in this method, which makes elaborate analytical studies on the exposed samples difficult. A further disadvantage of the method is the limitation of the exposure temperature to a maximum of 40 °C.

4.2.2 Saturated salt solutions

A very convenient method to adjust specific relative humidities is the use of saturated salt solutions [67]. The oversaturated salt solution made up as a slushy mixture from distilled water and chemically pure salt, is typically enclosed in a sealed chamber (desiccator) and the tested material is exposed to the moist gas atmosphere. The storage conditions using this method are described in **paper 4**.

The advantage of this method is that the sample can be exposed to a specific relative humidity on a larger scale. Also, the sample holder can be directly placed into the desiccator which enables further analysis of the sample without impacting the surface (**Figure 8**).

4.2.3 Climate chamber

To produce prehydrated material on a large scale (kg), use of a climate chamber is required. In a climate chamber heated to the required temperature, the samples were spread out on a plastic tray as a thin layer (1 mm) and exposed for different periods of time to air possessing a controlled relative humidity, as is shown in **Figure 10**.

4 Experimental

The major advantage of this method is that the temperature inside the chamber can be increased up to + 100 °C or decreased to - 10 °C. This allows to simulate storage conditions e. g. in a cement silo where the temperature is high, or during transport and storage of cement in winter when the temperature is low.

The major disadvantages are the slow rate of reaching a constant weight (sorption equilibrium), particularly at high relative humidities, and the error introduced in opening and closing the chamber for sampling.

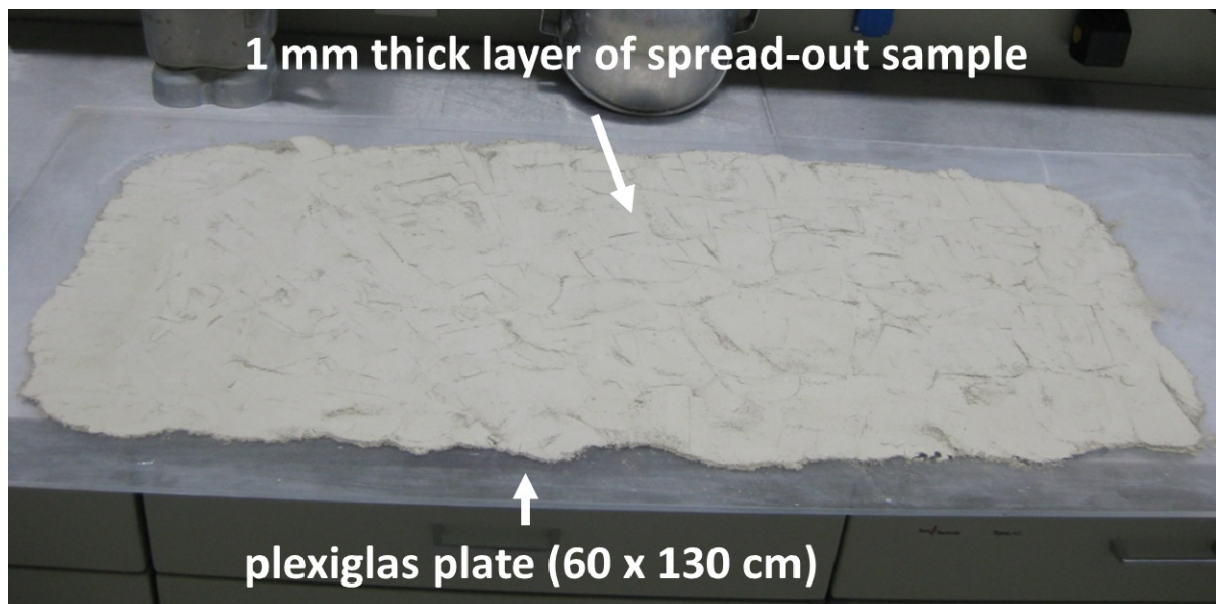


Figure 10: Moisture exposure of the sample in a climate chamber: a thin layer (~ 1 mm) of material is spread out on the plexiglas plate

5 METHODS

This chapter presents an overview of the main methods used in this work. Whereby the focus was placed first on the characterisation of the prehydration products formed on the surface of cement constituents during their exposure to different RH values, followed by the bulk analysis of the prehydrated samples with regards to their conventional hydration after mixing with water. The sample preparation and further details about the measurements performed can be found in the attached publications.

5.1 Surface analysis

Several methods were applied to study the very early interactions of water vapour with individual cement constituents and cement. Prehydration is predominantly a surface reaction, hence common bulk analysis methods are not useful. The main limitations of performing the surface analysis arise from the presence of an only few nanometer thin layer of different hydration products containing amorphous and crystalline products (**Figure 11**).

Thus, the surface analysis requires the use of complementary techniques. In this thesis, the following surface characterisation methods were applied: x-ray diffraction (XRD), x-ray photoelectron spectroscopy (XPS), FTIR-ATR spectroscopy, micro-Raman analysis, TOF-SIMS and (E)SEM/ EDX investigations.

Some of those methods are well-established and frequently used in cement chemistry while others (micro-Raman and TOF-SIMS analysis) were introduced as new additional methods. All of them have their advantages and limitations. **Table 4** presents a summary of the changes detected on the surface upon ageing and describes the corresponding analytical method. The basic principles of all methods are summarised in the following.

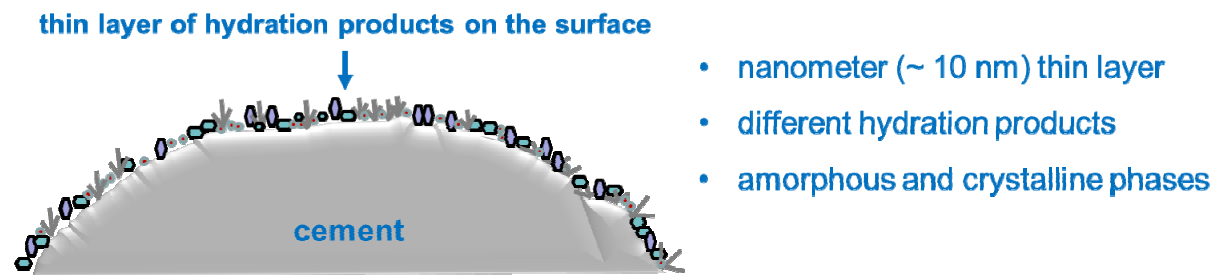


Figure 11: Schematic illustration of a thin layer of hydration products occurring on the surface of a cement particle upon exposure to moist air

Table 4: Methods used to characterise the structural changes on the surfaces of samples exposed to moist air

Method	Structural changes and phases detected
XRD	Excellent for crystalline phases such as ettringite, portlandite, CaCO_3 polymorphs, crystalline C-A-H phases if present in sufficient quantity
XPS	Surface – specific detection of C-S-H and C-A-H phases at the early stage of prehydration; enrichment of special elements on the surface (e.g. sodium)
FTIR-ATR	Changes in the water state: adsorption on the surface or absorption into the bulk
micro-RAMAN	Excellent for detecting very early amorphous CaCO_3 nuclei
TOF-SIMS	Determination of the thickness of the hydration layer (depth profiling)
(E)SEM/ EDX	Morphological changes due to the formation of hydrates, particularly useful for detection of crystalline products with characteristic morphology such as ettringite; observation of amorphous C-S-H gels

5.1.1 X-ray diffraction analysis

X-ray diffraction (XRD) is one of the most important techniques used to identify and quantify the crystalline phases in cement [68]. X-rays are used to produce the diffraction pattern because their wavelength λ is typically within the same order of magnitude (1–100 Å) as the d-spacing between layers in the crystals. This correlation is described by Bragg's equation (Figure 12).

However, the intensity of the diffraction signals strongly depends on the crystallinity of the sample. Amorphous materials are lacking the long-range order in the arrangement of their atoms as compared to the high degree of order observed in well-crystallised substances. As a consequence, amorphous materials give rise to very diffuse and weak diffraction signals, sometimes referred to as 'amorphous humps', e. g. as detected for some C-S-H phases.

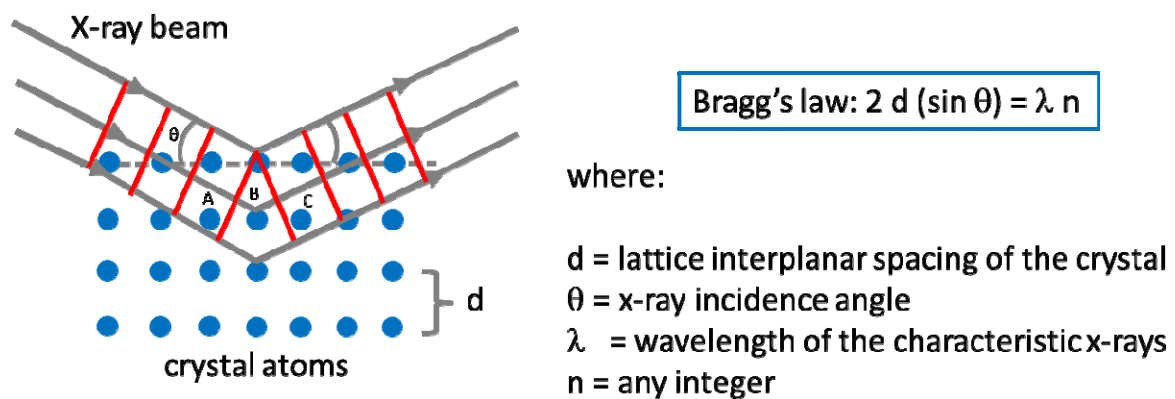


Figure 12: Schematic illustration of the principles of x-ray diffraction (XRD) analysis

5.1.2 X-ray photoelectron spectroscopy

X-ray photoelectron spectroscopy (XPS) can provide information on the composition and speciation of the prehydrated surface, without interference from the unaffected bulk material [69]. In XPS, the sample is irradiated with low-energy x-rays (~1.5 keV) in order to provoke the photoelectric effect, with the energy of the emitted photoelectrons being characteristic of the element from which they are emitted. Slight changes in the bonding environment of a

given element results in changes of the photoelectron spectra. The low energy of the photoelectrons ensures that only those emitted from the surface of the irradiated sample are detected. Consequently, XPS allows the analysis of surface layers with thicknesses of 1 to 12 nm only, with all elements except hydrogen being identifiable. **Figure 13** illustrates the basic principle of the XPS technique. BLACK *et al.* have shown that XPS can be a useful tool in the investigation of pure C₃S and C₂S clinkers after aging. They applied XPS analysis also for the characterization of various fresh and carbonated C-S-H phases [70–72]. More recently, BELLMANN *et al.* used XPS to investigate the surface of C₃S during the induction period [73].

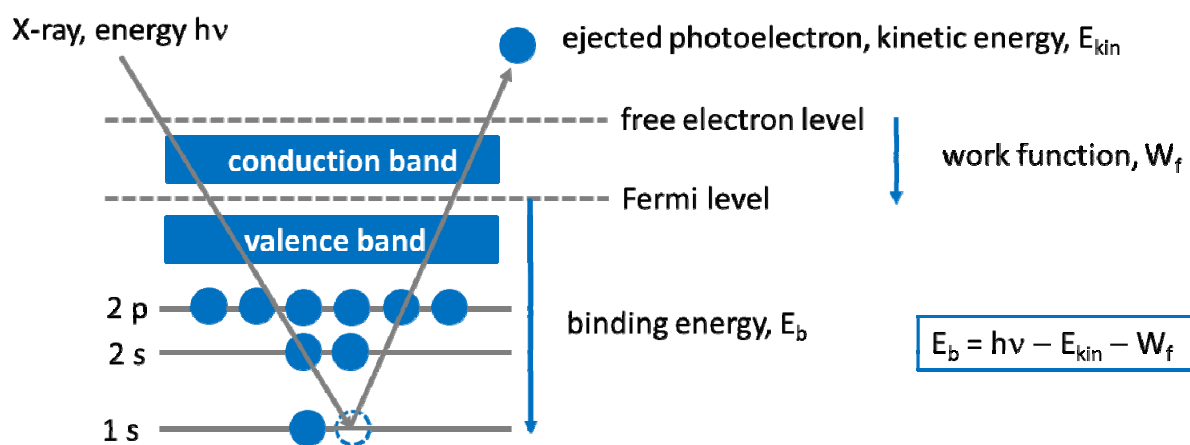


Figure 13: Schematic illustration of the principle of x-ray photoelectron spectroscopy (XPS)

5.1.3 IR spectroscopy and Raman analysis

In infrared spectroscopy, molecules or groups of atoms on large molecules absorb different wavelengths of infrared light as a factor of the constituents present in a molecule or group, the geometry and the immediate surroundings. It can therefore be used to study both crystalline and amorphous samples.

Raman spectroscopy yields similar, but complementary, information. It relies on inelastic scattering of monochromatic light, usually from a laser in the visible, near infrared, or near ultraviolet range. The laser light interacts with molecular vibrations, phonons or other excitations in the system, resulting in the energy of the laser photons being shifted up or down. The shift in energy gives information about the vibrational modes in the system. The

potential of Raman spectroscopy for the characterisation of cementitious materials was demonstrated by BENSTED and a review on this subject has been published recently by BLACK [74, 75].

Attenuated total reflectance (ATR) is a sampling technique used in conjunction with infrared spectroscopy which enables samples to be examined directly in the solid without further preparation [76]. ATR uses a property of total internal reflection called the evanescent wave. A beam of infrared light is passed through the ATR crystal in such a way that it is reflected at least once on the internal surface of the crystal in contact with the sample. This reflection forms the evanescent wave which extends into the sample, typically by a few micrometers (Figure 14).

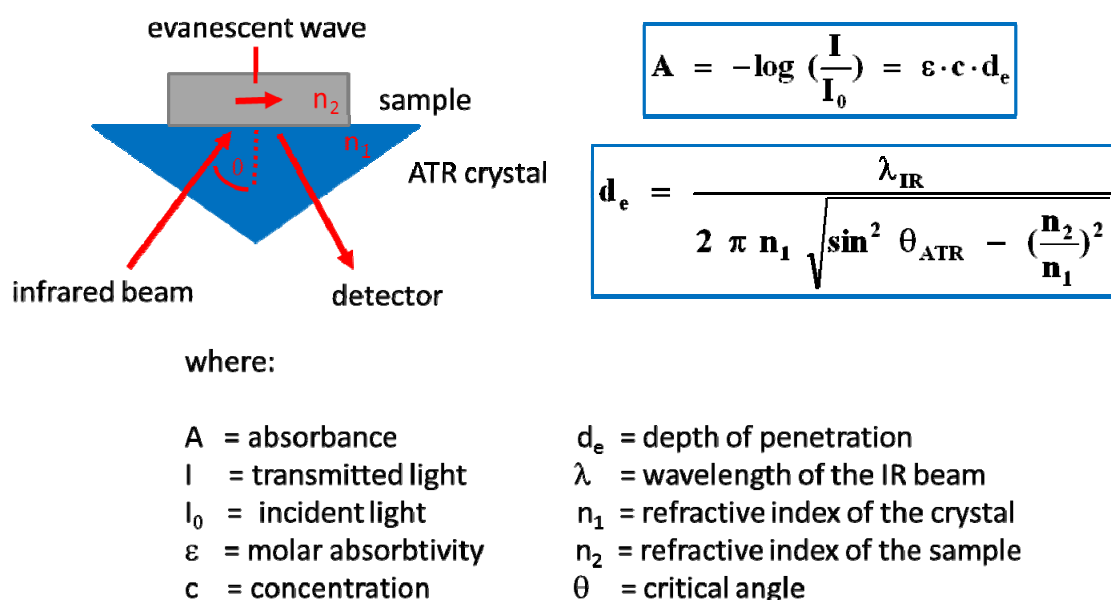


Figure 14: Schematic illustration of the principle of FTIR-ATR spectroscopy

5.1.4 Time-of-flight secondary ion mass spectrometry (TOF-SIMS)

Time-of-flight secondary ion mass spectrometry (TOF-SIMS) is a surface-sensitive analytical method that uses a pulsed primary ion beam (typically Cs or Ga) to desorb and ionize species from a sample surface (Figure 15). The species are removed in atomic monolayers from the surface (secondary ions). The resulting secondary ions are accelerated and transferred to a mass spectrometer, where they are mass analysed by measuring their time-of-flight from the sample surface to the detector [77, 78].

TOF-SIMS can provide an analysis of the chemical composition, imaging for determining the distribution of chemical species, and depth profiling for thin films. However, this method does not produce a quantitative analysis. At best, it is semi-quantitative. In cement chemistry, the first attempt to study the hydration of cement using SIMS was performed by GERHARD [79]. More recently, TOF-SIMS was applied to study the chemical distribution of elements on the surfaces of hydrated clinkers, with and without deposition of superplasticizers [80].

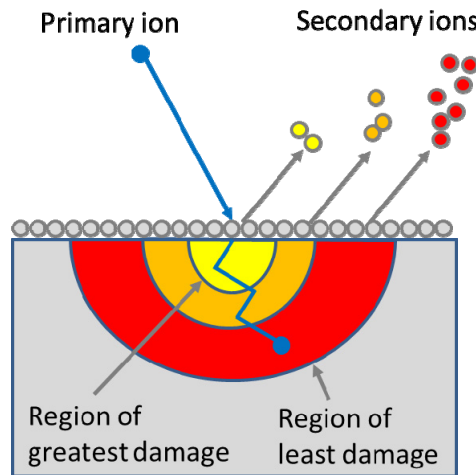


Figure 15: Schematic illustration of the principle of time-of-flight secondary ion mass spectrometry (TOF-SIMS)

5.1.5 Scanning electron microscopy

The use of scanning electron microscopy can provide information about the microstructure of pure cement clinker phases and industrial cements after exposure to moisture. Environmental scanning electron microscopy (ESEM) operates under a low water vapour pressure and is an ideal technique for studying the effects of a controlled humidity environment. It enables to follow the structural changes accompanying cement hydration at the micron level and, through energy-dispersive x-ray analysis (EDX), gives complementary information on the local chemical composition [81]. **Figure 16** exhibits a SEM micrograph obtained from a prehydrated C_3A (stored for 3 days at 80 °C and 80 % RH). Well-formed calcite ($CaCO_3$) crystals with a size of $\sim 2 - 5 \mu m$ are visible, while amorphous gibbsite $Al(OH)_3$ can be detected by using EDX elemental analysis.

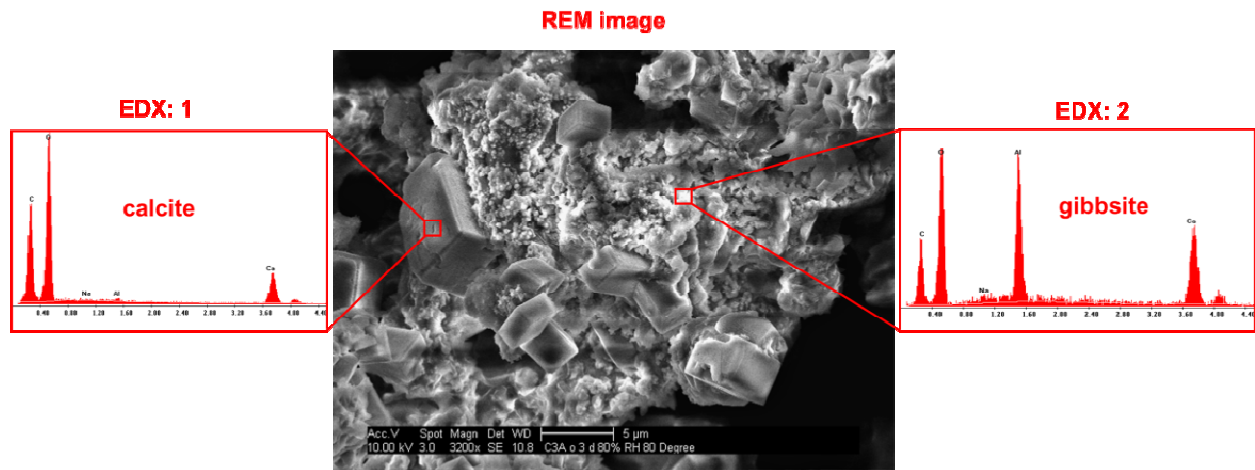


Figure 16: SEM micrograph of prehydrated C₃A; indicated are two EDX spots confirming the formation of crystalline calcite and amorphous gibbsite

5.2 Bulk analysis

To study the impact of prehydration on the bulk properties of cement, isothermal calorimetry and *in-situ* XRD analysis were combined to correlate the changes in cement phases with the rates of chemical reactions occurring during the first 48 h of cement hydration.

Isothermal calorimetry tracks the kinetics of cement hydration as a function of heat released. Results of isothermal calorimetry typically consist of a data set providing the instantaneous heat evolution rate versus time. These raw data can be integrated to obtain a curve for the cumulative heat release versus time. The advantage of this technique is that the hydration process can be followed continuously *in-situ* without stopping the hydration process. The disadvantage is that only the overall heat evolution can be measured which is the sum of the heat evolved by all the reactions occurring at any particular time.

To overcome this disadvantage, *in-situ* XRD can be applied. Using this technique, individual hydration reactions from dissolution of clinker phases as well as formation of hydrate phases such as e. g. ettringite or portlandite can be observed. **Figure 17** demonstrates a typical rate of heat evolution for a cement hydrated for 48 hours and the corresponding *in-situ* XRD patterns. The calorimetric curve indicates the acceleration period of the hydration process occurring after about 3 hours, which correlates well with the initiation of the silicate hydration

observed from the formation of portlandite in the *in-situ* XRD. Furthermore, formation of ettringite can be observed after dissolution of gypsum within the first 2.5 hours of hydration.

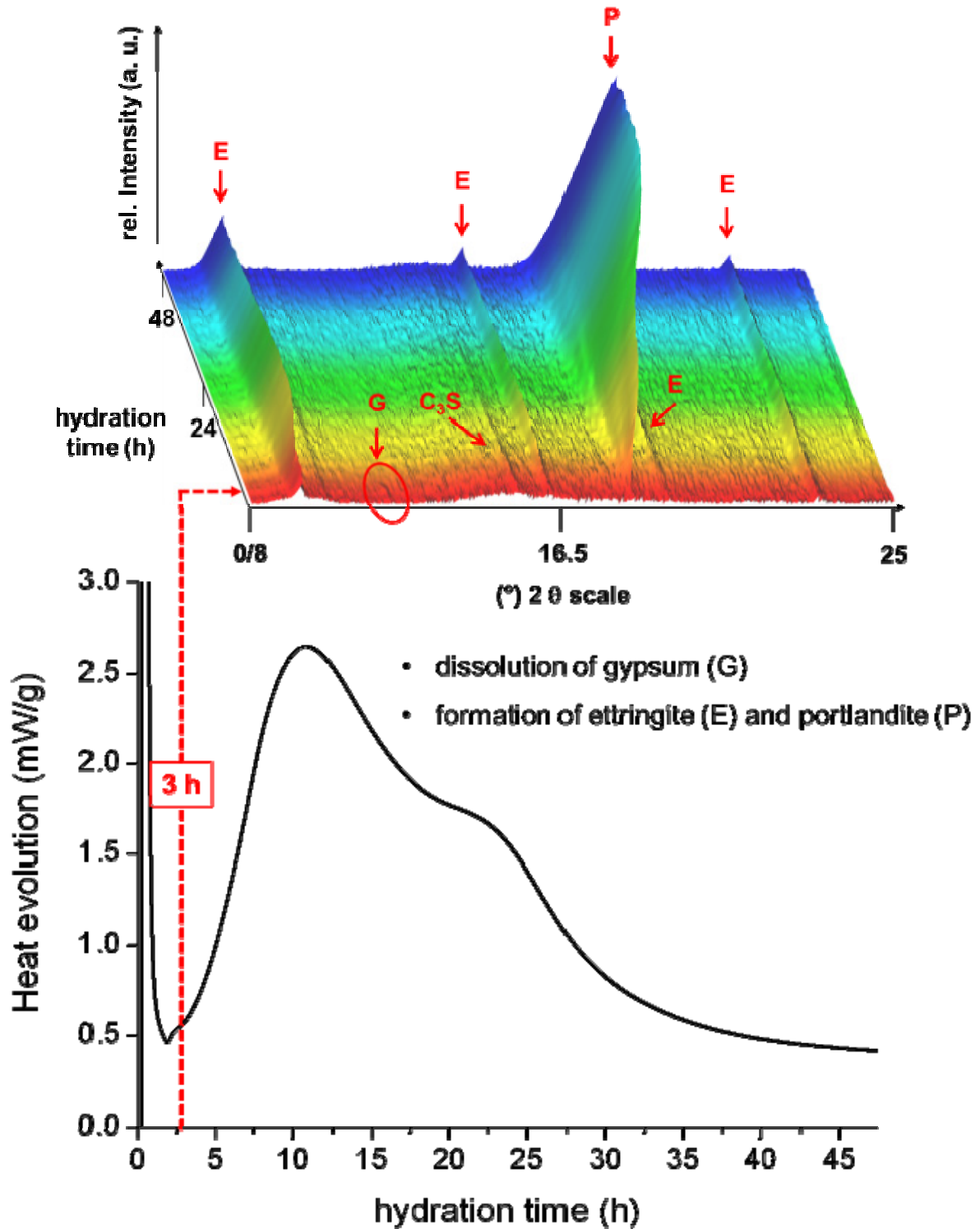


Figure 17: Isothermal calorimetric curve and corresponding *in-situ* XRD patterns of a CEM I 52.5 N, measured during the first 48 h of hydration at $w/c = 0.5$

5.3 Interactions with admixtures

Several methods were applied to characterise the interactions of Portland cement with various admixtures. The main methods used in this work can be summarised as follows:

- Rheology (mini slump test)
- Adsorption (TOC)
- Zeta potential
- Calorimetry
- *In-situ* XRD

First, investigations on a simplified system containing cubic C₃A and calcium sulphate hemihydrate in presence of β -naphthalene sulfonate formaldehyde (BNS) were performed. Second, the behavior of a prehydrated industrial cement in the presence of different admixtures was studied. The third project was to study a basic dry mix mortar formulation containing different chemical admixtures.

Rheological measurements (mini slump test) were performed to test the fluidity (workability) of different pastes, to determine the water demand of the system and to quantify the dispersing effect of superplasticizers as specified in the modified DIN EN 1015-3 test using a Vicat cone (height: 2.5 cm, internal diameter: 1.3 cm) [82]. Flowability of cement paste over time was measured according to EN 12706 [83]. A detailed elaboration of the procedural method can be found in **papers 6 and 7**.

Adsorption isotherms were collected to determine the amount of admixtures adsorbed on solid particles contained in the aqueous slurries of the materials tested. Adsorption was calculated using the depletion method. For this purpose, the concentration of admixture present in the mixing water before contact with the clinker or cement, and the non-adsorbed portion of the admixture remaining in solution was determined. Admixture content in the filtrate was measured by total organic content (TOC) analysis using combustion at 890 °C in a High TOC II instrument (Elementar, Hanau, Germany). Filtrate was recovered by centrifugation of the slurry for 10 min at 8500 rpm, then filtered through a 0.45 μ m Nylon filter by pressure filtration and stabilized by addition of 5 mL of 0.1 mol/L hydrochloric acid to 1 mL of filtrate. The percentage of admixture adsorbed on clinker or cement was calculated from the TOC

content using a reference admixture solution of known concentration. Further information on the preparation of the slurries can be found in **paper 6**.

The surface charges on the pastes prepared from fresh and aged cements were determined by zeta potential measurement (DT 1200 from Dispersion Technology Inc., Bedford Hills, USA) in distilled water after 4 and 20 minutes of hydration. The zeta potential instrument measures a vibration current induced by an acoustic wave which causes the aqueous phase to move relative to the cement particles. From that, a potential difference which can be measured is designated as zeta potential [84, 85].

Calorimetric measurements and *in-situ* XRD analysis for samples containing chemical admixtures were recorded in the same matter as described in chapter **5.2**.

6 RESULTS AND DISCUSSIONS

The main findings from all publications developed within this thesis are presented in this chapter. They are ordered according to their topics. Results of this research work which have not yet been published are summarised in the last sub-chapter.

6.1 Sorption balance study on anhydrous cement minerals - paper 1

A sorption balance study of water vapour sorption on anhydrous cement minerals and cement constituents is presented in **paper 1**.

The experiments were conducted to gain an understanding of the principle effects on individual cement clinker phases (monoclinic C_3S , monoclinic β - C_2S , cubic and orthorhombic C_3A and orthorhombic C_4AF) as well as of different sulphates ($CaSO_4$, β - $CaSO_4 \cdot \frac{1}{2} H_2O$, $CaSO_4 \cdot 2 H_2O$) and of free lime (CaO) after storage in moist environment.

In this investigation, the RH levels at which prehydration of the cement constituents starts to occur, and the amount of water sorbed per unit area of cement component surface were determined.

Figure 18 summarises the RH values at which the uptake of water begins (the “on-set points”) as obtained from the mass change profiles for all cement constituents tested.

The experiments demonstrated that among all cement components, CaO and orthorhombic C_3A are the ones which start to sorb water at particularly low RH values (< 55 %). Additionally, they sorb the highest amounts of water. Cubic C_3A and C_4AF follow next while C_3S and C_2S , the main clinker constituents, are the least reactive phases (**Figure 19**).

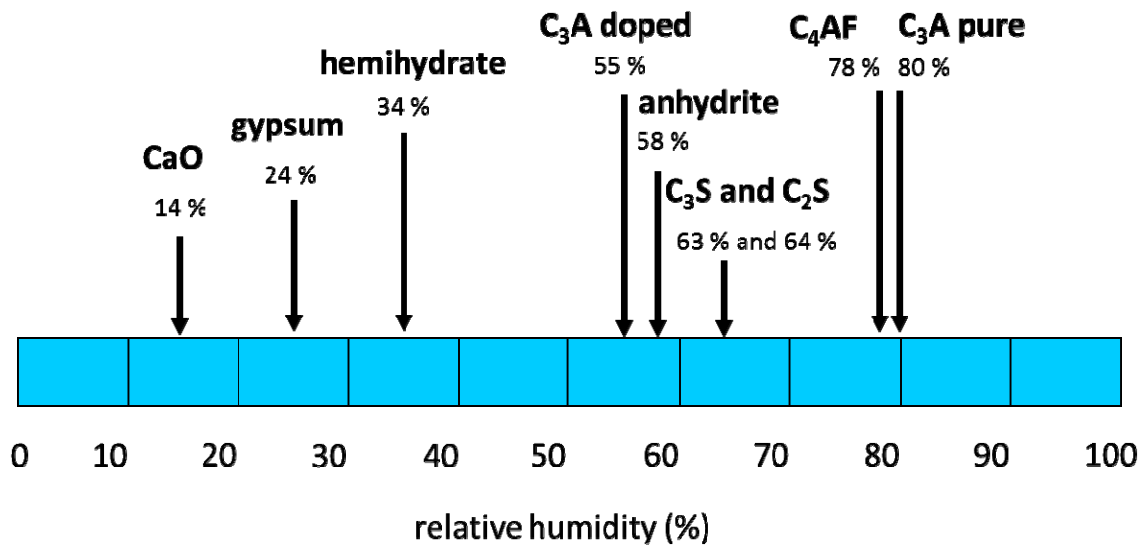


Figure 18: Threshold values of relative humidity at which individual cement constituents start to sorb water, measured on a sorption balance instrument at 20 °C using the ramp mode

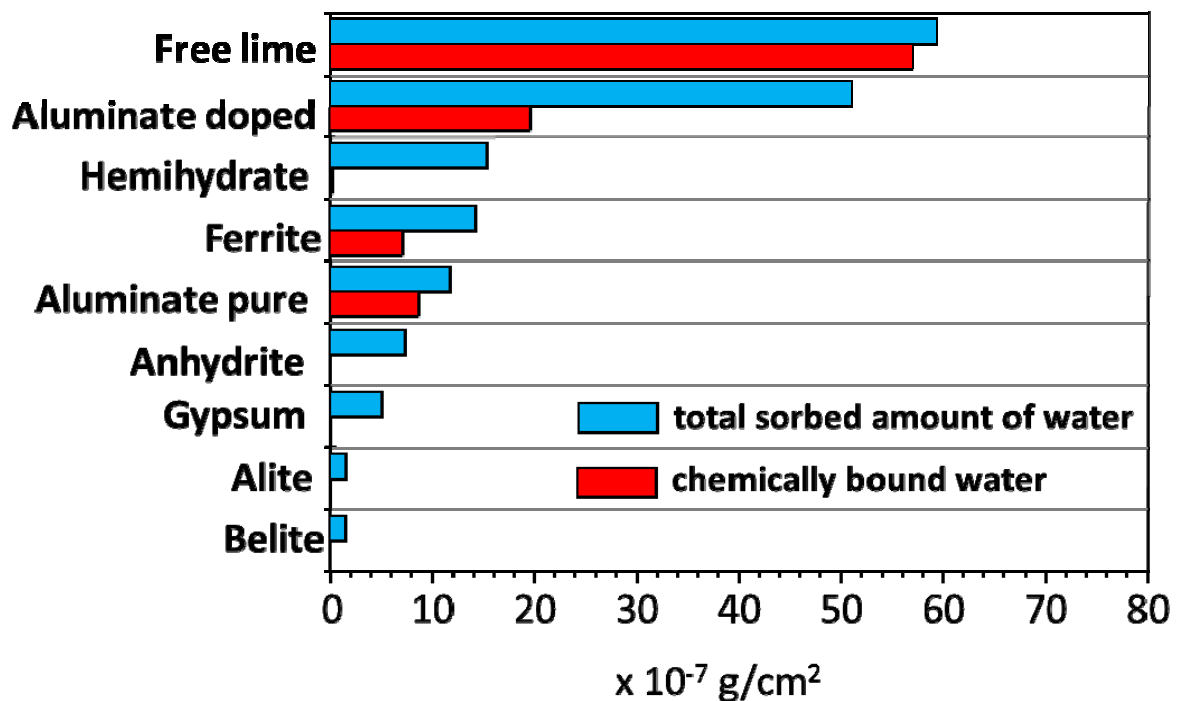


Figure 19: Comparison of relative amounts of water sorbed per unit of specific surface area for different cement constituents, tested in ramp mode at 20 °C

Emphasis was placed on understanding the ratio between physically and chemically sorbed water, and the reversibility of this process. Three different kinds of water uptake were observed:

- Water vapour is mostly sorbed chemically; the water is bound irreversibly to the phase and cannot be removed by drying for 1 h at 1 % RH and 20 °C. An example for this behaviour is free lime (CaO).
- Water vapour is sorbed both chemically and physically; the physically sorbed part of water is removed by drying at 1 % RH; whereas, the chemically sorbed part cannot be removed by drying. This behaviour is represented for example by orthorhombic C₃A.
- Water vapour is mostly sorbed physically and can be removed almost completely by drying at 1 % RH. Such behaviour is exemplified by β -CaSO₄ · ½ H₂O or the silicates C₃S and C₂S.

For all samples, the moisture sorption capacity profiles were also measured at 40 °C to elucidate the effect of temperature on water vapour sorption. Comparison of the sorption profiles obtained at 20 °C and 40 °C, respectively, indicates that increased temperature shifts the on-set point where water sorption begins to occur to lower RHs. Additionally, increasing the temperature also led to a significantly higher water uptake as is shown in **Figure 20**. This phenomenon can be explained by the different values of absolute humidity existing in the gas phase at different temperatures.

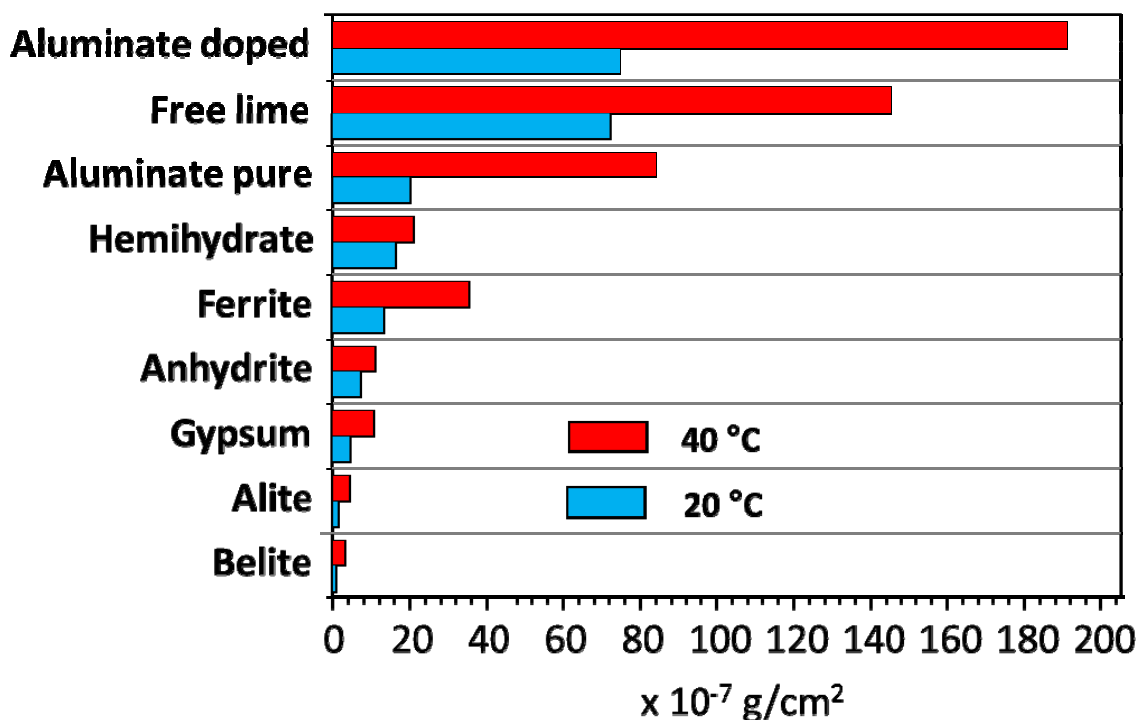


Figure 20: Temperature-dependent mass changes for samples, tested in step and down mode at 20 °C and 40 °C, respectively

6.2 X-ray photoelectron spectroscopic study on C₃A polymorphs - paper 2

In the **papers 1** it was demonstrated that of all the cement clinker phases, CaO and C₃A react preferably with water vapour when cement is prehydrated. However, the cubic and orthorhombic C₃A polymorphs exhibit different behaviours when exposed to water vapour. For orthorhombic C₃A, the onset point at which water sorption starts to occur was found to lie at 55 % RH, compared to 80 % RH for cubic C₃A.

In [57], distinct differences were noticed between the XPS spectra of cubic and orthorhombic C₃A prehydrated in moist air (85 % RH) for just 1 h. Here, emphasis was placed on separation of the effects caused by water vapour and carbon dioxide. Therefore, in this study, the impact of initial exposure of cubic and orthorhombic C₃A to moisture, followed by interaction with atmospheric CO₂, was investigated by XPS.

From the results presented in **paper 2** it was aimed to understand why when prehydrated in air, orthorhombic C_3A is more sensitive to moisture than cubic C_3A .

In the absence of CO_2 , both C_3A polymorphs showed the formation of C_4AH_{13} on their surfaces, but the extent was more pronounced for the orthorhombic modification. Surface enrichment of sodium, in the form of sodium hydroxide, was evident after prehydration of orthorhombic C_3A which was doped with 4 wt. % of Na_2O (**Figure 21 a**). The increased pH induced by the separation of NaOH on the surface may account for the increased rate of reaction.

Exposure to ambient air containing CO_2 led to further changes in the Na 1s spectra (**Figure 21 a**), namely a large growth in intensity and a slight shift back to lower binding energies, with the signal centred at 1071.3 eV. Such binding energy corresponds to either Na_2CO_3 or $NaHCO_3$, both of which produce a peak at 1071.3 eV [86]. This finding suggests that the initially formed NaOH then carbonated to form Na_2CO_3 which constitutes the final product from the prehydration and carbonation process.

Accordingly, prehydrated cubic C_3A produced only monocarbo aluminate ($3 CaO \cdot Al_2O_3 \cdot CaCO_3 \cdot 11 H_2O$) on its surface, while carbonation of orthorhombic C_3A resulted in significant Na_2CO_3 formation besides monocarbo aluminate. This explains why orthorhombic C_3A undergoes increased carbonation, compared to its cubic counterpart (**Figure 21 b**).

The formation of surface Na_2CO_3 on orthorhombic C_3A was confirmed by SEM imaging (**Figure 22**). After exposure to air, bright crystalline specks which were identified by EDX as Na_2CO_3 were visible on the surface of sample.

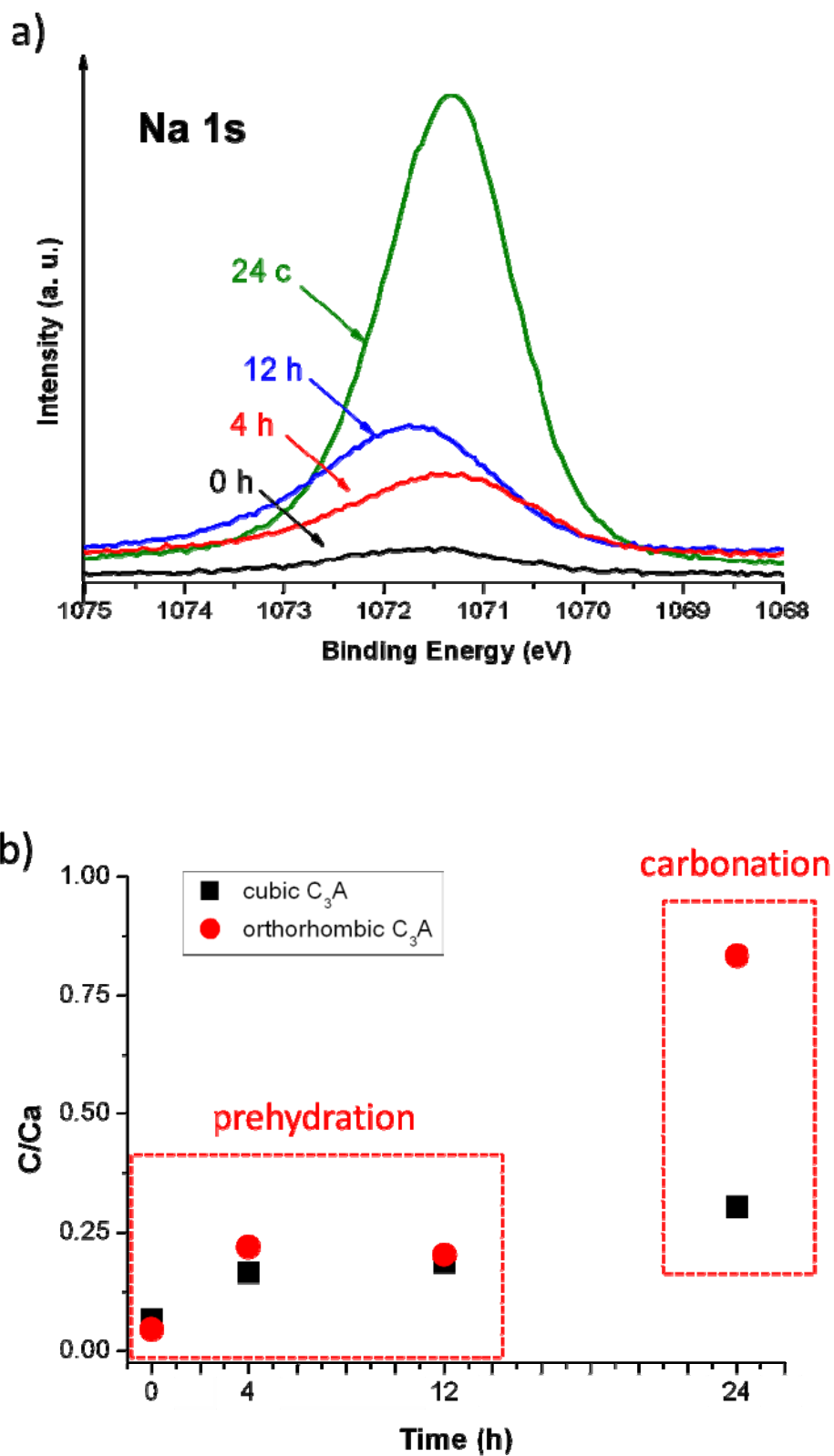


Figure 21: Na 1s XPS spectra of fresh and aged orthorhombic C₃A sample (a) and normalised elemental ratios of C/Ca occurring on the surfaces of cubic and orthorhombic C₃A as a function of ageing period and mode, as measured by XPS (b)

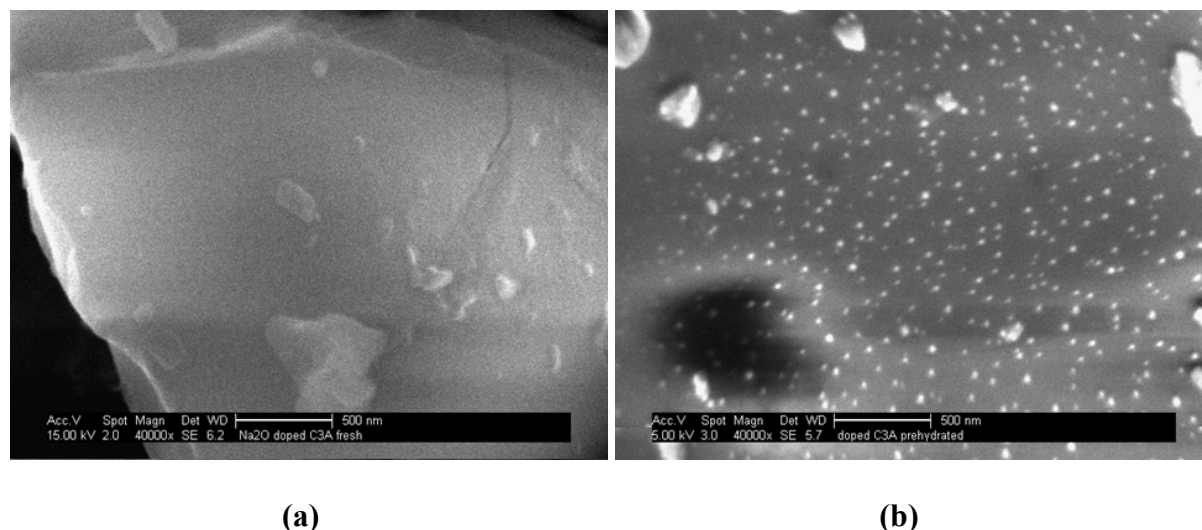


Figure 22: SEM images of the surfaces of fresh (a) and 24 hrs prehydrated and carbonated orthorhombic C₃A (b) showing Na₂CO₃ crystals on the prehydrated sample

6.3 Raman spectroscopic study on CaO - paper 3

At 20 °C, among all cement components free lime (CaO) showed the lowest threshold value for water sorption of ~ 14 % RH only. Also, CaO can sorb large quantities of water which are chemically bound (**paper 1**). This pronounced ability of CaO to bind atmospheric moisture quickly and irreversibly may possibly reduce or even prevent the prehydration of other clinker constituents when cement is exposed to moisture. Therefore, information on the reaction of CaO, or its subsequently formed hydrate, Ca(OH)₂ with moist air can provide insight into the behaviour of industrial cements and for example their storage history.

The aim of this study, reported in **paper 3**, was to simulate storage conditions for CaO (80 °C and relative humidities between 10 and 80 %) which can occur in the cement silo and to investigate the impact of those conditions on the reaction of CaO with atmospheric water and CO₂. Special attention was given to the amount and type of CaCO₃ polymorphs formed during exposure to moist air. The combination of micro-Raman spectroscopy, x-ray diffraction analysis and SEM imaging allowed tracking of the changes occurring on the surface of CaO exposed to moist air at 80 °C.

After exposure to low RH, total conversion of CaO to Ca(OH)₂ was observed. Subsequently, initially formed Ca(OH)₂ underwent partial carbonation into amorphous calcium carbonate.

6 Results and discussions

At low humidities (10 – 20 % RH), this reaction was observed only by Raman spectroscopy and not by x-ray diffraction. Exposure to higher relative humidities (> 40 %) led to the formation of crystalline calcium carbonates which were x-ray detectable. At this RH (40 %), the three different calcium carbonate polymorphs (calcite, aragonite and vaterite) co-exist while at increasing RH, calcite becomes increasingly prevalent (**Figure 23**). Exposure to different RH levels also impacts the crystal sizes of the reaction products, with larger crystals produced at higher RHs.

The results confirm the potential of Raman spectroscopy in the study of the hydration behaviour of minor cement constituents, particularly when amorphous products are involved in the reaction processes.

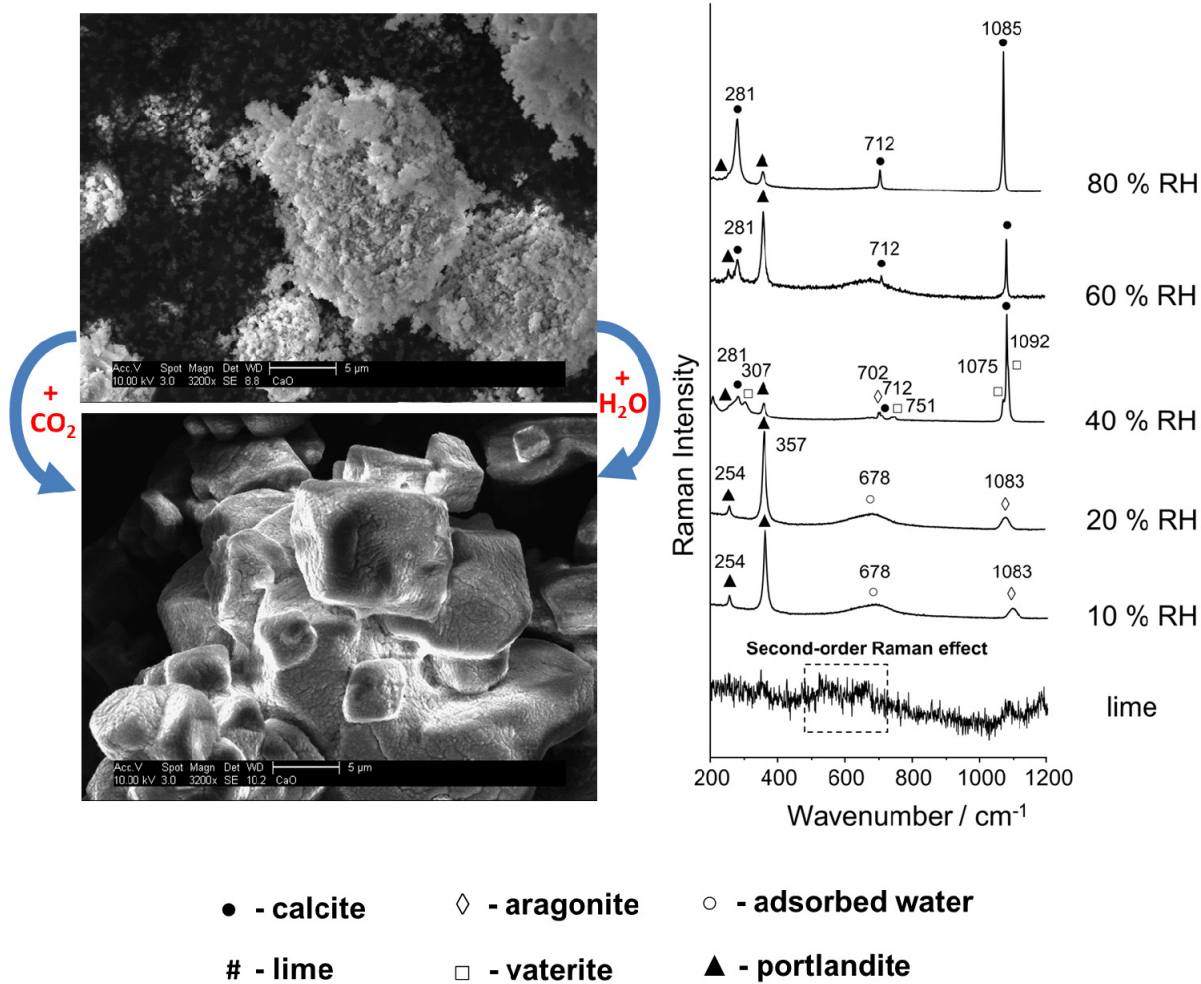


Figure 23: SEM images and micro-Raman spectra of freshly calcined and prehydrated CaO showing the formation of different hydration and carbonation products

6.4 Sorption balance study on binary mixtures - paper 4

The studies on prehydration of individual cement constituents presented before does not account for interactions between different phases which can take place during prehydration of actual cements. Therefore, in **paper 4** specific water sorption experiments were performed to gain an understanding of the principle interactions occurring during prehydration between the C_3A polymorphs in the absence and presence of calcium sulphate hemihydrate.

The objective of this study was to demonstrate the effect which water vapour may have on the different C_3A polymorphs in the presence of sulphate, and to provide insight into the mechanism of a potential interaction by using dynamic and static water vapour sorption methods.

In the presence of calcium sulphate hemihydrate, ettringite (AF_t phase) was observed as the predominant prehydration product for both C_3A modifications. This signifies that an ion transport had occurred between C_3A and sulphate. ESEM imaging also revealed that in a moist atmosphere, a liquid water film condenses on the surfaces of the phases as a consequence of capillary condensation between the particles. C_3A and sulphate can then dissolve and react with each other. Similar water films were also directly observed in the ESEM chamber when C_3A polymorphs were exposed to high RH levels ($> 80\%$) without hemihydrate, as is shown in **Figure 24**.

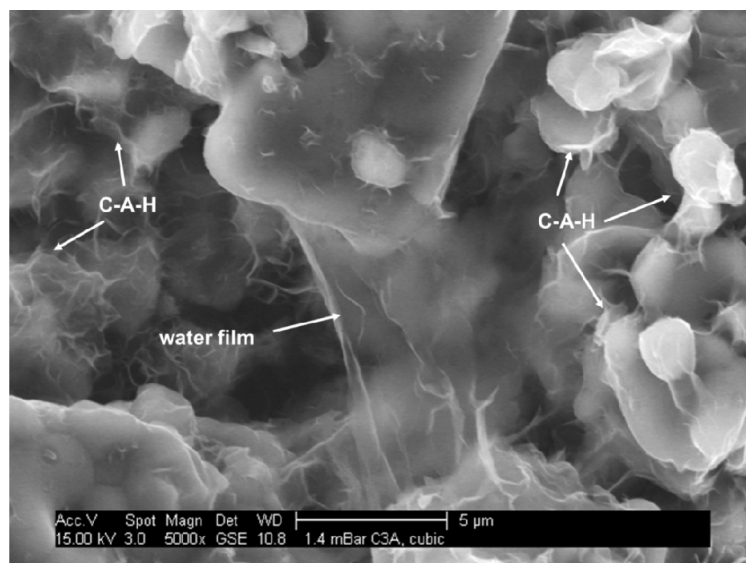


Figure 24: ESEM image of cubic C_3A , prehydrated for 30 min in the ESEM chamber at 4.5 °C and 85 % RH, exhibiting a film of condensed liquid water between the particles

Obviously, prehydration not only involves surface interaction with gaseous water molecules; but also capillary condensation between C_3A particles, thus allowing C_3A and sulphate to react according to the well-known clinker dissolution/oversaturation/precipitation scheme observed for conventional cement hydration. This finding is of fundamental importance because it signifies that during prehydration, similar hydrates are formed as during normal cement hydration when cement is mixed with water, although the morphology might be dependent on the conditions (chemical potential of water, temperature and duration of exposure to RH). Ettringite crystals were shorter when RH was lower, and longer and thicker when RH increased (**Figure 25**).

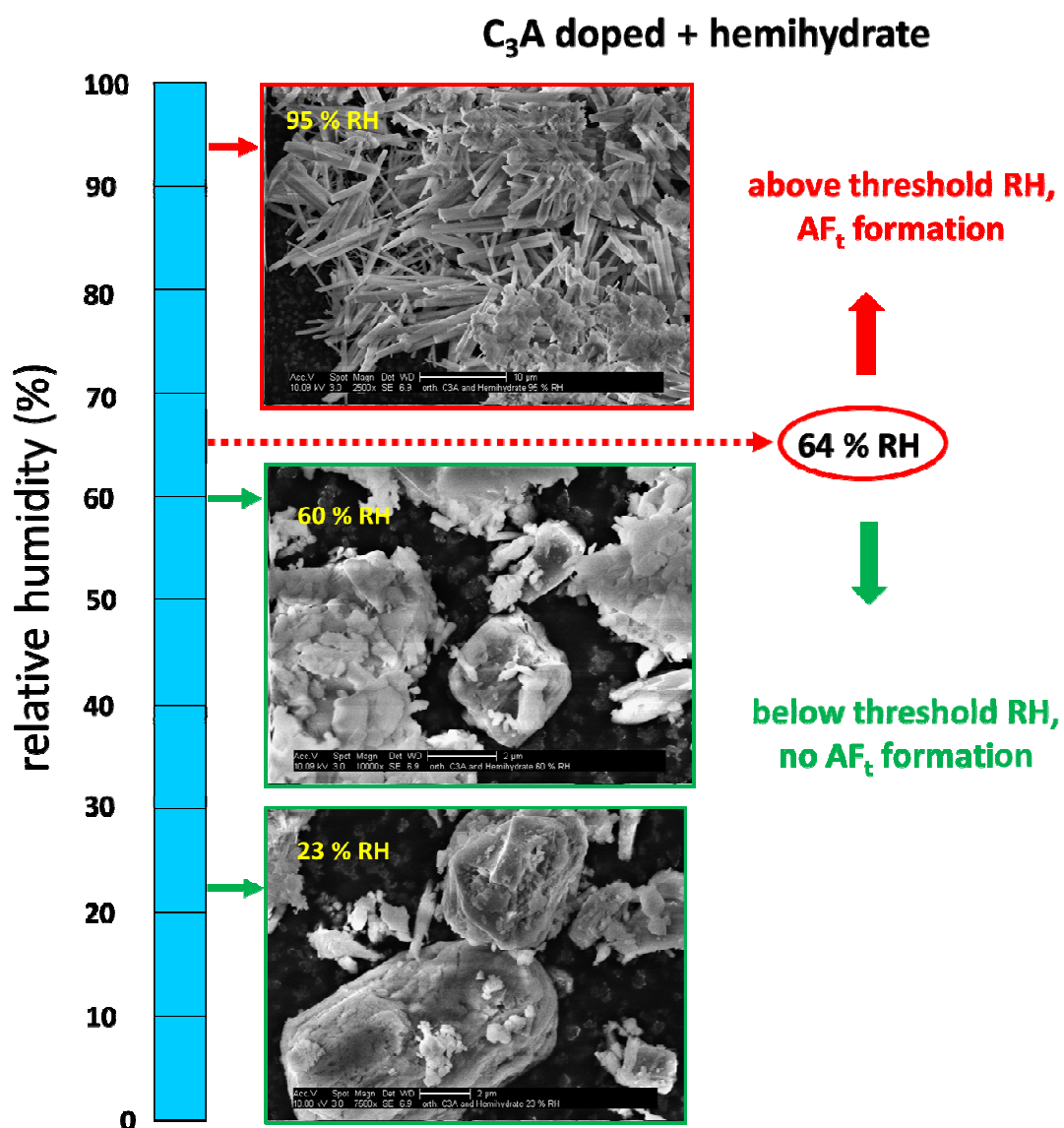


Figure 25: SEM images of orthorhombic C_3A prehydrated below and above the threshold value of 64 % RH in the presence of hemihydrate for 21 days at 20 °C and at different RH levels

Below 70 % RH, cubic C₃A did not react with calcium sulphate hemihydrate; while orthorhombic C₃A formed ettringite crystals already beginning at 64 % RH. Below these threshold values no chemical reaction occurs between C₃A and hemihydrate, thus the mixtures sorb minimal amounts of moisture on their surfaces, possibly by hydrogen bonding, but no ettringite was found in the samples as presented in **Figure 25** for the binary mixture containing orthorhombic C₃A and hemihydrate.

6.5 The effects of prehydration on the adsorption of BNS superplasticizer - paper 5

Based on the results reported in **paper 4**, the cumulative amount of water sorbed by the individual phases was compared with that of the binary mixture. Furthermore, the RH value at which the ettringite (AF_t) phase starts to appear in large amounts was determined.

In the second part of **paper 5** it was investigated how ettringite formed during the prehydration can affect the adsorption and dispersing power of a BNS superplasticizer. For this experiment, a binary mixture of cubic C₃A and calcium sulphate hemihydrate was prehydrated for 48 hours below and above its onset point of 70 % RH. Subsequently, adsorption of BNS superplasticizer on the prehydrated mixture was determined.

The results implied that the formation of ettringite which occurs above the threshold value can influence the adsorption of the BNS superplasticizer. A noticeably (20 %) higher adsorbed amount of BNS superplasticizer than for the non-prehydrated binary mixture was observed. Whereas, prehydration of the binary mixture below the onset point does not much affect BNS adsorption. There, no ettringite was found. However, it must be noted that ettringite formation influenced the adsorption of BNS only at such dosages (> 1.5 by weight of the binary mixture) which are above typical application additions of 0.1 – 1 wt. %. These findings are schematically summarised in **Figure 26**.

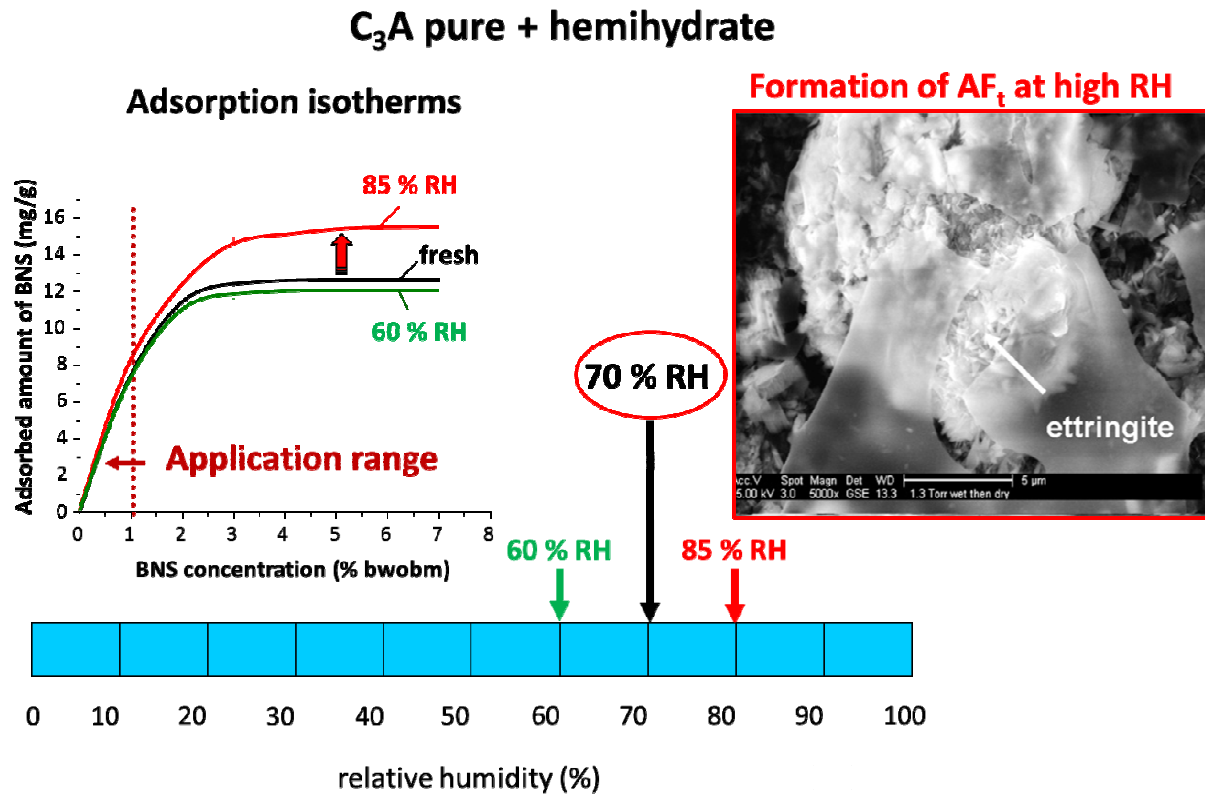


Figure 26: Adsorption isotherms for BNS added to a binary mixture of cubic C₃A and β-hemihydrate (w/bm = 5) prehydrated below and above the threshold value of 70 % RH: fresh (black); prehydrated at 60 % RH (green); prehydrated at 85 % RH (red); ESEM image of the binary mixture, exposed to moist air for 90 min in the ESEM chamber at 4.5 °C and 85 % RH, showing ettringite formation and water films on the surface of cubic C₃A

The results presented in **paper 5** demonstrate that prehydration of cubic C₃A in the presence of calcium sulphate hemihydrate may affect the dosage levels of superplasticizers in concrete or mortar. Consequently, owed to the nano crystallinity of ettringite formed during prehydration and its associated huge specific surface area, exposure of cements containing high amounts of C₃A to moisture may result in higher consumption of superplasticizer. Understanding of the conditions leading to the formation of nano-sized cement hydrates during cement manufacturing and storage may help to prevent the unwanted effects of prehydration on admixture performance.

6.6 The effects of prehydration on the performance of chemical admixtures - paper 6

The aim of this study which is presented in **paper 6** was to obtain a broader view of the influence of prehydration on the interaction of aged cement with chemical admixtures.

For this purpose, CEM I 52.5 N was exposed at 35 °C to moist air (90 % RH) for 1 and 3 days. These conditions were chosen to simulate the uptake of moisture over an extended period of time at lower humidities and therefore provide an accelerated time scale.

Three superplasticizers (NSF, PCE and casein), a water-retention agent (MHEC) and two accelerators (Ca formate and amorphous Al_2O_3) were investigated as chemical admixtures. All admixtures used were commercial products to ensure practical relevance.

The results presented here show that the uptake of moisture and the carbonation can cause a significant change in the flow, water retention and setting behaviour patterns of mortar or concrete. Both the specific surface area and the surface charge of a cement are changed as a result of partial surface hydration, which has a substantial effect on the interaction with admixtures. The following correlations were found:

- The effectiveness of superplasticizers in prehydrated cement is generally less than in fresh cement. The dispersing power of the biopolymer-based superplasticizer casein is less strongly affected by moist storage, while polycarboxylates and NSF are severely affected as is presented in **Figure 27**.
- Aged cement exhibits a significantly improved water retention capacity with, at the same time, a higher water demand to achieve suitable workability required in application. Therefore, prehydrated cement requires a lower dosage of methylcellulose to reach a high water retention.
- In aged cement, effectiveness of set accelerators (Ca formate and amorphous Al_2O_3) is significantly decreased. When cement was exposed to moisture for 3 d, they can even turn into a retarder.

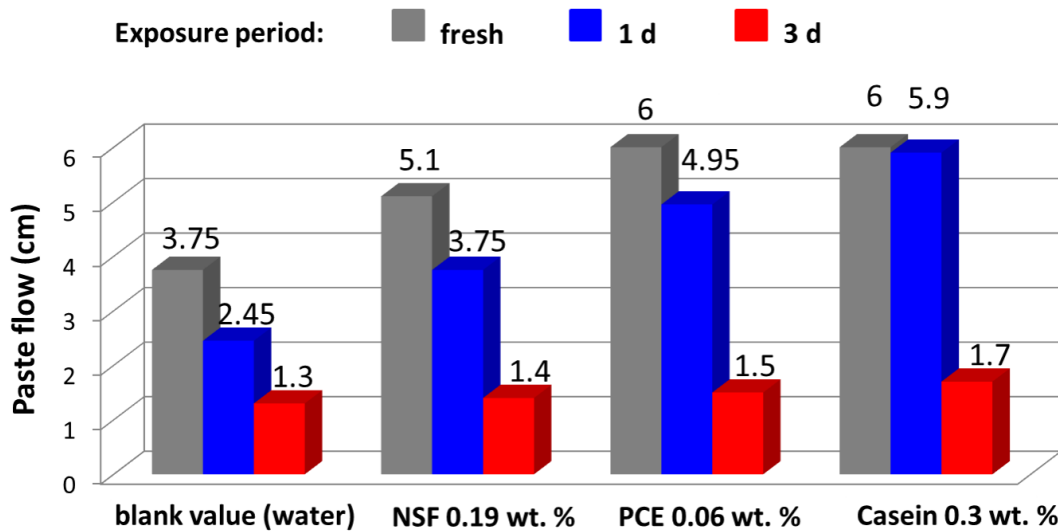


Figure 27: Flow spreads of cement pastes ($w/c = 0.55$) made from fresh (grey) and prehydrated CEM I 52.5 N with and without superplasticizers (blue: storage time 1 d; red: 3 d)

Therefore, Portland cement that was exposed for an extended period of time to moist air can exhibit significantly changed behaviour in combination with admixtures. The effects of this partial surface hydration can be both positive and negative with respect to the behaviour of superplasticizers, although the detrimental effects are more prevalent (**Figure 27**).

6.7 The effects of prehydration on the performance of drymix mortars - paper 7

In **paper 7**, the impact of prehydration on the performance of retarders and of casein superplasticizer in a SLU formulation based on a ternary binder system containing OPC, calcium aluminate cement (CAC) and calcium sulphate was studied. This system was chosen as an example for a very common dry mix mortar formulation.

In the experiments, a basic SLU formulation without retarder was exposed at 35 °C to moist air (90 % RH) for 1 and 3 days and characterised. Afterwards, the aged SLU mortar was formulated with tartrate or citrate retarder and their effectiveness in such prehydrated formulation was studied. In a parallel experiment, a SLU formulation containing casein as

superplasticizer was exposed to moist air, and the effects of this ageing on the flow properties of the mortar were investigated.

From the results it was hoped to gain insight into the mechanism underlying the decreased performance of admixtures in aged dry mix mortars.

The experiments signified that when exposed to moist air, SLU formulations undergo significant ageing which negatively impacts their shelf-life stability. In wet atmosphere, especially CAC and anhydrite react to form abundant ettringite crystals which cover the surfaces of the binders (**Figure 28**).

This massive formation of ettringite causes three major effects:

- Modification of the chemical composition and electrical surface charge of the binder particles
- Imbalance of sulphate in the system, due to premature consumption of anhydrite
- Incomplete or delayed hydration of some binder particles, as a result of hindered access of water to these surfaces

Also, the performances of chemical admixtures can be severely impacted by moisture exposure of the dry mortar. Here, it was found that effectiveness of tartrate as retarder was reduced while citrate gained from partial surface hydration of the SLU powder. Another admixture, casein superplasticizer, underwent chemical decomposition and quickly lost its dispersing ability. Apart from these chemical effects, prehydration of a SLU blend was found to also negatively impact engineering properties such as flow behaviour or compressive strength development.

This study demonstrated that proper storage of dry mix mortars which excludes the potential of moisture uptake is essential for their shelf-life stability. However, considering the harsh environments of actual construction sites one has to acknowledge that storage conditions there are not always ideal. Therefore, dry mortar producers are recommended to use high quality packaging, e.g. with moisture barriers such as PE or aluminium foils, to bag their products.

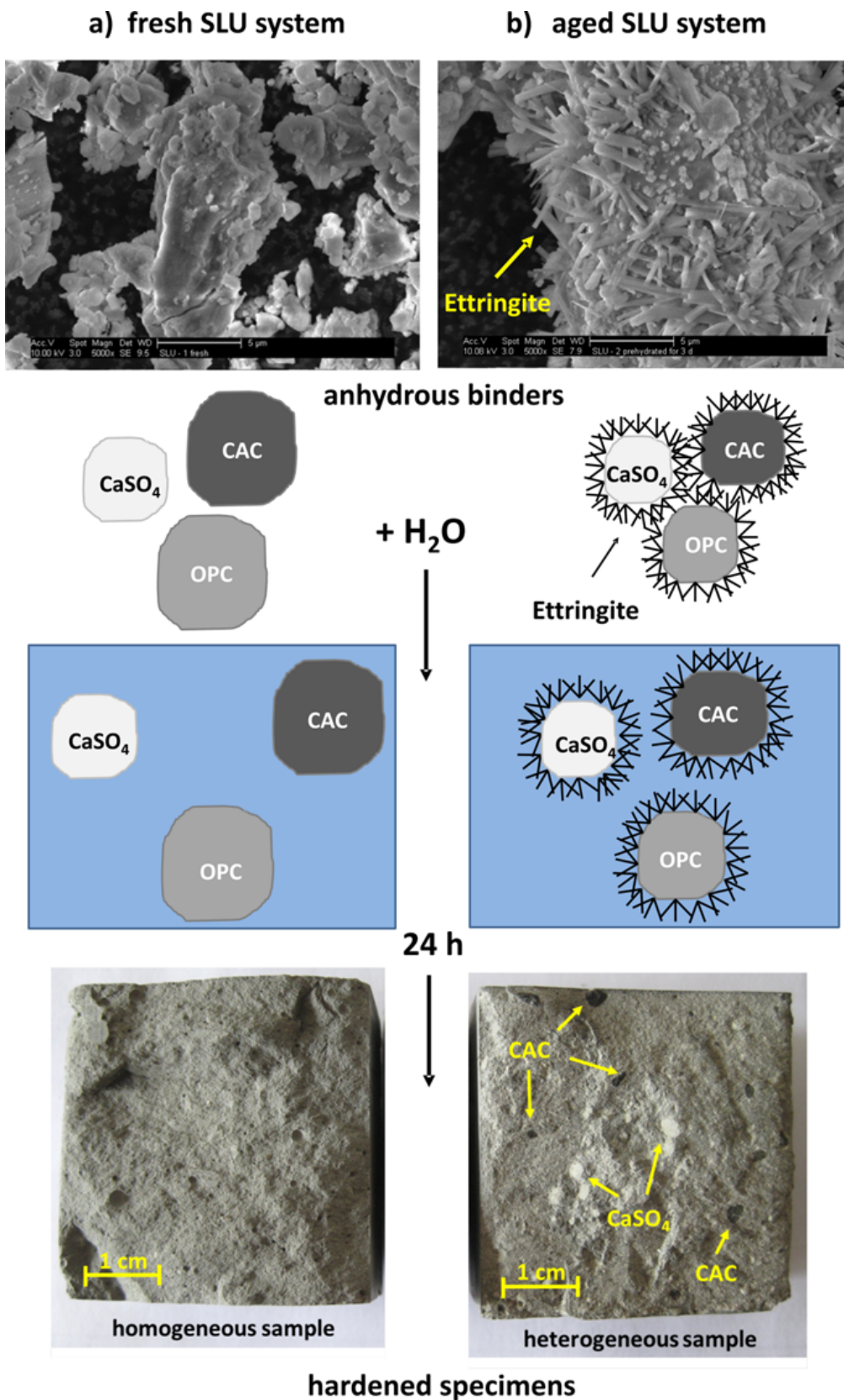


Figure 28: Schematic illustration of effects influencing the flow behaviour, water demand and fractal surfaces of 24 h hardened specimens of fresh (a) and aged (b) SLU formulations mixed with water

6.8 Further preliminary results

Results of this research work which have not yet been published are summarised in this chapter.

6.8.1 An attempt to utilise SIMS technique in the analysis of cement prehydration

In order to determine the thickness of the prehydration layer which is formed during exposure of a clinker phase to moist air, TOF-SIMS analysis was utilised. This requires a flat surface of the clinker sample. For this experiment, alite was chosen. The motivation for selecting this phase was to compare the layer thickness of hydrates which in XPS analysis was found at ~ 10 – 15 nm with result from SIMS. In the preparation, the freshly sintered alite was embedded into a resin and polished. **Figure 29** displays a SEM image of the sample.

Prehydration of the sample was performed with D₂O vapour at 60 °C for 16 hours. For this purpose, a saturated solution of KCl in D₂O instead of H₂O was prepared. Experimental conditions were chosen such as to exclude any impact which may arise from the contact of the sample surface with atmospheric water during sample preparation.

Figure 30 summarises all steps which were performed during the preparation of the sample and subsequent analysis.

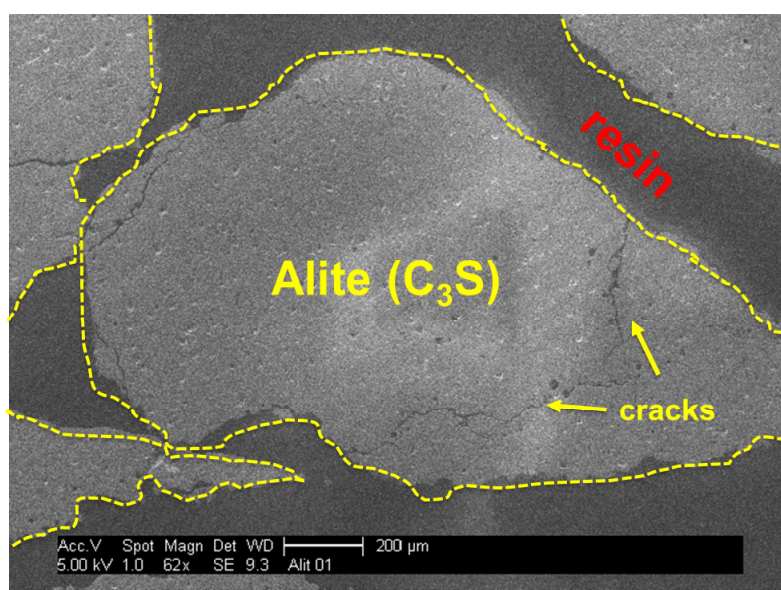


Figure 29: SEM image of alite embedded in resin during sample preparation

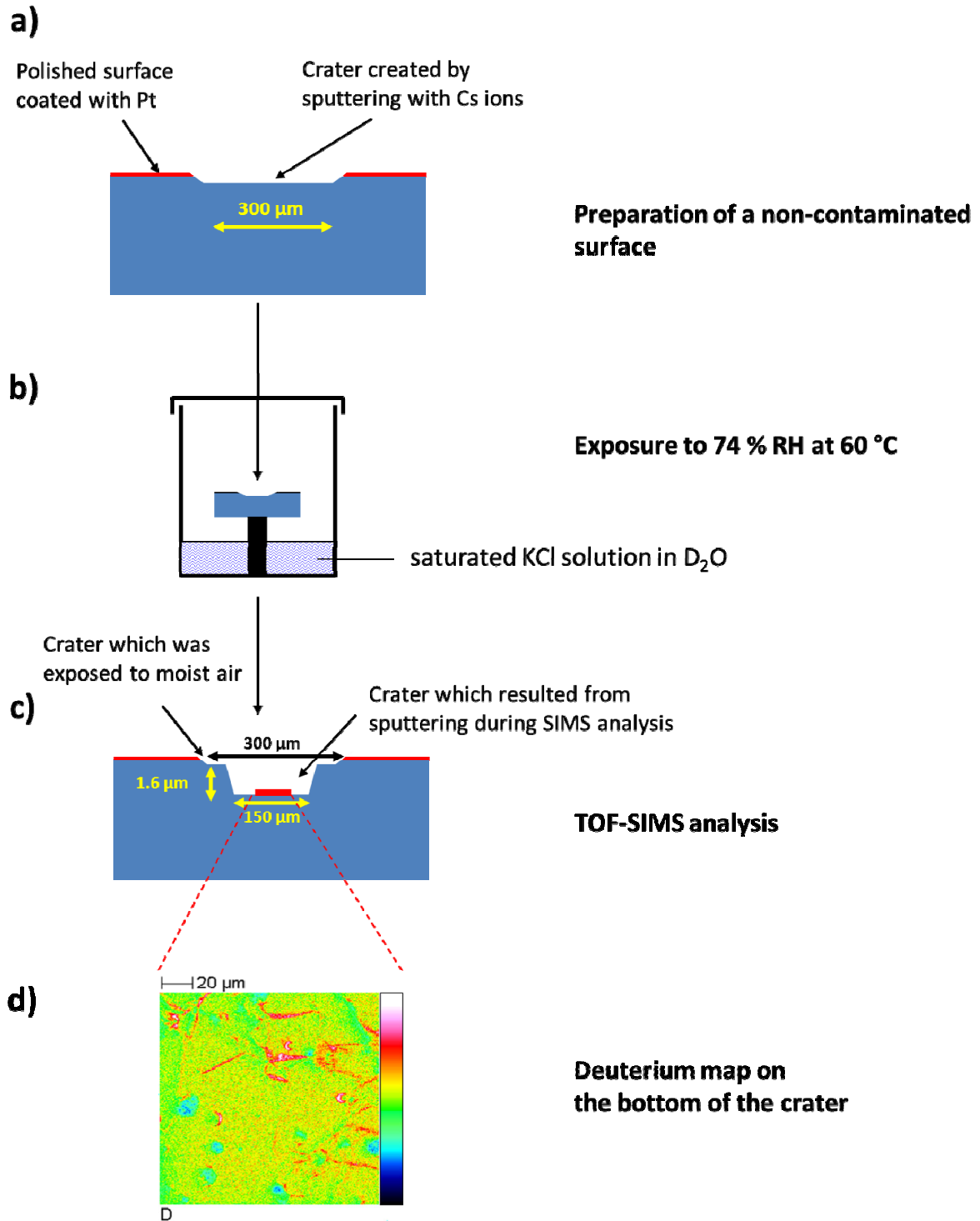


Figure 30: Steps performed during TOF-SIMS analysis: **a)** creating of a non-contaminated surface by sputtering of the Pt-coated C_3S surface with Cs ions; **b)** exposure of this surface at 60 °C for 18 hours to 74 % RH; **c)** depth profiling in TOF-SIMS analysis; **d)** deuterium map taken from the bottom of the crater

First, a polished section of C_3S (**Figure 29**) was covered with platinum to overcome the electrostatic charge of the sample. Prior to exposure to moist air, the sample surface was thoroughly sputtered in order to remove any contaminations from polishing and handling (**Figure 30 a**).

In the next step, the freshly prepared, non-contaminated surface of C_3S was exposed for 16 hours to 74 % RH at 60 °C as is shown in **Figure 30 b**.

This prehydrated C_3S sample was then analysed utilising a TOF-SIMS instrument (IONTOF TOF-SIMS IV, Münster, Germany). The instrument was equipped with a pulsed Ga^+ source. For sputter depth profiling, an O_2^+ or Cs^+ sputter gun was used, depending on the ion detection polarity chosen. The measurement was performed by using four different sputter erosion modes over the total depth of 1.6 μm (**Figure 31**).

Unfortunately, deuterium ions were detectable during the entire analysis. Even at the bottom of the crater elemental mapping showed the presence of deuterium ions (**Figure 30 c**). Such deep penetration of deuterium ions into the C_3S sample after 16 hours of exposure to humid air is unlikely to be caused by prehydration. Obviously, migration of deuterium through the cracks had occurred. Therefore, this attempt to determine the thickness of the hydration layer caused by prehydration had failed. Nevertheless, it was shown in principle that prehydration with D_2O presents a valid method to study the interaction of cement with humid air. It demonstrated that the successful preparation of a crackless surface is most critical to utilise TOF-SIMS for depth profiling.

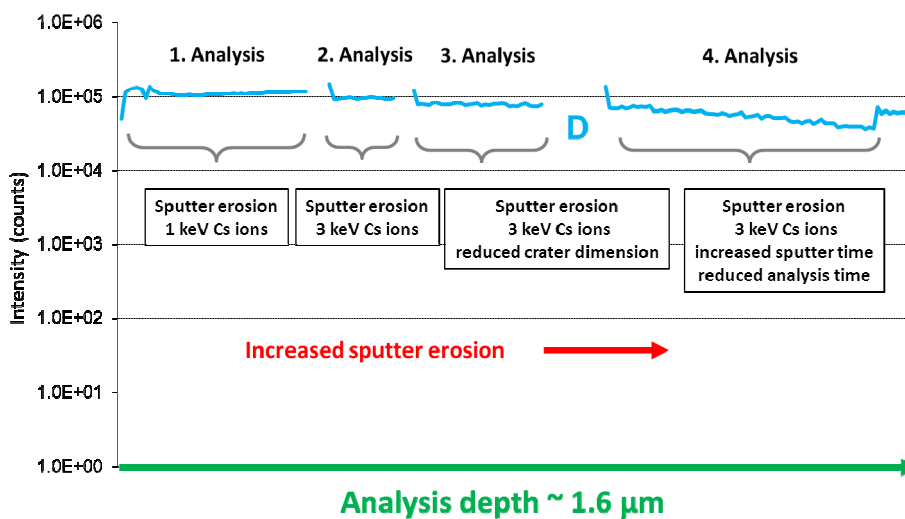


Figure 31: Time resolved detection of ion fragments from prehydrated C_3S over a total profile depth of 1.6 μm using TOF-SIMS analysis

6.8.2 Study on the sorption kinetics applying a shrinking core model

The objective of this study was to elucidate the kinetics of the process of surface hydration of C₃A and calcium sulphate hemihydrate. For this purpose, the rate limiting steps involved in the reactions were investigated by applying the shrinking core model as proposed by YAGI and KUNII [87].

The shrinking core model approach is widely used to explain fluid – solid reactions [88]. It is generally applicable to initially non-porous particles which react with a reagent leaving a layer of reaction products around the non-reacted core. This type of reaction can be described as follows:



Such situation may occur when a binary mixture containing C₃A and calcium sulphate hemihydrate is exposed to a relative humidity above their threshold values. First, water vapour will condense on the surfaces of the solid particles. Then, C₃A and calcium sulphate hemihydrate will react in the water films to form ettringite (**Figure 32**). According to this model, the rate-limiting step can be one of the following three:

- (1) Gas phase/liquid film diffusion control: condensation and diffusion of water from the liquid film to the surface of the solid particle
- (2) Shell layer diffusion control: diffusion through the hydrate solid layer (e. g. of ettringite)
- (3) Chemical reaction diffusion control: chemical reaction at the surface of the unreacted particle

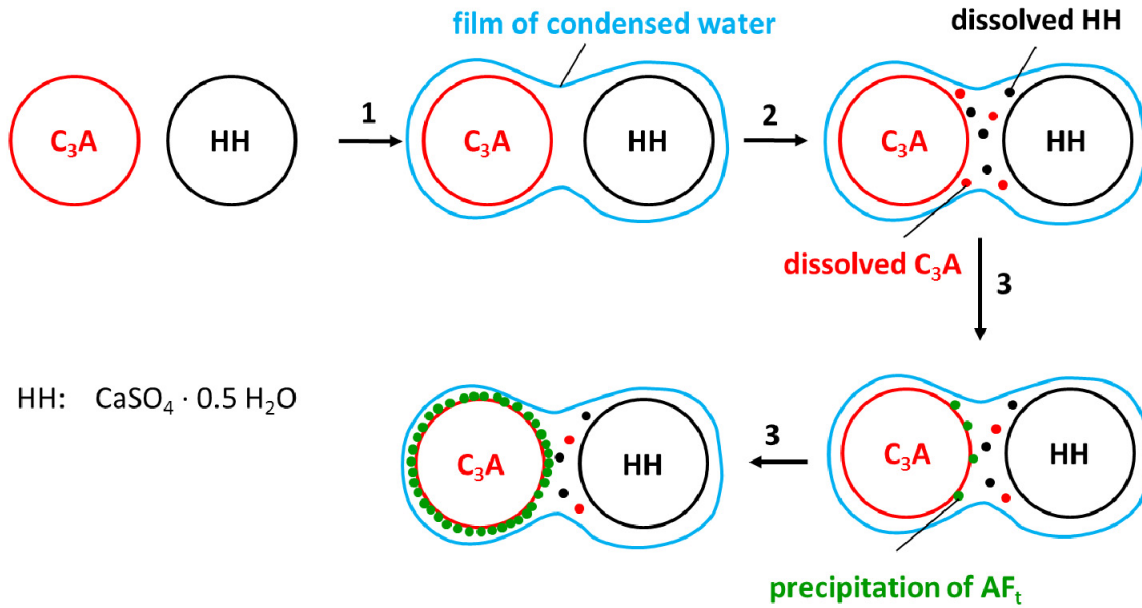


Figure 32: Schematic illustration of the processes occurring during exposure of a binary mixture containing C_3A and calcium sulphate hemihydrate to RH above their threshold values

By applying the shrinking core model the rate-determining step for the reaction fluid – solid can be assigned to either the diffusion control (mass transfer) or the chemical reaction model.

As is common for all chemical reactions involving solids, the observed rate of reaction (R) can be expressed in terms of a rate r per unit area of the reaction interface, multiplied by the surface area (S) newly generated which may evolve in many possible ways at time t :

$$R(T, C_i, t) = r(T, C_i) \cdot S(t) \quad \text{equation (6)}$$

Whereby T is the temperature and C_i are the concentrations of the reactants, intermediates and products. In case of water sorption, the progress of a reaction (α) at time t can be expressed by the ratio of the sorbed water $\Delta m(t)$ at the time t to the mass of the mixture at the dynamic equilibrium $\Delta m(\text{EQ})$:

$$\alpha(t) = \frac{\Delta m(t)}{\Delta m(\text{EQ})} \quad \text{equation (7)}$$

To distinguish between the three different rate-limiting steps, the following equations can be used [89]:

(1) Gas phase/liquid film diffusion control:

$$t = k_1 \cdot \alpha \quad \text{equation (8)}$$

(2) Shell layer diffusion control:

$$t = k_{2s} \cdot \alpha^2 [1 - (1 - \alpha)^{2/3} + 2(1 - \alpha)] \quad \text{equation (9)}$$

(3) Chemical reaction diffusion control

$$t = k_{3s} [1 - \sqrt[3]{1 - \alpha}] \quad \text{equation (10)}$$

In all equations k_i is defined as a specific rate of reaction and “s” stands for the assumption that the solids particles involved in the reaction are spherical.

Equations 8 – 10 can be generalised in linear form with a dimensionless function $a(\alpha(t))$:

$$t = k \cdot a(\alpha(t)) \quad \text{equation (11)}$$

So, for example, if the reaction of the binary mixture was limited by shell layer diffusion control, then **equation 9** can be expressed as:

$$t = k_{2s} [1 - (1 - \alpha)^{2/3} + 2(1 - \alpha)] = k_{2s} \cdot a_{2s}(\alpha(t)) \quad \text{equation (12)}$$

with $a_{2s}(\alpha(t)) = [1 - (1 - \alpha)^{2/3} + 2(1 - \alpha)]$ and $a(\alpha(t)) = \frac{t}{k}$

from **equation (11)**

Equation (11) can be rewritten in logarithmic form as follows:

$$\ln a(\alpha(t)) = \ln t - \ln k \quad \text{equation (13)}$$

To determine k , $\ln a(\alpha(t))$ needs to be plotted against $\ln t$. The intercept of this straight line with the y axis then is the reciprocal value of $\ln k$, with the specific rate of reaction k in minutes.

When **equation 13** is applied, the slope $d(\ln a(\alpha))/d(\ln t)$ should be “1” when the assumed rate-determining step of a reaction is correct.

The abovementioned calculations were applied for the water sorption isotherms of orthorhombic C_3A with calcium sulphate hemihydrate (**Figure 33**). The experimental conditions for the water sorption experiment are reported on page 8, section 2.2.1 in **paper 4**. At relative humidities below the onset point at 64 %, only minor amounts of water were sorbed (less than 2 wt. %). Therefore, the mechanism controlling the process of surface hydration of C_3A and calcium sulphate hemihydrate were studied only for RH levels above the threshold value.

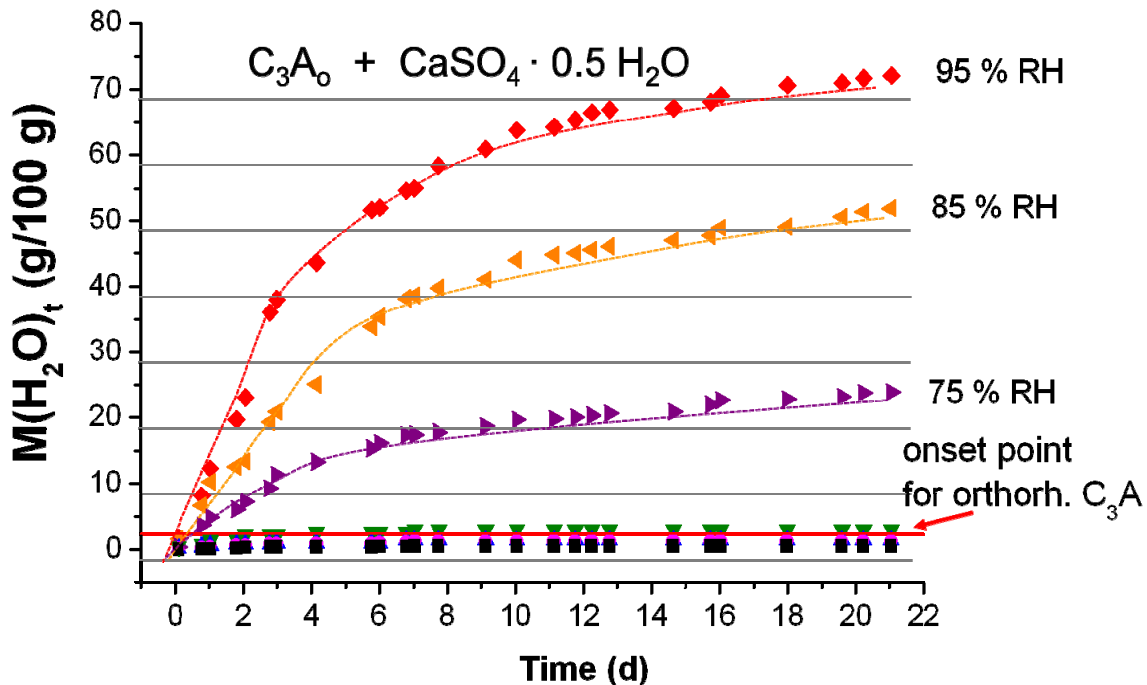


Figure 33: Water sorption isotherms for a binary mixture of orthorhombic C_3A + hemihydrate studied at 20 °C and 23 – 95 % RH as a function of time

From the experimental data presented in **Figure 33**, $\ln a(\alpha)$ was plotted against $\ln t$. Within the first 3 days of the exposure of the binary mixture to high RH levels, gas phase/liquid film diffusion control was found to be the most probable rate-limiting step because it fits the model best. **Figure 34** displays the corresponding plots for 75 %, 85 % and 95 % RH. The coefficient of determination R^2 for all three plots is ~ 0.97 . The value for the slope $d(\ln a(\alpha))/d(\ln t)$ is ~ 0.8 .

However, after 3 days of exposure gas phase/liquid film diffusion control no longer describes the mechanism of sorption well, as the calculated points are below the ideal fit. This indicates that diffusion via the gas phase/liquid film no longer presents the rate-limiting step.

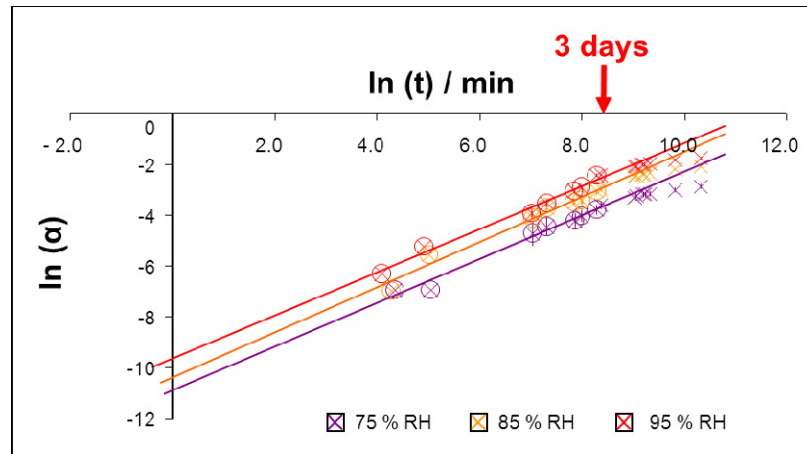


Figure 34: Plots of $\ln a(\alpha)$ against $\ln t$ according to **equation 8** for data obtained from sorption isotherms of orthorhombic C_3A with calcium sulphate hemihydrate at 75 %, 85 % and 95 % RH, respectively

Obviously, after 3 days of exposure diffusion through the solid layer of hydrates (e. g. ettringite) is the rate-limiting step. **Figure 35** displays the corresponding plots according to **equation 9**. Here, the coefficient of determination R^2 for all three plots is ~ 0.92 . The value for the slope $d(\ln a(\alpha))/d(\ln t)$ is ~ 0.85 . Between 3 and 8 days of storage at high RH values, diffusion through the ettringite layer obviously is the main rate-limiting step.

The shrinking core model does not explain the slowdown in water sorption after 8 days. There are several potential reasons for it. First, the shrinking core model was developed for

individual solid materials which undergo reactions. In this system, a binary mixture of two materials is involved in the chemical reaction.

Second, one of the assumptions was that the particles involved in the reaction are spherical. From SEM imaging it is obvious that C_3A as well as calcium sulphate hemihydrate are not spherical at all (**Figure 36**).

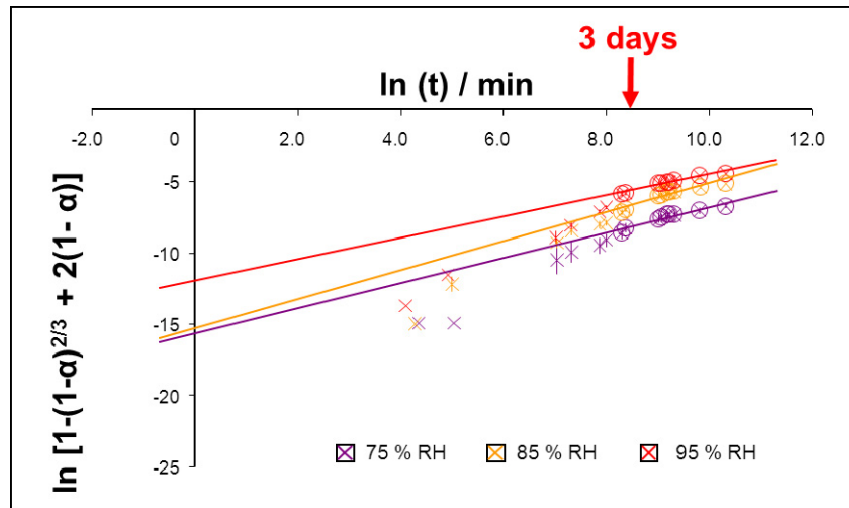


Figure 35: Plots of $\ln a(\alpha)$ against $\ln t$ according to **equation 9** for data obtained from sorption isotherms of orthorhombic C_3A with calcium sulphate hemihydrate at 75 %, 85 % and 95 % RH, respectively

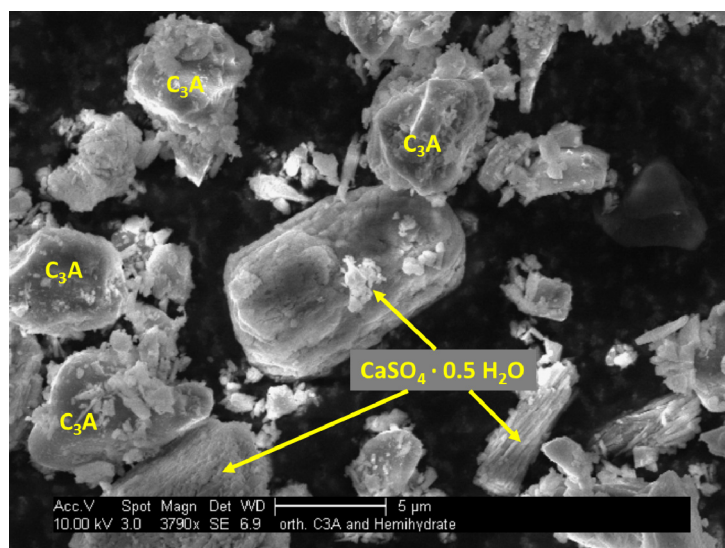


Figure 36: SEM image of the binary mixture of orthorhombic C_3A with calcium sulphate hemihydrate

From these results it can be concluded that within the first three days of the storage at high RH, condensation and diffusion of water from the liquid film to the surfaces of the solid particles plays an important role; while after 3 days, diffusion through the ettringite layer presents the rate-limiting step.

The same sorption experiments and calculations were also performed for a binary mixture containing cubic C_3A and calcium sulphate hemihydrate. This binary mixture sorbed only half the amount of water compared to that containing orthorhombic C_3A . For cubic C_3A , the change from gas phase/liquid film diffusion to diffusion through the ettringite layer occurred already after ~ 12 hours of exposure, compared to 3 days for the binary mixture containing orthorhombic C_3A .

Obviously, both C_3A polymorphs exhibit different sorption kinetics when prehydrated in the presence of calcium sulphate hemihydrate. A potential reason for the different behaviours is the presence of sodium ions in the liquid water film when orthorhombic C_3A is exposed to moist air. Surprisingly, sodium ions appear to impact the degree of permeability of the ettringite layer formed on the C_3A particles, making it less dense than in case of cubic C_3A . Further experiments are required to proof this hypothesis.

6.8.3 Prehydration of different calcium sulphates at 80 % RH and 80 °C

Previously it has been reported that during the grinding process of the clinker at temperatures above 42 °C, gypsum can dehydrate and react to more soluble hemihydrate or anhydrite [11]. However, in this study no report about the behaviour of other calcium sulphates was given.

Therefore, the purpose of this experimental series was to study the prehydration products of gypsum, hemihydrate and anhydrite on their surfaces after exposure to moist air (80 % RH) at 80 °C for 1, 3 and 7 days by using x-ray diffraction.

The corresponding XRD patterns are shown in **Figure 37**. Even at such high RH level gypsum partially dehydrates to anhydrite which was detected already after 1 day of exposure (**Figure 37 a**).

However, at the given conditions hemihydrate does not dehydrate at all. In fact, hemihydrate partially even sorbs water and shows reflections of gypsum which became less intense when the sample was stored for 7 days. This indicates that initially formed gypsum later starts to release its crystal water (**Figure 37 b**).

Anhydrite does not exhibit any changes after storage for 1 day, however after 3 days, similar to hemihydrate, weak reflections for gypsum appear in the XRD scan. After prolonged storage (7 d), this gypsum dehydrates completely and no signals other than those for anhydrite can be detected (**Figure 37 c**).

This experiment shows that calcium sulphates are very sensitive to relative humidity and can easily sorb and desorb water at high temperature and relative humidity. The amount of crystal water does not only change the chemical structure of sulphates, but also influences their solubility as was shown in **Table 2 (Chapter 3.1, p. 6)**. In industrial cements the amount of sulphate ions present at the early stage of hydration plays an important role, because sulphate controls the setting behaviour of the C₃A phase and thus the workability of a mortar or concrete. Therefore, more attention should be paid to the solubility of sulphates when cement was exposed to high RH and temperature during its storage.

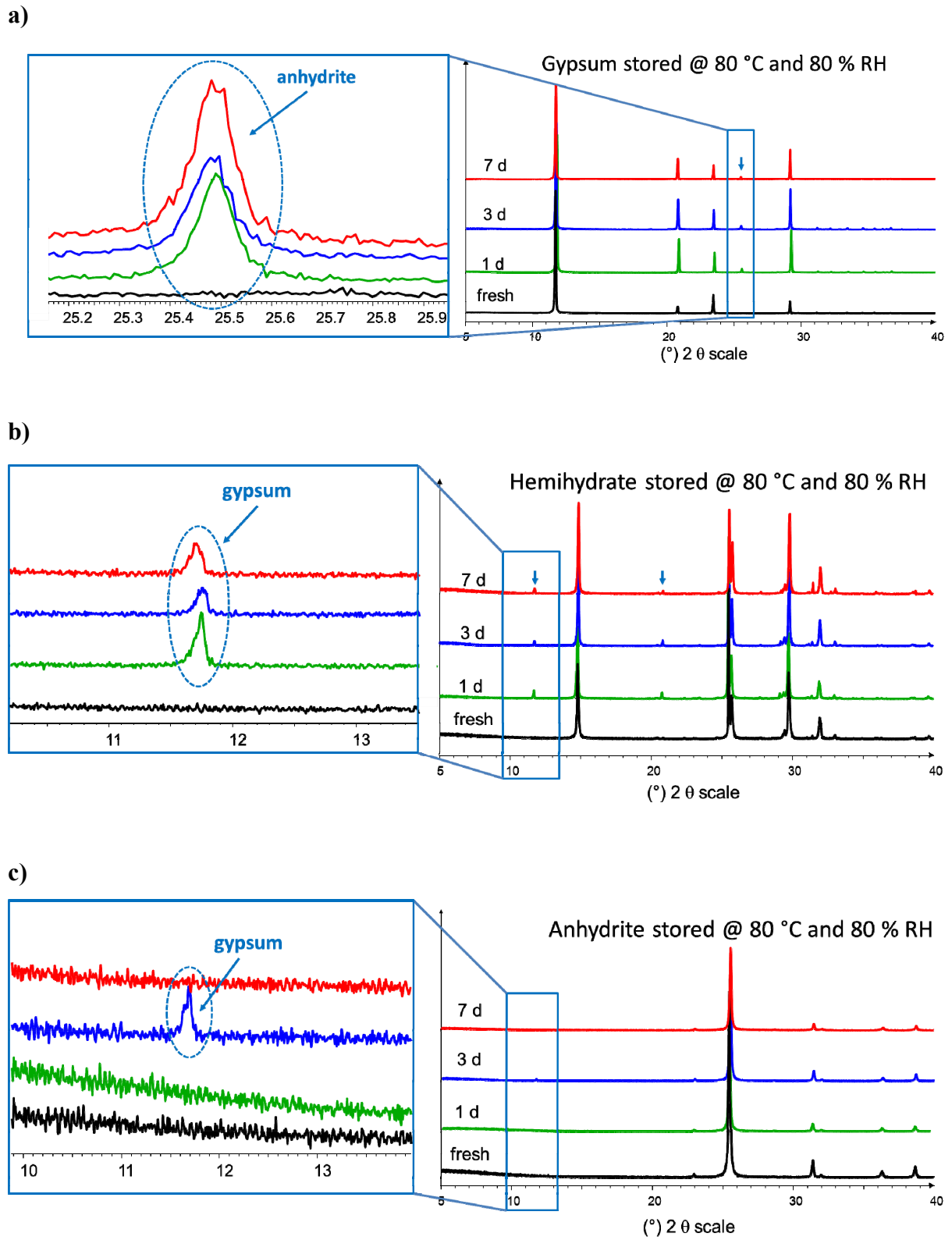


Figure 37: XRD patterns of gypsum (a), hemihydrate (b) and anhydrite (c) stored at 80 °C and 80 % RH for 1, 3 and 7 days

6.8.4 CEM I prehydrated at 80 °C and 10 – 80 % RH

Cement clinker is produced at high temperature (1450 °C). Once the clinker is ground with sulphates, this hot cement is stockpiled in storage silos where the elevated temperature, especially in warm climates, is not readily abated [90].

Summer months exacerbate the situation since ambient temperatures are generally high and cement consumption increases. On one hand the warmer temperatures reduce the ability of hot cement to release large quantities of heat to the ambient air. On another hand, increased consumption of cement in warm months means that freshly ground cement is stored only short before being shipped to ready-mixed plants for use in batching. Consequently, the temperature occurring in the cement silo can be high. Also, the relative humidity of air varies according to the season.

Therefore, CEM I 52.5 N was stored at 80 °C and different RH levels (10, 20, 40, 60 and 80 %) for 1, 3 and 7 days to simulate storage conditions which can occur in the cement silo. Subsequently, the performance of the exposed cement was tested in the absence and presence of BNS superplasticizer.

Mini slump tests revealed that the storage of cement at 80 °C and low RH levels (below 60 %) does not impact its performance in the presence of BNS superplasticizer (**Figure 38**). At high RH levels (≥ 60 %), a significant decrease in the dispersing power of BNS was observed. The effect became even stronger with increased exposure period.

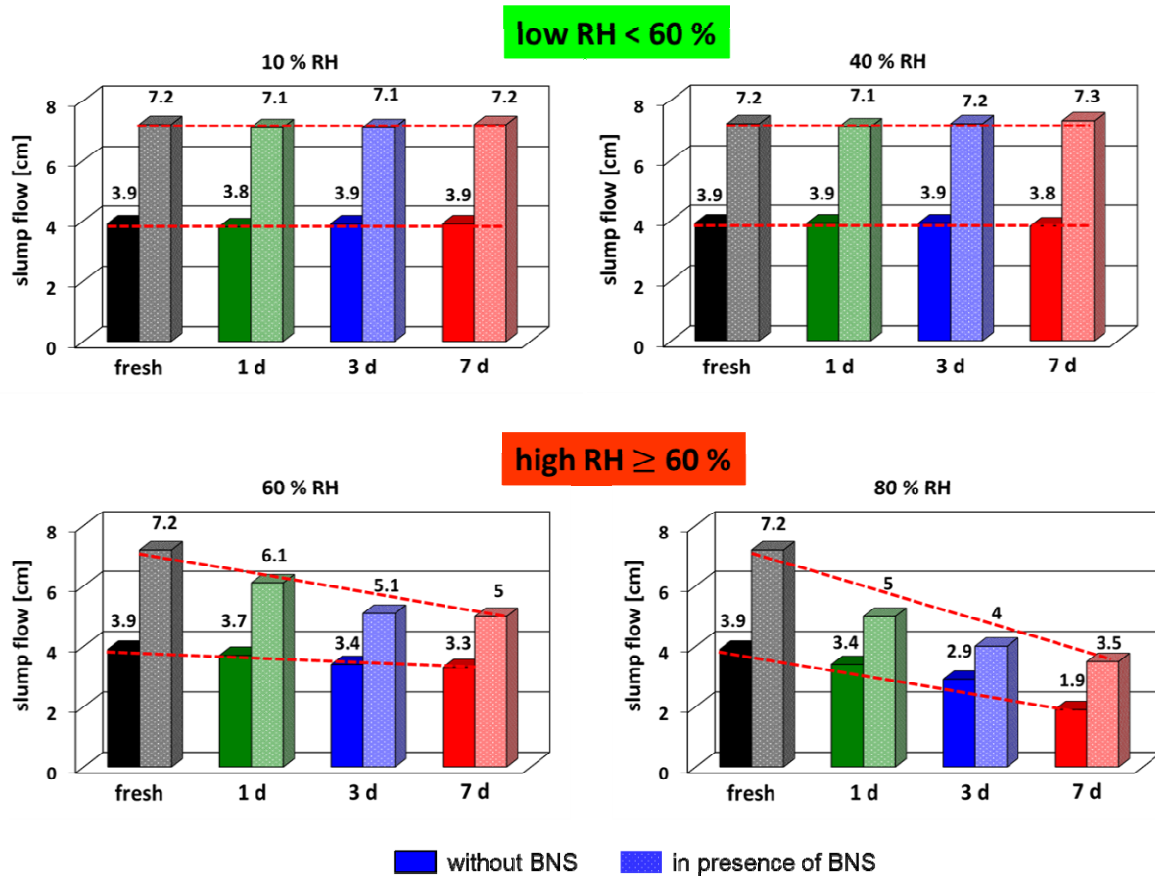


Figure 38: Flow spread of cement pastes ($w/c = 0.55$) made from CEM I 52.5 N with and without BNS, fresh (black) and prehydrated at 80 °C and different RHs levels (10, 40, 60 and 80 %) (storage time green: 1 d; blue: 3 d; red: 7 d); Dosage of BNS: 0.5 wt. %

6.8.5 CEM II / A-LL prehydrated at 35 °C and 90 % RH

In Germany about 45 % of the domestic cement sales are OPCs. Blast furnace cements account for ~ 11 % and other cements for ~ 1 %, leaving a market share of ~ 40 % for Portland-composite cements (CEM II/III). In Europe as a whole the ratio between OPC (CEM I) and Portland-composite cements is at ~ 32 % for Portland cement and ~ 55 % for blended cements [91 – 93].

Therefore, it is important to know how such composite cements interact with environmental moisture. For this purpose, one typical CEM II cement (CEM II / A-LL 32.5 R) was chosen as an example for a limestone blended cement. Its chemical composition is presented in **Table 5**.

6 Results and discussions

The cement was exposed at 35 °C to air containing 90 % RH for 1 and 3 days and then analysed.

SEM micrographs revealed the formation of hydration products on the surface of the prehydrated CEM II, as is shown in **Figure 39**. Ettringite (AF_t) was identified via XRD as the main phase formed during exposure to moist air (**Figure 40**).

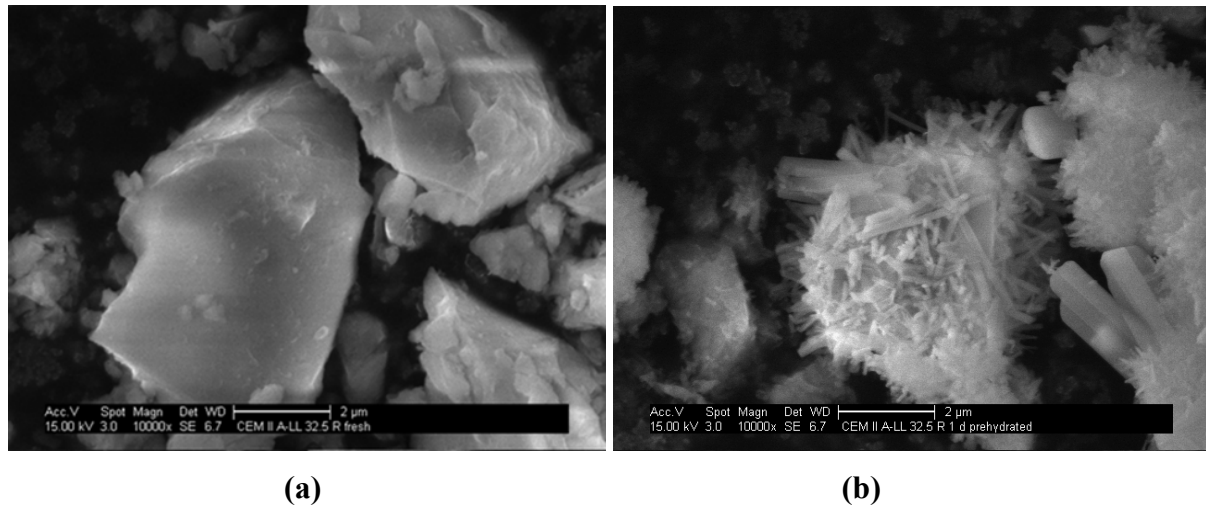


Figure 39: SEM images of CEM II / A-LL 32.5 R fresh (a) and prehydrated for 1 d at 35 °C and 90 % RH (b)

Table 5: Phase composition and specific properties of the CEM II / A-LL 32.5 R sample (Schwenk, Allmendingen plant)

Phase composition	wt. %
C_3S	45.1
C_2S	19.1
C_3A	5.1
C_4AF	7.4
free lime (CaO)	0.2
anhydrite ($CaSO_4$)	1.4
bassanite ($CaSO_4 \cdot 0.5 H_2O$)	1.9
dihydrate ($CaSO_4 \cdot 2 H_2O$)	0.8
calcite ($CaCO_3$)	16.3
quartz (SiO_2)	0.7
LOI	1.9
specific surface area (<i>Blaine</i>)	4632 cm^2/g

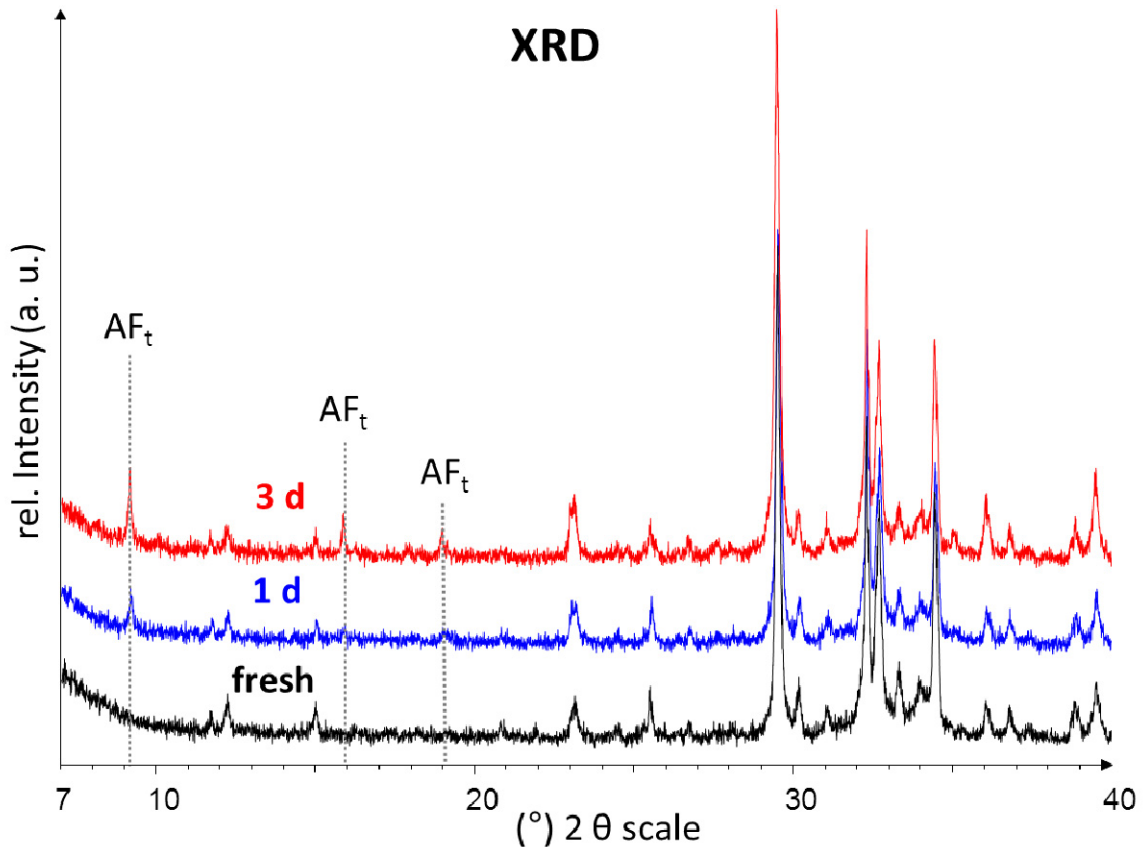


Figure 40: XRD patterns of the fresh and aged CEM II / A-LL 32.5 R

The hydration behaviour of this aged CEM II cement was investigated by means of isothermal calorimetry as is shown in **Figure 41**. Similar as reported in [57] for CEM I, the investigated CEM II also showed retardation of hydration and a reduction in heat flow (**Figure 41**).

However, the calorimetric curves of the CEM II exposed to moisture exhibited similar shapes for 1 and 3 days, while the CEM I cement after longer storage exhibited a more pronounced retardation (**paper 6**). This result indicates that the capacity of CEM II to sorb water vapour during exposure to moist air is less than for CEM I. Thermogravimetric measurements shown in **Figure 42** confirmed that prolonged storage of CEM II does not much impact its loss of ignition (LOI) while in CEM I this value increased when the storage time was extended from 1 to 3 days.

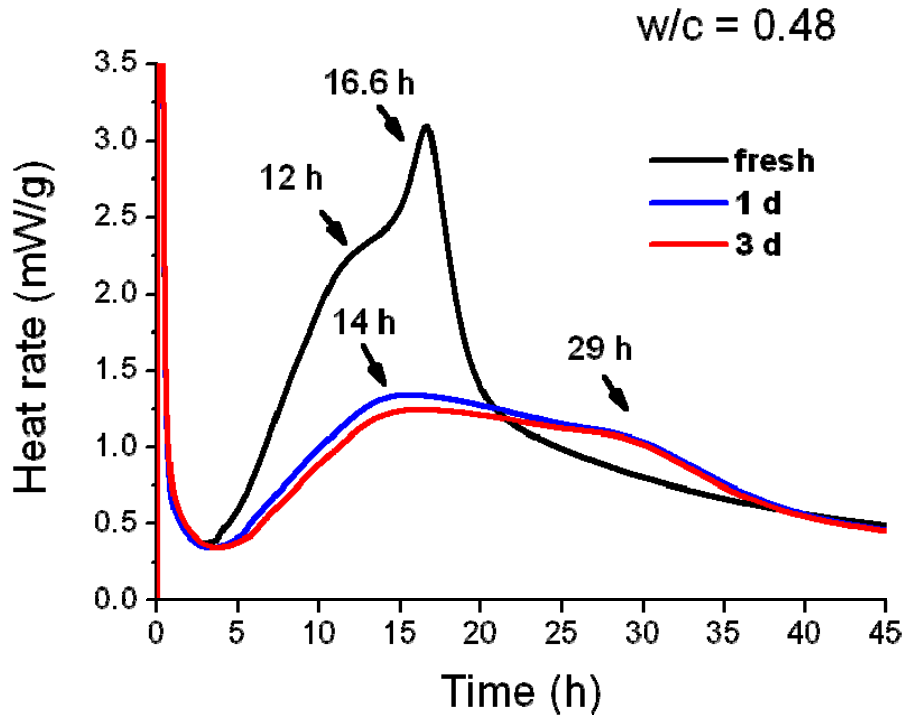


Figure 41: Isothermal calorimetry performed on fresh and aged CEM II / A-LL 32.5 R over a period of 45 h (w/c = 0.48)

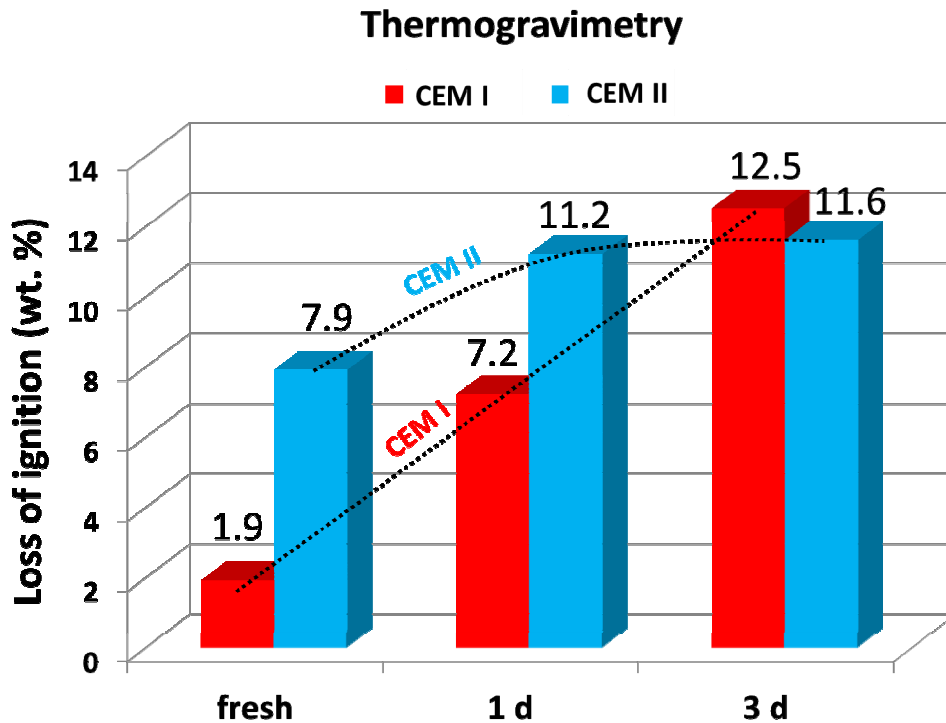


Figure 42: Thermogravimetric measurements obtained for fresh and aged CEM I 52.5 N and CEM II / A-LL 32.5 R

7 CONCLUSIONS AND OUTLOOK

7.1 Conclusions

In this thesis, the general phenomenon of cement prehydration was scientifically investigated under laboratory conditions.

First, the physicochemical surface effects of water sorption and their impact on the hydraulic properties of cement were investigated on individual clinker phases and cement constituents to gain an understanding of the effects on the individual minerals before studying a typical sample of OPC. It was shown that cement constituents exhibit fundamentally different onset points at which water sorption starts to occur. The amount of water sorbed per specific surface area was differentiated for each cement constituent. It was found that water can be bound physically, chemically, or in both ways. The experiments demonstrated that both free lime and orthorhombic C_3A sorb particularly large amounts of water. CaO is especially hygroscopic and possibly reduces or even prevents the prehydration of other clinker constituents when cement is exposed to moisture. CaO and C_3A are followed by β - $CaSO_4 \cdot \frac{1}{2} H_2O$ and cubic C_3A . C_4AF , gypsum and anhydrite sorb low amounts of water, whilst the silicates C_3S and C_2S sorb almost no water at all. A comparison of the sorption isotherms at 20 °C and 40 °C indicated that for all clinker phases, increasing temperature causes moisture uptake to occur at lower RHs. Obviously, different cement constituents exhibit very different behaviour towards water vapour at high temperature.

Prehydration is predominantly a surface reaction, hence common bulk analysis methods such as x-ray diffraction are not always useful. Instead, surface specific analytical techniques such as x-ray photoelectron spectroscopy (XPS) or micro-Raman analysis were utilised to collect information on the composition of the prehydrated surface, without interference from the unaffected bulk material. The results confirmed the potential of micro-Raman spectroscopy in the study of the hydration behaviour of minor cement constituents, particularly when amorphous products are involved in the reaction processes.

X-ray photoelectron spectroscopy provided deeper insights into the mechanisms of “water vapour/air – clinker” interactions. In the XPS spectra, clear differences were observed for cubic and orthorhombic C_3A after prehydration with water vapour and subsequent

carbonation in air. Orthorhombic C_3A which was doped with 4 wt. % of Na_2O was more sensitive toward humidity and carbonation as the cubic modification. The presence of sodium ions in orthorhombic C_3A was found to account for its higher sensitivity towards humidity and atmospheric carbon dioxide. Thus, the experiments suggest that when high amounts of Na-doped, orthorhombic C_3A are present in a cement sample, it may undergo more pronounced prehydration during storage than a cement containing the same amount of cubic C_3A .

In the second step, binary mixtures of the C_3A polymorphs with calcium sulphate hemihydrate were studied. ESEM imaging revealed that ettringite formation occurs via a condensed liquid water film. Obviously, prehydration does not much involve surface interaction with gaseous water molecules, but mainly relies on capillary condensation between the particles, thus allowing C_3A and calcium sulphate to react according to the well-known clinker dissolution/oversaturation/precipitation scheme observed for conventional cement hydration. This finding is of fundamental importance because it signifies that during prehydration, similar hydrates are formed as during normal cement hydration when cement is mixed with water, although their morphology might be dependent on the specific conditions.

Finally, the impact of prehydration and carbonation on cement hydration and the interaction of aged cement with admixtures was investigated. It was found that prehydration of C_3A in the presence of calcium sulphate hemihydrate may affect the dosage level of superplasticizer to be used for concrete or mortar. Consequently, owed to the nano crystallinity of ettringite formed during prehydration and its associated huge specific surface area, exposure of cements containing high amounts of C_3A to moisture may result in a higher consumption of superplasticizer.

CEM I cement that was exposed for an extended time period to moist air was found to exhibit a significantly altered behaviour not only with Superplasticizers, but also with other admixtures. The effects of this partial surface hydration of cement can be both positive and negative, although the detrimental effects are predominant in most of the cases. The results indicated that storage of CEM I 52.5 N at high temperature (80 °C) does not affect its properties when the RH level is kept below 60 %.

Preliminary results obtained for a limestone blended cement showed that a typical CEM II can also undergo prehydration, but the extent of the effects is less than for a CEM I cement.

Prehydration generally occurs when the ambient RH exceeds the threshold value at which moisture uptake begins. This implies that storing cements below this critical RH value would prevent prehydration. Therefore, throughout the production and storage period of a cement, ideally the ambient RH should be below the onset point of the most active clinker phases. However, under actual conditions where cement is produced, stored, distributed and applied, the control of RH to the required levels is practically impossible. Careful packaging and storage are the only measures which can help to minimise the effects from prehydration and to extend the shelf-life stability of cement or dry mixed mortar.

7.2 Outlook

The subject of cement prehydration is highly interesting for cement manufacturers and applicators. Therefore, several questions on this phenomenon should be clarified in further research. For example, the study on the impact of water vapour on the behaviour of various Portland blended cements as well as on dry mixed mortar formulations should be continued.

But also the mechanisms behind the interactions of aged cement with various admixtures are not yet fully understood, owed to the complex nature and interdependence of numerous chemical reactions.

The focus of this present work was placed on the investigation of “water vapour – cement” interactions and less on the impact of carbon dioxide. However, some results presented in this work showed the significance of atmospheric CO₂ on the ageing phenomenon of cement. Therefore, further experiments in this direction should be performed.

Also, research utilising additional analytical techniques is needed to understand the effects which could not be explained by the present methods. For example, the measurements using the secondary ion mass spectrometry (SIMS) which failed in a first attempt should be reactivated and extended to phases other than C₃S.

8 REFERENCES

- [1] Schneider M., Romer M., Tschudin M., Bolio H., *Sustainable cement production—present and future*, Cem. Concr. Res. 41 (7), (2011), 642–650.
- [2] International Energy Agency World Business Council for Sustainable Development, *Cement Technology Roadmap 2009: Carbon Emissions Reductions up to 2050* (2009).
- [3] Winnefeld F., *Influence of cement ageing and addition time on the performance of superplasticizers*, ZKG Int. 61 (11), (2008), 68–77.
- [4] Maltese C., Pistolesi C., Bravo A., Cella F., Cerulli T., Salvione D., *Effect of moisture on the setting behavior of Portland cement reacting with an alkali-free accelerator*, Cem. Concr. Res. 37 (6), (2007), 856–865.
- [5] Sprung V. S., *Effect of storage conditions on the properties of cements*, ZKG Int. 30 (6), (1978), 305–309.
- [6] Silk I. M., *Exposure to moisture alters well cement*, Pet. Eng. Int. 58 (3), (1986), 45–49.
- [7] Barbic L., Tinta V., Lozar B., Marincovic V., *Effect of storage time on the rheological behavior of oil well slurries*, J. Am. Ceram. Soc. 74 (5), (1991), 945–949.
- [8] Dubina E., *Physikalisch-chemische Oberflächeneffekte bei der Adsorption von Wasser und deren Bedeutung für die Hydratation von Portlandzement und reinen Zementklinkern*, Master Thesis, 2008, Technische Universität München.
- [9] Stark J., Wicht B., *Zement und Kalk - Der Baustoff als Werkstoff*, Birkhäuser Verlag (Berlin), 2000.
- [10] Lea M. F., *The chemistry of cement and concrete*, 4 ed., New York: Chemical Publishing Co., Inc. 1997.
- [11] Mould A. E., Williams D. W., *The effects of high ambient temperatures on gypsum plasters*, Build. Sci. 9, (1974), 243–245.

- [12] Bensted J., *Effects of the clinker - gypsum temperature upon early hydration of Portland cement*, Cem. Concr. Res. 12 (3), (1982), 341–348.
- [13] Sprung S., *Effect of mill atmosphere on the setting and strength of cement*, ZKG Int. 27 (5), (1974), 259–267.
- [14] Jawed I., Skalny J., *Alkalies in cement: a review. I: Forms of alkalies and their effect on clinker formation*, Cem. Concr. Res. 7 (6), (1977), 719–730.
- [15] Kim B.-G. *Compatibility between cements and superplasticizers in high performance concrete: influence of alkali content in cement and of the molecular weight of PNS on the properties of cement pastes and concretes*, in Département de génie civil, 2000, Université de Sherbrooke: Sherbrooke, Canada.
- [16] Bullard J. W., Jennings H. M., Livingston R. A., Nonat A., Scherer G. W., Schweitzer J. S., Scrivener K. L., Thomas J. J., *Mechanisms of cement hydration*, Cem. Concr. Res. 41 (12), (2011), 1208–1223.
- [17] Thomas J. J., *A new approach to modeling the nucleation and growth kinetics of tricalcium silicate hydration*, J. Am. Ceram. Soc. 90 (10), (2007), 3282–3288.
- [18] Bishnoi S., Scrivener K. L., *Studying nucleation and growth kinetics of alite hydration using μ ic*, Cem. Concr. Res. 39 (10), (2009), 849–860.
- [19] Dove P. M., Han N., *Kinetics of mineral dissolution and growth as reciprocal microscopic surface processes across chemical driving force*, AIP Conference Proceedings, Vol. 916, (2007), 215–234.
- [20] Juilland P., Gallucci E., Flatt R., Scrivener K. L., *Dissolution theory applied to the induction period in alite hydration*, Cement Concr. Res. 40 (6), (2010), 831–844.
- [21] Gartner E. M., Young J. F., Damidot D. A., Jawed I., *Hydration of Portland cement*, in: J. Bensted, P. Barnes (Eds.), *Structure and Performance of Cements*, 2nd Edition, Spon Press, New York, (2002), 57–113.

- [22] Bullard J. W., Flatt R. J., *New insights into the effect of calcium hydroxide precipitation on the kinetics of tricalcium silicate hydration*, J. Am. Ceram. Soc. 93 (7), (2010), 1894–1903.
- [23] Kumar A., Scrivener K. L., *Modelling early age hydration kinetics of alite*, Cem. Concr. Res. 42 (7), (2012), 903–918.
- [24] Juilland P., Kumar A., Gallucci E., Flatt R. J., Scrivener K. L., *Effect of mixing on the early hydration of alite and OPC systems*, Cem. Concr. Res. 42 (9), (2012), 1175–1188.
- [25] Rixom M. R., Mailvaganam N. P., *Chemical admixtures for concrete*, E&FN Spon Ltd, London, UK, 1999.
- [26] EN 934-2, *Admixtures for concrete, mortar and grout, Part 2: Concrete admixtures – Definitions, requirements, conformity, marking and labeling*, 2009 from <http://www2.din.de/>.
- [27] Cheung J., Jeknavorian A., Roberts L., Silva D., *Impact of admixtures on the hydration kinetics of Portland cement*, Cem. Concr. Res. 41 (12), (2011), 1289–1309.
- [28] Taylor H. F. W., "Cement chemistry", 2 ed., London, Academic Press Ltd., 1990.
- [29] Yamada K., *Basics of analytical methods used for the investigation of interaction mechanism between cements and superplasticizers*, Cem. Concr. Res. 41 (7), (2011), 793–798.
- [30] Patural L., Marchal P., Govin A., Grosseau P., Ruot B., Devès O., *Cellulose ethers influence on water retention and consistency in cement-based mortars*, Cem. Concr. Res. 41 (1), (2011), 46–55.
- [31] Bülichen D., Kainz J., Plank J., *Working mechanism of methyl hydroxyethyl cellulose (MHEC) as water retention agent*, Cem. Concr. Res. 42 (7), (2012), 953–959.
- [32] Bishop M., Barron A. R., *Cement hydration inhibition with sucrose, tartaric acid and lignosulfonate: analytical and spectroscopic study*, Ind. Eng. Chem. Res. 45 (21), (2006), 7042–7049.

- [33] Thomas N. L., Birchall J. D., *The retarding action of sugars on cement hydration*, Cem. Concr. Res. 13 (6), (1983), 830–842.
- [34] Juenger M. C. G., Jennings H. M., *New insights into the effects of sugar on the hydration and microstructure of cement pastes*, Cem. Concr. Res. 32 (3), (2002), 393–399.
- [35] Peterson V. K., Juenger M. C. G., *Time-resolved quasielastic neutron scattering study of the hydration of tricalcium silicate: effects of CaCl₂ and sucrose*, Phys. B 385–386 (1), (2006), 222–224.
- [36] Meyers S. L., *Heat Developed by Cement While Setting and Hardening*, Rock Prod. 35, (1932), 22.
- [37] Woods H., Steinour H. H., Starke H. R., *Effect of composition of Portland cement on heat evolved during hardening*, Ind. Eng. Chem. 24 (1932), 1207–1241.
- [38] Davis R. E., Carlson R. W., Kelly J. W., Troxell E., *Cement investigations for Hoover dam*, Proc. Am. Conc. Inst., 29 (1933), 413–431, see 30 (1934), 485–497 for another report on the same subject.
- [39] Hornibrook, F. B., Kalousek, G. L., Jumper, C. H., *Effects of partial prehydration and different curing temperatures on some of the properties of cement and concrete*, J. Res. Natl. Bur. Stand. 16 (5), (1936), 487–509.
- [40] Weithase H., *Über Änderung der Bindezeit von Portlandzement*, Zement 20, (1931), 187–192.
- [41] Hansen W. C., *Aeration cause of false set in Portland cement*, ASTM Proceedings 58 (1958), 1044–1050.
- [42] Kalousek G. L., *Abnormal set of Portland cement, causes and correctives*, U. S. Department of the Interior, Bureau of Reclamation, General Report Nr. 45, Denver, CO, 1969.
- [43] Kalousek G. L., *Hydration processes at the early stages of cement hardening*, 6th Symposium on the Chemistry of Cement, Moscow, 1974.

- [44] Havard Mork J., Gjoerv O., E., *Effect of Gypsum-hemihydrate Ratio in Cement on Rheological Properties of Fresh Concrete*, Am. Cer. Inst. 94, (1997), 142–146.
- [45] Hewlett P., *Lea's Chemistry of Cement and Concrete*, Butterworth-Heinemann, 2004.
- [46] Hills L. M., *Water Spray in Cement Finish Mills: A Literature Review*, PCA R&D Serial No. 2889, Portland Cement Association, 2006.
- [47] Hansen F. E., Clausen H. J., *Cement strength and cooling by water injection during grinding*, ZKG 27 (7), (1974), 333–336.
- [48] Theisen K., Johansen V., *Prehydration and strength development of Portland cement*, J. Am. Ceram. Soc. Bull. 54 (9), (1975) 787–791.
- [49] Matouschek F., *Beitrag zur Erklärung der Knollenbildung im Zement*, ZKG Int. 25, (1972), 395–396.
- [50] Whittaker M., Dubina E., Al-Mutawa F., Arkless L., Plank J. and Black L., *The effect of prehydration on the engineering properties of CEM I Portland cement*, Adv. Cem. Res. (2012), in print.
- [51] Richartz V. W., *Effects of Storage on the Properties of Cement*, ZKG Int. 2, (1973), 67–74.
- [52] Bensted G., Bier T. A., Wutz K., Maier M., *Characterization of the Ageing Behaviour of Premixed Dry Mortars and its Effect on their Workability Properties*, ZKG Int. 60 (6), (2007), 94–103.
- [53] Zurbriggen R., Götz-Neunhoeffler F., *Mechanism and resulting damages of prolonged retardation in aged dry mixes: A case study of mixed-binders containing tartaric acid*, GDCh monograph, Vol. 37, (2007), 111–118.
- [54] Breval E., *Gas-phase and liquid-phase hydration of C₃A*, Cem. Concr. Res. 7 (3), (1977), 297–304.
- [55] Breval E., *The Effects of Prehydration on the Liquid Hydration of 3 CaO · Al₂O₃ with CaSO₄ · 2 H₂O*, J. Am. Ceram. Soc. 62 (7-8), (1979), 395–398.

- [56] Jensen O. M., Hansen F. P., Lachawski E. E., Glasser F. P., *Clinker Mineral Hydration at Reduced Relative Humidities*, Cem. Concr. Res. 29 (9), (1999), 1505–1512.
- [57] Dubina E., Black L., Sieber R., Plank J., *Interaction of water vapour with anhydrous cement minerals*, Adv. Appl. Cer. 109 (5), (2010), 260–268.
- [58] Brutsaert W., *Evaporation into the Atmosphere: Theory, History, and Applications*, Boston, Kluwer Academic Publishers, 1991.
- [59] Meyer G., Schiffner E., *Technische Thermodynamik*, 2. ed. Fachbuchverlag Leipzig, 1983.
- [60] Albert B., Guy B., Damidot D., *Water chemical potential: A key parameter to determine the thermodynamic stability of some hydrated cement phases in concrete?*, Cem. Concr. Res. 36 (5), (2006), 783–790.
- [61] Baquerizo L., Matschei T., Scrivener K., *Impact of water activity on the water of cement hydrated*, ibausil, (2012), Vol. 1, 0249–0259.
- [62] Rose J., *Dynamic Physical Chemistry*, New York, Wiley, 1961.
- [63] Wesselsky A., Jensen O. M., *Synthesis of pure Portland cement phases*, Cem. Concr. Res. 39 (11), (2009), 973–980.
- [64] Franke B., *Bestimmung von Calciumoxyd und Calciumhydroxyd neben wasserfreiem und wasserhaltigem Calciumsilikat*, Z. Anorg. Allg. Chem. 247 (1-2), (1941), 180–184.
- [65] Anderberg, A., Wadsö L., *Method for simultaneous determination of sorption isotherms and diffusivity of cement-based materials*, Cem. Concr. Res. 38 (1), (2008), 89–94.
- [66] Wadsö L., Markova N., *Comparison of three methods to find the vapour activity of a hydration step*, Eur. J. Pharm. Biopharm. 51, (2001), 77–81.
- [67] Greenspan L., *Humidity fixed points of binary saturated aqueous solutions*, J. Research Nat. Bur. Stand. Sec - A, Phys. and Chem. 81A (1), (1977), 89–96.

- [68] Taylor J. C., Aldridge L. P., Matulis C. E., Hinczak I., *X-ray powder diffraction analysis of cements*, in: Bensted J., Barnes P. (eds.), *Structure and Performance of Cements*, 2nd ed., Spon Press, **2002**.
- [69] Grant J. T., Briggs D., *Surface Analysis by Auger and X-ray Photoelectron Spectroscopy*, Chichester, IM Publications, **2003**.
- [70] Black L., Stumm A., Garbev K., Stemmermann P., Hallam K. R., Allen G. C., *X-ray photoelectron spectroscopy of the cement clinker phases tricalcium silicate and β -dicalcium silicate*, *Cem. Concr. Res.* 33 (10), (**2003**), 1561–1565.
- [71] Black L., Garbev K., Stemmermann P., Hallam K. R., Allen G. C., *Characterisation of crystalline C-S-H phases by X-ray photoelectron spectroscopy*, *Cem. Concr. Res.* 33 (6), (**2003**), 899–911.
- [72] Black L., Garbev K., Gee I., *Surface carbonation of synthetic C-S-H samples: A comparison between fresh and aged C-S-H using X-ray photoelectron spectroscopy*, *Cem. Concr. Res.* 38 (6), (**2008**), 745–750.
- [73] Bellmann F., Sowoidnich T, Ludwig H.-M., Damidot D., *Analysis of the surface of tricalcium silicate during the induction period by X-ray photoelectron spectroscopy*, *Cem. Concr. Res.* 42 (9), (**2012**), 1189–1198.
- [74] Bensted J., *Uses of Raman spectroscopy on cement chemistry*, *J. Am. Ceram. Soc.* 59, (**1976**), 140–143.
- [75] Black L., *Raman spectroscopy of cementitious materials*, *Spectrosc. Prop. Inorg. Organomet. Compd.* 40, (**2009**), 72–123.
- [76] de Paiva L. B., Rodrigues F. A., *Early-hydration of β -Ca₂SiO₄ followed by FTIR/ATR spectroscopy*, *J. Mat. Sci.*, 39 (18), (**2004**), 5841–5843.
- [77] Vickerman J. C., Brown A., Reed N. M. (Eds), *Secondary Ion Mass Spectrometry, Principles and Applications*, Oxford University Press, **1989**.
- [78] Vickerman J. C., Briggs D., *ToF-SIMS: Surface Analysis by Mass Spectrometry*, IM Publications and Surface Spectra, **2001**.

- [79] Gerhard W., *The hydration of cement studied by secondary ion mass spectrometry (SIMS)*, Cem. Concr. Res. 13 (6), (1983), 849–859.
- [80] Ferrari L., Bernard L., Deschner F., Kaufmann J., Winnefeld F., Plank J., *Characterization of Polycarboxylate-Ether Based Superplasticizer on Cement Clinker Surfaces*, J. Am. Ceram. Soc. 95 (7), (2012), 2189–2195.
- [81] Deng C.-S., Breen C., Yarwood J., Habesch S., Phipps J., Craster B., Maitland G., *Ageing of oilfield cement at high humidity: a combined FEG-ESEM and Raman microscopic investigation*, J. Mater. Chem. 12 (10), (2002), 3105–3112.
- [82] German Institute for Standardization: DIN EN 1015-3, Methods of test for mortar for masonry – Part 3: Determination of consistence of fresh mortar (by flow table); German version, Berlin, Beuth Verlag, 2007.
- [83] German Institute for Standardization: DIN EN 12706, Adhesives - Test methods for hydraulic setting floor smoothing and/or levelling compounds - Determination of flow characteristics, German version, Berlin, Beuth Verlag, 1999.
- [84] Dukhin S. S., *Electrochemical characterization of the surface of a small particle and nonequilibrium electric surface phenomena*, Adv. Colloid and Interface Sci. 61 (1995), 17–49.
- [85] Dukhin A. S., Goetz P. J., *Characterization of Liquids, Nano- and Microparticulates, and Porous Bodies Using Ultrasound; Chapter 5: Electroacoustic Theory*, Studies in Interface Science, Volume 24, 2010.
- [86] Moulder J. F., Stickle W. F., Sobol P. E., Bomben K. D., in: J. Chastain (Ed.), *Handbook of X-Ray Photoelectron Spectra – A Reference Book of Standard Spectra for Identification and Interpretation of XPS Data*, Perkin-Elmer, Eden Prairie, Minnesota, 1992, p. 229.
- [87] Yagi S., Kunii D., *Studies on combustion of carbon particles in flames and fluidized beds*, Proceedings 5th Int. Symp. on Combustion, 1955.
- [88] Levenspiel O., *Chemical Reaction Engineering*, 3rd ed., John Wiley & Sons, Inc. New

York, 1999.

[89] Bamford C. H., Tipper C. F. H., Compton R. G., *Comprehensive Chemical Kinetics*, Vol. 21, Elsevier, 119–149, **1984**.

[90] http://www.cement.org/tech/cct_hot_cement.asp (downloaded on 23.10.2012).

[91] Müller Ch., *Performance of Portland-composite cements*, *Cem. Int.* 2 (4), (**2006**), 2–9.

[92] Damtoft J. S., Lukasik J., Herfort D., Sorrentino D., Gartner E. M., *Sustainable development and climate change initiatives*, *Cem. Concr. Res.* 38 (2), (**2008**), 115–127.

[93] Zahlen und Daten 2010-2011. Bundesverband der Deutschen Zementindustrie.



A sorption balance study of water vapour sorption on anhydrous cement minerals and cement constituents

E. Dubina^a, L. Wadsö^b, J. Plank^{a,*}

^a Technische Universität München, Chair for Construction Chemicals, Garching, Lichtenbergstraße 4, 85747, Germany

^b Lund University, Building Materials LTH, Box 118, 221 00 Lund, Sweden

ARTICLE INFO

Article history:

Received 28 October 2010

Accepted 25 July 2011

Keywords:

Prehydration

Humidity (A)

Clinker (B)

Aging (C)

Sulfate (D)

ABSTRACT

The phenomenon of water vapour sorption by powdered cement constituents exposed to different relative humidities and temperatures was studied. The individual clinker phases C_3S , C_2S , C_3A , C_4AF , calcium sulfates and CaO were tested. Using a water sorption balance, the amount of chemically and physically sorbed water per unit of surface area of the powders and the relative humidity at which water sorption starts to occur on the phases were determined. Various cement clinker phases prehydrate very differently. CaO and C_3A were found to be most reactive towards water vapour whereas the silicates react less. CaO starts to sorb water at very low RHs and binds it chemically. Beginning at 55% RH, orthorhombic C_3A also sorbs significant amounts of water and binds it chemically and physically. Water sorption of C_3S and C_2S only begins at 74% RH, and the amount of water sorbed is minor. Calcium sulfates sorb water predominantly physically.

© 2011 Elsevier Ltd. All rights reserved.

1. Introduction

The phenomenon of water vapour sorption by cement powders exposed to humidity is known as prehydration of cement. Industrial cements may undergo some prehydration already during the manufacturing process. There, a first contact with water can occur in the mill where clinker is ground together with gypsum at elevated temperature (90–120 °C). Under these conditions, gypsum dehydrates and releases water which can react with the clinker. Furthermore, cement producers sometimes lower the milling temperature by spraying e.g. 2% of water into the mill. Even during storage in the cement silo where temperature may get as high as 70–80 °C, prehydration may proceed due to the continuous release of water from the interground gypsum as long as the temperature exceeds 42 °C [1]. Therefore, cement may already be prehydrated before it is delivered to the customer. Thus, the properties of cement can fluctuate considerably, depending on its history of manufacture and storage.

After delivery and in industrial use, cement may be further stored for several months or even a year before usage. For dry-mix mortars, for example, the usual shelf life is 6 months to 1 year, as stated on the bags. Alteration of the cement properties during storage is highly undesirable, but has been repeatedly noticed by users [2–5]. Such phenomenon may lead to cement failure and is prevalent in climates characterized by relatively high temperature and humidity. The

principal consequences of prehydration for the engineering properties of cement are increased setting time, decreased compressive strength and heat of hydration, altered rheological properties and poor response to superplasticizer addition [6–9].

In particular, the surface composition of the individual clinker phases may be affected due to prehydration. Thus, the quality of cement must be assessed based on a profound understanding of the processes occurring during its fabrication and storage. Despite its importance, due to its complex nature and the difficulties associated with the analysis of hydration layers which extend to only a few nanometers in thickness, prehydration of cement is not well understood from the aspect of the interdependency of numerous chemical reactions. Obviously, prehydration of cement is far more complex than the sum of each individual prehydration reaction. Thus, this study on prehydration of pure clinker phases was performed to provide an understanding of the key processes taking place during sorption of water in the complex system of cement.

Ordinary Portland cement (OPC) consists of several clinker phases. The main constituents are variants of: calcium silicates (Ca_3SiO_5 and Ca_2SiO_4), calcium aluminate ($Ca_3Al_2O_6$), and ferrite ($Ca_4Al_{4-x}Fe_xO_{10}$) which are commonly denominated as C_3S , C_2S , C_3A and C_4AF , respectively. Jensen et al. showed that the clinker minerals C_3S , C_2S and C_3A have fundamentally different sensitivities to moisture [10]. For example, C_3A was shown to hydrate at lower relative humidities than either C_3S or C_2S . However, while some factors that govern clinker reactivity towards water vapour such as e.g. the free energy of the mineral's surface are known [11], we still lack in a complete understanding of the mechanisms by which certain cement components are more sensitive to prehydration than others.

* Corresponding author. Tel.: +49 89 289 13151; fax: +49 89 289 13152.
E-mail address: sekretariat@bauchemie.ch.tum.de (J. Plank).

Table 1
Physicochemical properties of the starting materials.

Material	Source	Purity (wt.%)	Average particle size d_{50} value (μm)
CaCO ₃	Merck	98.5	14
Al ₂ O ₃	Nabaltec	99.5	20
SiO ₂	Euroquarz	99	7
Fe ₂ O ₃	Lanxess	96	3
MgO	Merck	99	4
NaNO ₃	Merck	99	5

Even more important is the question whether prehydration is solely a reaction between cement and water vapour, or whether it occurs via water vapour condensation, followed by reactions between liquid water and cement. This latter case would entail that prehydration follows the well-known route of dissolution–oversaturation–precipitation in the same manner as during hydration of ordinary cement. Whereas in the first case, a totally different mechanism of prehydration leading to different hydration products may occur.

Generally, water vapour can be sorbed by cement either physically or chemically, or in both ways. Water molecules can physically bind to the surface of cement by van der Waals forces (adsorption), forming mono- and multilayers. At higher relative humidity, capillary condensation and capillary water uptake may occur. Both processes are physical by nature. Additionally, water can react chemically with clinker phases, yielding crystalline hydration products. The chemical incorporation of water into amorphous solids and the formation of early hydration products on the surface of cement particles can result in changes of the properties of cement powder. Generally, physically bound water will be reversibly desorbed when the water vapour pressure is decreased or the temperature is increased. In this case, the forces between the solid (adsorbent) surface and the vapour molecules (adsorbate) are weak. The forces involved in chemical reactions are much greater than those in physical adsorption. Therefore, chemically bound water will not be released by lowering RH to 1% for a short period of time. In this study, physically bound water was defined as water which can be removed by drying at 1% RH for 1 h only, while irreversibly sorbed water was considered to be bound chemically.

In the present work, the physicochemical effects of water sorption on the surfaces of pure clinker phases (monoclinic C₃S, monoclinic β -C₂S, cubic and orthorhombic C₃A and orthorhombic C₄AF) as well as of different sulfates (CaSO₄, β -CaSO₄ · ½H₂O, CaSO₄ · 2H₂O) and of free lime (CaO) were investigated using a water vapour balance instrument. The experiments were conducted to gain an understanding of the principle effects on individual cement constituents.

In this investigation, the RHs at which prehydration of the cement constituents starts to occur, and the amount of water sorbed per unit area of cement component surface were determined. Emphasis was placed on understanding the ratio between physically and chemically sorbed water, and the reversibility of this process. Measurements were

conducted at both 20 °C and 40 °C. Finally, the products formed as a result of sample exposure to water vapour were visually investigated by ESEM.

2. Materials and methods

2.1. Materials

Pure cement clinker minerals were prepared by calcination of the respective oxides or carbonates. The characteristics of the starting materials are given in Table 1. From the starting materials, mixtures with molar ratios corresponding to theoretical values were prepared according to Table 2 and homogenized by grinding in a ball mill for about 10 min. Powders were transferred into platinum crucibles and heated to the specific synthesis temperature (Table 2).

C₃S (alite) in monoclinic modification was stabilized by incorporation of 2 wt.% MgO and 1 wt.% Al₂O₃.

The sintering protocol for this phase included a 2 h heating ramp from 100 °C to 1450 °C, then maintaining a constant temperature of 1450 °C for 4 h. Immediately thereafter, the sample was quenched via rapid cooling by removing it from the oven. The sintering process was repeated 3 times until no reflections due to CaO could be observed by X-ray diffraction.

β -C₂S (belite in monoclinic modification) was stabilized by incorporation of 0.5 wt.% B₂O₃. The sintering protocol included 1 h 45 min heating ramp from 100 °C to 1300 °C, then keeping a constant temperature of 1300 °C for 3 h. Subsequently, the sample was quenched in the same manner as for alite. The disappearance of the peaks due to CaO and SiO₂ and progressing formation of β -C₂S was followed via X-ray diffraction.

Preparation of C₃A and C₄AF generally followed the procedures described by Wesselsky et al. [12]. Pure, undoped C₃A and orthorhombic C₃A doped with 4 wt.% Na₂O were prepared. The sintering protocol for cubic C₃A included a 1 h 50 min heating ramp from 100 °C to 1350 °C for the homogenized powders of CaCO₃ and Al₂O₃ mixed at stoichiometric ratio (3:1), followed by sintering the sample for 4 h at 1350 °C. Subsequently, the sample was quenched. After the first sintering process, mayenite (C₁₂A₇) and free lime were detected as minor byproducts. The sintering process was repeated 3 times to reduce the amount of mayenite and free lime to less than 0.1 wt.% each. For orthorhombic C₃A, NaNO₃ was first manually ground in an agate mortar for 10 min; then homogenized with CaCO₃ and Al₂O₃ in a ball mill for about 10 min. The homogenized powder was heated for 1 h 50 min from 100 °C to 1350 °C, then sintered at 1350 °C for 3 h and subsequently quenched. The sintering process was repeated several times. After the first burn, the amount of NaNO₃ was adjusted depending on the amount of free lime detected by XRD to exclude cubic C₃A as byproduct which can be attributed to the volatility of sodium at high temperatures.

Brownmillerite (C₄AF) was synthesized by sintering an idealized mixture of CaO, Al₂O₃ and Fe₂O₃ at molar ratios of 4:1:1. The oxides were first ground in a ball mill, then heated from 100 °C to 1250 °C

Table 2
Proportions, sintering temperature and periods used for the preparation of 100 g of each clinker phase.

Clinker phase	Amounts in g of							T (°C)/ time (h) ^a
	CaCO ₃	SiO ₂	Al ₂ O ₃	Fe ₂ O ₃	MgO	B ₂ O ₃	NaNO ₃	
Monoclinic C ₃ S (alite)	127.1	25.8	1.0	–	2.0	–	–	1450/4 h
Monoclinic β -C ₂ S (belite)	116.2	34.9	–	–	–	0.5	–	1300/3 h
Cubic C ₃ A (pure aluminate)	111.1	–	37.7	–	–	–	–	1350/6 h
Orthorhombic C ₃ A (doped aluminate)	98.1	–	34.5	–	–	–	14.5	1350/3 h
C ₄ AF (brownmillerite)	82.4	–	21.0	32.9	–	–	–	1250/4 h
CaO (free lime)	178.5	–	–	–	–	–	–	1000/3 h

^a The sintering process was repeated several times with intermediate grindings to exclude impurities in the form of minor phases.

and finally kept at 1250 °C in an oven for about 4 h. The sample was quenched by rapid cooling. The sintering process was repeated three times until no reflections due to CaO, Al₂O₃ and Fe₂O₃ could be observed by X-ray diffraction.

Free lime was prepared by calcination of CaCO₃ over 3 h at 1000 °C.

Grinding of all samples prepared was performed in a ball mill (Planetary Mono Mill PULVERISETTE 6 classic line, Fritsch, Idar-Oberstein, Germany) for 10 min at 250 rpm under air at a temperature of 21 °C and RH of 20%.

As calcium sulfates, gypsum (purity 98 wt.%), β-hemihydrate (purity 97 wt.%) and anhydrite (purity 99 wt.%) from Sigma-Aldrich were used.

Purity of synthesised phases was checked by quantitative X-ray powder diffraction (XRD) using a Bruker D8 Advance X-ray diffractometer (Bruker AXS, Karlsruhe, Germany) with a Bragg–Brentano geometry, equipped with a two-dimensional detector (Vantec-1®, Bruker AXS, Karlsruhe, Germany). The clinker phases were found to be pure within an accuracy of ± 1 wt.% for C₂S/C₃S and ± 0.5 wt.% for C₃A/C₄AF (Software for Rietveld analysis: Topas 3.0, Bruker AXS, Karlsruhe, Germany).

XRD patterns of all cement components tested in this study are presented in Fig. 1.

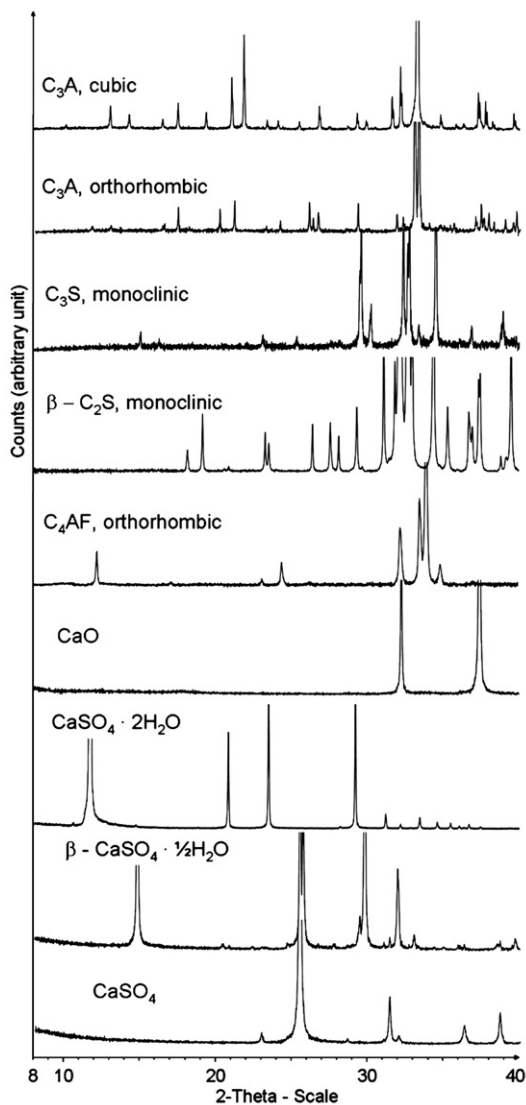


Fig. 1. XRD patterns of clinker phases as prepared and of cement components tested, shown in the range of 8–40° 2θ.

Table 3
Properties of synthesized pure clinker phases and cement constituents.

Cement constituent	Source	Chemical notation	Average particle size d_{50} value (μm)	Specific surface area (BET) (cm ² /g)
C ₃ S ^a , monoclinic	Self-prepared	Ca ₃ SiO ₅	8.1	5700
C ₂ S ^b , monoclinic	Self-prepared	Ca ₂ SiO ₄	7.4	5500
C ₃ A, cubic	Self-prepared	Ca ₃ Al ₂ O ₆	6.2	7800
C ₃ A, orthorhombic ^c	Self-prepared	Ca _{8,5} NaAl ₆ O ₁₈	9.0	7100
C ₄ AF, orthorhombic	Self-prepared	Ca ₄ Al ₂ Fe ₂ O ₁₀	12.9	2800
CaO	Self-prepared	CaO	4.7	24000
Gypsum	Sigma-Aldrich	CaSO ₄ · 2H ₂ O	32.2	7900
Hemihydrate	Sigma-Aldrich	CaSO ₄ · ½H ₂ O	10.4	12000
Anhydrite	Sigma-Aldrich	CaSO ₄	5.9	14000

^a Doped with 1 wt.% Al₂O₃ and 2 wt.% MgO.

^b Stabilized with 0.5 wt.% B₂O₃.

^c Doped with 4 wt.% Na₂O.

The average particle size (d_{50} value) of all phases tested was measured by laser granulometry (Cilas 1064, Cilas, Marcoussis, France). Specific surface area of all samples was determined by N₂ adsorption (BET method) employing a NOVA 4000e surface area analyzer from Quantachrome (Odelzhausen, Germany). The results are presented in Table 3.

2.2. Sorption balance instruments

Two sorption balances (DVS-1000 and DVS Advantage, both from Surface Measurement Systems Ltd., London, UK) were used to measure the moisture uptake of clinker phases, sulfates and CaO. Both sorption balances have similar mode of operation and differ merely in their software. Generally, a sorption balance allows automatic and quantitative measurement of sorption and desorption of water vapour or other gases on small scale samples (5–150 mg) [13]. Sorption balances have been employed successfully to determine the water sorption behaviour and kinetics of materials as diverse as textiles and food preparations [14,15]. The general set-up of a sorption balance is presented in Fig. 2. To conduct the measurement, the sample is placed in a sample pan of the microbalance. Both temperature and relative humidity can be programmed separately. The moisture uptake by the sample is measured while it is exposed to a nitrogen flow with a well defined RH of ±1%. RH is controlled by mixing dry and water vapour saturated nitrogen gas. The relative humidity can be changed either in steps or in ramps, and it can be increased or decreased. The microbalance has a resolution of 0.1 μg. In our experiments, nitrogen was supplied from a Nitrogen generator (G2, Domnick Hunter Ltd, Gateshead, England).

2.3. Experimental program for water vapour sorption

The moisture uptake can be investigated by different relative humidity programs constructed from RH-steps and RH-ramps [16,17]. In the present study, both ramp and step programs to investigate different aspects of the moisture uptake process were used. In all cases, the temperature was held constant at 20 °C or 40 °C during each measurement.

Fig. 3 shows the ramp program used in our study. There, RH is continuously increased from 1% to 95% RH at a constant rate of about 0.16% RH per minute. It is important to stabilise the sample for 1 h at 1% RH

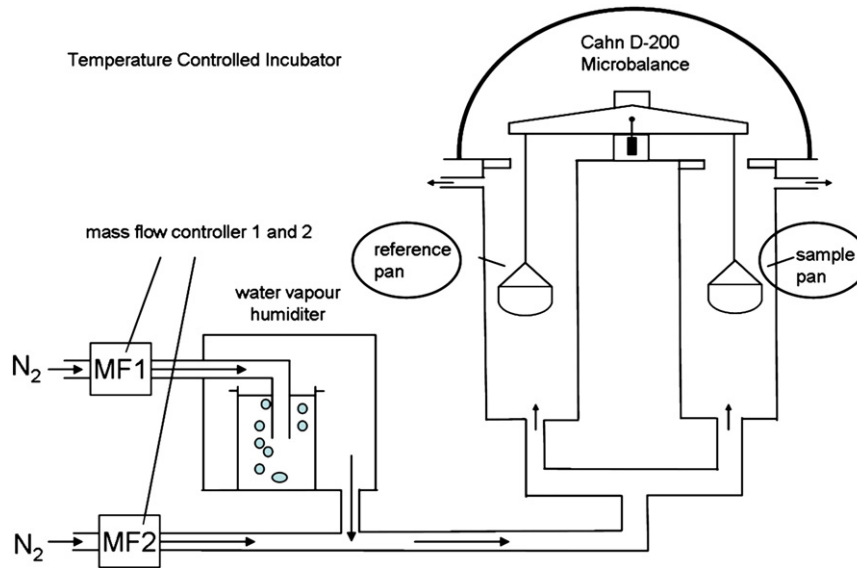


Fig. 2. Schematic illustration of a DVS instrument.

before increasing the relative humidity. Furthermore, at the end of the exposure to water vapour, each sample was subjected to 1%RH to distinguish between physically and chemically bound water. Whereas, with the ramp program it is possible to obtain a mass change profile for the sample. This makes it possible to assess the threshold value of RH (onset point) at which a sample starts to sorb water.

Fig. 4 shows the step and down program for relative humidities of between 60% and 95%. In this program, RH is increased from 1% to the desired RH, and then decreased again to 1% RH. This program makes it possible to distinguish between physically and chemically bound water. The physically bound water can be removed by drying at 1%RH (reversible process); while the chemically bound water cannot be removed from the surface after reaction with water vapour (irreversible process). All experiments in this mode were performed at high RHs between 60% and 95%. For calculation of the reversibly and irreversibly bound mass of water (w), the following formula was used:

$$w = \frac{m(\varphi)_i - m_0}{m_0} \quad (1)$$

where φ is the relative humidity, $m(\varphi)_i$ is the mass of the sample after water vapour sorption, and m_0 is the initial dry mass of the sample. All experiments with the program in step and down mode were done at both 20 °C and 40 °C to determine the temperature influence on the water vapour uptake. The limitation of this method is that it requires samples to achieve the sorption–desorption equilibrium within 1 h. This may or may not be the case with the samples tested here, and establishment of equilibrium conditions was not checked here. A further problem in the interpretation of the data may relate to the potential presence of induction period phenomena occurring in the reactive processes involved here [11]. Therefore, values obtained according to this method should be interpreted as qualitative, and not be taken as quantitative and final.

2.4. SEM imaging

Scanning electron microscopy (SEM) images were obtained from a FEI XL 30 FEG microscope equipped with a large field detector under low vacuum conditions (1 mbar H₂O pressure, corresponding to ~4% RH at room temperature). Observations on the morphology of the products

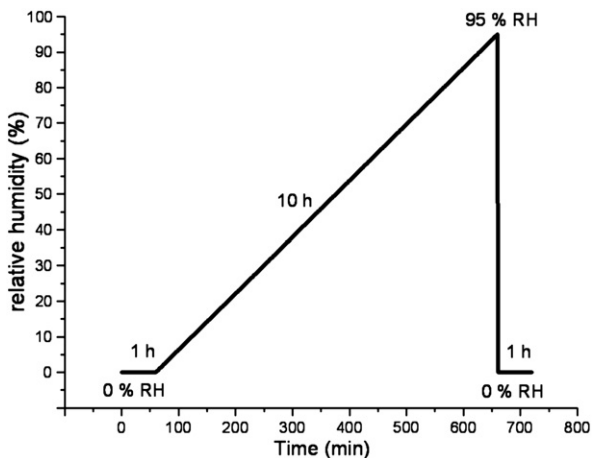


Fig. 3. Development of relative humidity over time used in the ramp program.

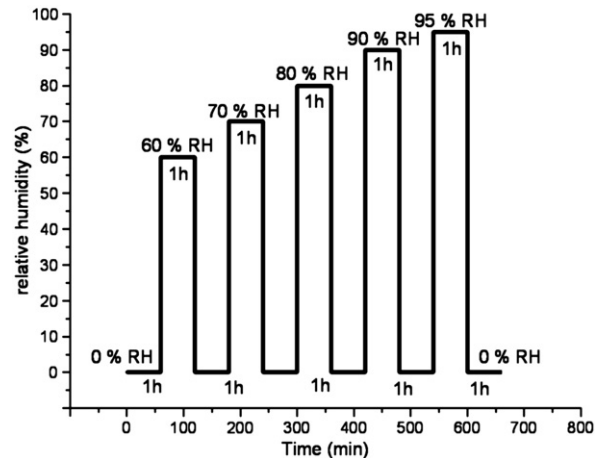


Fig. 4. Relative humidity program used in the step and down mode.

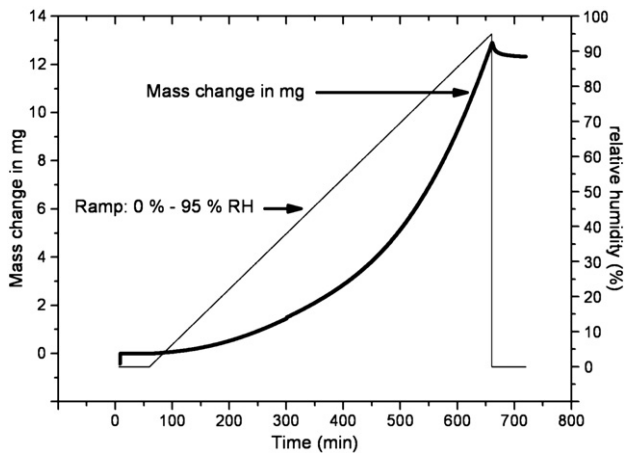


Fig. 5. Water vapour sorption of CaO, determined on a sorption balance at 20 °C using the ramp mode and measured over a period of 11 h (initial mass of sample: 90.2192 mg).

were performed on uncoated samples before and after exposure to relative humidity after storage in the sorption balance instrument.

3. Results and discussion

3.1. Total water sorption

The cement constituents tested showed significantly different mass change profiles in the range between 1% and 95% RH. Generally, three different behaviours were observed.

First, CaO (free lime) already starts to sorb water at very low relative humidity (<10% RH). Its uptake of water increases exponentially with RH. Fig. 5 shows the mass change profile of CaO using the ramp program. The CaO sample investigated sorbed a total of 0.14 mg of water per mg CaO over a period of 11 h. This amount corresponds to ~40% conversion of CaO to portlandite $\text{Ca}(\text{OH})_2$. Obviously, free lime strongly attracts water vapour and possibly acts as a drying agent (desiccant) in cement. When in the final part of the experiment humidity was decreased from 95% to 1% RH, not much desorption of water did occur.

Thus, it confirms that almost all of the water sorbed by CaO is irreversibly (chemically) bound.

Second, some clinker minerals such as C_3A or C_4AF exhibit a very minor uptake of water until a specific threshold RH value is exceeded. This point – “the threshold point” or on-set – varies with type of clinker phase, temperature and specific surface area of the individual phase. Fig. 6 shows

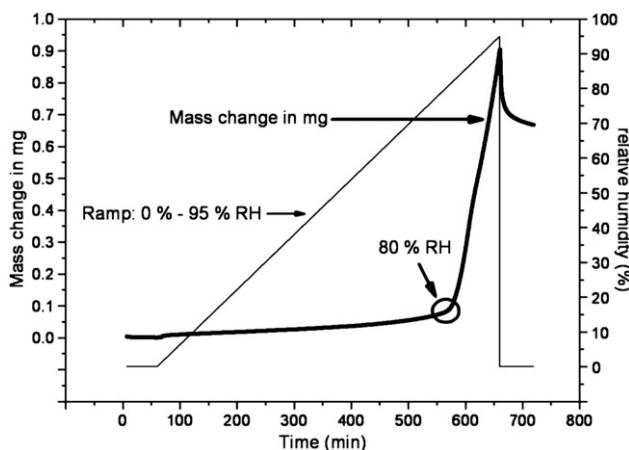


Fig. 6. Water vapour sorption of cubic C_3A , determined on a sorption balance at 20 °C using ramp mode and measured over a period of 11 h (initial mass of sample: 97.3439 mg).

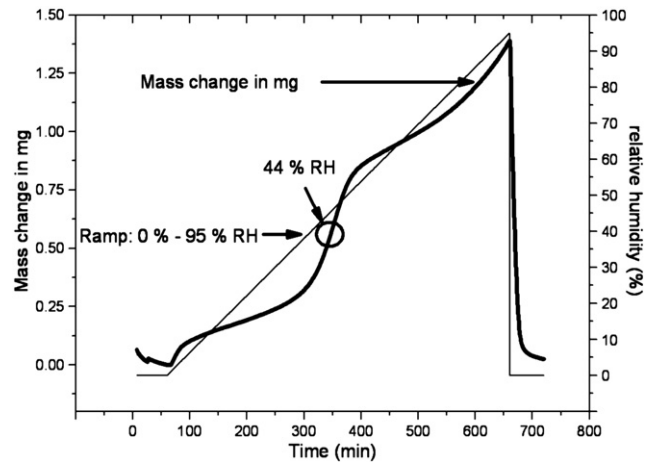


Fig. 7. Water vapour sorption of $\beta\text{-CaSO}_4 \cdot \frac{1}{2}\text{H}_2\text{O}$, measured on a sorption balance at 20 °C, using ramp mode, measured over a period of 11 h (initial mass of sample: 74.9417 mg).

as an example the mass change profile for cubic C_3A . Beginning at 80% RH, cubic C_3A starts to take up a noticeable amount of water vapour. In this experiment, C_3A sorbed ~0.9 wt.% of water, based on the dry mass of C_3A . From this value, 0.7 wt.% was not removable and thus bound by chemical reaction of C_3A .

The third category is represented by the sulfates. At increasing humidity, they exhibit a characteristic, step-wise uptake of water. Fig. 7 displays a typical mass change diagram for $\beta\text{-CaSO}_4 \cdot \frac{1}{2}\text{H}_2\text{O}$. Its mass change profile developed in the ramp mode shows an on-set point for water sorption at around 34% RH and several inflexion points, the most significant one at 44% RH. This behaviour can be interpreted such that at ~34% RH, rapid hydration of β -hemihydrate begins until it slows down at RH values beyond 60%.

Table 4 summarizes the RH values of the on-set point for water uptake (i.e. the RHs at which water sorption starts to occur) for all cement constituents tested as obtained from the mass change profiles.

3.2. Distinction between chemically and physically sorbed water

The amount of chemically and physically bound water can be differentiated by studying water sorption using the step mode. Tests performed at RHs between 60% and 95% again showed different types of water vapour sorption behavior by the cement constituents tested.

Three different kinds of water uptake were observed:

- Water vapour is mostly sorbed chemically; the water is bound irreversibly to the phase and cannot be removed by drying for 1 h at 1% RH and 20 °C. An example for this behaviour is free lime (see Fig. 8).
- Water vapour is sorbed both chemically and physically; the physically sorbed part of water can be removed by drying at 1%

Table 4

Relative humidities at which cement constituents start to take up water vapour, measured on a sorption balance at 20 °C using the ramp mode.

Cement constituents	Relative humidity at which water sorption starts (%)
CaO	<10
$\text{CaSO}_4 \cdot 2\text{H}_2\text{O}$	24
$\beta\text{-CaSO}_4 \cdot \frac{1}{2}\text{H}_2\text{O}$	34
C_3A , orthorhombic	55
CaSO_4	58
C_2S , monoclinic	64
C_3S , monoclinic	63
C_4AF , orthorhombic	78
Pure C_3A , cubic	80

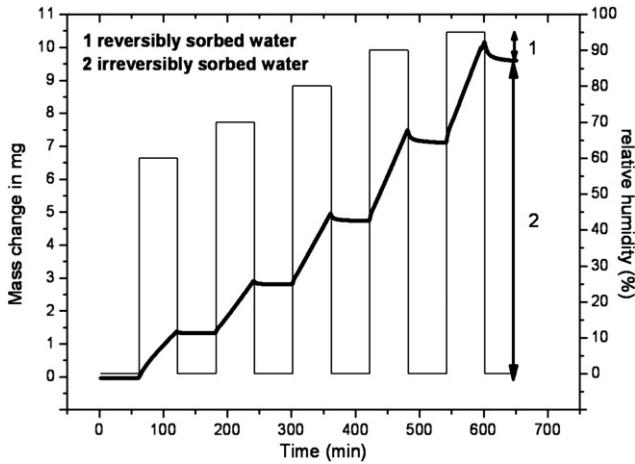


Fig. 8. Determination of physically (1) and chemically (2) sorbed water on CaO, measured on a DVS instrument at 20 °C using step and down mode (initial mass of sample was: 58.5219 mg).

RH; whereas, the chemically sorbed part cannot be removed by drying. This behaviour is represented by cubic C₃A (see Fig. 9).
 (c) Water vapour is mostly sorbed physically and can be removed almost completely by drying at 1% RH. Such behaviour is exemplified by β-CaSO₄ · ½H₂O (see Fig. 10).

Free lime sorbs all water vapour irreversibly and reacts to form portlandite. Only at very high RHs (around 90–95%), a small amount of physically bound water can be removed. This pronounced ability of CaO to sorb water vapour very quickly and irreversibly can possibly reduce or even prevent prehydration of other constituents when cement is exposed to moisture during storage. Thus, cements exhibiting a relatively high content of free lime possibly sorb more water than cements possessing a low amount of free lime. Cubic C₃A, on the other hand, is an example of a cement constituent which shows both physical and chemical sorption. Its chemical sorption leads to the formation of C-A-H phases.

For β-CaSO₄ · ½H₂O, most of the water vapour uptake is reversible, and thus can be removed by drying at 1% RH. This result is unexpected, because β-CaSO₄ · ½H₂O is known to react almost instantaneously with liquid water to form gypsum. For this reason, it is commonly applied with set retarders to achieve practical setting times in building products. However, this reaction normally occurs via the dissolution–oversaturation–precipitation mechanism. Here, β-

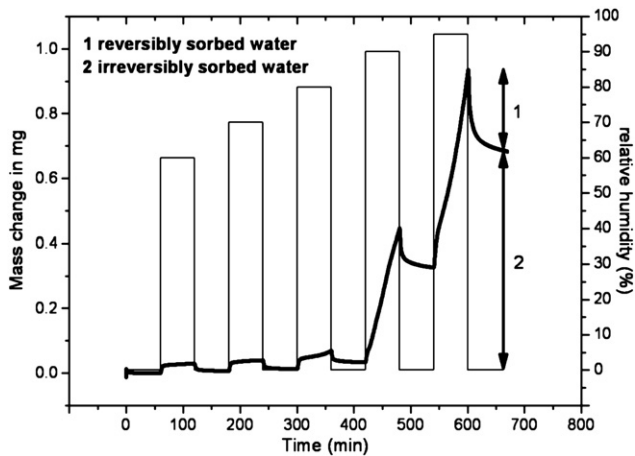


Fig. 9. Determination of physically (1) and chemically (2) sorbed water on cubic C₃A, measured on a DVS instrument at 20 °C using step and down mode (initial mass of sample: 58.8794 mg).

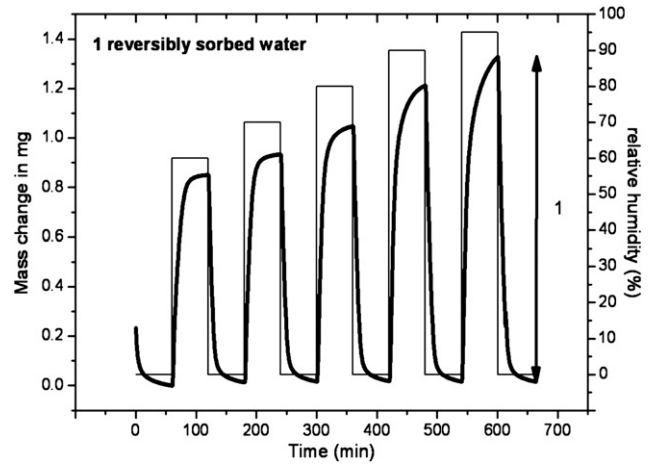


Fig. 10. Determination of physically (1) sorbed water on β-CaSO₄ · ½H₂O, measured on a DVS instrument at 20 °C using step and down mode (initial mass of sample: 68.4202 mg).

CaSO₄ · ½H₂O obviously does not dissolve and react, but sorbs water molecules only physically.

Table 5 presents a summary on the water sorption measured for all samples tested by using the two different methods (ramp and step and down mode). There, the amount of water sorbed by each cement constituent tested at 20 °C over a period of 11 h is presented as wt.% of original mass of sample and as mass per unit of specific surface area of sample. It becomes obvious that free lime and – to less extent – doped orthorhombic C₃A sorb the highest amount of water, followed by the calcium sulfates. Whereas, the silicates show only a minor uptake of water.

Because water vapour sorption first and above all is a surface process, the uptake of water by a surface is directly linked to its granular size which is expressed by its specific surface area. To account for this, the amount of water sorbed per unit area was calculated using the values for the specific surface area (BET method) of the fresh, non-prehydrated samples as shown in Table 3. Additionally, it was found that the BET surface area of the fresh samples did not change much as a result of water sorption. Thus, the values shown in Table 5 represent the amount of water sorbed per unit of surface area of the non-prehydrated sample. Generally, the relative order of the samples was found to be independent of the test mode. Fig. 11 shows a comparison of relative water uptake per specific surface area for different cement constituents tested. There, it becomes obvious that free lime and doped, orthorhombic C₃A by far sorb the highest amounts of water per surface area (~50–60 · 10⁻⁷ g/cm²). This is followed at some distance by β-CaSO₄ · ½H₂O

Table 5

Total mass changes of cement constituents obtained from DVS measurements for two different modes of exposure to humidity.

Cement constituent	Mass change after exposure to max. 95% relative humidity at 20 °C			
	Ramp method		Step and down method	
	(wt.%)	($\frac{10^{-7} \text{g}}{\text{cm}^2}$)	(wt.%)	($\frac{10^{-7} \text{g}}{\text{cm}^2}$)
CaO	14.24	59.3	17.35	72.3
C ₃ A, orthorhombic	3.62	51.0	5.29	74.5
CaSO ₄ · ½H ₂ O	1.85	15.4	1.94	16.2
C ₄ AF, orthorhombic	0.40	14.3	0.37	13.2
C ₃ A, cubic	0.92	11.8	1.57	20.1
CaSO ₄	1.03	7.4	1.01	7.2
CaSO ₄ · 2H ₂ O	0.40	5.1	0.36	4.6
C ₃ S, monoclinic	0.09	1.6	0.08	1.4
C ₂ S, monoclinic	0.09	1.6	0.04	0.7

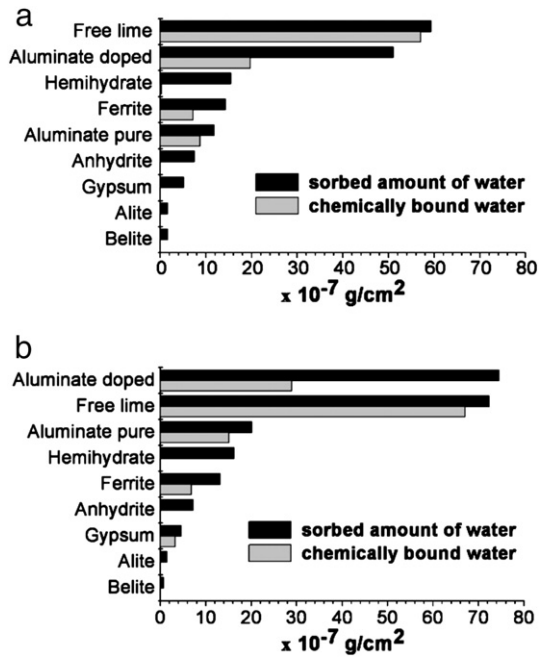


Fig. 11. Comparison of relative water uptake per unit of specific surface area for different cement constituents tested in a) ramp mode and b) step and down mode.

($\sim 15 \cdot 10^{-7} \text{ g/cm}^2$), C_4AF ($\sim 14 \cdot 10^{-7} \text{ g/cm}^2$) and undoped, cubic C_3A ($\sim 12 \cdot 10^{-7} \text{ g/cm}^2$). While the silicates sorb a surprisingly low amount of water ($\sim 1.6 \cdot 10^{-7} \text{ g/cm}^2$). Taking into account that the density of sorbed water is roughly 1 g/cm^3 we can estimate the equivalent thicknesses of the water layers sorbed on the surfaces of CaO and C_3S as $\sim 60 \text{ nm}$ and 1.6 nm , respectively.

This result instigates that in some cases such as for the silicates, prehydration entails only a very minor portion of the bulk substance. In this case, an ultra-thin layer of only few nanometer thickness is being formed. Still, these small amounts of sorbed water can affect the chemical and engineering properties of the calcium silicates, causing for example retardation of hydration and decreased early strength [9]. While for other cement constituents, prehydration probes much deeper into the bulk material and affects a large portion of it. A representative example for this behaviour is free lime where a significant portion of the bulk material is chemically converted to portlandite.

3.3. ESEM imaging

Fig. 12 shows ESEM images of fresh, anhydrous cubic C_3A and of the same sample prehydrated with water vapour at 20°C in the step and down program. The specimen exposed to water vapour exhibits numerous platelets of C-A-H phases whereas the surface of the anhydrous C_3A is free of them.

Additional ESEM images of both fresh and prehydrated $\beta\text{-CaSO}_4 \cdot \frac{1}{2}\text{H}_2\text{O}$ are in perfect agreement with the results obtained from sorption balance measurements. No changes on the surface of the binder were detected after prehydration (Fig. 13).

3.4. Effect of temperature on water vapour sorption

For all samples, the moisture capacity profiles were also measured at 40°C in the step and down mode to elucidate the effect of temperature on water vapour sorption. Comparison of the sorption profiles obtained at 20°C and 40°C , respectively, indicates that increased temperature shifts the on-set point where uptake of water begins to lower RHs. The strongest effect of increased temperature was observed for pure C_3A (Fig. 14). Additionally, increasing the

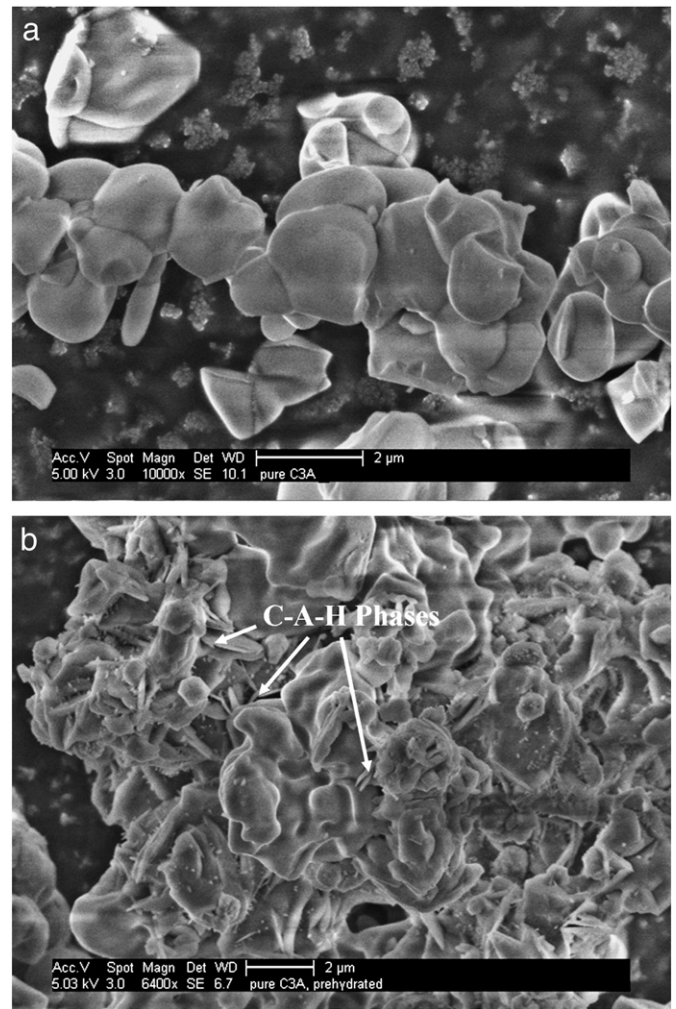


Fig. 12. ESEM images of cubic C_3A : a) fresh, anhydrous; b) prehydrated over 5 h at 60–95% RH and subsequently dried at 1% RH for 1 h at 20°C .

temperature also led to a significantly higher water uptake. For C_3A , at 40°C and 80%RH, the total amount of sorbed water is ~ 5 times higher than that at 20°C . At both temperatures, the amount of water chemically bound by C_3A generally increases when RH exceeds 80% RH. This phenomenon is explained by the different values of absolute humidity existing in the gas phase at different temperatures. Generally, the water vapour pressure at saturation is a function of temperature. Consequently, the absolute water content occurring at a constant RH increases with temperature. At any RH, at 40°C there is about three times more water vapour present in the atmosphere than at 20°C . This higher concentration of water increases the rate of water sorption and results in faster achievement of the sorption equilibrium.

For CaO , increased temperature accelerated water sorption so much that already between 60% and 70%RH, most of the CaO was completely hydrated (Fig. 15). Sorption by CaO was largely irreversible and occurred at a significantly higher rate at 40°C . Obviously, the rate of reaction with water inside the CaO particles is significantly increased by higher temperature. As a rule of thumb, chemical reactions double their kinetics every 10 K, so the increase observed for CaO is to be expected. At 40°C and 80% RH, still a small amount of physically, reversibly bound water was found for CaO . This instigates that at this stage, CaO is almost completely converted to $Ca(OH)_2$ which can sorb water only via physical sorption. This amount is removed by drying at 1% RH.

Opposite to CaO , for some cement constituents, an increase of temperature only slightly affected their water sorption. For example,

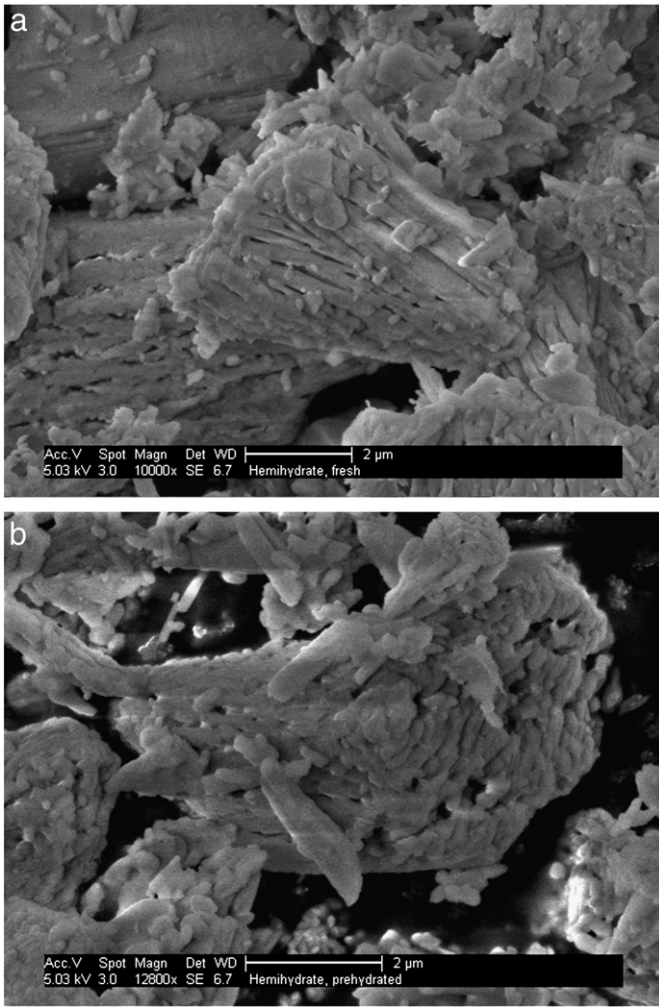


Fig. 13. ESEM images of $\beta\text{-CaSO}_4 \cdot \frac{1}{2}\text{H}_2\text{O}$: a) fresh; b) prehydrated at 20 °C over 5 h at 60–95% RH and subsequently dried at 1% RH for 1 h.

at 40 °C $\beta\text{-CaSO}_4 \cdot \frac{1}{2}\text{H}_2\text{O}$ does not show a significant increase in the total amount of sorbed water (Fig. 16). This behavior instigates that this phase sorbs water only through physical sorption which is quite independent of temperature.

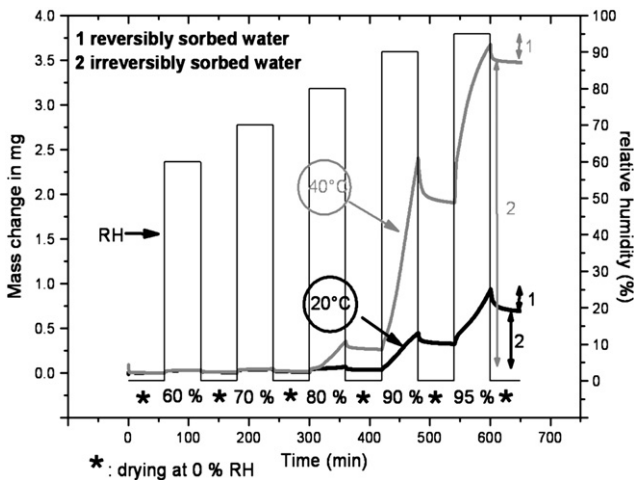


Fig. 14. Water vapour sorption isotherms for pure C_3A , measured at 20 °C and 40 °C, respectively, in step and down mode (initial masses of samples: $m(20\text{ °C}) = 58.8794\text{ mg}$, $m(40\text{ °C}) = 56.2018\text{ mg}$).

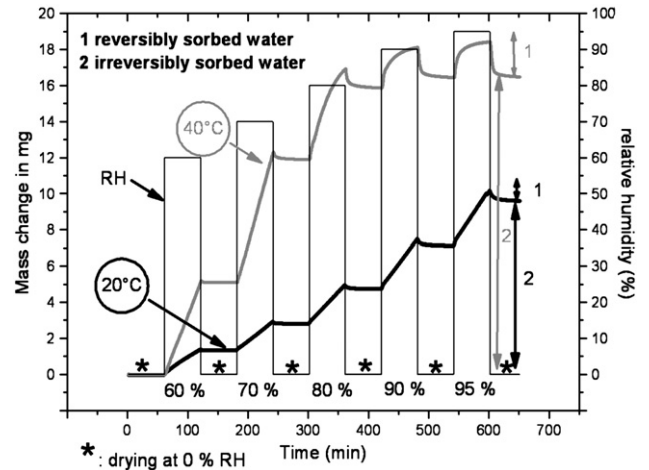


Fig. 15. Water vapour sorption isotherms for CaO measured at 20 °C and 40 °C, respectively, in step and down mode (initial masses of samples: $m(20\text{ °C}) = 58.5219\text{ mg}$; $m(40\text{ °C}) = 53.005\text{ mg}$).

Finally, Table 6 gives a comparison of the total amounts of water sorbed at 20 °C and 40 °C, respectively, for all samples tested. The values in the table present the amount of water sorbed in percentage, milligram and per unit of specific surface area (BET method). The results show that increased temperature which results in an increased amount of water content in the gas phase affects the samples quite differently. Some cement constituents, e. g. C_3A and CaO, sorb more water at 40 °C whereas others (e. g. $\beta\text{-CaSO}_4 \cdot \frac{1}{2}\text{H}_2\text{O}$) respond less to an increase in temperature, because they only show physical adsorption which is more rapid.

4. Conclusions

This study demonstrated that a dynamic vapour sorption balance is a very useful instrument to investigate the interaction between gaseous water and cement constituents. The sorption of water vapour on pure clinker phases, calcium sulfates and CaO was studied at different RHs and temperatures using ramp and step and down programs for adjusting RH. Investigation via ESEM complemented and confirmed the results obtained with the sorption balance instrument. From the aforementioned results of this study, the following conclusions could be obtained:

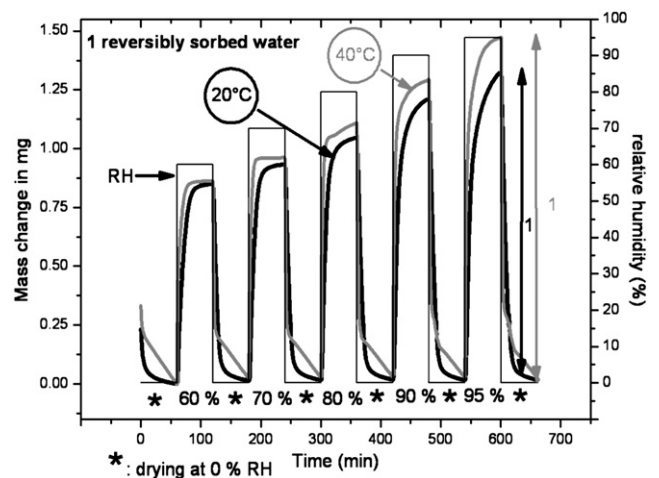


Fig. 16. Water vapour sorption isotherms for $\beta\text{-CaSO}_4 \cdot \frac{1}{2}\text{H}_2\text{O}$ measured at 20 °C and 40 °C, respectively, in step and down mode (initial masses of samples: $m(20\text{ °C}) = 68.4202\text{ mg}$; $m(40\text{ °C}) = 59.3159\text{ mg}$).

Table 6

Comparison of mass changes for samples tested at 20 °C and 40 °C, respectively, in step and down mode.

Cement constituent	Mass change after exposure to humidity					
	T = 20 °C			T = 40 °C		
	(wt.%)	(mg)	$\left(\frac{10^{-7} \text{g}}{\text{cm}^2}\right)$	(wt.%)	(mg)	$\left(\frac{10^{-7} \text{g}}{\text{cm}^2}\right)$
C ₃ A, orthorhombic	5.29	3.45	74.5	13.55	11.22	190.8
CaO	17.35	10.10	72.3	34.75	18.42	144.8
C ₃ A, cubic	1.57	0.93	20.1	6.53	3.67	83.7
β-CaSO ₄ · ½H ₂ O	1.94	1.32	16.2	2.48	1.47	20.7
C ₄ AF, orthorhombic	0.37	0.27	13.2	0.99	0.91	35.4
CaSO ₄	1.01	0.93	7.2	1.52	3.06	10.9
CaSO ₄ · 2H ₂ O	0.36	0.21	4.6	0.85	0.42	10.8
C ₃ S, monoclinic	0.08	0.07	1.4	0.24	0.18	4.2
C ₂ S, monoclinic	0.04	0.01	0.7	0.17	0.18	3.1

Cement constituents show fundamentally different onset points at which water uptake starts to occur. The amount of sorbed water per specific surface was differentiated for each cement constituent. It showed that sorbed water can be bound physically, chemically or in both ways. The experiments demonstrated that both free lime and orthorhombic C₃A sorb large amounts of water. They are followed by β-CaSO₄ · ½H₂O and cubic C₃A. C₄AF, gypsum and anhydrite sorb very low amounts of water, whilst the silicates C₃S and C₂S sorb almost no water at all.

A comparison of the sorption isotherms at 20 °C and 40 °C indicates that for all clinker phases, increasing temperature causes moisture uptake to occur at lower RHs. Obviously, different cement constituents exhibit very different behaviour towards water vapour at high temperature.

The subject of prehydration of cement is highly interesting for cement manufacturers and applicators. Therefore several questions on this phenomenon should be clarified in further investigations. For example, the impact of water vapour on the behaviour of binary mixtures, with a focus on C₃A mixed with different calcium sulphates, should be studied in more detail. Such experiment may give an answer to the question whether the mechanism behind prehydration is solely based on a topochemical reaction between cement and water vapour, or whether it entails a reaction with liquid condensed water which follows the well known route of cement hydration characterized by a dissolution–oversaturation–precipitation process.

Furthermore, prehydration of pure clinker phases and other cement constituents should be studied in presence of CO₂ to understand the synergistic impact of CO₂ and water vapour on the ageing of cement.

Acknowledgments

The authors are grateful to Nanocem (Core Project # 7) for the financial support of this work. Additionally, the authors like to thank Leon Black, University of Leeds/U.K and Holger König, HeidelbergCement, Leimen/ Germany for their input in many discussions.

References

- [1] A.E. Mould, D.W. Williams, The effects of high ambient temperatures on gypsum plasters, *Build. Sci.* 9 (1974) 243–245.
- [2] C. Maltese, C. Pistolesi, A. Bravo, F. Cella, T. Cerulli, D. Salvione, Effect of moisture on the setting behavior of Portland cement reacting with an alkali-free accelerator, *Cem. Concr. Res.* 37 (2007) 856–865.
- [3] G. Schmidt, T.A. Bier, K. Wutz, M. Maier, Characterization of the ageing behavior and its effect on their workability properties, *ZKG Int.* 60 (6) (2007) 94–103.
- [4] C.-S. Deng, C. Breen, J. Yarwood, S. Habesch, J. Phipps, B. Caster, G. Maitland, Ageing of oilfield cement at high humidity: a combined FEG-ESEM and Raman microscopic investigation, *J. Mater. Chem.* 12 (2002) 3105–3112.
- [5] F. Winnefeld, Influence of cement ageing and addition time on the performance of superplasticizer, *ZKG Int.* 61 (11) (2008) 68–77.
- [6] V.S. Sprung, Effect of storage conditions on the properties of cements, *ZKG Int.* 30 (6) (1978) 305–309.
- [7] K. Theisen, V. Johansen, Prehydration and strength development of Portland cement, *J. Am. Ceram. Soc. Bull.* 54 (9) (1975) 787–791.
- [8] L. Barbic, V. Tinta, B. Lozar, V. Marinkovic, Effect of storage time on the rheological behavior of oil well cement slurries, *J. Am. Ceram. Soc.* 74 (5) (1991) 945–949.
- [9] E. Dubina, L. Black, R. Sieber, J. Plank, Interaction of water vapour with anhydrous cement minerals, *Adv. Appl. Ceram.* 109 (5) (2010) 260–268.
- [10] O.M. Jensen, P. Hansen, E.E. Lachowski, F.P. Glasser, Clinker mineral hydration at reduced relative humidities, *Cem. Concr. Res.* 29 (1999) 1505–1512.
- [11] O.M. Jensen, Thermodynamic limitation of self-desiccation, *Cem. Concr. Res.* 25 (1995) 157–164.
- [12] A. Wesselsky, O.M. Jensen, Synthesis of pure Portland cement phases, *Cem. Concr. Res.* 39 (2009) 973–980.
- [13] A. Anderberg, L. Wadsö, Method for simultaneous determination of sorption isotherms and diffusivity of cement-based materials, *Cem. Concr. Res.* 38 (2008) 89–94.
- [14] D. Enke, M. Rückriem, A. Schreiber, J. Adolphs, Water vapour sorption on hydrophilic and hydrophobic nanoporous materials, *Appl. Surf. Sci.* 256 (2010) 5482–5485.
- [15] Ch.C.W. Spackman, Sh.J. Schmidt, Characterising the physical state and textural stability of sugar gum pastes, *Food Chem.* 119 (2010) 490–499.
- [16] L. Wadsö, N. Markova, Comparison of three methods to find the vapour activity of a hydration step, *Eur. J. Pharm. Biopharm.* 51 (2001) 77–81.
- [17] L. Wadsö, A. Anderberg, I. Åslund, O. Söderman, An improved method to validate the relative humidity generation in sorption balances, *Eur. J. Pharm. Biopharm.* 72 (2009) 99–104.

Paper 2

Impact of Water Vapour and Carbon Dioxide on Surface Composition of C₃A Polymorphs Studied by X-ray Photoelectron Spectroscopy

E. Dubina¹, L. Black², J. Plank¹

*¹Technische Universität München, Lehrstuhl für Bauchemie, Lichtenbergstr. 4, 85747 Garching bei München,
Germany*

²Institute for Resilient Infrastructure, School of Civil Engineering, University of Leeds, Leeds, LS2 9JT, UK

To be submitted to Cement and Concrete Research

Abstract

The surface specific analytical method, x-ray photoelectron spectroscopy (XPS), was used to study the effects of water vapour and CO₂ on the cubic and orthorhombic polymorphs of C₃A. Significant differences were observed in the XPS spectra. Upon exposure to water vapour, both polymorphs produced C₄AH₁₃ on their surfaces. Additionally, o-C₃A developed NaOH and traces of C₃AH₆ on its surface. Subsequent carbonation yielded monocarboaluminate on both polymorphs. Large amounts of Na₂CO₃ were also formed on the surface of o-C₃A as a result of carbonation of NaOH. Furthermore, the extent of carbonation was much more pronounced for o-C₃A than for c-C₃A modification.

Key words: Ca₃Al₂O₆ polymorphs (D), water vapour, carbonation (C), X-ray photoelectron spectroscopy

1. Introduction

Tricalcium aluminate (C₃A) constitutes ~ 2 – 12 wt. % of an ordinary Portland cement (OPC, CEM I). In industrial cement, C₃A usually occurs as one of two polymorphs: cubic or orthorhombic. It is well known that C₃A can incorporate a large number of minor and trace elements into its crystal structure [1 – 4]. The impact of these elements on the crystal structure as well as the hydration behaviour and kinetics has been thoroughly discussed in previous works [5 – 7].

Among those impurities, alkalis (K₂O, Na₂O) appear to be the most important modifying oxides. These oxides are able to change the crystal system of C₃A from cubic to orthorhombic and to monoclinic [8], and sodium oxide plays a significant role in stabilising different modifications of C₃A. The structure of pure, undoped, cubic C₃A has been determined by

Mondal and Jeffery. They also discussed the solid solutions of the $\text{Na}_2\text{O}-\text{C}_3\text{A}$ series [9]. Isomorphic substitution of calcium by sodium in solid solutions formed at 1250 °C leads to crystallisation into the cubic polymorph at Na_2O contents of 0 - 2.5 % (by mass), the orthorhombic polymorph at 3.5 - 4.2 % Na_2O , and the monoclinic polymorph at > 4.2 % Na_2O [10].

C_3A is the most reactive cement clinker phase. In the absence of soluble sulphates, it instantaneously forms massive amount of hydration products, mainly calcium aluminate hydrates (C-A-H phases of different stoichiometric compositions). Owing to this high reactivity, C_3A can react with atmospheric water vapour during storage and cause a phenomenon known as prehydration of cement [11]. It has been demonstrated that of all the cement constituents, C_3A reacts preferably with water vapour when cement is prehydrated [12], with an impact on the setting behaviour of the cement [13]. However, the cubic and orthorhombic C_3A polymorphs exhibit different behaviours when exposed to water vapour. For orthorhombic C_3A , the onset point at which water sorption starts to occur lies at 55 % relative humidity (RH) compared to 80 % RH for cubic C_3A [14].

Prehydration is predominantly a surface reaction, hence common bulk analysis methods such as x-ray diffraction are not useful. Instead, surface specific analytical techniques such as x-ray photoelectron spectroscopy (XPS) can provide information on the composition and speciation of the prehydrated surface, without interference from the unaffected bulk material. In XPS, the sample is irradiated with low-energy (~1.5 keV) x-rays in order to provoke the photoelectric effect, with the energy of the emitted photoelectrons being characteristic of the element from which they are emitted and the chemical state of the element. The low energy of the photoelectrons ensures that only those emitted from the surface of the irradiated sample

are detected. Consequently, XPS allows the analysis of surface layers with thicknesses of 1 to 12 nm only, with all elements bar hydrogen being capable of identification [15].

In the present study, the impact of initial exposure of C_3A to moisture, followed by interaction with atmospheric CO_2 , was investigated by XPS. Furthermore, the influence of Na_2O , present in the orthorhombic modification of C_3A , on these processes was studied. From the results it was aimed to develop an understanding of the actual chemical composition occurring in the surface of prehydrated and slightly carbonated C_3A samples.

2. Materials and Methods

2.1 Synthesis of C_3A polymorphs

Pure, undoped cubic C_3A and orthorhombic C_3A doped with 4 wt. % Na_2O were synthesised according to the literature using calcium carbonate and aluminium oxide as starting materials [14]. In the preparation of orthorhombic C_3A , sodium nitrate was used as Na_2O source to achieve the doping. The sintered samples were removed from the oven, allowed to cool in air for 3 minutes in covered Pt crucibles and then immediately placed in the cup of a steel ball mill (Planetary Mono Mill PULVERISETTE 6 classic line, Fritsch, Idar-Oberstein, Germany). Grinding was performed in air at 250 rpm for 10 minutes at a temperature of 21 °C without the addition of a grinding agent. The ground samples were stored in sealed 20 mL glass bottles placed in a vacuum desiccator.

According to quantitative X-Ray diffraction (XRD) analysis of freshly prepared samples, the C_3A phases were 99 ± 0.5 wt. % pure. Their XRD patterns are presented in **Figure 1**. Furthermore, FTIR-ATR spectra of the synthesised C_3A samples were obtained to confirm phase purity. **Figure 2** shows the characteristic differences between the two polymorphs: for

orthorhombic C_3A , the number of IR bands decreases as a result of altered symmetry of the Al_6O_{18} ring ($C_3 \rightarrow C_1$). Furthermore, partial substitution of Ca^{2+} by Na^+ leads to disordering of the structure and thus broadening of the bands [2].

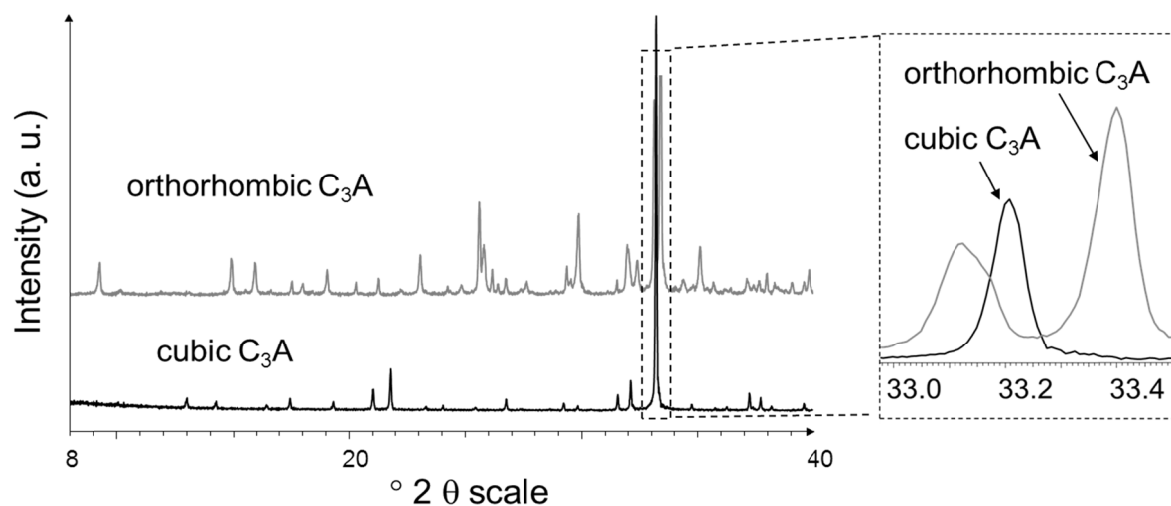


Fig. 1. XRD patterns of cubic and orthorhombic C_3A phases as prepared, shown in the range of 8 – 40 ° 2θ scale

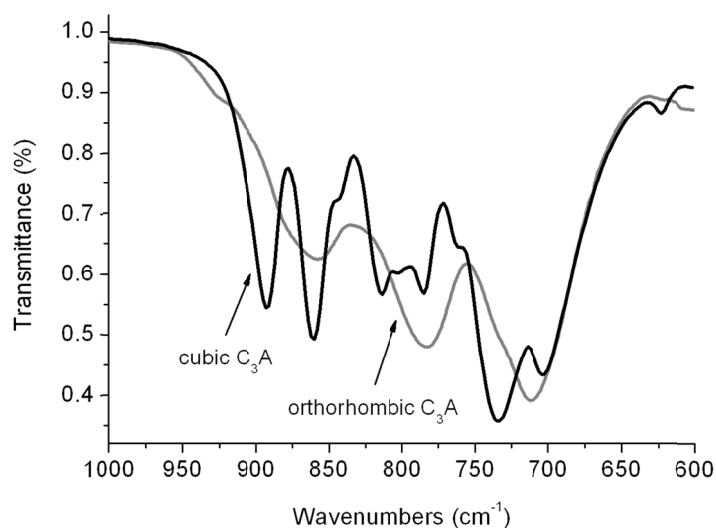


Fig. 2. FTIR-ATR spectra of cubic and orthorhombic C_3A phases as prepared, shown in the range between 600 – 1000 cm^{-1}

The surface of orthorhombic C_3A was investigated by scanning electron microscopy (SEM) using a FEI XL 30 FEG microscope equipped with a large field detector under low vacuum

conditions (1 mbar H₂O pressure, corresponding to ~ 4 % RH at room temperature). The sample exposure was as for the XPS experiments.

2.2 Water and CO₂ exposure of samples

200 mg of powdered C₃A were pressed into pellets (d = 13 mm) at a pressure of 50 N/mm² using a hydraulic press. The pellets of cubic and orthorhombic C₃A were then refired at 1350 °C for 3 h (c-C₃A) or 20 minutes (o-C₃A) to achieve complete dehydration and decarbonation.

However, preliminary XPS analysis of the C₃A pellets still showed evidence for slight carbonation. Thus, to obtain a completely pristine surface, all samples were etched by argon ion bombardment under vacuum in the photoelectron spectrometer, prior to any exposure to water vapour and CO₂.

To study the impact of water vapour on the C₃A polymorphs the pellets were exposed to a N₂ gas atmosphere containing a defined amount of water vapour. Pellets were placed in a nitrogen gas filled desiccator, which was placed in a glove box. The relative humidity over the samples was adjusted to 85 % via the use of a saturated potassium chloride solution placed in the desiccator [16]. Subsequently, carbonation was studied by exposing the pellets to air at a RH of 70 % and 24 °C, also in the desiccator.

Each sample was subjected to three different exposure cycles. At first, the freshly calcined pellet was introduced into the vacuum system of the XPS instrument, etched by Ar ion bombardment to remove surface contamination and then transferred back to the desiccator, under nitrogen and over a saturated KCl solution. After four hours the sample was transferred

back into the XPS chamber and analysed. Subsequently, the same sample was prehydrated, again in the desiccator, for 8 further hours, thus giving a total time of prehydration of 12 hours, and analysed as before. The third, and final, cycle involved exposing the previously prehydrated sample to atmospheric conditions, i.e. containing CO₂, for a further 12 hours. Throughout the rest of the manuscript samples are identified as 0 h, 4 h, 12 h and 24 c, where h and c indicate exposure to humidity or CO₂ respectively and the number indicates the duration of exposure.

2.3 XPS analysis

Each pellet was stuck onto a double-sided adhesive copper tape and inserted into the vacuum chamber for analysis. The samples were analysed using a SCIENTA ESCA 300 photoelectron spectrometer (located at the National Centre for Electron Spectroscopy and Surface Analysis, NCESS, Daresbury, UK) fitted with a high power rotating anode (8 kW) and a monochromatic Al K_α ($h\nu = 1486.7$ eV) X-ray source. The X-ray beam was focused on a 6 mm × 0.5 mm area on the sample via a large, seven crystal double focusing monochromator. The Al K_α line profile had a FWHM (full width at half maximum) energy width of 0.26 eV. The detection system consisted of hemispherical analyser possessing a radius of 300 nm and a multi-channel detector. The system was operated with 0.8 mm slits and 150 eV pass energy, giving an overall instrument resolution of 0.30 eV ± 0.05 eV FWHM. Because the samples were often extremely good electrical insulators, a flood gun was used to compensate for sample charging.

Following an initial survey scan, high resolution spectra were recorded for the elements of interest: Na 1s, Ca 2p, O 1s, C 1s, Al 2p. Derived sensitivity factors were applied to convert signal intensities to atomic compositions [17].

Data were extracted from the spectra via peak fitting using CasaXPS software. A Shirley background was assumed in all cases. Spectra were corrected for charging effects using the adventitious hydrocarbon peak at 284.8 eV binding energy (BE). This peak is ubiquitous due to carbon contamination from the vacuum systems [18]. The presence of inorganic carbon, as carbonate, was always looked for in high-resolution scans.

3. Results and discussion

3.1 XPS analysis of fresh C₃A polymorphs

At first, unaged samples of cubic and orthorhombic C₃A were studied and used as reference in the study. **Figures 3 and 4** show the Al 2p and C 1s XPS spectra obtained from both polymorphs after each exposure. The corresponding binding energies, element ratios and chemical shifts are tabulated in **Tables 1 – 4**.

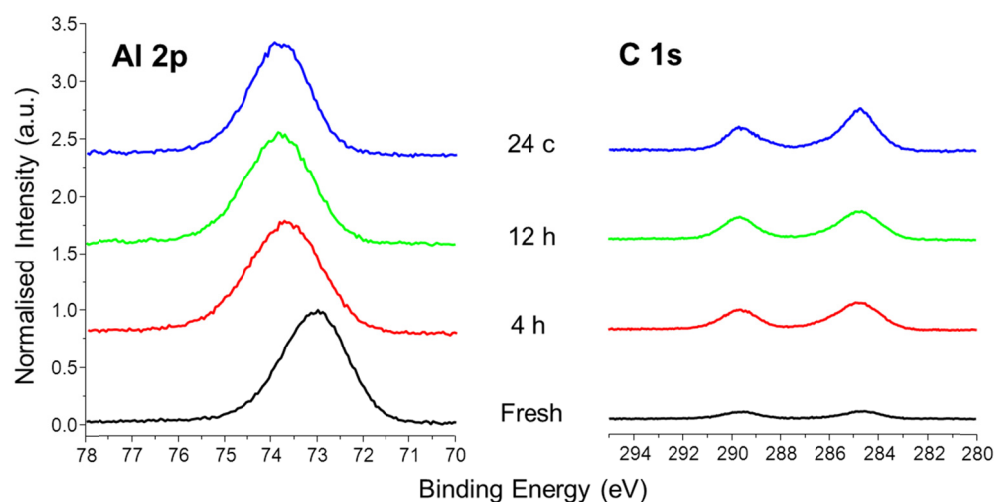


Fig. 3 XPS spectra of non-doped, cubic C₃A sample, fresh and aged, showing the evolution of the Al 2p (left) and C 1s (right) peaks during exposure to water vapour and subsequent carbonation

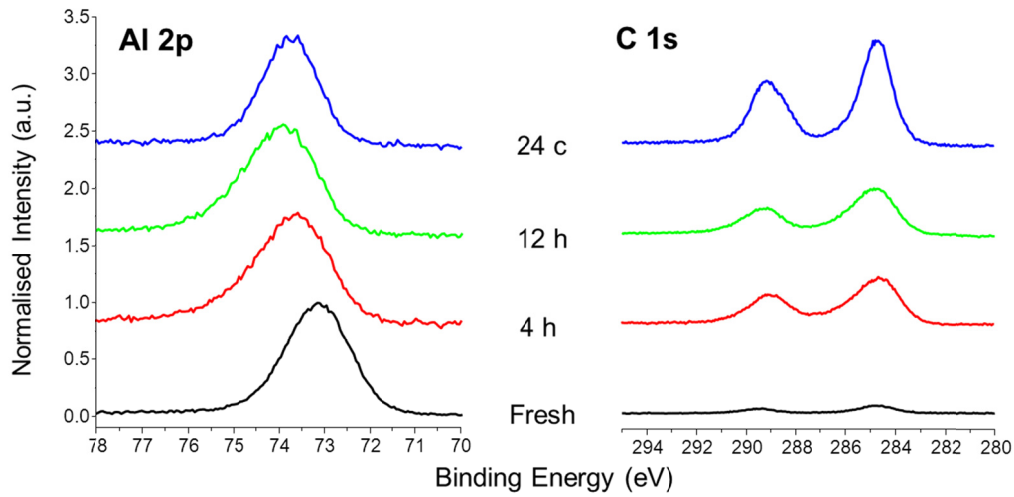


Fig. 4 XPS spectra of orthorhombic C_3A sample, fresh and aged, showing the evolution of the Al 2p (left) and C 1s (right) peaks during exposure to water vapour and subsequent carbonation

Table 1 Binding energies of fresh and aged cubic C_3A , as obtained by XPS

Element	Binding energy (eV)* after exposure period/mode			
	0 h (fresh)	4 h	12 h	24 c
Ca 2p _{2/3}	346.4(4)	347.0(6)	347.1(8)	347.1(7)
O 1s	529.7(4)	531.1(9)	531.3(1)	531.2(9)
	531.3(6)	531.6(6)	531.7(0)	531.6(7)
Al 2p	72.9(2)	73.5(0)	73.7(0)	73.7(7)
	73.5(3)	74.1(4)	74.3(3)	74.7(3)
C 1s	289.6(5)	289.6(7)	289.6(8)	289.5(7)

* Shifts relative to C 1s = 284.8 eV

Table 2 Element ratios and chemical shifts of fresh and aged cubic C_3A , as obtained from XPS analysis

El. ratios	Element ratios and chemical shifts (eV)* after exposure period/mode			
	0 h (fresh)	4 h	12 h	24 c
Ca/Al*	1.5	1.47	1.48	1.47
C/Ca	0.07	0.17	0.19	0.3
Δ_{Ca-Al}	273.4(4)	273.3(6)	273.3(4)	273.3(7)
Δ_{Ca-C}	56.7(9)	57.4(0)	57.5(1)	57.6(0)

*: Values represent normalized ratios based on the assumption that etched sample possesses the ideal composition $Ca_3Al_2O_6$.

Table 3 Binding energies of fresh and aged orthorhombic C₃A derived from XPS analysis

Element	Binding energy (eV)* after exposure period/mode			
	0 h	4 h	12 h	24 c
Ca 2p _{2/3}	346.4(3)	346.6(8)	346.9(5)	346.7(7)
O 1s	529.8(5)	530.9(7)	531.2(0)	531.1(7)
	531.6(7)	531.7(7)	531.8(6)	532.6(8)
Al 2p	73.1(1)	73.5(3)	73.7(2)	73.7(4)
	74.0(5)	74.4(6)	74.5(4)	-
Na 1s	1071.5(6)	1071.5(1)	1071.5(1)	1071.3(7)
	1072.2(2)	1072.3(3)	1072.3(5)	1072.2(4)
C 1s	289.5(8)	289.3(4)	289.2(3)	289.3(4)

* Shifts relative to C 1s = 284.8 eV

Table 4 Element ratios and chemical shifts of fresh and aged orthorhombic C₃A, as obtained from XPS analysis

El. ratios	Element ratios and chemical shifts (eV)* after exposure period /mode			
	0 h (fresh)	4 h	12 h	24 c
Ca/Al*	1.4(2)	2.0(5)	2.0(1)	1.9(8)
Na/Ca*	0.1(2)	0.5(5)	0.9(1)	2.9(4)
C/Ca	0.0(4)	0.2(2)	0.2(0)	0.8(3)
Na/C	0.4(7)	0.4(3)	0.7(8)	0.7(5)
$\Delta_{Ca - Al}$	273.2(8)	272.9(1)	272.9(9)	272.9(9)
$\Delta_{Ca - C}$	56.9(1)	57.6(0)	57.6(2)	57.6(9)
$\Delta_{Na - C}$	782.1(6)	782.4(1)	782.4(9)	782.3(1)

*: Values represent normalized ratios based on the assumption that etched sample has the ideal composition Ca_{8.5}NaAl₆O₁₈.

The Al 2p spectra for the fresh phases were slightly asymmetrical, with the calcium-rich cubic C₃A having a slightly lower binding energy than orthorhombic C₃A (**Figures 3 and 4**). The Al 2p spectra for the fresh samples show two contributions, namely at ~ 72.9 and 73.5 eV for the cubic and at ~ 73.1 and 74.0 eV for the orthorhombic C₃A polymorph (**Tables 1 and 3**). The values found here for cubic C₃A are very close to that of 73.1 eV reported by *Ball et al.* [19]. Aluminium binding energies are dependent upon the coordination number [20]. In both C₃A modifications, Al is always tetrahedrally coordinated and occurs as AlO₄. Six such tetrahedra form an Al₆O₁₈¹⁸⁻ ring in orthorhombic C₃A which becomes deformed upon replacement of Ca²⁺ by the slightly less electronegative Na⁺ in the centre of the Al₆O₁₈¹⁸⁻ ring

[21]. Thus, the slight changes in binding energy from cubic to orthorhombic C_3A may be due to the symmetry change ($C_3 \rightarrow C_i$) or change in electronegativity caused by the incorporation of Na_2O into doped C_3A .

The Ca 2p binding energies for both fresh polymorphs were the same and in good agreement with the value of 346.3 eV obtained by *Ball et al.* [19]. Unlike the Al 2p spectra, changes in Ca 2p spectra would not be expected upon replacement of calcium by sodium. In addition to the binding energies, changes in the Ca 2p – Al 2p energy separation (Δ_{Ca-Al}) were determined (Tables 2 and 4). In previous studies on calcium silicate hydrates, these values have been shown to provide valuable information related to changes in their chemical structure, in particular the degree of silicate polymerisation in calcium silicate hydrates [18]. This approach also overcomes problems due to charging when analysing insulating samples. Here, the incorporation of sodium into the C_3A lattice, with the conversion from cubic to orthorhombic modification, did not induce changes in polymerisation, but there was a slight reduction in Δ_{Ca-Al} from 273.4 to 273.2 eV, likely as a result of the reduced electronegativity of sodium compared to calcium.

3.2 Exposure to water vapour and CO_2

In a previous investigation, we noticed distinct differences between the XPS spectra of the surfaces of cubic and orthorhombic C_3A prehydrated in moist air (85 % RH) for just 1 h [22]. Here, emphasis was placed on separation of the effects caused by water vapour and carbon dioxide.

Prehydration under water vapour only (no CO_2 present) was slower than in the previous study where prehydration was performed in moist, CO_2 -containing air. Still, the impact of water

vapour led to visible changes in the binding energies, particularly in the Al 2p peak (**Figures 3 and 4**). For both modifications, exposure to water vapour caused a shift to higher Al 2p binding energies. Furthermore, the Al 2p spectra broadened upon prehydration and two peaks were required to fit them, signifying a change in the chemical state of Al, plausibly due to formation of C-A-H phases. An Al 2p binding energy of 73.8 eV has previously been reported for pure C_4AH_{13} [22]. Here, after exposure of both C_3A polymorphs to water vapour for 12 h, a peak could be fitted at ~ 73.7 eV, likely indicative of C_4AH_{13} formation. The second peak in the Al 2p spectra was centred at ~ 74.3 eV for the cubic and at ~ 74.5 eV for the orthorhombic modification. The peaks at 74.3 – 74.5 eV might be attributable to C_3AH_6 (katoite), but analysis of a standard sample of this hydrate would be necessary to confirm this assumption.

Concerning changes upon carbonation, i.e. exposure to air, the Al 2p spectra of both C_3A polymorphs showed a shift to lower BE from the previous state, but a higher BE compared to the fresh samples. Furthermore, the Al 2p spectra sharpen after carbonation. In previous work it has been established that XPS peak widths reflect, among other things, more ordered structures [23]. Thus, the changes observed here suggest that when the supply of carbon dioxide is limited, carbonation is slight, leading to the formation of a poorly ordered phases on the surface of C_3A , while ready access of more CO_2 leads to ample formation of ordered phases. Additionally, formation of carbonate was observed in the C 1s spectra, as indicated by a peak at ~ 289 eV (**Fig 3 and 4**). Furthermore, the carbonate peaks narrowed, with the FWHM decreasing from 1.7 to 1.6 eV for cubic and from 2.1 to 1.7 eV for orthorhombic C_3A .

For the cubic modification, the relative peak areas of the Ca 2p and C 1s spectra (Ca 2p spectra not shown here) suggest a C/Ca ratio of 0.3 (**Table 2**), indicating the formation of calcium monocarboaluminate ($3 CaO \cdot Al_2O_3 \cdot CaCO_3 \cdot 11 H_2O$). This is in agreement with the bulk carbonation behaviour of C_3A pastes, as analysed by Raman spectroscopy [24]. The

mechanism of the monocarboaluminate formation is based on the reaction of CO_2 with $\text{C}_4\text{A} \cdot n\text{H}_2\text{O}$ which possesses a disordered layered structure. In this process, the interlayer OH^- is replaced by CO_3^{2-} [25]. The ion exchange stabilises the layered structure and results in shrinkage of the basal spacing from 1.08 nm in C_4AH_{13} to 0.76 nm for the carbonated species [26].

The C 1s spectra indicate that carbonation of orthorhombic C_3A was more extensive than for the cubic modification. The 24 c sample revealed a C/Ca ratio of 0.8 (Table 4). This ratio was too high to be explained solely by calcium monocarboaluminate formation, and indicated the presence of another carbonate species.

Figure 5 shows the changes in C/Ca and Ca/Al ratios with exposure for both aged C_3A modifications. Both polymorphs behaved comparably with regards to their C/Ca values up to 12 h of prehydration, but behaved very differently upon exposure to ambient air for a further 12 hours.

Exposure to water vapour led to a very minor decrease in the Ca/Al ratio of cubic C_3A . However, in case of orthorhombic C_3A there is a trend towards Ca/Al ratio of 2, i.e. C_4AH_x , which agrees with the slightly increased rate of hydration. This may be explained by the increased Na^+ content increasing the pH of the water film on the surface of the C_3A .

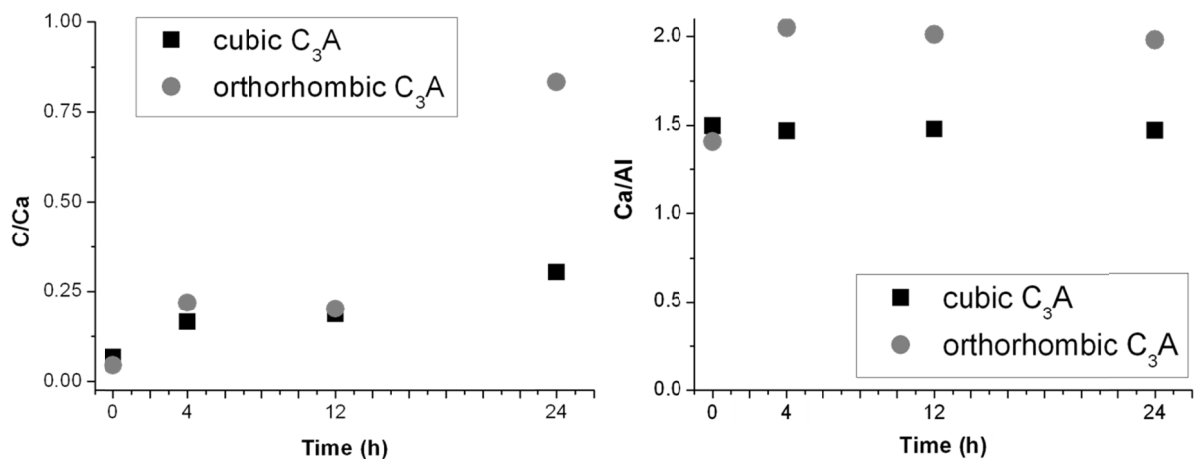


Fig. 5 Normalised ratios of C/Ca (left) and Ca/Al ratios (right) occurring on the surfaces of cubic and orthorhombic C₃A as a function of ageing period and mode, as measured by XPS

3.3 Impact of Na₂O

Examination of high resolution Na 1s spectra revealed how the presence of sodium affected the reactivity of orthorhombic C₃A, and the Na/Ca ratios were calculated and shown in **Figure 6**.

The freshly calcined sample exhibited a Na 1s signal which comprised two signals: the main peak centred at ~ 1071.5 eV and a second minor peak at ~ 1072.2 eV. The main peak at ~ 1071.5 eV can be attributed to incorporated Na₂O within the o-C₃A structure. The minor peak corresponds to the value of 1072.2 eV reported for NaOH [27].

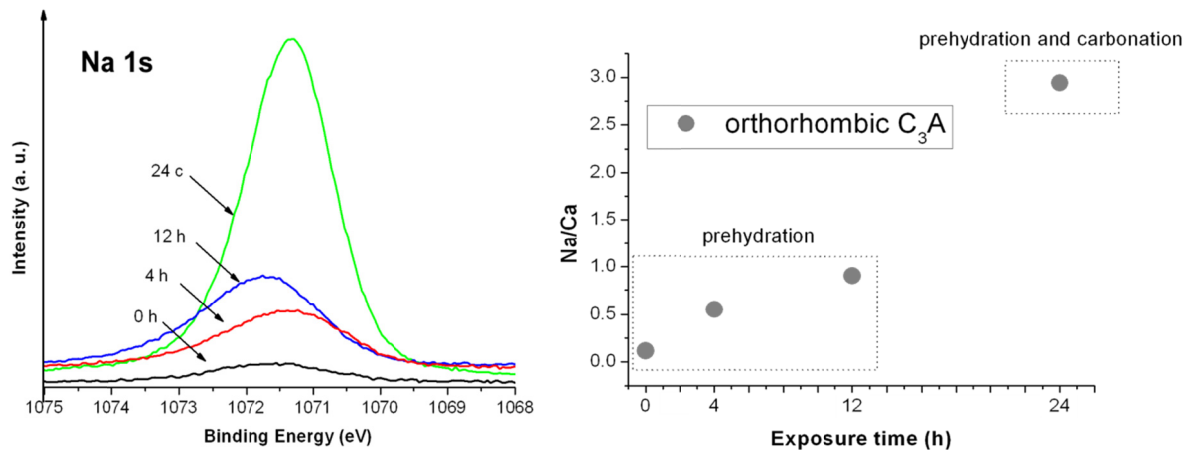


Fig. 6 Na 1s XPS spectra of fresh and aged orthorhombic C_3A samples (left) and Na/Ca ratios after exposure of orthorhombic C_3A sample to moisture and CO_2 in air (right)

For the o- C_3A sample prehydrated with moisture only, there was a gradual increase in the intensity of the signal centred at ~ 1072.2 eV. This signified less and less sodium bound within the crystal structure of orthorhombic C_3A , with the increased intensity due to mobilisation of sodium upon exposure to water vapour and its migration to the sample surface. This finding agrees with results from Glasser *et al.* who observed that Na^+ can dissolve into the aqueous phase more rapidly than Ca^{2+} or Al^{3+} [5]. According to literature, NaOH shows a Na 1s peak at ~ 1072.2 eV [27]. Thus, upon abstraction from the crystal structure, sodium appears to combine with water to form NaOH on the surface.

Exposure to ambient air, containing CO_2 , led to further changes in the Na 1s spectra, namely a large growth in intensity and a slight shift back to lower binding energies, with the signal centred at 1071.3 eV. Such binding energy corresponds to either Na_2CO_3 or $NaHCO_3$, both of which produce a peak at 1071.3 eV [28]. This finding suggests that the initially formed NaOH then carbonated to form Na_2CO_3 , which constitutes the main product from the prehydration and carbonation process.

The formation of surface Na_2CO_3 on o- C_3A was confirmed by SEM imaging (**Fig. 7**). Bright crystalline specks were visible on the surface of sample 24 c. These particles were identified by energy dispersive x-ray (EDX) spectroscopy as Na_2CO_3 .

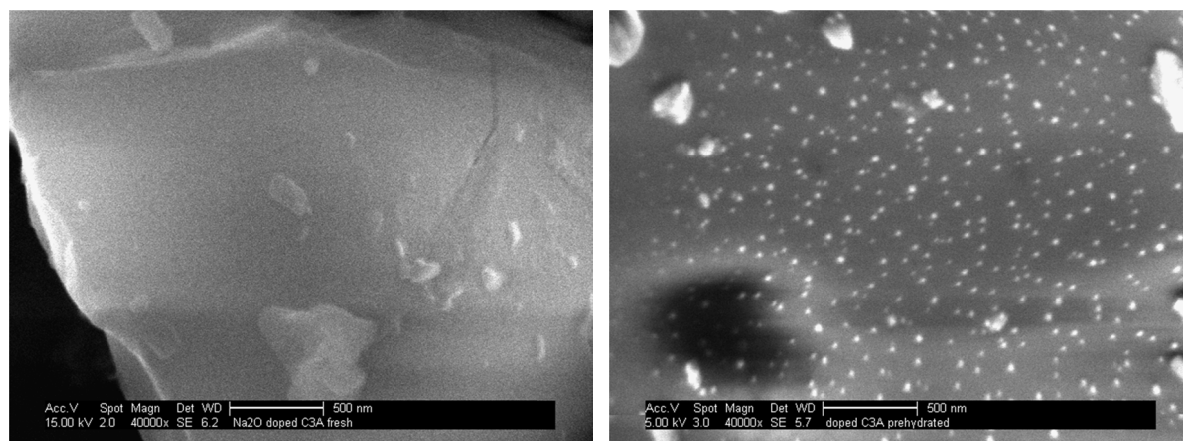


Fig. 7 SEM images of the surfaces of 0 h fresh (left) and 24 c (prehydrated and carbonated) orthorhombic C_3A (right), showing Na_2CO_3 crystals on the prehydrated sample

4. Conclusions

X-ray photoelectron spectroscopy has been used to follow the interactions of cubic and orthorhombic C_3A polymorphs with environmental moisture and CO_2 under defined storage conditions.

In the XPS spectra, clear differences were observed for cubic and orthorhombic C_3A after prehydration with water vapour and subsequent carbonation in air. During prehydration in the absence of CO_2 , both C_3A polymorphs showed the formation of C_4AH_{13} on their surfaces, but the extent was more pronounced for the orthorhombic modification. Surface enrichment of sodium, in the form of sodium hydroxide, was observed after prehydration of orthorhombic C_3A which was doped with 4 wt. % of Na_2O . The increased pH induced by the surface NaOH may account for the increased rate of reaction.

Additionally, the impact of sodium on carbonation of orthorhombic C_3A was studied. Prehydrated cubic C_3A produced monocarboaluminate ($3 CaO \cdot Al_2O_3 \cdot CaCO_3 \cdot 11 H_2O$) on its surface, while carbonation of orthorhombic C_3A resulted in additional extensive Na_2CO_3 formation. The reason is the high amount of NaOH formed after the initial prehydration at the surface of orthorhombic C_3A . This explains why orthorhombic C_3A undergoes increased carbonation, compared to its cubic counterpart.

The findings bear significance also for the interaction of prehydrated cements with admixtures such as superplasticizers. It is well established that their interaction to a large extent relies on the surface charge of the aluminate hydrates. As has been demonstrated above, aging of cement can lead to various prehydration products which possess different surface charges. Consequently, the effectiveness of admixtures may differ, depending on the storage conditions of the cement.

Acknowledgments

E. Dubina is grateful to Nanocem (Core Project # 7) for financial support of this work. The authors also like to acknowledge the support from EPSRC (grant reference EP/E025722/1) for supporting this work through the Daresbury NCESS Facility. They also want to thank Dr. Danny Law for his support at NCESS. Additionally, Dr. Holger König and Dr. Maciej Zajac, both from HeidelbergCement, Leimen/ Germany are thanked for their input in many discussions.

References

- [1] H. F. W. Taylor, *Cement Chemistry*, Academic Press, London, 1990.
- [2] A. I. Boikova, A. I. Domansky, V. A. Paramonova, G. P. Stavitskaja and V. M. Nikuschenko, "The influence of Na₂O on the structure and properties of 3CaO·Al₂O₃", *Cem. Concr. Res.* 7, 1977, 483 – 492.
- [3] L. Gobbo, L. Sant'Agostino, L. Garcez, "C₃A polymorphs related to industrial clinker alkalies content", *Cem. Concr. Res.* 34, 2004, 657 – 664.
- [4] D. Stephan, H. Maleki, D. Knöfel, B. Eber, R. Härdtl, Influence of Cr, Ni, and Zn on the properties of pure clinker phases: Part II. C₃A and C₄AF, *Cem. Concr. Res.* 29, 1999, 651 – 657.
- [5] F. P. Glasser, M. B. Marinho, "Early stages of the hydration of tricalcium aluminate and its sodium containing solid solutions", *Br. Ceram. Proc.* 35, 1984, 221 – 236.
- [6] S. Wistuba, D. Stephan, G. Raudaschl-Sieber, J. Plank, "Hydration and hydration products of two-phase Portland cement clinker doped with Na₂O", *Adv. Cem. Res.* 19, 2007, 125 – 131.
- [7] A. P. Kirchheim, V. Fernández-Altable, P. J. M. Monteiro, D. C. C. Dal Molin, I. Casanova, "Analysis of cubic and orthorhombic C₃A hydration in presence of gypsum and lime", *J. Mater. Sci.* 44, 2009, 2038 – 2045.
- [8] H. Pöllmann, Composition of cement phases. In *Structure and Performance of Cements* (BENSTED J. and BARNES P. (eds.)). Spon Press, London, 2002, 25 – 56.
- [9] P. Mondal, J.W. Jeffery, "The crystal structure of tricalcium aluminate Ca₃Al₂O₆", *Acta Cryst. B* 31, 1975, 689 – 697.
- [10] C. Ostrowski, J. Żelazny, "Solid Solutions of Calcium Aluminates C₃A, C₁₂A₇ and CA with Sodium Oxide", *J. Therm. Anal. Calorim.*, 75 (3), 2004, 867 – 885.
- [11] E. Breval, "Gas-phase and liquid-phase hydration of C₃A", *Cem. Concr. Res.* 7, 1977, 297 – 304.

- [12] K. Theisen, V. Johansen, “Prehydration and strength development of Portland cement”, *J. Am. Cer. Soc.*, 54 (9), 1975, 787 – 791.
- [13] M. Whittaker, E. Dubina, F. Al-Mutawa, L. Arkless, J. Plank, L. Black, “The effect of prehydration on the engineering properties of CEM I Portland cement”, *Adv. Cem. Res.*, 2012, in print.
- [14] E. Dubina, L. Wadsö, J. Plank, “A sorption balance study of water vapour sorption on anhydrous cement minerals and cement constituents”, *Cem. Concr. Res.* 41, 2011, 1196 – 1204.
- [15] J. T. Grant and D. Briggs “Surface Analysis by Auger and X-ray Photoelectron Spectroscopy”, published by IM Publications, 2003, Chichester, UK.
- [16] L. Greenspan, “Humidity Fixed Points of Binary Saturated Aqueous Solutions”, *J. Res. Nat. Bur.*, 8 (1), 1977, 89 – 95.
- [17] C. D. Wagner, L. E. Davis, M. V. Zeller, J. A. Taylor, R. H. Raymond, L. H. Gale, “Empirical atomic sensitivity factors for quantitative analysis by electron spectroscopy for chemical analysis”, *Surf. Interface Anal.*, 3 (5), 1981, 211 – 225.
- [18] L. Black, K. Garbev, I. Gee, “Surface carbonation of synthetic C-S-H samples: A comparison between fresh and aged C-S-H using X-ray photoelectron spectroscopy”, *Cem. Concr. Res.*, 38, 2008, 745 – 750.
- [19] M. C. Ball, R. E. Simmons, I. Sutherland, “Surface composition of anhydrous tricalcium aluminate and calcium aluminoferrite”, *J. Mater. Sci.*, 22, 1987, 1975 – 1979.
- [20] T. L. Barr, S. Seal, K. Wozniak, J. Klinowski, “ESCA studies of the coordination state of aluminium in oxide environments”, *J. Chem. Soc., Faraday Trans.*, 93, 1997, 181 – 186.
- [21] Y. Takeuchi, F. Nishi, I. Maki, “Crystal-chemical characterization of the tricalcium aluminate-sodium oxide ($3\text{CaO} \times \text{Al}_2\text{O}_3\text{-Na}_2\text{O}$) solid solution series”, *Z. Kristallogr.* 152 (3-4), 1980, 259 – 307.

- [22] E. Dubina, L. Black, R. Sieber, J. Plank, “Interaction of water vapour with anhydrous cement minerals”, *Adv. Appl. Ceram.*, 109 (5), 2010, 260 – 268.
- [23] L. Black, K. Garbev, G. Beuchle, P. Stemmermann, D. Schild, “X-ray photoelectron spectroscopic investigation of nanocrystalline calcium silicate hydrates synthesised by reactive milling”, *Cem. Concr. Res.*, 36, 2006, 1023 – 1031.
- [24] L. Black, C. Breen, J. Yarwood, J. Phipps and G. Maitland, “In situ Raman analysis of hydrating C₃A and C₄AF pastes in presence and absence of sulphate”, *Adv. Appl. Ceram.*, 2006, 105, 209 – 216.
- [25] R. Fischer, H.J. Kuzel, “Reinvestigation of the system C₄A · nH₂O – C₄A · CO₂ · nH₂O” *Cem. Concr. Res.*, 12, 1982, 517 – 526.
- [26] R. Gabrovšek, T. Vuk, V. Kaučič, “The Preparation and Thermal Behavior of Calcium Monocarboaluminate”, *Acta Chim. Slov.*, 55, 2008, 942 – 950.
- [27] R. A. Zarate, S. Fuentes, J. P. Wiff, V. M. Fuenzalida, A. L. Cabrera, “Chemical composition and phase identification of sodium titanate nanostructures grown from titania by hydrothermal processing”, *J Physics Chemistry Solids*, 68, 2007, 628 – 637.
- [28] J. F. Moulder, W.F. Stickle, P.E. Sobol, K.D. Bomben, in: J. Chastain (Ed.), *Handbook of X-Ray Photoelectron Spectra – A Reference Book of Standard Spectra for Identification and Interpretation of XPS Data*, Perkin-Elmer, Eden Prairie, Minnesota, 1992, p. 229.

Paper 3

Influence of Water Vapour and Carbon Dioxide on Free Lime During Storage at 80 °C Studied by Raman Spectroscopy

E. Dubina¹, L Korat², L. Black³, J. Strupi Šuput², J. Plank¹

¹*Technische Universität München, Lehrstuhl für Bauchemie, Lichtenbergstr. 4, 85747 Garching bei München,
Germany*

²*Slovenian National Building and Civil Engineering Institute, Dimičeva 12, 1000 Ljubljana, Slovenia*

³*Institute for Resilient Infrastructure, School of Civil Engineering, University of Leeds, Leeds, LS2 9JT, UK*

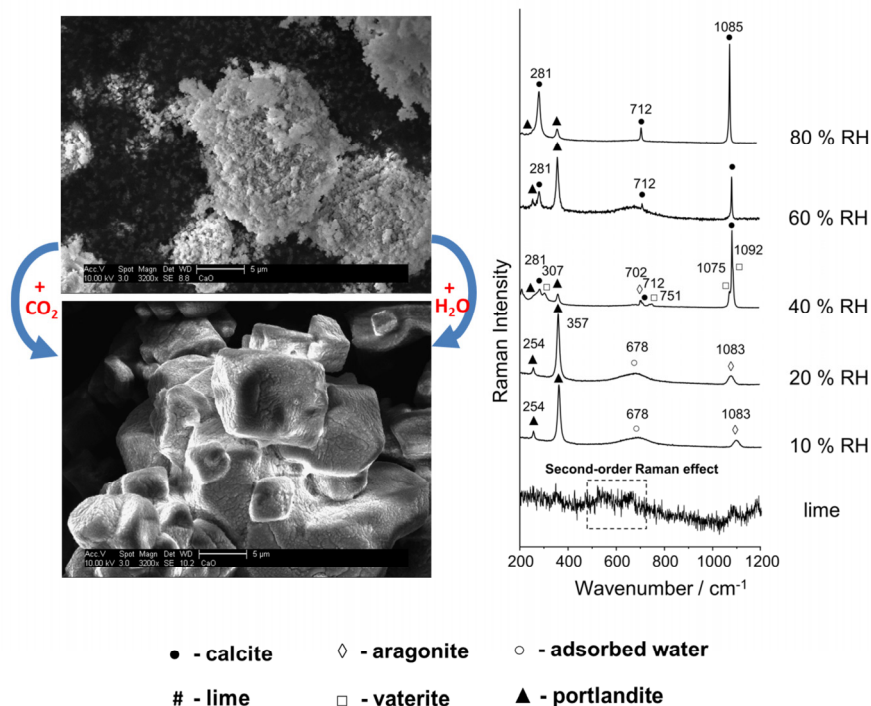
Submitted on 9/11/2012 to Spectrochimica Acta Part A

Abstract

Micro-Raman spectroscopy has been used to follow the reaction of free lime (CaO) exposed for 24 hours to moist air at 80 °C under conditions of different relative humidities (10 – 80 % RH). X-ray diffraction and SEM imaging were applied as complementary techniques. The conversion of lime to calcium hydroxide and its subsequent carbonation to various calcium carbonate polymorphs was found to strongly depend on the relative humidity. At low RH (10 – 20 %), only Raman spectroscopy revealed the formation of early amorphous CaCO₃ which in the XRD patterns was detected only at ≥ 40 % RH. However, XRD analysis could identify the crystalline polymorphs formed at higher relative humidities. Thus, between 20 and 60 % RH, all three CaCO₃ polymorphs (calcite, aragonite and vaterite) were observed via XRD whereas at high relative humidity (80 %), calcite was the predominant reaction product. The results demonstrate the usefulness of Raman spectroscopy in the study of minor cement constituents and their reaction products on air, especially of amorphous character.

Keywords: micro-Raman; calcium oxide; moisture; carbonation;
calcium carbonate polymorphs; REM/EDX

Graphical abstract



Introduction

By volume, ordinary Portland cement (OPC) presents the most abundant industrially manufactured material and it also constitutes one of the world's most commonly used building materials ^[1]. Unfortunately, cement powder is highly hygroscopic and eagerly sorbs water vapour in a process generally known as surface prehydration of cement ^[2, 3]. This phenomenon may occur already during the manufacturing process, e. g. in the clinker mill, or later during storage in cement silos where the temperature often is 80 °C and high relative humidities occur as a consequence of gypsum dehydration ^[4, 5]. The interaction of cement with water vapour has detrimental effects on its engineering properties. Those include decreased compressive strength and workability, increased setting time and higher water demand ^[6-8]. The extent to which these phenomena occur depends on the temperature and relative humidity ^[9].

Recently we have investigated the physicochemical effects of water vapour sorption by pure cement clinker phases and free lime. There, the relative humidity values (“thresholds”) above which prehydration starts to occur were determined ^[10]. Among all cement components, free lime (CaO) showed the lowest threshold value of 14 % relative humidity (RH) only. Also, CaO can sorb large quantities of water which are chemically bound. This pronounced ability of CaO to bind atmospheric moisture quickly and irreversibly possibly reduces or even prevents the prehydration of other clinker constituents when cement is exposed to moisture. In current cements, typically about 0.5 – 1.5 wt. % of free lime are present ^[11]. Therefore, information on the reaction of CaO, or its subsequently formed hydrate, Ca(OH)₂ with moist air can provide insight into the behaviour of industrial cement and for example its storage history.

The potential of Raman spectroscopy for the characterisation of cementitious materials was first demonstrated in 1976 ^[12]. Also, more recently a review on this subject has been published ^[13]. New instruments are available now which offer the potential for micro-Raman spectroscopy. These enable capture of spectra from the surfaces of samples just a few microns thick and with minimal interference from environmental moisture ^[14]. Moreover, whilst for example x-ray diffraction requires crystalline analytes, Raman spectroscopy allows the detection of amorphous phases and provides information on the local chemical environment. Raman spectra can be obtained from almost all components present in anhydrous cement and from cement hydrate phases. One exception is calcium oxide which is Raman inactive.

However, it is possible to observe second order effects which give rise to sharp bands at 530 and 660 cm^{-1} , as well as a broad signal at about 1000 cm^{-1} [15].

The aim of this study was to simulate storage conditions for CaO (80 °C and relative humidities between 10 and 80 %) which can occur in the cement silo and to investigate the impact of those conditions on the reaction of CaO with atmospheric water and CO₂. Special attention was given to the amount and type of CaCO₃ polymorphs formed during exposure to moist air.

Experimental

Preparation of CaO

CaO was prepared by calcination of CaCO₃ (Merck, 98.5 % purity) for 3 h at 1000 °C and subsequent grinding to particles possessing an average size of 4.7 μm (d_{50} value) and a specific surface area of 2.4 m^2/g (N₂, BET). Precautions were taken to prevent reaction with atmospheric CO₂ and water vapour by storing samples in sealed 20 mL glass vials under nitrogen.

Ageing of CaO

To establish the cause of the ageing phenomenon under those storage conditions, CaO powder was spread out as a thin layer (1 mm) on a plastic tray and exposed for 24 hours to air possessing controlled relative humidities (10, 20, 40, 60 and 80 %) in a climate chamber heated to 80 °C.

Sample Characterisation

All fresh and prehydrated samples were analysed by x-ray diffraction, XRD, (D8 Advance, Bruker axs, Karlsruhe, Germany) using a Cu K _{α} X-ray source. Diffractograms were taken from 7 – 40 ° 2 θ at 21 °C, with a step size of 0.008 ° and a dwell time of 54 s. The mineralogical phases were identified by comparison with Diffract Plus EVA Application V.8.0 and JCPDS PDF-2 database [16].

Micro-Raman measurements were performed at room temperature using a Horiba Jobin Yvon HR 800 LabRAM instrument (Villeneuve d'Ascq, France) equipped with an Olympus BX40 microscope (focus graduation 1 μm), a laser working at $\lambda = 785 \text{ nm}$ and a multi channel air-

cooled CCD detector. Each spectrum was acquired over the spectral range of 200 – 1200 cm^{-1} using a 10x objective. Prior to each experiment, the Raman shift was calibrated against the 520 cm^{-1} peak of silicon. Data handling was performed using LabSpec 5 software.

Scanning electron microscopic (SEM) images were obtained on uncoated samples using a FEI XL 30 FEG instrument (FEI, Eindhoven, Netherlands) under low vacuum conditions (1 mbar H_2O pressure) and an accelerating voltage of 10 kV. Dispersive x-ray spectroscopy was performed using a SUTW-Sapphire detector (EDAX, Mahwah, U.S.A.) under the same conditions as SEM imaging, however accelerating voltage was 15 kV.

Results and Discussion

The x-ray diffraction patterns of fresh lime and of samples exposed to air at 80 °C are displayed in **Figure 1**. There, reflections for unreacted CaO were visible only for the freshly calcined sample which was not yet exposed to air. After storage at low relative humidity (10 % RH), complete hydration of CaO to portlandite ($\text{Ca}(\text{OH})_2$) was observed. No carbonation of this phase was detected at or below 20 % RH. However, after storage at 40 %, intensity of the reflections from portlandite decreased and partial carbonation became evident as signified by the appearance of new reflections attributable to CaCO_3 polymorphs. Namely, well defined and intense reflections for calcite and aragonite, and traces of vaterite were detected. In samples exposed to higher relative humidities (60 – 80 %), only portlandite and calcite were found. There, as RH increased, the reflections from calcite became more intense and sharp.

The micro-Raman spectra of the CaO samples exposed to different relative humidities are presented in **Figure 2**. They exhibited several distinct differences as compared to the XRD patterns. Apparently, Raman spectroscopy was able to capture also amorphous reaction products.

Analysis of the freshly calcined CaO showed very weak bands at ~ 530 and 660 cm^{-1} due to a second order Raman effect of lime. Following exposure of CaO to lower humidities (10 – 20 %), new bands at 254 and 357 cm^{-1} became visible which are characteristic for portlandite. Additionally, a broad band attributed to water adsorbed on the surfaces of portlandite appeared at 678 cm^{-1} . It has been reported earlier that surface adsorption of water occurs when CaO has quantitatively reacted to $\text{Ca}(\text{OH})_2$ which then via van der Waals forces can

physically bind additional water molecules on its surface as mono or multilayers [10]. Furthermore, a broad signal centred at 1083 cm^{-1} which was attributed to symmetric stretching of carbonate groups present in amorphous calcium carbonate became visible [17]. Thus, it became clear that already at 10 % RH partial carbonation of CaO had occurred which was not evident from the XRD patterns. There, the first carbonation products were found only at 40 % RH and higher. This signifies that compared to XRD, Raman spectroscopy constitutes a more sensitive technique to monitor early carbonation reactions.

In a similar study, rapid carbonation of portlandite present in hydrated calcium silicates has been investigated by Black *et al.*, also using micro-Raman spectroscopy. Like in our study, amorphous calcium carbonate was identified there as the first carbonation product [18].

Increasing the exposure RH to 40 % led to a sharper carbonate ν_1 (symmetrical stretching) band in the range of $1000\text{--}1100\text{ cm}^{-1}$, thus indicating formation of crystalline calcium carbonates. Deconvolution of the signal revealed a number of overlapping bands at 1075, 1085 and 1092 cm^{-1} . Also, a number of weaker ν_4 carbonate bands at around 700 cm^{-1} were detected. The precise positions of these various bands are influenced by the symmetry of the carbonate anion, thus enabling polymorph identification when the entire spectrum and not just individual bands are looked at. The doublet at 1075 and 1092 cm^{-1} can be attributed to vaterite which normally exhibits a characteristic triplet at 1075, 1081 and 1092 cm^{-1} [19]. Here, the band at 1081 cm^{-1} is overlapped by the more intense ν_1 carbonate band at 1085 cm^{-1} assigned to the aragonite and calcite polymorphs. Also, at $701\text{--}703\text{ cm}^{-1}$ ν_4 carbonate bands corresponding to aragonite were observed.

In the Raman spectra of the samples exposed to 60 and 80 % RH, bands at 1085 cm^{-1} , 712 cm^{-1} , 357 cm^{-1} and 281 cm^{-1} were recorded. The band at 357 cm^{-1} is characteristic for portlandite, whilst the others are attributable to calcite [20]. Intensity of the calcite bands increased with increasing RH.

The exposure of CaO to air possessing different RHs not only led to changes in the mineralogical composition, but also increased the crystal sizes of the samples. **Figure 3** exhibits SEM images of the fresh and aged samples. Exposure to water vapour led to the appearance of deposits over the entire substrate. Storage at high RH favoured the formation of larger crystals, compared with exposure to low RH. Furthermore, energy dispersive x-ray spectroscopy showed higher carbon and oxygen contents in samples stored at higher RH levels, thus indicating the presence of larger amounts of calcium carbonate in these samples.

In CaO exposed to 40 % RH, a slightly higher oxygen content than in other samples was detected, indicating the simultaneous presence of Ca(OH)₂ as well as of CaCO₃ on the hydrated surface.

Conclusion

In the present work, the influence of relative humidity and atmospheric carbon dioxide on CaO (free lime), a minor constituent of Portland cement, was investigated. The combination of micro-Raman spectroscopy, x-ray diffraction analysis and SEM imaging allowed tracking of the changes occurring on the surface of CaO exposed to moist air at 80 °C. After exposure to low RH, total conversion of CaO to Ca(OH)₂ was observed. Subsequently, initially formed Ca(OH)₂ underwent partial carbonation into amorphous calcium carbonate. At low humidities (10 – 20 % RH), this reaction was observed only by Raman spectroscopy and not by x-ray diffraction. Exposure to higher relative humidities (≥ 40 %) led to the formation of crystalline calcium carbonates which were x-ray detectable. At moderate RH (40 %), the three different calcium carbonate polymorphs (calcite, aragonite and vaterite) co-exist while at increasing RH, calcite becomes increasingly prevalent. Exposure to different RH levels also impacts the crystal sizes of the reaction products, with larger crystals produced at higher RHs. The results confirm the potential of Raman spectroscopy in the study of the hydration behaviour of minor cement constituents, particularly when amorphous products are involved in the reaction processes.

Acknowledgements

The authors are grateful to Nanocem (Core Project # 7) for financial support of this work. ED wishes to thank Dr. Holger König and Dr. Maciej Zajac, HeidelbergCement, Leimen, Germany for their valuable contributions in many discussions.

Figures (1 - 3):

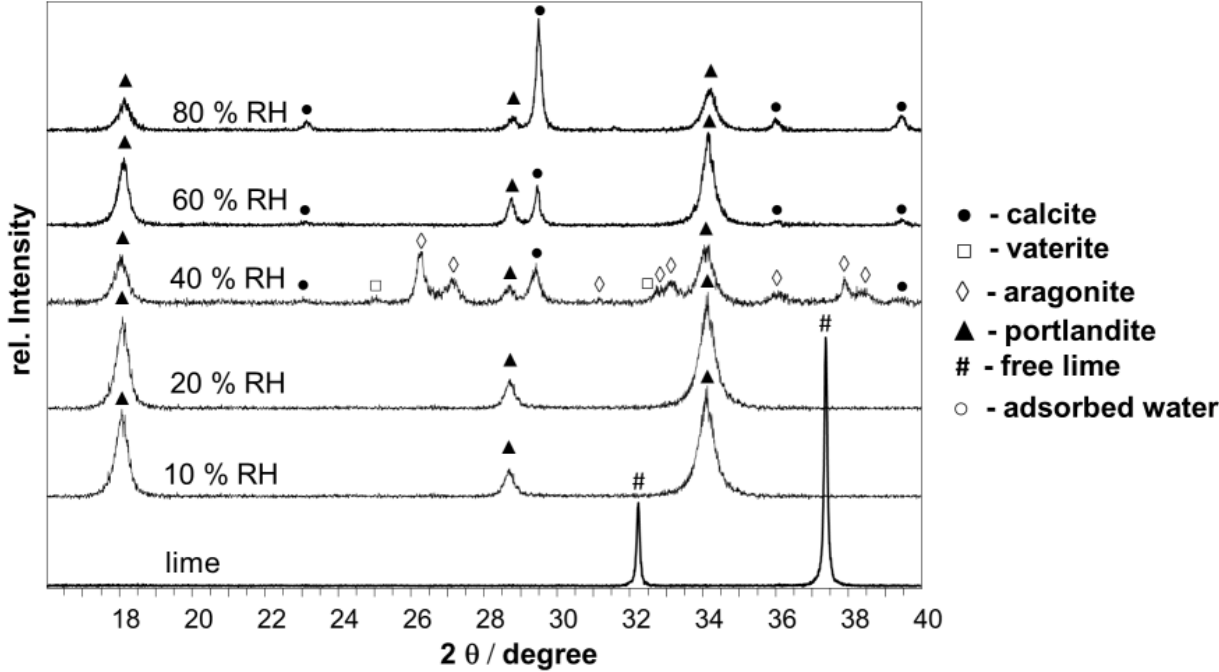


Figure 1. X-ray diffraction patterns of fresh and exposed CaO to moist air showing the formation of different hydration and carbonation products

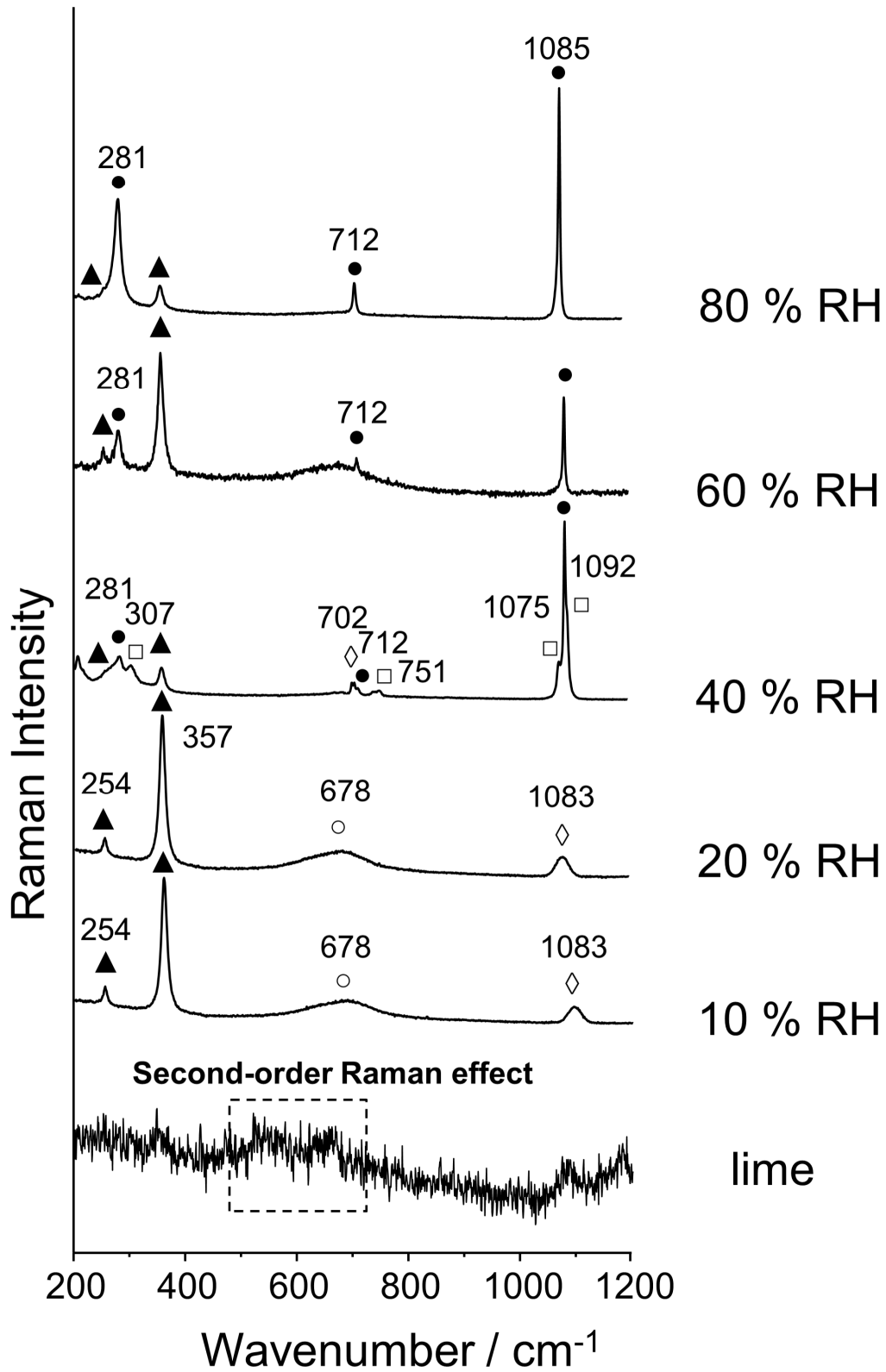


Figure 2. Micro-Raman spectra of fresh and exposed CaO to moist air showing the formation of different hydration and carbonation products

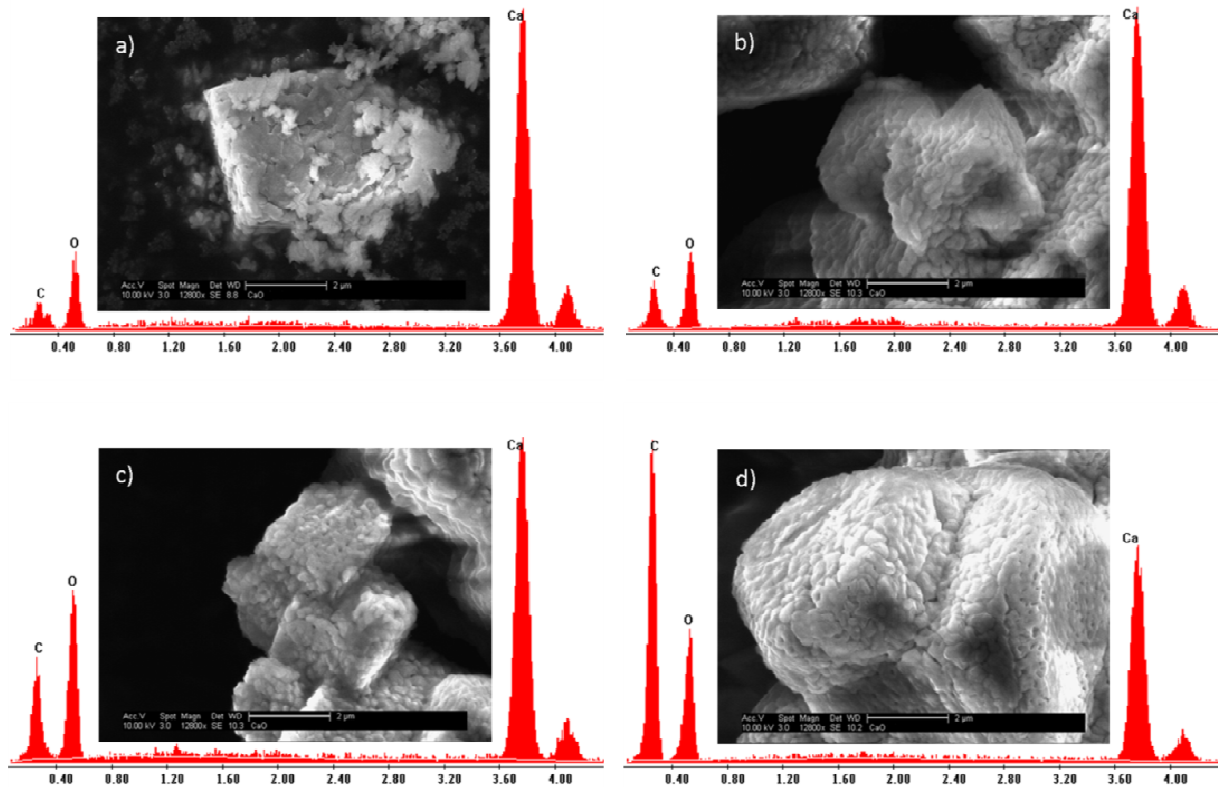


Figure 3. SEM micrographs and EDX spectra of CaO samples, fresh **(a)** and stored at 20 % RH **(b)**, 40 % RH **(c)** and 80 % RH **(d)**; (storage conditions: 80 °C, 24 hours); magnification: 12800 x

References

- [1] J. M. Crow, *Chemistry World* (2008), 62 – 66.
- [2] O. M. Jensen, P. Hansen, E. E. Lachowski, F. P. Glasser, *Cem. Concr. Res.* 29, (1999), 1505 – 1512.
- [3] E. Dubina, L. Black, R. Sieber, J. Plank, *Adv. App. Cer.* 109 (5), (2010), 260 – 268.
- [4] S. Sprung, *ZKG International* 31 (6), (1978), 305 – 309.
- [5] F. E. Hansen, H. J. Clausen, *ZKG International* 27 (7), (1974), 333 – 236.
- [6] K. Theisen, V. Johansen, *Am. Cer. Soc.* 54 (9), (1975), 787 – 791.

- [7] F. Winnefeld, *ZKG International* 61 (11), (2008), 68 – 77.
- [8] G. Schmidt, T. A. Bier, K. Wutz, M. Maier, *ZKG International* 60 (6), (2007), 94 – 103.
- [9] M. Whittaker, E. Dubina, F. Al-Mutawa, L. Arkless, J. Plank, L. Black, *Adv. Cem. Res.* (2012), in print.
- [10] E. Dubina, L. Wadsö, J. Plank, *Cem. Concr. Res* 41 (11), (2011), 1196 – 1204.
- [11] P. C. Hewlett, *Lea's Chemistry of Cement and Concrete*, 4 ed., Butterworth-Heinemann, 2004.
- [12] J. Bensted, *J. Am. Ceram. Soc.* 59, (1976), 140 – 143.
- [13] L. Black, *Spectrosc. Prop. Inorg. Organomet. Compd.* 40, (2009), 72 – 123.
- [14] S. Martinez-Ramirez, M. Frías, C. Domingo, *J. Raman Spectrosc.* 37, (2006), 555 – 561.
- [15] M. S. Seehra, *J. Solid State Chem.*, 63, (1986), 344 – 345.
- [16] JCPDS PDF-2 release 2003, ICDD Newton Square, PA, USA.
- [17] M. M. Tlili, M. Ben Amor, C. Gabrielli, S. Joiret, G. Maurin, P. Rousseau, *J. Raman Spectrosc.* 33, (2001), 10 – 16.
- [18] L. Black, K. Garbev B. Gasharova, C. Breen, J. Yarwood, P. Stemmermann, *J. Am. Ceram. Soc.* 90 (3), (2007), 908 – 917.
- [19] A. L. Soldati, D. E. Jacob, U. Wehrmeister, W. Hofmeister, *Mineral. Mag.* 72 (2), (2008), 579 – 592.
- [20] S. Gunasekaran, G. Anbalagan, *Spectrochim. Acta Part A* 68 (2007) 656 – 664.

Paper 4

Interaction of Environmental Moisture with Cubic and Orthorhombic C₃A in the Absence and Presence of Sulfates

E. Dubina¹, J. Plank¹, L. Black², L. Wadsö³

¹*Technische Universität München, Lehrstuhl für Bauchemie, Lichtenbergstr. 4, 85747 Garching bei München, Germany*

²*Institute for Resilient Infrastructure, School of Civil Engineering, University of Leeds, Leeds, LS2 9JT, UK*

³*Building Materials, Lund University, P. O. Box 118, 221 00 Lund, Sweden*

Submitted on 16/10/2012 to *Advances in Cement Research*

(under review)

Abstract

The phenomenon of water vapour sorption by anhydrous C_3A polymorphs both in the absence and in the presence of $CaSO_4 \cdot 0.5 H_2O$ was studied utilizing dynamic and static sorption methods. It was found that orthorhombic C_3A starts to sorb water at 55 % relative humidity (RH) and cubic C_3A at 80 % RH. Also, C_3A_o sorbs a higher amount of water which is predominantly physically bound while C_3A_c preferentially interacts with water by chemical reaction.

In the presence of calcium sulphate hemihydrate, ettringite was observed as predominant prehydration product for both C_3A modifications, i.e., that ion transport had occurred between C_3A and sulphate. ESEM imaging revealed that in a moist atmosphere, a liquid water film condenses on the surface of the phases as a consequence of capillary condensation between the particles. C_3A and sulphate can then dissolve and react with each other. Seemingly, prehydration is mainly facilitated through capillary condensation and less through surface interaction with gaseous water molecules.

Key words: Prehydration, Sulphate, $Ca_3Al_2O_6$, Moisture

List of notations:

AF_t	calcium aluminate trisulphate hydrate, ettringite
AF_m	calcium monosulfoaluminate hydrate, monosulphate
BET	Brunauer, Emmett, Teller
c	cubic
conc.	concentration
C_3A	tricalcium aluminate
C-A-H	calcium aluminate hydrate phases
d_{50}	average particle size
ESEM	environmental scanning electron microscope
Pa	Pascal
mg	milligrams
M_t	amount of water sorbed by the sample at time t
o	orthorhombic
RH	relative humidity
t	time
W_0	weight of the sample at the beginning of the experiment
W_t	weight of the sample at sorption time t
wt. %	weight percentage
XRD	X-Ray Diffraction

1. Introduction

Ordinary Portland cement (OPC) is a moisture sensitive material and may take up water vapour during the manufacturing process or later on by inappropriate conditions occurring during its transport or storage [1 – 3]. The phenomenon of water vapour sorption by cement powder exposed to humidity is known as prehydration of cement [4 – 5]. Prehydration of cement may lead to failures, that are more prevalent in climates characterised by high temperatures and humidities. In previous works, several consequences of prehydration for the chemical and engineering properties of cement have been reported. Those include: increased setting time, decreased compressive strength and heat of hydration, altered rheological properties and poor response to superplasticizer addition [6 – 12].

In order to secure control of cement performance in the field and thus also of concrete performance, it is important to understand the mechanisms behind the interactions of cement with water vapour. Due to the complex nature of cement, it is challenging to identify the key processes occurring during sorption of water on the surfaces of cement particles. Previous studies have shown that the individual clinker minerals C_3S , C_2S , C_3A and C_4AF have fundamentally different sensitivities to moisture [13 – 14].

We recently investigated the physicochemical effects of water sorption on the surfaces of pure individual clinker phases, plus those of different sulphates and free lime [15]. There, we determined the relative humidity (RH) thresholds at which early stage hydration (up to 11 hours) of these cement constituents in moist atmospheres starts to occur, and the amount of water sorbed per unit of surface area. The experiments demonstrated that among all cement components, orthorhombic C_3A and free lime are the ones which start to sorb water at particular low RH values ($< 55\%$). Additionally, they sorb the highest amounts of water.

Cubic C_3A and C_4AF follow next while C_3S and C_2S , the main clinker constituents, are the least reactive phases.

However, the study of prehydration of individual cement constituents does not account for interactions between different phases, which can take place during prehydration of actual cements. For example, it is well established that at the early stage of its hydration with liquid water, C_3A can react with sulphates to form AF_m or AF_t phases [16 – 19]. Thus, formation of those phases may significantly affect further sorption of water vapour by cement. Furthermore, *Kirchheim et al.* showed that there are important differences between the hydration of the two C_3A polymorphs (cubic and orthorhombic) with gypsum [20]. Therefore, it is of interest to have a better understanding of the interaction of each C_3A polymorph with calcium sulphates when exposed to different relative humidities.

In an earlier study it was reported that cubic C_3A reacts with gypsum when it is prehydrated [21]. Yet there are no studies which compare the behaviour of the two C_3A polymorphs (cubic and orthorhombic) when exposed to moisture in the presence of calcium sulphate hemihydrate, and the mechanism underlying this prehydration reaction. More specifically, it is unknown whether prehydration is solely a reaction between C_3A with sulphates and gaseous water vapour, or whether it occurs as a consequence of water vapour condensation, which then allows C_3A and sulphate to react in solution.

In this study, specific water sorption experiments were performed to gain an understanding of the principle interactions occurring during prehydration between the C_3A polymorphs in the absence and presence of calcium sulphate hemihydrate (subsequently abbreviated as “hemihydrate”, and chosen for its higher solubility and dissolution rate compared to gypsum or anhydrite). From this, the behaviours of the two C_3A polymorphs were compared.

The objective of this study was to demonstrate the effect which water vapour may have on the different C₃A polymorphs in the presence of sulphate, and to provide insight into the mechanism of a potential interaction by using dynamic and static water vapour sorption methods.

2. Materials and Methods

2.1 Materials

Pure, undoped cubic C₃A and orthorhombic C₃A doped with 4 wt. % Na₂O were synthesized from calcium carbonate and aluminium oxide according to [15]. In the preparation of C₃A₀, sodium nitrate was used as a source for Na₂O. The sintered samples were removed from the oven, allowed to cool in air for 3 minutes and then immediately placed in the cup of a ball mill (Planetary Mono Mill Pulverisette 6 classic line, Fritsch, Idar-Oberstein, Germany). Grinding was performed for 10 minutes at 250 rpm at a temperature of 21 °C and a relative humidity of 20 %. No grinding agent was added in the milling process.

Precautions were taken to prevent reaction with atmospheric carbon dioxide and water vapour by storing the freshly ground samples in sealed 20 mL glass bottles placed in a vacuum desiccator containing silica gel as a drying agent.

According to quantitative XRD analysis using *Rietveld* refinement, the C₃A phases were 99 ± 0.5 wt. % pure. The XRD patterns of the cubic and orthorhombic C₃A samples are presented in **Fig. 1**. Their average particle size (d₅₀ value) and specific surface area (BET, N₂) are given in **Table 1**.

The sample of β -modification of calcium sulphate hemihydrate (purity 97 wt. %) was obtained from Sigma-Aldrich (Taufkirchen, Germany). The average particle size and specific surface area were 10.4 μm and 12 000 cm^2/g , respectively (**Table 1**).

Binary mixtures of individual cubic and orthorhombic C_3A respectively with hemihydrate were prepared by manually blending the C_3A and hemihydrate powders at a molar ratio of 1:1.

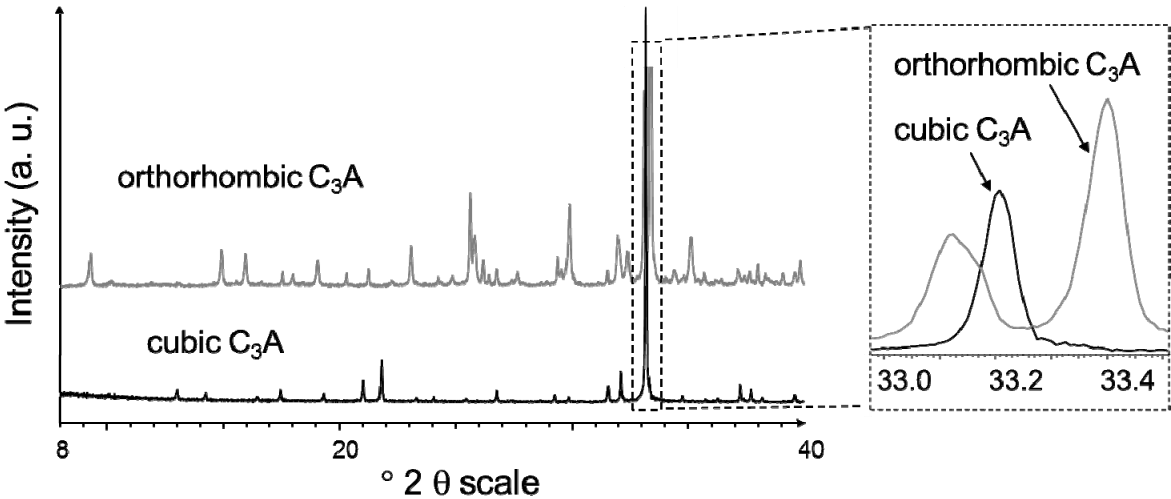


Fig. 1. XRD patterns of cubic and orthorhombic C_3A phases as prepared, shown in the range of 8 – 40 $^\circ 2\theta$ scale

Table 1 Average particle size (d_{50} value) and specific surface area (BET) of the cubic and orthorhombic C_3A modifications prepared for this study

Phase	Average particle size (d_{50} value)	Specific surface area (BET)
	(μm)	(cm^2/g)
cubic C_3A	6.2	7 800
orthorhombic C_3A	10.0	7 000

2.2 Methods

2.2.1 Exposure of samples to water vapour

For the determination of the water vapour sorption behaviour of the various samples, both dynamic and semi-equilibrium (static) water sorption methods were used. In both experiments, the temperature was held constant at 20 °C.

A sorption balance (DVS Advantage, Surface Measurement Systems Ltd., London, UK) was used to measure the moisture uptake using the dynamic method. Further details on this instrument and the general set-up can be found in a previous article [15]. For analysis, 0.015 – 0.05 g of a binary mixture (C₃A + hemihydrate) were placed in a sample pan which was then transferred into a climate chamber where the desired relative humidity was obtained by mixing a proportional amount of dry and humid nitrogen gas. Two different exposure protocols were used during the dynamic vapour sorption tests:

In the first regime, RH was continuously increased from 1 % to 95 % RH at a constant rate of approximately 0.16 % RH per minute, as described in [15]. This ramp regime provided a mass change profile and made it possible to assess the threshold value of RH (onset point) at which a sample started to sorb water. In the second regime, RH was increased from 1 % to 95 % RH in 10 % RH steps to the desired RH and then kept at this level, as shown in **Figure 2**. The duration of exposure at each RH was set at either 1 hour for short-time experiments and at 5 hours for long-time experiments. At the beginning and end of each experiment, RH was set to 1 % RH.

In this study, physically bound water is defined as water which can be removed by drying at 1 % RH for 1 hour only, while non-removable water was considered to be bound chemically (irreversibly sorbed).

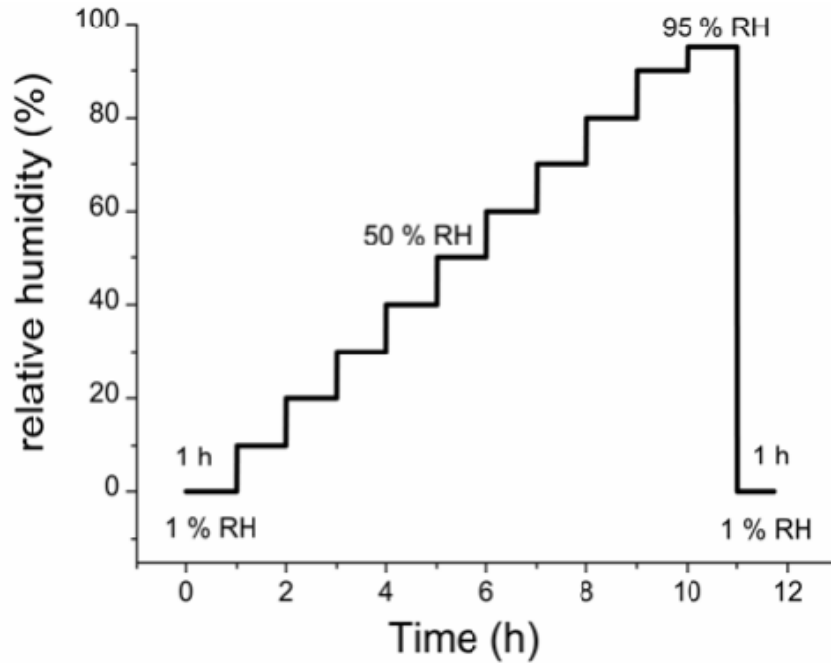


Fig. 2. Test protocol for the dynamic water vapour sorption experiment whereby relative humidity is increased in 1 hour steps over time

For the semi-equilibrium (static) regime the relative humidity environment was realised by keeping the samples (0.15 – 0.50 g) in a desiccator above saturated salt solutions. Exposure period was 21 days. The salts used and their relative humidity values are given in **Table 2**.

For the experiments in the presence of calcium sulphate hemihydrate, the binary mixtures were weighed accurately (this value was designated as W_0), and then stored for 21 days at a constant temperature of $20\text{ }^\circ\text{C} \pm 1\text{ }^\circ\text{C}$ under different relative humidities. The weight increase of the samples at sorption time t was measured by quickly weighing them on a digital balance. This value was noted as W_t . The weight increases were monitored over a period of 21 days. The percentage mass of water sorbed by a binary mixture at time t was calculated as:

$$M_t = \frac{W_t - W_0}{W_0} \times 100\% \quad (1)$$

Table 2: The saturated salt solutions used in the experiments, the corresponding relative humidity values at 20 °C obtained from them and the values for H₂O partial pressure calculated from the saturation vapour pressure of water (2.34 kPa) at RH = 100 % [22].

Salt	K-acetate	MgCl ₂	K ₂ CO ₃	NaBr	NaCl	KCl	KNO ₃
conc. / g/L*	2700	700	1350	1200	500	500	500
RH / %	23	33	43	60	75	85	95
p(H ₂ O) / kPa	0.54	0.77	1.01	1.40	1.76	1.99	2.22

* with solid salt at the bottom of the salt solution

2.2.2 Instrumentation

Samples were analysed by quantitative XRD using a Bruker D8 Advance X – ray diffractometer (Bruker AXS, Karlsruhe, Germany) with Bragg – Brentano geometry, equipped with a two dimensional detector (Vantec – 1, Bruker AXS, Karlsruhe, Germany) operated at an accelerating voltage of 40 keV on a CuK_α anode, irradiation intensity of 30 mA, and 40 scans in steps of 0.02 °/s. Cement hydrates were identified by comparison with Diffract Plus EVA Application V.8.0 and JCPDS PDF-2 database [23].

The average particle size (d₅₀ value) of all phases tested was measured by laser granulometry (Cilas 1064, Cilas, Marcoussis, France) using isopropyl alcohol as a base fluid and ultrasound to disagglomerate the particles before the measurement.

The specific surface area of all samples was determined by N₂ adsorption (BET method) employing a NOVA 4000e surface area analyzer from Quantachrome (Odelzhausen, Germany).

Environmental scanning electron microscopic (ESEM) and scanning electron microscopic (SEM) images were obtained on a FEI XL 30 FEG instrument (FEI, Eindhoven, Netherlands) equipped with a Peltier cooling stage and a gaseous secondary electron detector. One set of samples was investigated under low vacuum conditions (1 mbar H₂O pressure, corresponding to ~ 4 % RH at room temperature). Samples were not coated and were examined before and after their exposure to relative humidity in a sorption balance or in a desiccator over various periods of time.

For selected samples, *in-situ* observations of the development of prehydration products were performed using the ESEM mode. For this, anhydrous samples were placed on the cooling stage in the microscope chamber whereupon the temperature was lowered to 3 °C and the water vapour pressure was raised to ~ 6.3 mbar (corresponding to 85 % RH) for 1.5 hrs. To allow high resolution imaging, the pressure was lowered to ~ 1.7 mbar (corresponding to ~ 7 % RH) during imaging.

3. Results and discussion

3.1 Water sorption behaviour of individual C₃A polymorphs

3.1.1 Total water sorption

Applying the ramp regime, cubic and orthorhombic C₃A showed significantly different behaviours (**Fig. 3**). Orthorhombic C₃A started to sorb water already at ~ 55 % RH which is far below the onset point of 80 % RH observed for cubic C₃A. This indicates that orthorhombic C₃A is more susceptible to moisture than cubic C₃A.

Under these conditions, when RH reached 95 %, cubic C₃A had sorbed ~ 0.9 wt. % of water, based on its dry mass. Thereafter, when RH was lowered to 1 %, 0.7 wt. % could not be

removed and thus were considered as bound by chemical reaction. In comparison, orthorhombic C_3A had sorbed a total of ~ 3.4 wt. % of water, with ~ 1.4 wt. % bound chemically.

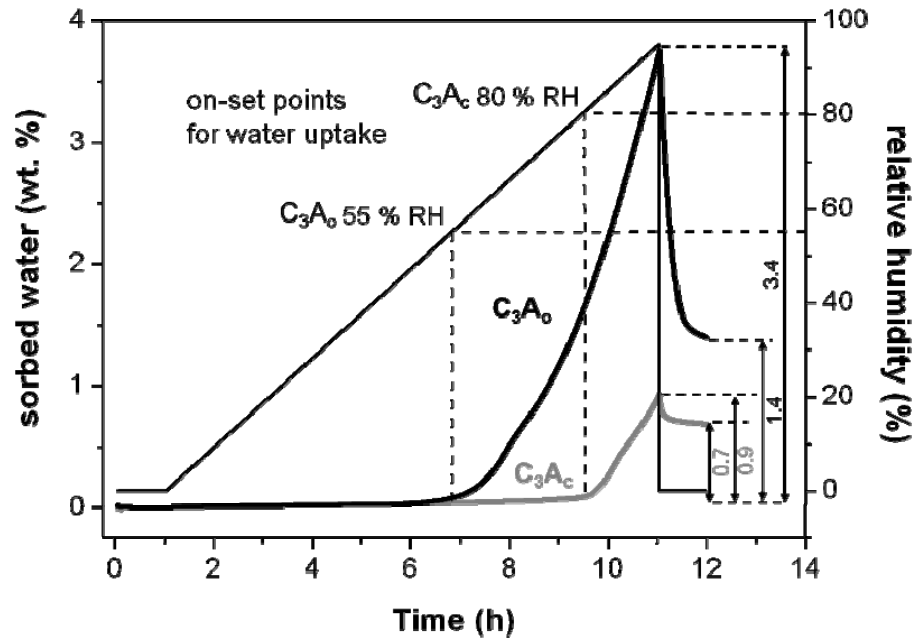


Fig. 3. Water vapour sorption isotherms of cubic and orthorhombic C_3A , determined on a sorption balance at $20\text{ }^\circ\text{C}$ using ramp mode and measured over a period of 11 hours

Following the water vapour sorption experiment, all samples were analysed by XRD and SEM. XRD revealed no discernable differences between prehydrated and fresh samples with the amount of surface hydrates formed being insignificant compared to the non-reacted bulk material.

However, SEM analysis revealed significant differences in the surface appearance of the two polymorphs (**Fig. 4**). Undoped C_3A_c showed considerable fewer prehydration products than C_3A_o . For cubic C_3A , preferential nucleation of C-A-H phases between grains or on grain edges was observed. For the sodium doped C_3A_o , after water vapour exposure the initially smooth surface was almost completely covered by very fine crystals of Na_2CO_3 , as indicated by elemental EDX mapping. Additionally, C-A-H phases were found on the surface.

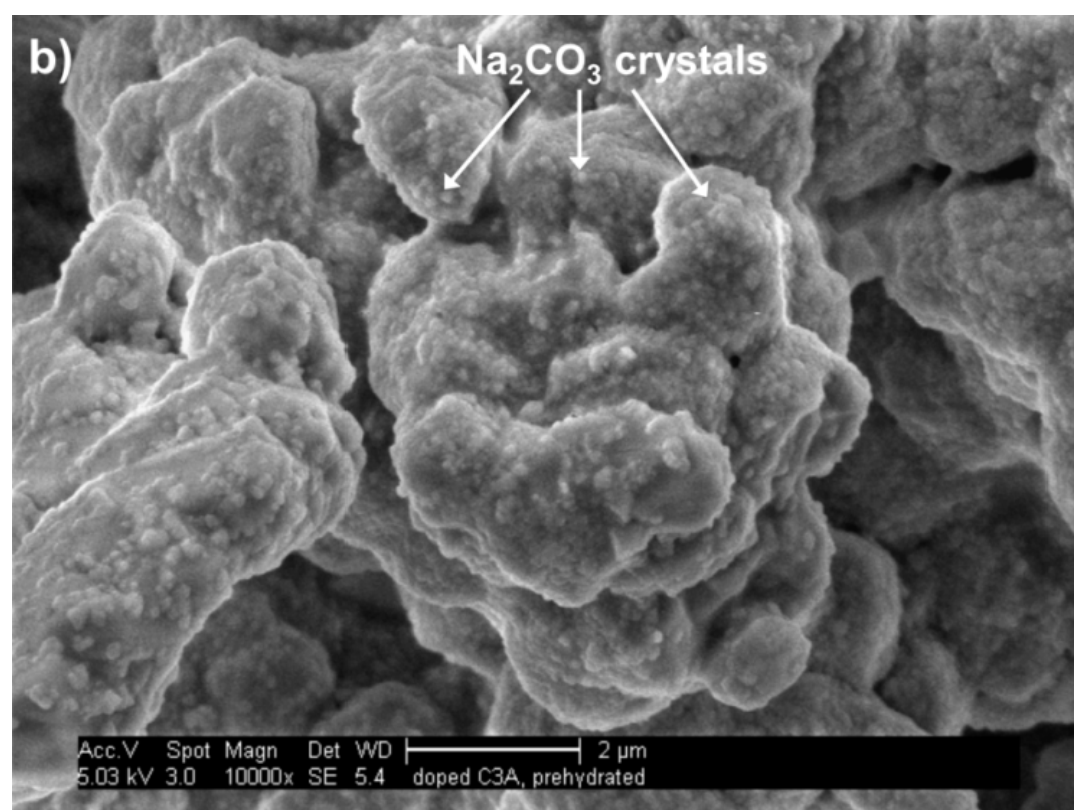
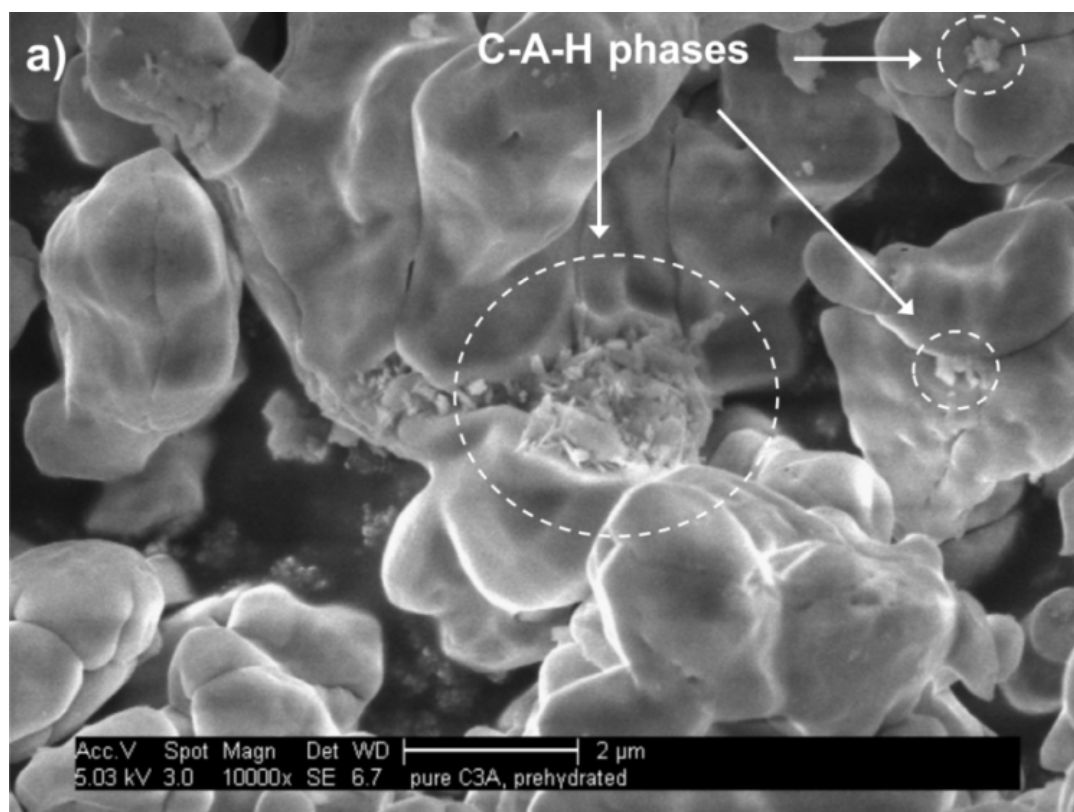


Fig. 4. SEM images of the C_3A polymorphs prehydrated for 10 hours using ramp regime and subsequent drying at 1 % RH for 1 hour at 20 °C: a) pure, cubic C_3A ; b) doped, orthorhombic C_3A

The presence of alkalis has a major impact on the water vapour sorption behaviour of C_3A . Orthorhombic C_3A shows a tendency for selective dispartage of sodium ions from its crystal structure [24]. This process can change both the surface characteristics and also the bulk properties of C_3A . When orthorhombic C_3A comes in contact with water vapour, then it reacts to form C-A-H phases and sodium ions are released as NaOH which will then quickly undergo carbonation.

Most interesting and important, however, was evidence of condensed water films, occurring mainly in the interstitial spaces and sometimes on the surfaces of the C_3A particles exposed to moisture. **Figure 5** shows as example an *in-situ* ESEM image of C_3A_c exposed for 30 min to 85 % RH in the microscope chamber. The micrograph reveals a thin water film which bridged two adjacent C_3A particles. Such films were also observed when studying C_3A_0 samples.



Fig. 5. ESEM image of cubic C_3A , prehydrated for 30 min in the ESEM chamber at 4.5 °C and 85 % RH, exhibiting a film of condensed liquid water between the particles.

Obviously, interaction of these phases with humidity is not limited to physicochemical reactions with gaseous water molecules, but also involves interaction with liquid water whereby the phases dissolve and hydrates are precipitated from an oversaturated solution. This mechanism is based on capillary condensation of water in the interstitial spaces between the clinker particles which can be described by *Kelvin's* equation:

$$\ln\left(\frac{p}{p_0}\right) = - \frac{\sigma}{R \cdot T \cdot \rho \cdot r} \quad (2)$$

Whereby p = partial pressure of H_2O under actual test conditions, p_0 = partial H_2O pressure at saturation, σ = surface tension of water, R = universal gas constant, ρ = density of the sample and r = radius of the pores or initial spaces.

According to this equation it is obvious that the smaller the pore size, the lower the RH at which capillary condensation occurs. In this study, a broad distribution of pore sizes ranging from 50 nm to 1 μm was evident between the C_3A particles (**Figs. 4 and 5**). Electron micrographs showed evidence of water films on all samples after only a few minutes of exposure to moist air, and the first hydration products become visible immediately after the films appeared. The amount of hydrates became more abundant with exposure time.

The observation that prehydration – at least partially – occurs via a liquid film of condensed water is of great significance. It suggests that during the process of prehydration, cement constituents can interact with each other in a similar manner as during normal hydration after mixing cement with water. This concept was probed further when the binary mixtures of C_3A and hemihydrate were tested later.

3.1.2 Impact of exposure time on water sorption

The water vapour sorption process is dependent on different factors, such as temperature, exposure time, RH and specific properties of the material under investigation. Since a system may take time to reach equilibrium, the amount of sorbed water may vary with respect to time when the sample is exposed to humidity. To study the impact of storage time on the amounts of chemically and physically bound water, cubic and orthorhombic C₃A samples were exposed to humidity using the step mode.

Figure 6 shows the time-dependent evolution of mass change for both samples at increased RH. The exposure time for each RH step was increased from 1 hour (short exposure) to 5 hours (long exposure), and the amounts of physically and chemically bound water were calculated based on the initial dried mass of samples.

The extended exposure times had no influence on the thresholds for water uptake. Orthorhombic and cubic C₃A samples started to take up noticeable amounts of water vapour at RH values of 50 % RH and 80 % RH respectively (**Fig. 6**). These RH values are in good agreement with the onset points found before using the ramp regime (55 % RH for orthorhombic C₃A and 80 % RH for cubic C₃A; see **Fig. 3**). However, the duration of the experiments did affect the total amounts of water sorbed by each sample. When exposed to 5 hour steps, cubic C₃A sorbed almost 7 times more water than when exposed to 1 hour steps, while orthorhombic C₃A sorbed 4 times more water. Despite this, for cubic C₃A the ratio between chemically and physically bound water was independent of the duration of the experiment, remaining at ~ 3 for both short (2.1 / 0.7 wt. %) and long (14.2 / 4.9 wt. %) exposure. For orthorhombic C₃A, however, the ratio changed significantly. When humidity was increased in 1 hr steps, the ratio of chemically to physically bound water was 0.7. It decreased to 0.3 for the experiments applying 5 hr steps. This indicates that under prolonged exposure to humidity, orthorhombic C₃A undergoes less chemical reactions and preferentially sorbs water physically. Consequently, independent of exposure times, cubic C₃A generally

predominantly interacts with water vapour through chemical reactions while orthorhombic C_3A preferentially sorbs water physically.

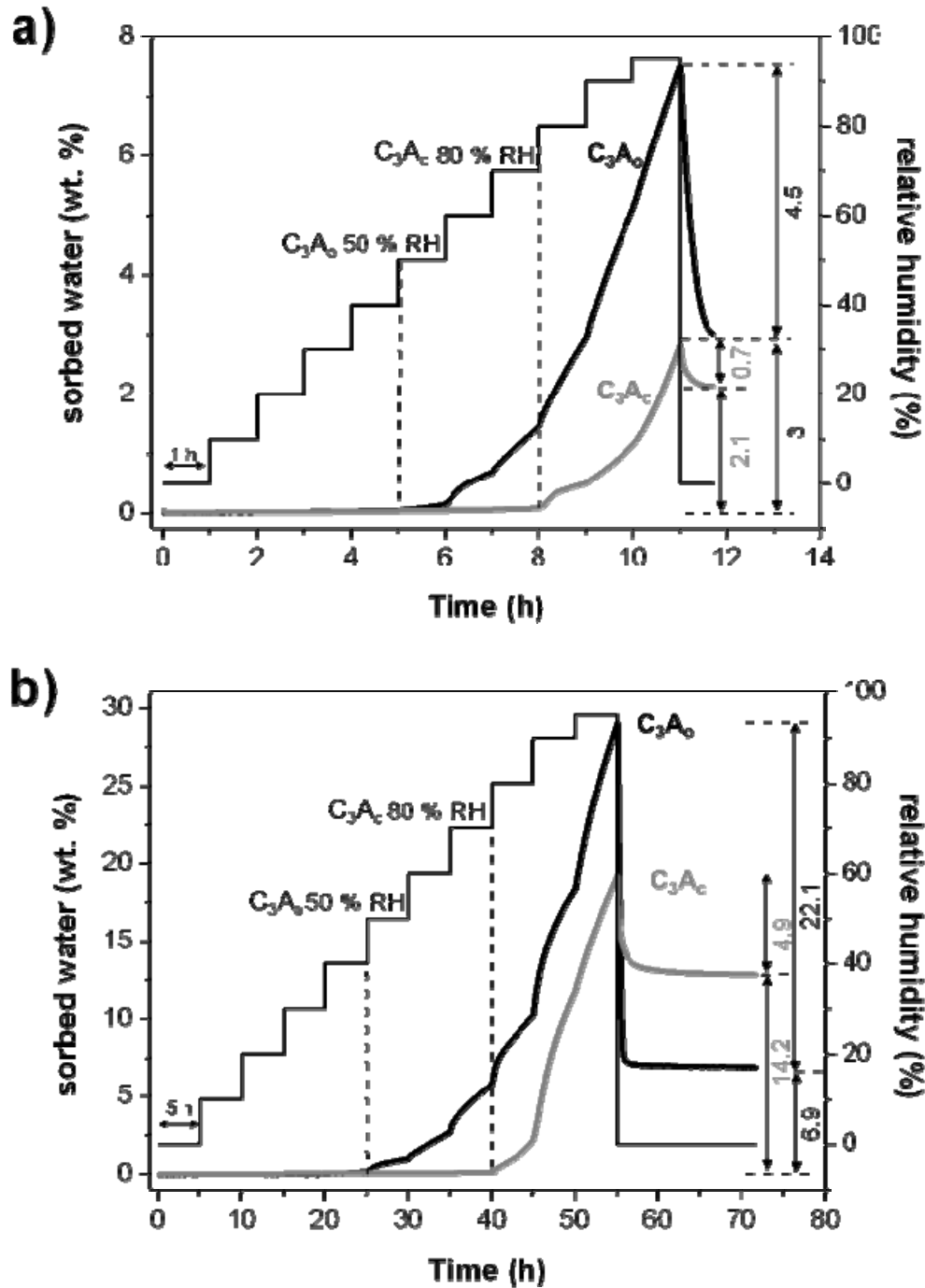


Fig. 6. Water vapour sorption isotherms of cubic and orthorhombic C_3A , determined on a sorption balance at 20 °C using the RH step mode and measured over a total time period of a) 11 hours and b) 55 hours

Another significant difference was observed in the total amounts of water bound chemically on each sample after drying at 1 % RH. Here, after longer exposure times, cubic C_3A bound more water chemically than orthorhombic C_3A (14.2 wt. % vs. 6.9 wt. %). Characterisation of the samples by XRD after exposure to humidity showed no apparent changes after short exposure (11 hrs). However, for orthorhombic C_3A reflections for katoite (C_3AH_6) were observed after long exposure (**Fig. 7**). No additional reflections from sodium containing phases (e. g. Na_2CO_3) were found for the orthorhombic phase.

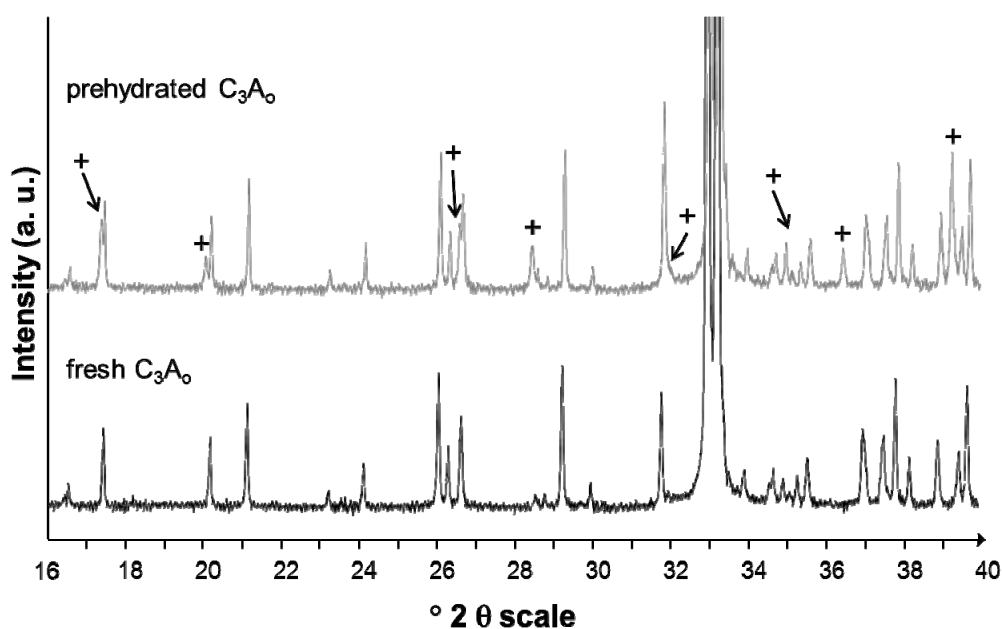


Fig. 7. X-Ray diffraction patterns recorded before and after exposure of orthorhombic C_3A to RH over a period of 55 hours using the ramp regime; “+” = katoite (JCPDS No. 24-0217), unlabeled reflections belong to orthorhombic C_3A

It should be noted that under real conditions, when a C_3A or cement sample is exposed to humid air, no subsequent drying will occur at the end of the exposure period. Thus, the total amount of water sorbed there will also include physically bound water. Additionally, throughout this experiment carbon dioxide was rigorously excluded to minimise the formation

of various carbonate species. Such a condition differs significantly from actual storage environments.

3.1.3 Influence of particle size on water sorption

Another factor which may greatly influence the total amount of water sorbed is the particle size and therefore the specific surface area of a sample and the pore sizes for capillary condensation. To determine the impact of particle size on the water vapour sorption behaviour, orthorhombic C_3A with an initial average particle size (d_{50} value) of $10\ \mu\text{m}$ was ground to $5\ \mu\text{m}$ and $2\ \mu\text{m}$ respectively. **Figure 8** shows the isotherms obtained for the three samples over 55 hours of exposure. As expected, smaller samples, which possess higher specific surface areas, sorbed greater amounts of water. For example, the C_3A powder ground to $2\ \mu\text{m}$ sorbed $\sim 57\%$ of its own mass, versus 30% for the $10\ \mu\text{m}$ sample. To determine the impact of surface area, the values of sorbed mass of water per unit mass of phase were converted into values per unit of surface area, and the results shown in **Figure 9**. The amount of water sorbed per unit surface is independent of particle size and lies at $\sim 0.05\ \text{mg}/\text{cm}^2$. Similarly, the onset of water uptake was independent of particle size. It started when RH reached 50% , in good agreement with the results presented earlier (see **Fig. 3**).

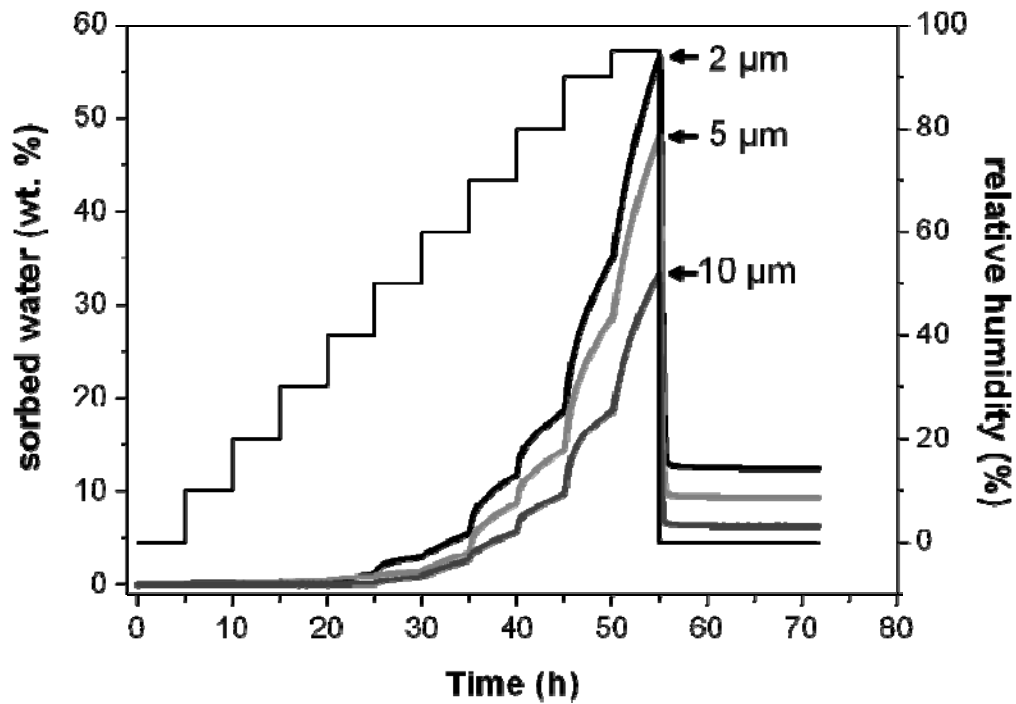


Fig. 8. Water vapour sorption isotherms for orthorhombic C_3A ground to average particle sizes of $10\ \mu\text{m}$, $5\ \mu\text{m}$ and $2\ \mu\text{m}$ respectively, determined on a sorption balance at $20\ ^\circ\text{C}$ over a period of 55 hours using step mode

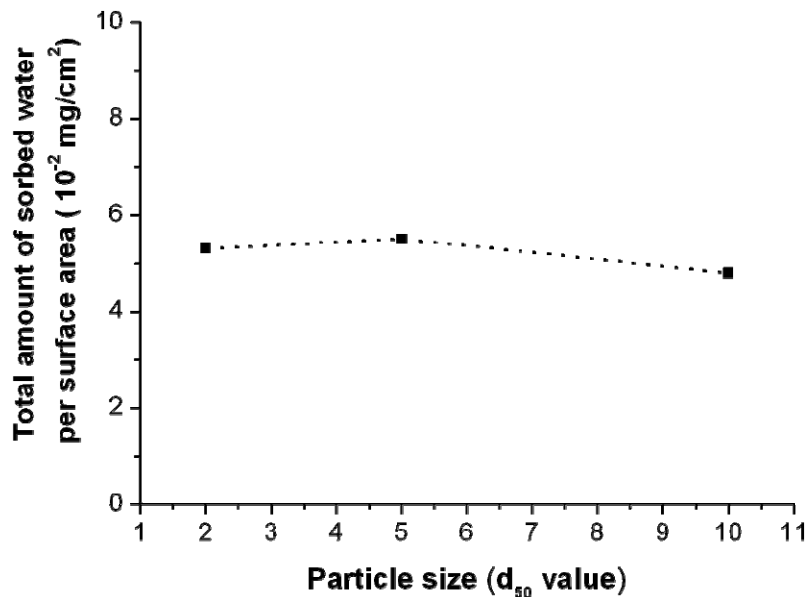


Fig. 9. Plot of total amount of sorbed water per surface area (after exposure of sample to RH at $20\ ^\circ\text{C}$ for 55 hours using the step mode) as a function of particle size (d_{50} value) of C_3A_0

3. 2 Binary mixtures

3.2.1 Dynamic water vapour sorption

To study the behaviour of water sorption in the presence of sulphates, the cubic and orthorhombic C_3A polymorphs were exposed to a ramped RH regime in the presence of hemihydrate.

Figure 10 shows the cumulative amount of water sorbed by the binary mixtures. Below 64 % RH, the sorption profiles of both C_3A polymorphs exhibit almost identical characteristics. Furthermore, both modifications show step-like mass increase over the range 34 % to 60 % RH, which can be attributed to the hemihydrate. This step also occurred in the mass profile of pure hemihydrate exposed to humidity [15], where pure hemihydrate showed two onset points, one at ~ 34 % RH and one at ~ 78 % RH, with an inflection point at ~ 44 % RH.

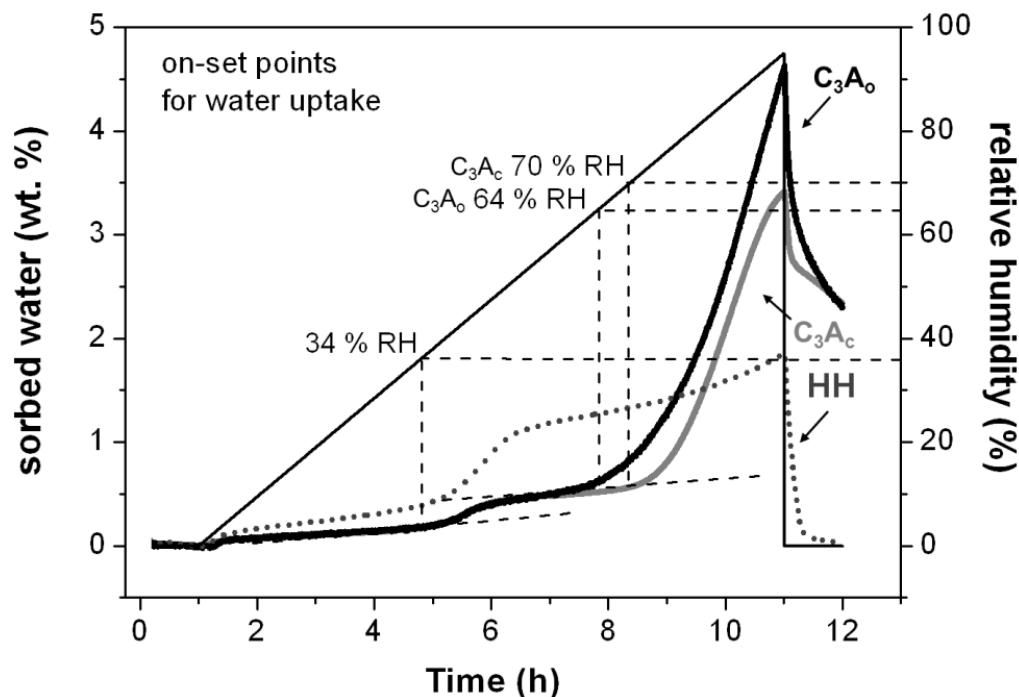


Fig. 10. Water vapour sorption isotherms for pure $CaSO_4 \cdot 0.5 H_2O$ and for cubic and orthorhombic C_3A dry-blended with hemihydrate, determined on a sorption balance at 20 °C over a period of 11 hours using the ramp regime

The shapes of the water sorption profiles of the binary mixtures imply that at lower RHs, no chemical reaction occurs between C₃A and hemihydrate during prehydration; the mixtures sorb minimal amounts of moisture on their surfaces, possibly by hydrogen bonding. Additionally, for the binary mixture containing orthorhombic C₃A, the onset point occurred at a slightly lower RH (64 %) than for the binary mixture containing cubic C₃A (70 % RH). This suggests that the sodium ions present in orthorhombic C₃A lower the onset point.

Table 3 gives a comparison of the total amounts of water sorbed by cubic and orthorhombic C₃A at 20 °C in the absence and presence of hemihydrate using the ramp regime. The table presents the amount of water sorbed by mass percentage and per unit of surface area (BET) of C₃A. The values show that when hemihydrate was present, both C₃A polymorphs sorbed higher amounts of water than in the absence of sulphate, with the effect on cubic C₃A being much more pronounced than for C₃A₀. XRD analysis performed for the binary mixtures after exposure to moisture showed formation of ettringite for both modifications, confirming that C₃A reacts chemically with hemihydrate (**Fig. 11**).

Table 3 Comparison of the total amounts of water sorbed by cubic and orthorhombic C₃A at 20 °C in the absence and presence of hemihydrate over 11 hours using the ramp program

C ₃ A polymorph	mass change after exposure to humidity			
	hemihydrate absent		hemihydrate present	
	[wt.%]	[10 ⁻⁷ g/cm ²]	[wt.%]	[10 ⁻⁷ g/cm ²]
cubic	0.92	11.8	3.42	38.9
orthorhombic	3.60	51.4	4.60	54.8

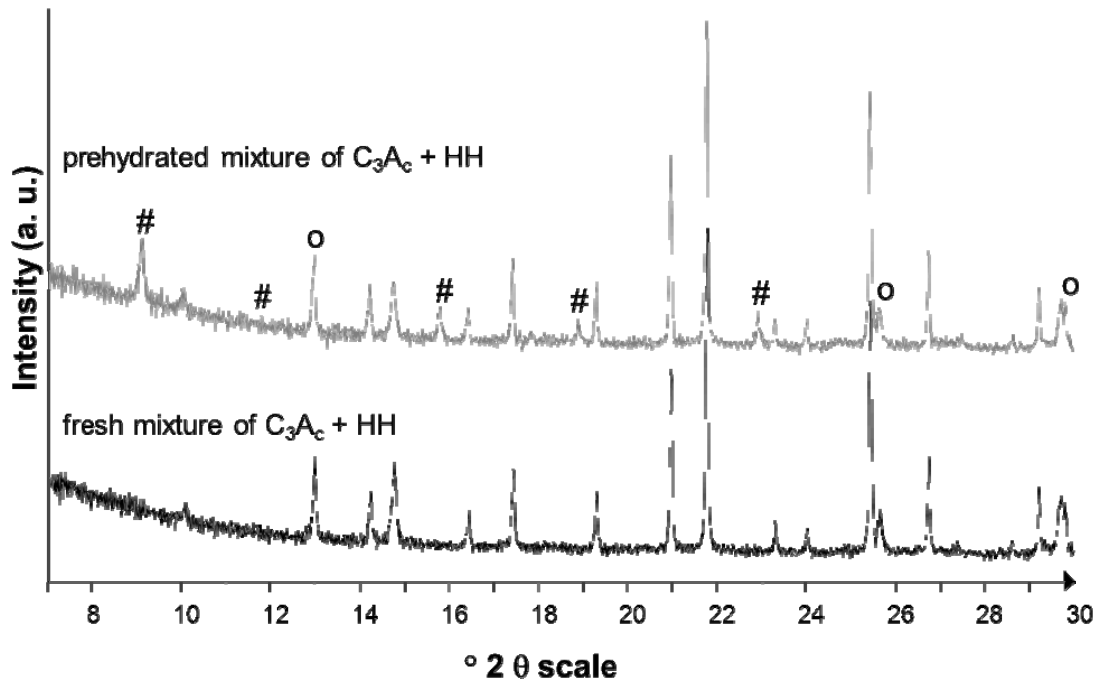


Fig. 11. X-Ray diffraction patterns of a binary mixture of cubic C_3A with hemihydrate recorded before and after exposure to RH over a period of 11 hours using a ramp regime; # = ettringite (JCPDS No. 42 – 1451), o = hemihydrate (JCPDS No. 41 – 0224), unlabelled reflections belong to cubic C_3A

In order to determine whether the prehydration reaction observed between C_3A and hemihydrate occurs with water vapour (gas molecules) or via condensation of water vapour followed by liquid-phase reactions, *in-situ* ESEM monitoring of the prehydration of C_3A with hemihydrate was performed. For this purpose, the binary mixtures were exposed to 85 % RH at 4.5 °C for 1.5 hours in the chamber of an ESEM instrument. **Figure 12a** clearly shows evidence of a liquid water film immediately at the beginning of the imaging. Later on, formation of nano-sized ettringite needles on the surface of C_3A (here: orthorhombic polymorph) was evidenced, as shown in **Figure 12b**. This result is most interesting because ettringite formation is possible only if ions are dissolved from both C_3A and hemihydrate and then react in the liquid phase into ettringite. Thus, this experiment shows that prehydration mainly occurs via a liquid condensed water film and less from interaction with gaseous water

molecules. It also confirms the observations made before for the individual clinker phases (see Fig. 5).

At lower RHs (< 60 %), the liquid water films were found to be thinner compared to higher RH values. Thicker water layers enable greater ion transport, thus accelerating the chemical reactions occurring between C_3A and hemihydrate and producing more early hydration products.

The same results were obtained for the binary mixture containing cubic C_3A (images not shown here). Again, liquid water films were found in-between the particles and on the surfaces, and nano-sized ettringite crystals were identified as prehydration products, thus confirming a reaction between dissolved ion species.

These findings suggest that during improper storage of actual cements, capillary condensation may occur between the cement particles, initiating partial surface hydration and resulting in products identical to those formed under normal hydration conditions. Also, this process will be accelerated for cements possessing particularly small particle sizes (e. g. CEM I 52.5 type). Such cement will require more careful storage than coarser cements.

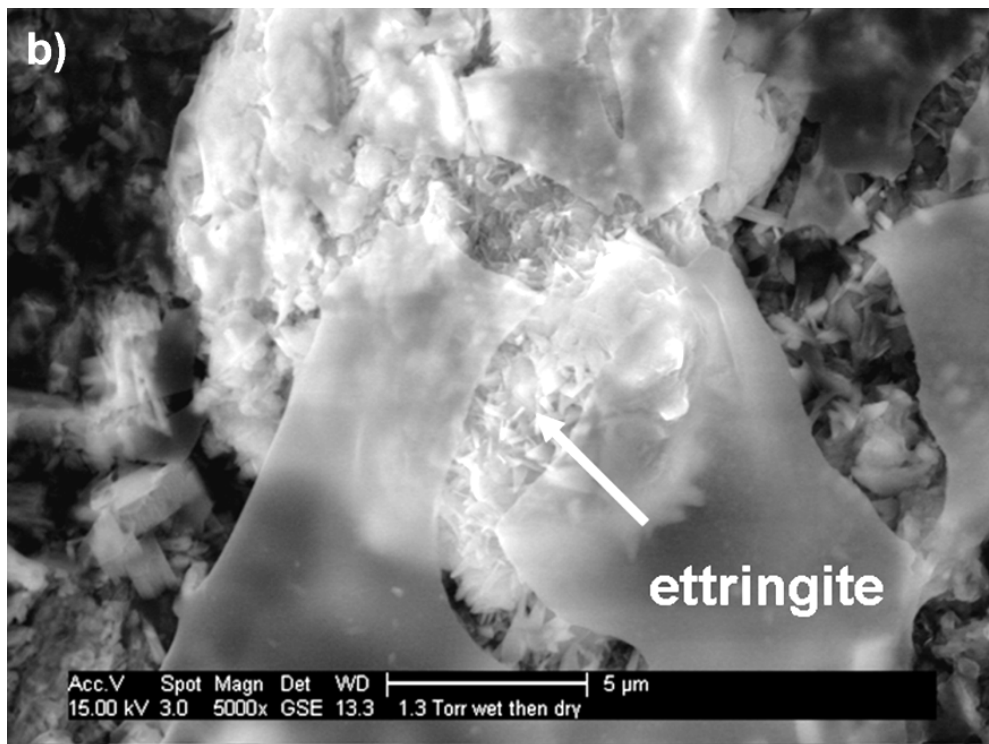
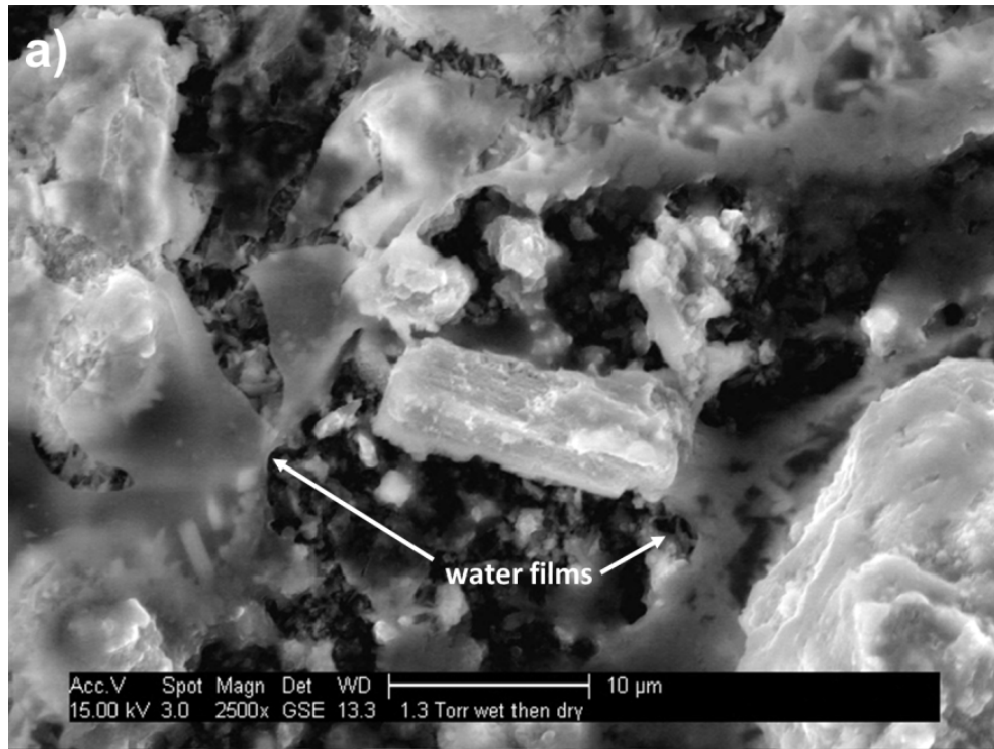


Fig. 12. *In-situ* ESEM monitoring of the prehydration of cubic C_3A with hemihydrate at 85 % RH: **a)** formation of a liquid water film within minutes after moisture exposure; **b)** ettringite needles formed on the surface of a C_3A particle and water films present after 1.5 hrs of moisture exposure

3.2.2 Static water vapour sorption

Complementary to the dynamic water vapour sorption, a static method was employed to examine the behaviour of the binary mixtures over longer time periods (21 days) of exposure.

Figure 13 shows the sorption isotherms obtained for both mixtures over the range 23 – 95 % RH.

The results for both static and dynamic methods were found to be in good agreement. The onset points obtained via the dynamic method were comparable with those from static measurements. At relative humidities below the onset points, only minor amounts of water were sorbed (less than 2 wt. %). The binary mixture containing orthorhombic C_3A sorbed almost twice the amount of water compared to that containing cubic C_3A . Ettringite was found in all samples prehydrated above the onset point, while below those RH values no ettringite was detected. The presence of sodium ions in orthorhombic C_3A leads to a more rapid water uptake by the mixture within the first three days. This result implies that also in the presence of sulphate, sodium ions enhance the water uptake significantly, as was found before for the individual phases (see **Fig. 6**).

The SEM images of samples prehydrated for 21 days. Again, no ettringite was observed for the samples prehydrated below the onset point (**Fig. 14**). Above the threshold however, needle-like ettringite crystals were observed. It was noticed that the shape of the ettringite crystals can vary from very thin needles produced at lower RH (75 %) to long and thick crystals at 95 % RH.

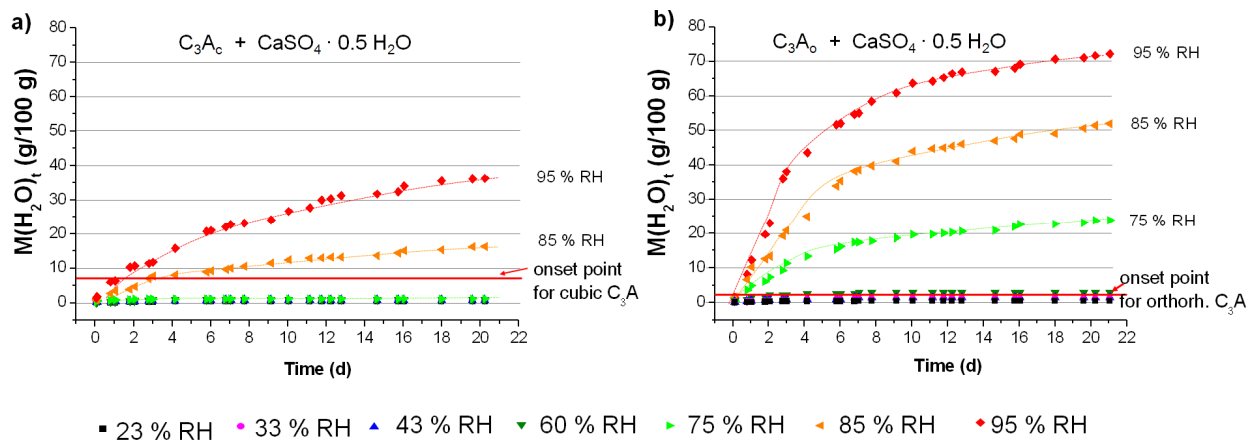


Fig. 13. Water sorption isotherms for binary mixtures at 20 °C and 23 – 95 % RH as a function of time: **a)** cubic C_3A + hemihydrate; **b)** orthorhombic C_3A + hemihydrate

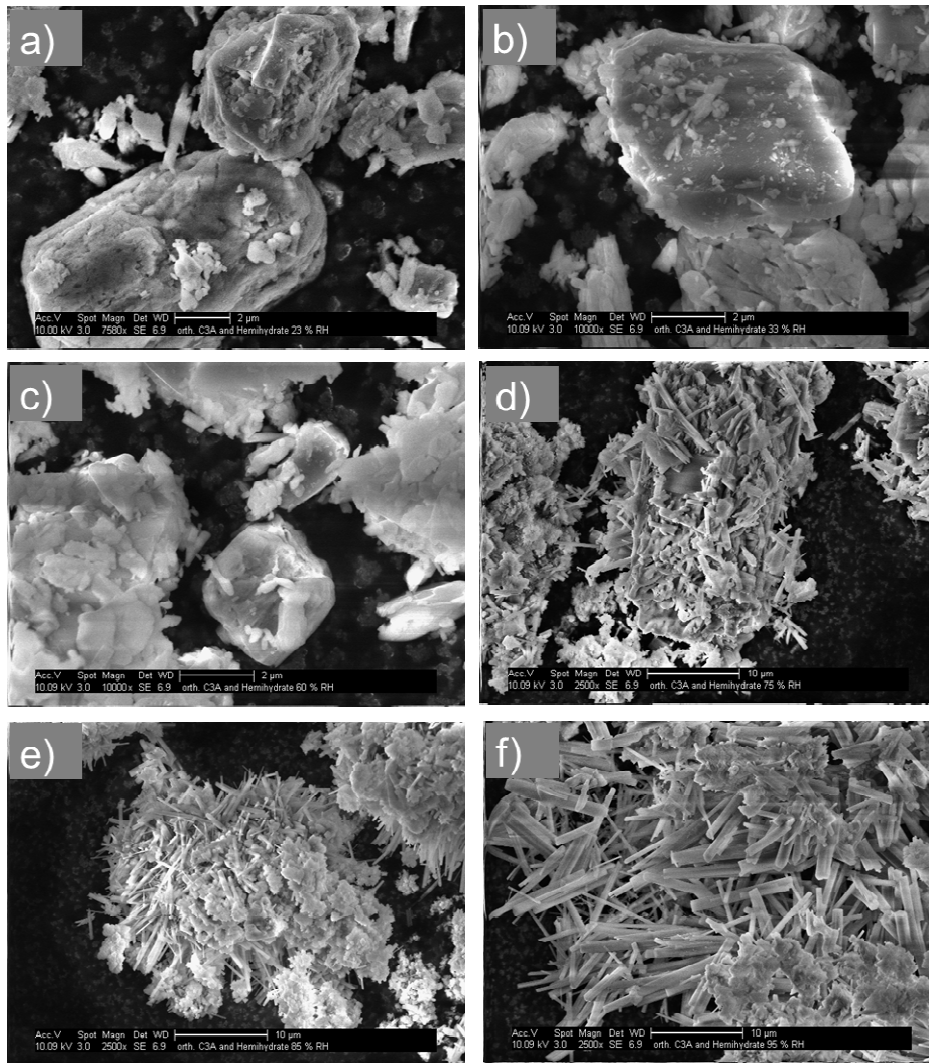


Fig. 14. SEM images of orthorhombic C_3A prehydrated in presence of hemihydrate for 21 days at 20 °C and at different relative humidities: **a)** 23 % RH **b)** 33 % RH **c)** 60 % RH **d)** 75 % RH **e)** 85 % RH **f)** 95 % RH

4. Conclusions

Dynamic and static methods of water vapour sorption were used to follow the interactions of cubic and orthorhombic C_3A polymorphs with gaseous water in the absence and in the presence of calcium sulphate hemihydrate.

It was found that both polymorphs behave differently in the presence of water vapour. The sodium ions present in orthorhombic C_3A lower the onset point to 55 % RH, compared to 80 % for undoped cubic C_3A . Additionally, C_3A_o sorbs a higher amount of water which is mainly bound physically while C_3A_c predominantly interacts with water chemically.

A linear relationship between the average particle size (d_{50} value) of a C_3A sample and the total amount of water sorbed exists. Smaller particles which possess higher surface areas take up more water. However, the amount of water sorbed per unit of surface area remained constant.

In the absence of sulphate, katoite was confirmed as prehydration product of C_3A by XRD. In the presence of calcium sulphate hemihydrate, ettringite was found as the main prehydration product. ESEM imaging revealed that ettringite formation occurred via a condensed liquid water film. Obviously, prehydration not only involves surface interaction with gaseous water molecules; but also capillary condensation between C_3A particles occurs, allowing C_3A and sulphate to react according to the well-known clinker dissolution/oversaturation/precipitation scheme observed for conventional cement hydration. This finding is of fundamental importance because it signifies that during prehydration, similar hydrates are formed as during normal cement hydration when cement is mixed with water, although morphology might be dependent on the conditions. Ettringite crystals were shorter when RH was lower, and longer and thicker when RH increased. Below 70 % RH, cubic C_3A did not react with calcium

sulphate hemihydrate; while orthorhombic C_3A formed ettringite crystals already from 64 % RH.

Thus, the experiments from this study suggest that when high amounts of Na-doped orthorhombic C_3A are present in a cement sample, it may undergo more pronounced prehydration during storage than a cement containing the same amount of cubic C_3A .

Prehydration occurs when the ambient RH exceeds the threshold value at which moisture uptake begins (onset point). This implies that storing cements below this critical RH value would prevent prehydration. Therefore, throughout the production and storage period of a cement, ideally the ambient RH should be below the onset point of the most active clinker phases. However, under actual conditions where cement is produced, stored, distributed and used, the control of RH to the required levels practically is impossible. Careful packaging and storage are the only measures which can help to minimize the effects from prehydration and to extend the shelf-life stability of cement.

Acknowledgments

E. Dubina is grateful to Nanocem (Core Project # 7) for financial support of this work. Additionally, the authors like to thank Holger König and Maciej Zajac, HeidelbergCement, Leimen, Germany as well as Ellis Gartner, Lafarge, France for their guidance and input in many discussions.

References

- [1] F. E. Hansen, H. J. Clausen, “Cement strength and cooling by water injection during grinding”, *ZKG*, 27 (7), 1974, 333 – 336.
- [2] W. Richartz, “Effect of storage on the properties of cement”, *ZKG*, 26 (2), 1973, 67 – 74.
- [3] S. Sprung, “Effect of storage conditions on the properties of cements”, *ZKG INTERNATIONAL* 30 (6) 1978, 305 – 309.
- [4] O. M. Jensen, P. Hansen, E. E. Lachowski, F. P. Glasser, “Clinker mineral hydration at reduced relative humidities”, *Cem. Concr. Res.* 29, 1999, 1505 – 1512.
- [5] E. Breval, “Gas-phase and liquid-phase hydration of C_3A ”, *Cem. Concr. Res.* 7, 1977, 297 – 304.
- [6] K. Theisen, V. Johansen, “Prehydration and strength development of Portland cement”, *J. Am. Ceram. Soc.*, 54 (9), 1975, 787 – 791.
- [7] H. M. Sylla, “Effect of clinker cooling on the setting and strength of cement”, *ZKG* 28 (9), 1975, 357 – 362.
- [8] C. Maltese, C. Pistolesi, A. Bravo, F. Cella, T. Cerulli, D. Salvione, “Effect of moisture on the setting behavior of Portland cement reacting with an alkali – free accelerator”, *Cem. Concr. Res.* 37, 2007, 856 – 865.
- [9] G. Schmidt, T. A. Bier, K. Wutz, M. Maier, “Characterization of the ageing behaviour of premixed dry mortars and its effect on their workability properties”, *ZKG INTERNATIONAL* 60 (6), 2007, 94 – 103.
- [10] C.-S. Deng, C. Breen, J. Yarwood, S. Habesch, J. Phipps, B. Caster, G. Maitland, “Ageing of oilfield cement at high humidity: a combined FEG-ESEM and Raman microscopic investigation”, *J. Mater. Chem.* 12, 2002, 3105 – 3112.
- [11] F. Winnefeld, “Influence of cement ageing and addition time on the performance of superplasticizer”, *ZKG INTERNATIONAL* 61 (11) 2008, 68 – 77.

- [12] M. Whittaker, E. Dubina, F. Al-Mutawa, L. Arkless, J. Plank, L. Black, “The effect of prehydration on the engineering properties of CEM I Portland cement”, *Adv. Cem. Res.*, 2012, in print.
- [13] O. M. Jensen, “Thermodynamic limitation of self-desiccation”, *Cem. Concr. Res.* 25, 1995, 157 – 164.
- [14] E. Dubina, L. Black, R. Sieber, J. Plank, “Interaction of water vapour with anhydrous cement minerals”, *Adv. Appl. Ceram.*, 109 (5), 2010, 260 – 268.
- [15] E. Dubina, L. Wadsö, J. Plank, “A sorption balance study of water vapour sorption on anhydrous cement minerals and cement constituents”, *Cem. Concr. Res.* 41, 2011, 1196 – 1204.
- [16] P. W. Brown, L. O. Libermann, G. Frohnsdorff, “Kinetics of the early hydration of tricalcium aluminate in solutions containing calcium sulfate”, *J. Am. Ceram. Soc.* 67, 1984, 793 – 795.
- [17] H. Minard, S. Garrault, L. Regnaud, A. Nonat, “Mechanisms and parameters controlling the tricalcium aluminate reactivity in the presence of gypsum”, *Cem. Concr. Res.* 37, 2007, 1418 – 1426.
- [18] S. Pourchet, L. Regnaud, J. P. Perez, A. Nonat, “Early C₃A hydration in the presence of different kinds of calcium sulphate”, *Cem. Concr. Res.* 39, 2009, 989 – 996.
- [19] L. Black, Ch. Breen, J. Yarwood, C.-S. Deng, J. Phipps, G. Maitland, “Hydration of tricalcium aluminate (C₃A) in the presence and absence of gypsum – studied by Raman spectroscopy and X-ray diffraction”, *J. Mater. Chem.* 16, 2006, 1263 – 1272.
- [20] A. P. Kirchheim, V. Fernández-Altable, P. J. M. Monteiro, D. C. C. Dal Molin, “Analysis of cubic and orthorhombic C₃A hydration in presence of gypsum and lime”, *J. Mater. Sci.* 44, 2009, 2038 – 2045.
- [21] E. Breval, “The Effects of Prehydration on the Liquid Hydration of 3CaO · Al₂O₃ with CaSO₄ · 2H₂O”, *J. Am. Ceram. Soc.*, 62, (7-8), 1979, 395 – 398.

- [22] L. Greenspan, “Humidity fixed points of binary saturated aqueous solutions”, *J. Res. Nat. Bur. Stand. Sect. A. Phys. Chem.*, 81A, 1, 1977, 89 – 96.
- [23] JCPDS PDF-2 release 2003, ICDD Newton Square, PA, USA.
- [24] F. P. Glasser, M. B. Marinho, “Early stages of the hydration of tricalcium aluminate and its sodium-containing solid solutions”, 1984, *Proc. Br. Ceram. Soc.*, 221 – 235.

Paper 5

The Effects of Prehydration of a Combination of Cubic C₃A with β-hemihydrate on Adsorption of BNS Superplasticizer

E. Dubina, J. Plank, L. Wadsö, L. Black

Proceedings of the XIII ICCI International Congress
on the Chemistry of Cement, Madrid/Spain, 2011, p. 250

ISBN: CD 978 – 84 – 7292 – 400 – 0.

The effects of prehydration of a combination of cubic C₃A with β-hemihydrate on adsorption of BNS superplasticizer

¹Dubina E., ¹Plank J.*, ²Wadsö L., ³Black L.

¹Technische Universität München, Lehrstuhl für Bauchemie, Lichtenbergstr. 4, 85747 Garching bei München, Germany

²Lund University, Building Materials LTH, Box 118, 221 00 Lund, Sweden

³University of Leeds, School of Civil Engineering, Woodhouse Lane, Leeds, LS2 9JT, UK

Abstract

Industrial cements can undergo some prehydration during their manufacturing process or during transportation and storage. In the cement plant, a first contact with water may occur from the dehydration of gypsum which is ground together with clinker in the mill at temperatures of 80 - 120 °C. Afterwards, during storage in a silo, cement may sorb water from continued dehydration of gypsum. Finally, because of improper packing and storage conditions, cement may undergo further surface hydration. The early uptake of water by cement is commonly referred to as the prehydration phenomenon. It can result in alteration of the cement properties during storage which is highly undesirable. Nevertheless, it has been reported repeatedly. The principal consequences of this cement prehydration may include decreased compressive strength and low heat of hydration, altered rheological properties and poor response to superplasticizer addition. Various cement clinker phases prehydrate very differently. Using a water sorption balance it was shown that, the amount of chemically and physically sorbed water and the relative humidity at which water sorption starts to occur differ significantly between clinker phases. Photoelectron spectroscopy (XPS) revealed that prehydration results in the formation of a nano layer of cement hydrates covering the surface of the clinker phases. In multi phase mixtures of cement constituents, moisture sorption can exhibit a more complex behaviour. Here, the moisture sorption profile of individual cubic C₃A and β - CaSO₄ · ½ H₂O was examined, and was compared with the behaviour of a binary mixture of C₃A with β - CaSO₄ · ½ H₂O. It was found that the extent of prehydration of C₃A was affected by the modification of C₃A, by temperature and the presence of the sulphate. Generally, binary mixtures were found to sorb significantly higher amounts of water than the individual phases. The prehydration products of this binary mixture were characterized by FTIR-ATR spectroscopy. ESEM imaging revealed that prehydration occurs via liquid condensed water which dissolves the cement constituents, and not via water vapour.

Originality

Due to the complex nature of cement, the mechanisms behind its prehydration are not yet fully understood. The prehydration of cement is obviously far more complex than the sum of each individual prehydration reaction. This paper highlights the question whether the mechanism behind prehydration is solely based on a topochemical reaction between cement and water vapour, or whether it follows the well known route of cement hydration characterized by a dissolution – oversaturation – precipitation process. The subject of prehydration of cement is highly interesting for cement manufacturers and applicators.

Chief contributions

It is commonly known that ageing of cement or inadequate storage can result in different engineering properties of concrete or mortar. In our study, the general phenomenon of prehydration of cement was scientifically investigated. With “cement prehydration”, we mean the interaction between cement and water vapour. Through specific experiments, it was possible to replicate the onsite problems in the laboratory and thus determine the causes and effects by using modern analytical methods. Currently, the knowledge of very early cement hydration and related analytical methods is still limited. Prehydration of cement is a surface process, whereby only a few methods like photoelectron spectroscopy (XPS) and FTIR-ATR spectroscopy can be utilised. The aim of this study is to fill this gap by enhancement of the current methods and by development of new analytical strategies for cement surface analysis of cement. Finally, the dosage and effectiveness of BNS superplasticizer used in combination with prehydrated C₃A/β - CaSO₄ · ½ H₂O is investigated.

Keywords: Prehydration, cement, C₃A, β-hemihydrate, adsorption, superplasticizer

¹ Corresponding author: Email sekretariat@bauchemie.ch.tum.de Tel + 49 – 089 – 289 – 13151, Fax + 49 – 089 – 289 – 13152

Introduction

Ordinary Portland cement (OPC) consists of several clinker phases. The main constituents include calcium silicates (Ca_3SiO_5 and Ca_2SiO_4), aluminate ($\text{Ca}_3\text{Al}_2\text{O}_6$), and ferrite ($\text{Ca}_4\text{Al}_{4-x}\text{Fe}_x\text{O}_{10}$) which are abbreviated to C_3S , C_2S , C_3A , and C_4AF respectively. In industrial application, cement may be stored for up to months or even a year before use. For dry-mixed mortars, for example, the usual shelf life is 6 months to 1 year, as stated on the bags. Alteration of the cement properties during storage is highly undesirable, but has been repeatedly noticed by users (Winnefeld, 2008; Maltese *et al.*, 2007). Cements that are stored for longer periods, especially in humid air, may fail in the field. The principal consequences of this phenomenon, otherwise known as prehydration, include increased setting time, decreased compressive strength and lower heat of hydration, altered rheological properties and poor response to superplasticizer addition (Sprung, 1978; Schmidt *et al.*, 2007; Barbic *et al.*, 1991; Whittaker *et al.*, 2010).

Thus, the quality of cement must be assessed based on a profound understanding of the processes occurring during its fabrication and storage. Despite its importance, prehydration of cement is not well understood, due to the complex nature, the interdependency of numerous chemical reactions, and the difficulties associated with the analysis of hydration layers which extend to only a few nanometers in thickness.

However, the study of prehydration of pure clinker phases enables an understanding of the key processes taking place in the complex system of cement. Jensen *et al.* showed that the clinker minerals C_3S , C_2S , and C_3A have fundamentally different sensitivities to moisture. For example, C_3A hydrates at lower humidities than either C_3S or C_2S (Jensen *et al.*, 1999). Theisen *et al.* discovered that the clinker mineral most easily attacked by water vapour is C_3A , which is therefore, expected to be the principally active component during prehydration of cement (Theisen *et al.* 1975). Brevet investigated the impact of water vapour on the prehydration of C_3A in presence of gypsum. He found that the degree of prehydration induced by water vapour impacted the hydration of C_3A with water (Brevet, 1977).

In previous work on prehydration, we used a combination of different analytical methods to study the changes occurring upon prehydration on the surface of clinker particles (Dubina *et al.*, 2010). We found that exposure of C_3S to water vapour led to the formation of a thin layer of C–S–H which acts as a barrier upon mixing with water, thus retarding hydration. Exposure of both pure and doped C_3A resulted in the formation of a calcium aluminate hydrates. X-ray diffraction indicated that katoite (C_3AH_6) was present, while XPS potentially revealed the initial formation of C_4AH_{13} which converted to katoite. The rate of C_4AF prehydration was less than that of the other clinker phases, as expected. As a consequence we conclude that cements possessing a higher C_4AF content are less sensitive to water vapour during storage in moist air. Conversely, a high content of C_3A in cement results in a higher sensitivity towards moisture. Thus, cements of different compositions behave extremely different upon prehydration.

In recently published work we investigated the physicochemical effects of water sorption on the surfaces of pure clinker phases as well as of different sulfates and of free lime (Plank *et al.*, 2010). By using a water vapour sorption balance, the relative humidities (RHs) at which early stage hydration (up to 11 hours) of the cement constituents starts to occur, and the amount of water sorbed per unit area of cement component surface were determined. Emphasis was placed on understanding the ratio between physically and chemically sorbed water, and the reversibility of this process. The results show that the various cement constituents have fundamentally different onset points at which water uptake starts to occur. Also, the water sorbed can be physically, chemically or in both ways, bound by the constituents. The experiments demonstrated that among all cement components, orthorhombic C_3A and free lime absorb the highest amounts of water. Here, we study the effects of prehydration on a binary system composed of cubic C_3A and β - $\text{CaSO}_4 \cdot \frac{1}{2} \text{H}_2\text{O}$ at a molar ratio of 1:1.

First, emphasis was placed on understanding the water vapour sorption behaviour of the binary mixture in comparison to the pure phases. The cumulative amount of water sorbed by the individual phases was compared with that of the binary mixture. Furthermore, we determined the RH at which

the AF_t phase starts to appear in large amounts. The prehydration products were characterized via XRD and visually observed by SEM.

In the second part it was studied how AF_t formation during prehydration affects the adsorption and dispersing power of a BNS superplasticizer. For this experiment, a binary mixture of cubic C₃A and β - CaSO₄ · ½ H₂O was prehydrated for 48 hours below and above its onset point of 72 % RH. Adsorption of BNS superplasticizer on the prehydrated mixture was determined. The goal was to uncover the reason behind the occasionally reported poor response of superplasticizers with prehydrated cements.

Experimental

(1) Materials

Cubic C₃A was prepared from a 3:1 stoichiometric and homogenized mixture of CaCO₃ and Al₂O₃ (both Merck). The sintering protocol for cubic C₃A included a 1 h 50 min heating ramp from 100 °C to 1350 °C, followed by sintering the sample for 4 h at 1350 °C. Afterwards, the sample was quenched. The purity of the products was checked by X-ray diffraction. After the first sintering process, mayenite (C₁₂A₇) and free lime were detected as minor byproducts. The sintering process was repeated 3 times to reduce the amount of mayenite and free lime to less than 0.1 wt. %.

Average particle size (d₅₀ value) and specific surface area were determined by laser granulometry (Cilas 1064, Cilas, Marcoussis, France) and Blaine measurement (Toni Technik, Berlin, Germany). The values obtained were 6.2 μm and 4,630 cm²/g, respectively.

β-Hemihydrate (purity 97 wt. %) was obtained from Sigma-Aldrich. Average particle size (d₅₀ value) and specific surface area of the sample were 10.4 μm and 4,250 cm²/g, respectively.

The binary mixture was prepared by manually blending cubic C₃A and β-hemihydrate at a molar ratio of 1:1.

For β-naphthalenesulfonate formaldehyde (BNS) polycondensate, a commercial sample (Melcret[®] 500 F from BASF, Trostberg, Germany) was used.

(2) Exposure of samples to water vapour

A sorption balances (DVS-1000 instrument from Surface Measurement Systems Ltd., UK) was used to measure the moisture storage capacity of individual phases and the binary mixture. It enables to monitor sorption kinetics in a gas flow containing pure nitrogen and water vapour in chosen proportion. Moisture uptake by the material was continuously followed with precision of 0.1 μg, and its variation with respect to time. Temperature and humidity were controlled to 0.1 °C and 0.5 % RH, respectively. Sample quantities were typically in the order of 20 to 30 mg. Prior to all experiments, the sample was kept at 0 % RH (pure nitrogen flow) for one hour until a constant mass (derivative less than 0.0005 % per min) was reached. Then, over a period of 10 hours the relative humidity was continuously increased from 0 % to 95 % RH at a constant temperature of 20 °C. In this mode, it is possible to obtain the profile of mass change for different samples. This allows to assess the “onset point” at which the sample starts to sorb water. The binary system was prehydrated at 60 % and 85 % RH, respectively for 48 hours using a large quantity (50 g). There, the relative humidity was controlled via the use of saturated salt solutions of sodium bromide (90.6 g/ 100 g H₂O) and potassium chloride (34.4 g/100 g H₂O) contained in a desiccator at 20 °C (Greenspan, 1977).

(3) Analysis of samples

All fresh and prehydrated samples were analysed by X-ray diffraction (D8 Advance, Bruker axs, Karlsruhe, Germany; Cu Kα X-ray source, measurements between 5 and 70° 2θ). Scanning electron microscopy (SEM) images were obtained from a FEI XL 30 FEG microscope (Philips, now FEI Company, Eindhoven, Netherlands) equipped with a large field detector under low vacuum (1 mbar H₂O pressure) conditions. Observations on the morphology of the prehydration products were performed on uncoated samples before and after exposure to relative humidity.

(4) Adsorption of BNS

BNS adsorption on fresh and prehydrated samples was determined by addition of the superplasticizer to aqueous slurry of the binary mixture. Adsorption was calculated using the depletion method. For this purpose, the concentration of BNS polymer present in the mixing water before contact with the binary mixture, and the non-adsorbed portion of the BNS remaining in solution was determined. The binary mixture slurries were prepared by adding 1 g of the binary mixture to 5 mL of aqueous solution containing different polymer dosages. Filtrate was recovered by centrifugation of the slurry for 10 min at 8500 rpm, then filtered through a 0.45 μm Nylon filter by pressure filtration and stabilized by addition of 5 mL of 0.1 mol/L hydrochloric acid to 1 mL of filtrate. BNS content in the filtrate was measured by TOC analysis using combustion at 890 $^{\circ}\text{C}$ in a High TOC II instrument (Elementar, Hanau, Germany). The percentage of polymer adsorbed on cement was calculated from the TOC content using a reference BNS solution of known concentration.

Results and Discussion

(1) Water vapour sorption of individual C_3A and β -hemihydrate

Water vapour sorption of the individual phases was obtained with the use of a sorption balance instrument. **Figure 1** (left) displays the mass change profiles of individual cubic C_3A and β -hemihydrate in the range between 0 % and 95 % RH. The mass change profiles are very different. Beginning at 80 % RH, cubic C_3A starts to take up a significant amount of water vapour. In this experiment, C_3A absorbed 0.9 wt. % of water (based on dry C_3A); thereof, 0.7 wt. % was chemically bound. However, with increasing humidity, β -hemihydrate exhibits a step-wise uptake of water. The mass profile shows the first threshold value at around 34 % RH and an inflection point at around 44 % RH. This behaviour is characteristic of hydrate formation.

(2) Water vapour sorption of the binary mixture C_3A / β -hemihydrate

Figure 1 (right) shows the water sorption curve for the binary mixture in the range between 0 % and 95 % RH. There, it can be seen that the binary mixture starts to sorb large quantities of water beginning at 72 % RH.

From the mass change profiles of the individual phases presented in **Figure 1** (left), it is possible to calculate theoretical change in mass for the binary mixture of C_3A with β -hemihydrate at a molar ratio of 1:1. This result was compared with the experimental mass change profile of the binary mixture.

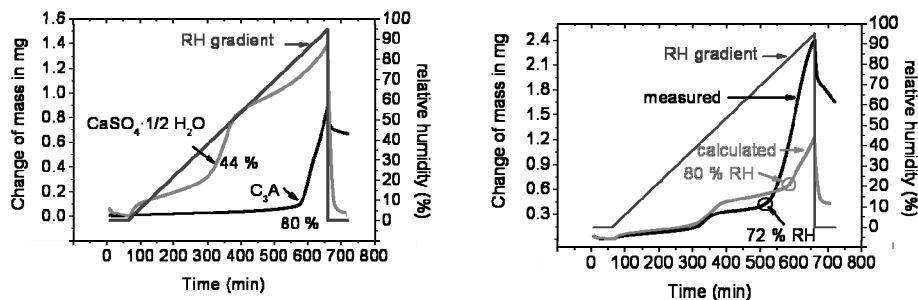


Figure 1: Water vapour sorption measured on a sorption balance instrument at 20 $^{\circ}\text{C}$, over a period of 10 hours using ramp mode; **left:** individual phases C_3A and β -hemihydrate; **right:** experimental and calculated mass change profiles for a binary mixture of C_3A with β -hemihydrate

There are several differences between the calculated and measured mass change profiles. Three stages can be distinguished:

- In the first interval between 0 % and 45 % RH, experimental values are in very good agreement with the calculated mass change profile. This implies that at low RHs, a chemical reaction between C_3A and β -hemihydrate does not occur during prehydration; the powders sorb minimal amounts of moisture at their surfaces by virtue of hydrogen bonding.

- In the second interval between 45 % and 75 % RH, experimental values are slightly lower than the calculated mass change profile. Additionally, for the binary mixture the experimentally detected sharp increase in mass (onset point) occurred at lower RH (72 % RH) than it was calculated from the mass change profiles of the individual phases (80 % RH).
- Upon increasing the relative humidity to above 75 % RH, great differences between the calculated and measured profiles become obvious. The binary mixture sorbed double the amount of water as predicted from addition of the mass change profiles of the individual phases. Here, significant formation of AF_t phase was analytical confirmed by FTIR spectra, thermogravimetric measurement (data not shown here) and in-situ ESEM imaging. This result is of great significance because ettringite formation only is possible if ions dissolved from both phases C_3A and β – hemihydrate can combine in a liquid phase which then becomes oversaturated and precipitates ettringite. Thus, this experiment reveals that prehydration occurs via liquid condensed water and not via water vapour. The formation of ettringite which can not occur when individual phases are exposed to water vapour appears to be the main reason for non-additive behaviour of the binary mixture in comparison to the individual phases. As mentioned before, in-situ ESEM imaging of the binary mixture exposed to 85 % RH for 1,5 hours reveals formation of nanosized ettringite needles, as shown in **Figure 2**.

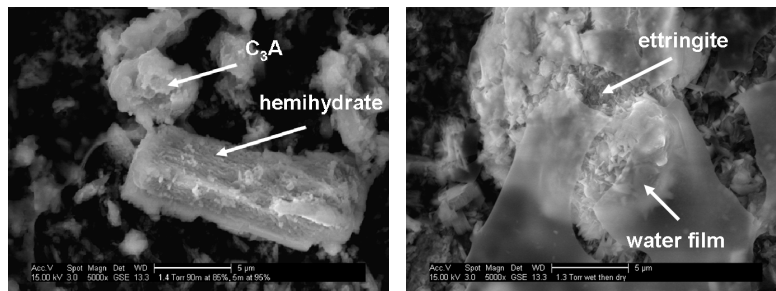


Figure 2 In-situ ESEM imaging of the binary mixture of C_3A_c and β – hemihydrate, exposed to 85 % RH for 1,5 hours; **(left)**: individual particles of C_3A_c and β – hemihydrate; **(right)**: films of liquid water between particles and presence of ettringite crystals on C_3A_c surface

Figure 3 summarises schematically the three stages of the water vapour sorption process in presence of the binary mixture of C_3A_c and β – hemihydrate

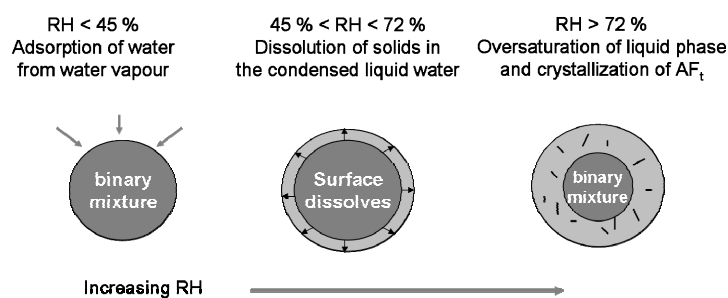


Figure 3: Schematic illustration of subsequent processes occurring when a binary mixture of cubic C_3A and β -hemihydrate is exposed to water vapour

(3) Adsorption of BNS on prehydrated binary mixture

To clarify how prehydration may affect the adsorption of BNS on the binary mixture, the blend of C_3A_c and β -hemihydrate was prehydrated for 48 hours at 60 % and 85 % RH, respectively. Those conditions are above and below the onset point for water sorption of the binary mixture which lies at 72 % RH (see **Fig. 1** right).

According to **Figure 4**, the binary mixture prehydrated at 85 % RH above the onset point took up significantly higher amounts of BNS than the non-prehydrated sample (15.4 mg/g vs. 12 mg/g).

Whereas, the binary mixture prehydrated below the onset (at 60 % RH) adsorbed similar amounts of BNS compared to the non-prehydrated sample (11.9 mg/g vs. 12 mg/g). The shape of the adsorption isotherms suggests a monolayer adsorption for all samples (LANGMUIR type isotherm). The saturated adsorption is reached for the binary mixture prehydrated at 85 % RH later than for the two other samples.

The data suggest that prehydration affects BNS adsorption noticeably when RH exceeds 72 %, which can be regarded as an onset point. As mentioned before, ettringite was found as the main prehydration product. It will be formed once RH reaches the onset point. **Figure 5** shows the X – ray diffraction patterns of fresh and prehydrated samples of the binary mixture. It confirms the formation of ettringite at 85 % RH, whereas no ettringite signals were found in the binary mixture prehydrated at 60 % RH.

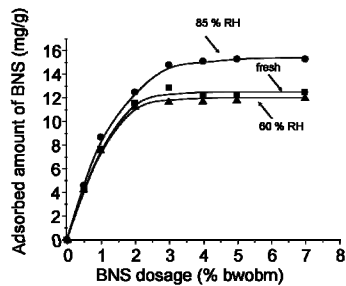


Figure 4: Adsorption isotherms for BNS added to binary mixture of C_3A_c and β -hemihydrate (w/bm = 5): fresh (■); prehydrated at 60 % RH (▲); prehydrated at 85 % RH (●)

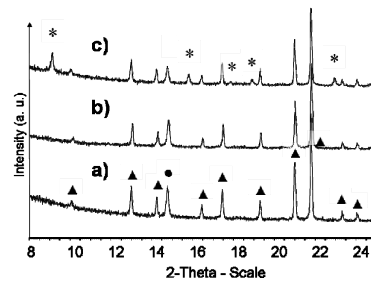


Figure 5: X-ray diffraction pattern of a binary mixture of C_3A_c a) fresh b) prehydrated over 48 h at 60 % RH and c) prehydrated over 48 h at 85 % RH binary mixtures of C_3A with β -hemihydrate (symbols: ▲ C_3A_c ; ● β -hemihydrate; * ettringite)

Obviously, the formation of ettringite leads to several changes of the surface properties of the binary mixture. For example, the total surface area will increase. Additionally, the surface charge and consequently the adsorption of superplasticizers would be greatly affected. As visualized by SEM images presented in **Figure 6**, the ettringite crystals formed during prehydration above the onset point are very thin with an average length of c.a. 100 – 500 nm. Previous work has shown that among the early cement hydrates, ettringite exhibits the most positive zeta potential and therefore instigates high adsorption of superplasticizer (Plank and Hirsch, 2003). Consequently, the increased adsorption of BNS onto the binary mixture prehydrated at 85 % RH can be explained by adsorption of BNS onto ettringite which was formed during prehydration.

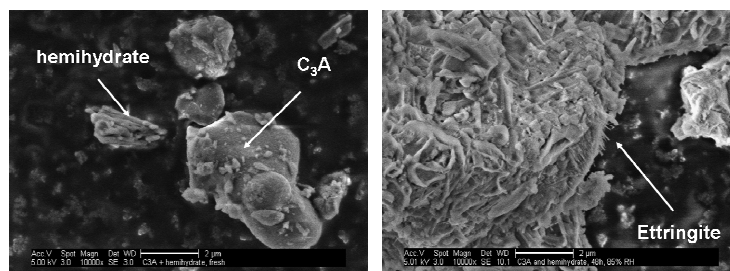


Figure 6: SEM images of non-prehydrated, C_3A_c and β -hemihydrate (left); and of a binary mixture of C_3A_c and β -hemihydrate, prehydrated for 48 hours at 85 % RH (right)

Conclusions

In this study, the effects of prehydration caused by water vapour on a binary mixture of cubic C_3A with β -hemihydrate at a molar ratio of 1:1 was investigated.

For individual clinker phases, use of a sorption balance instruments allows to determine the moisture uptake as a function of increasing relative humidity. For a binary systems composed of C_3A_c and β -hemihydrate, the water vapour sorption behaviour is more complex than for single component systems. It can be divided to three different stages. The onset point of the binary mixture was found to be lower than that of the pure individual phases. For the combine of C_3A_c and β -hemihydrate, ettringite formation starts when RH reaches the onset point of 72 % RH. Such substantial ettringite formation and is the reason for the nonadditive behavior of the binary mixture.

Additionally, it is shown that the formation of ettringite during prehydration significantly influences the adsorption of the BNS superplasticizer. There, a significantly (20 %) higher adsorbed amount of BNS superplasticizer than for the non-prehydrated binary mixture was observed. Whereas, prehydration of the binary mixture below the onset point does not much affect BNS adsorption, because there no ettringite is being formed.

Our experiments demonstrate that prehydration of C_3A_c in presence of β -hemihydrate may affect the dosage level of superplasticizer to be used on concrete or mortar. Consequently, owed to the nano-crystallinity of ettringite formed during prehydration and its associated huge specific surface area, exposure of cements containing high amounts of C_3A to moisture may result in higher consumption of superplasticizer. Understanding of the conditions leading to the formation of nano-sized cement hydrates during its manufacturing and storage may help to prevent the unwanted effects of prehydration on admixture performance.

Acknowledgment

The authors are grateful to Nanocem (Core Project # 7) for financial support of this work.

References

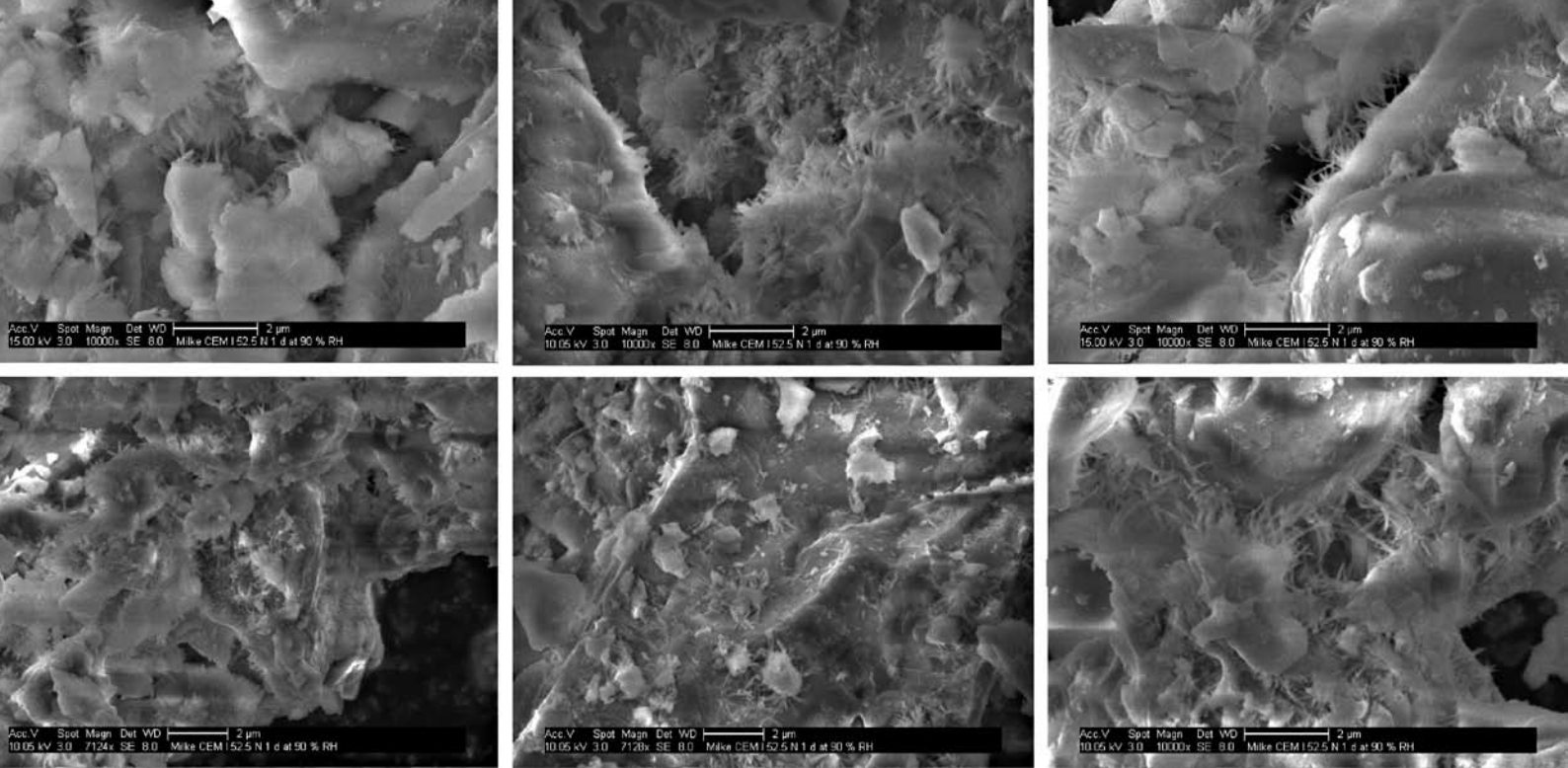
- Barbic, L., Tinta, V., Lozar, B., V. Marinkovic, "Effect of Storage Time on the Rheological Behavior of Oil Well Cement Slurries", *J. Am. Ceram. Soc.*, 74 (5), 1991, 945-949.
- Breval, E., "Gas-phase and liquid-phase hydration of C_3A ", *Cem. Concr. Res.*, 7 (3), 1977, 297-304.
- Dubina, E., Black, L., Sieber, R., Plank, J., "Interaction of water vapour with anhydrous cement minerals", *Adv. Appl. Ceram.* 109 (5), 2010, 260-268.
- Greenspan L., 'Humidity Fixed Points of Binary Saturated Aqueous Solutions', *J. Res. Nat. Bur.*, 8, (1), 1977, 89-95.
- Jensen, O. M., Hansen, P., Lachowski, E. E., Glasser, F. P., "Clinker mineral hydration at reduced relative humidities", *Cem. Concr. Res* 29 (9), 1999, 1505-1512.
- Maltese, C., Pistolesi, C., Bravo, A., Cella, F., Cerulli, T., Salvione, D., "Effect of moisture on the setting behavior of Portland cement reacting with an alkali-free accelerator", *Cem. Concr. Res.* 37 (6), 2007, 856-865.
- Plank, J., Hirsch, Ch., "Superplasticizer Adsorption on Synthetic Ettringite"; pp. 283-98 in Seventh CANMET/ACI Conference on Superplasticizers in Concrete. SP-217-19, Edited by V. M. Malhotra. ACI, Berlin, 2003.
- Plank, J., Dubina, E., Wadsö, L., "Surface prehydration of cement clinker phases and industrial cements, caused by water vapour", 7th International Symposium on Cement and Concrete (ISCC), 2010, Jinan (China).
- Schmidt, G., Bier, T. A., Wutz, K., Maier, M., "Characterization of the ageing behavior of premixed dry mortars and its effect on their workability properties", *ZKG INTERNATIONAL* 60 (6), 2007, 94-103.
- Sprung, V. S., "Effect of storage conditions on the properties of cements", *ZKG INTERNATIONAL* 30 (6) 1978, 305-309.
- Theisen, K., Johansen, V., "Prehydration and strength development of Portland cement", *Am. Cer. Soc. Bulletin* 54 (9), 1975, 787-791.
- Whittaker, M., Dubina, E., Plank, J., Black, L., "The effects of cement prehydration on engineering properties", *Cement and Concrete Science*, Birmingham, 2010, 101-104.
- Winnefeld, F., "Influence of cement ageing and addition time on the performance of superplasticizer", *ZKG INTERNATIONAL* 61 (11) 2008, 68-77.

Paper 6

Influence of Moisture- and CO₂-Induced Ageing in Cement on the Performance of Admixtures Used in Construction Chemistry

E. Dubina, J. Plank

ZKG International, 65 (10), (2012), 60 – 68.



Aging of cements Alterung von Zementen

Cement may exhibit altered properties during extended storage in moist atmospheres.

It is assumed that these effects are attributable to the take-up of atmospheric humidity and to carbonation at the surfaces of the cement particles.

TEXT Elina Dubina, Prof. Dr. Johann Plank*, Chair for Construction Chemicals, Technische Universität München, Garching/Germany

Zement kann während längerer Lagerung in feuchter Atmosphäre veränderte Eigenschaften zeigen.

Es wird angenommen, dass diese Effekte auf die Aufnahme von Luftfeuchtigkeit sowie Carbonatisierung an der Zementkornoberfläche zurückzuführen sind.

TECHNISCHE UNIVERSITÄT MÜNCHEN

Influence of moisture- and CO₂-induced ageing in cement on the performance of admixtures used in construction chemistry

Einfluss einer Feuchte- und CO₂-bedingten Zementalterung auf die Wirkung bauchemischer Zusatzmittel

1 Introduction

Cement may be affected by moisture and become slightly hydrated on the surface due to sorption of water both during production and during transport and subsequent storage in contact with atmospheric humidity [1 – 4]. Water vapour and possibly also CO₂ react with the sur-

1 Einleitung

Zement kann unter dem Einfluss von Feuchtigkeit sowohl während der Herstellung als auch dem Transport und der anschließenden Lagerung in Kontakt mit Luftfeuchtigkeit kommen und an der Oberfläche infolge Wassersorption geringfügig hydratisieren [1 – 4]. Dabei reagieren Wasser-

* corresponding author:
sekretariat@bauchemie.
ch.tum.de (Johann Plank)

face of the cement particles. The surface hydration may even begin during the production in the cement plant, e.g. as a consequence of the dehydration of gypsum during the grinding process in the cement mill. Some cement producers also spray up to 2% water into the clinker mill in order to keep the temperature of the mill feed below 115 °C. The take-up of water may also carry on during the storage of freshly produced cement in a silo because the gypsum releases more water of crystallization at elevated temperatures (> 42 °C) and this is then available for surface hydration. With dry pre-mixed mortar it is also possible that powdery additives, which as a rule have a residual moisture content of up to 5%, will give up water to the cement. In this case local annular layers of partially hydrated cement are formed around the additive particles.

Earlier investigations have shown that surface hydration can cause substantial changes in the properties of cement with respect to stiffening behaviour and strength development [5]. This led to a study of the behaviour of individual cement constituents in relation to atmospheric humidity. The threshold values for atmospheric humidity at which water sorption occurs were determined for all clinker phases and sulfate agents and for free lime with the aid of a water vapour sorption balance [6]. This showed that the individual constituents in the multi-component cement system sorb very different quantities of water vapour. Free lime and orthorhombic C_3A , which take up water above relative humidities of 14% and 55% respectively, are particularly hygroscopic. With cubic C_3A the water absorption starts at 80% relative humidity while the silicates (C_3S , C_2S) sorb only very small quantities of water above relative humidities of 63 and 64% respectively. The water is taken up both chemically and physically by the phases. It has been shown by photoelectron spectroscopy that chemical sorption leads to the formation of a layer of hydration products on the surfaces of these phases that is only a few nanometres thick.

It is therefore clear that cements can be expected to sorb different quantities of water vapour depending on their phase compositions. Cements containing high levels of free lime, orthorhombic C_3A and β - $CaSO_4 \cdot \frac{1}{2} H_2O$ react particularly sensitively to moisture. Increased care is necessary during their storage.

The changes at the surface of the cement particle can affect the action of the admixtures. Winnefeld, for example, used rheological measurements on cement suspensions to establish substantial differences in the action of superplasticizers in fresh and aged cements [7].

The intention of this study was to build on these individual findings and obtain a wider picture of the influence of pre-hydration on the interaction of cement with chemical admixtures. The chosen exposure conditions were 35 °C and 90% relative humidity. Although these conditions do not correspond to a central European climate they do simulate the take-up of considerable quantities of moisture and the effect of CO_2 over an extended period and therefore permit investigation on an accelerated time scale. Three superplasticizers (NSF, PCE and casein), a water-retention agent (MHEC)

dampf und ggfs. auch CO_2 mit der Zementkornoberfläche. Die Oberflächenhydratation kann bereits bei der Herstellung im Zementwerk beginnen, z. B. als Folge der Entwässerung von Gips während des Mahlvorganges in der Zementmühle. Außerdem sprühen einige Zementhersteller bis zu 2 % Wasser in die Klinkermühle, um die Temperatur des Mahlgutes unter 115 °C zu halten. Die Wasseraufnahme kann sich während der Lagerung eines frisch hergestellten Zements im Silo fortsetzen, da Gips bei erhöhter Temperatur (> 42 °C) weiter Kristallwasser freisetzt und somit für die Oberflächenhydratation zur Verfügung stellt. Bei Trockenmörteln besteht zudem die Möglichkeit, dass pulverförmige Zusatzmittel, die in der Regel eine Restfeuchte von bis zu 5 Gew.% aufweisen, Wasser an den Zement abgeben. In diesem Fall bildet sich eine lokale ringförmige Schicht von partiell hydratisiertem Zement um das Zusatzmittelkorn.

Frühere Untersuchungen zeigten, dass Oberflächenhydratation die Eigenschaften eines Zements bezüglich seines Rückstiefverhaltens und der Festigkeitsentwicklung erheblich verändern kann [5]. Dies gab Anlass, das Verhalten einzelner Zementbestandteile gegenüber Luftfeuchtigkeit zu studieren. Mit Hilfe einer Wasserdampfsorptionswaage wurden die Schwellenwerte an Luftfeuchtigkeit, ab denen Wassersorption auftritt, für alle Klinkerphasen, Sulfatträger sowie für Freikalk bestimmt [6]. Es zeigte sich, dass im Multikomponentensystem Zement die einzelnen Bestandteile sehr unterschiedliche Mengen an Wasserdampf sorbieren. Besonders hygroskopisch sind Freikalk und orthorhombisches C_3A , welche bereits ab 14% bzw. 55% relativer Luftfeuchte Wasser aufnehmen. Bei kubischem C_3A beginnt die Wasseraufnahme bei 80% rel. Feuchte, während die Silikate (C_3S , C_2S) ab 63 und 64% rel. Luftfeuchte sehr geringe Wassermengen sorbieren. Das Wasser wird von den Phasen sowohl chemisch als auch physikalisch aufgenommen. Mittels Photoelektronenspektroskopie konnte nachgewiesen werden, dass die chemische Sorption zur Bildung einer nur wenige Nanometer dicken Schicht an Hydratationsprodukten auf der Oberfläche dieser Phasen führt.

Somit wird deutlich, dass Zemente je nach Phasenzusammensetzung unterschiedliche Wasserdampfsorption erwarten lassen. Zemente mit hohen Gehalten an Freikalk, orthorhombischem C_3A und β - $CaSO_4 \cdot \frac{1}{2} H_2O$ reagieren besonders empfindlich auf Feuchtigkeit. Während ihrer Lagerung ist erhöhte Sorgfalt anzuwenden.

Die Veränderungen auf der Zementkornoberfläche können die Wirkung von Zusatzmitteln beeinflussen. So stellte Winnefeld anhand rheologischer Messungen an Zementsuspensionen erhebliche Unterschiede in der Wirkung von Fließmitteln in frischem und gealtertem Zement fest [7].

Aufbauend auf diesen Einzelerkenntnissen sollte in dieser Studie ein breiteres Bild über den Einfluss der Vorhydratation auf die Wechselwirkung von Zement mit bauchemischen Zusatzmitteln erlangt werden. Als Expositionsbedingungen wurden 35 °C und 90% rel. Luftfeuchtigkeit gewählt. Diese Bedingungen entsprechen zwar nicht einem mitteleuropäischen Klima, sie simulieren aber die Aufnahme beträchtlicher Feuchtemengen sowie die Einwirkung von CO_2 über einen längeren Zeitraum

and two accelerators (Ca formate and amorphous Al_2O_3) were investigated as the admixtures. The admixtures used were all commercial products to ensure practical relevance.

2 Materials and methods

2.1 Cement

A CEM I 52,5 N Portland cement (Milke®, Heidelberg-Cement AG, Geseke plant) was taken from current production immediately after the mill for the investigations. The mineralogical characterization was carried out by X-ray diffractometry (Bruker D8 advance) and subsequent Rietveld quantification (Topas 4.0 software). The free lime content was determined by the Franke method. The specific surface area was measured by N_2 adsorption (BET method, NOVA 4000e, Quantachrome) and by the Blaine method (EN 196-6). The results are shown in Table 1. Examination of the fresh cement by scanning electron microscopy showed absolutely no hydration products on the surface.

Pre-hydration of the cement was carried out at $35 \pm 2^\circ\text{C}$ and $90 \pm 3\%$ relative humidity (r.h.) in a climatic chamber for 1 or 3 days. The cement was spread over a Plexiglas plate in a 1 mm thick layer. The pre-hydrated cement samples were analyzed by X-ray diffraction, infrared spectroscopy (FTIR-ATR, Vertex 70, Bruker Optics, Karlsruhe) and thermogravimetry (STA 409, Netsch Gerätebau, Selb; temperature interval 30–900 °C, heating rate 20 K/min under synthetic air).

2.2 Additives

The following three commercial products were used as superplasticizers: a polycarboxylate ether powder (PCE, Melflux® 2651 F) from BASF Construction Polymers GmbH, Trostberg; a naphthalene sulfonic acid formaldehyde polycondensate (NSF, Melcret® 500 F) from BASF Construction Polymers GmbH, Trostberg, and casein from Ardex GmbH, Witten.

Tab. 1 Phase composition and specific material data for the CEM I 52,5 N cement sample in the fresh state

Phasenzusammensetzung und stoff-spezifische Daten der verwendeten Zementprobe CEM I 52,5 N in frischem Zustand

Phase	Content [mass %] Gehalt [M. %]
C_3S , m	52.0
C_2S , m	27.6
C_3A , c	4.4
C_3A , o	3.6
C_4AF , o	4.3
MgO	0.1
Free lime (Franke) Freikalk nach Franke	0.1
CaSO_4	2.1
$\text{CaSO}_4 \cdot 0.5 \text{H}_2\text{O}^*$	0.7
$\text{CaSO}_4 \cdot 2 \text{H}_2\text{O}^*$	0.4
K_2SO_4	0.5
CaCO_3	3.3
SiO_2	0.8
loss on ignition Glühverlust	1.9
density Dichte	3.3 g/cm ³
d_{50} value d_{50} -Wert	10.3 μm
specific surface area (BET) spezifische Oberfläche (BET)	1.4 m ² /g
specific surface area (Blaine) spezifische Oberfläche (Blaine)	0.33 m ² /g

* determined thermogravimetrically thermogravimetrisch bestimmt

und erlauben so eine Untersuchung im Zeitraffertempo. Als Zusatzmittel wurden drei Fließmittel (NSF, PCE und Casein), ein Wasserretentionsmittel (MHEC) und zwei Beschleuniger (Ca-Formiat sowie amorphes Al_2O_3) untersucht. Um Praxisrelevanz zu gewährleisten, wurden als Zusatzmittel ausschließlich kommerzielle Produkte eingesetzt.

2 Materialien und Methoden

2.1 Zement

Für die Untersuchungen wurde ein Portlandzement CEM I 52,5 N (Milke®, HeidelbergCement AG, Werk Geseke) der laufenden Produktion unmittelbar nach der Mühle entnommen. Die mineralogische Charakterisierung erfolgte mittels Röntgendiffraktometrie (Bruker D8 advance) und nachfolgender Rietveld-Quantifizierung (Topas 4.0 Software). Der Freikalkgehalt wurde nach Franke bestimmt. Die Messung der spezifischen Oberfläche erfolgte mittels N_2 -Adsorption (BET-Methode, NOVA 4000e, Quantachrome) und nach Blaine (EN 196-6). Die Ergebnisse sind in Tabelle 1 dargestellt. Eine rasterelektronenmikroskopische Betrachtung des frischen Zements zeigte keinerlei Hydratationsprodukte auf der Oberfläche.

Die Vorhydratation des Zements erfolgte in einer Klimakammer bei $35 \pm 2^\circ\text{C}$ und $90 \pm 3\%$ relativer Feuchtigkeit (r. F.) über 1 bzw. 3 Tage. Dazu wurde der Zement in einer 1 mm dicken Schicht auf einer Plexiglasplatte aufgetragen. Bei vorhydratisierten Zementproben wurden mittels Röntgenbeugung, Infrarotspektroskopie (FTIR-ATR, Vertex 70, Bruker Optics, Karlsruhe) und Thermogravimetrie (STA 409, Netsch Gerätebau, Selb; Temperaturintervall 30–900 °C, Aufheizrate 20 K/min unter synth. Luft) analysiert.

2.2 Zusatzmittel

Als Fließmittel wurden folgende drei kommerzielle Produkte eingesetzt: ein pulverförmiger Polycarboxylate-ther (PCE, Melflux® 2651 F) der Fa. BASF Construction Polymers GmbH, Trostberg; ein Naphthalinsulfonsäure-Formaldehyd-Polykondensat (NSF, Melcret® 500 F) der Fa. BASF Construction Polymers GmbH, Trostberg sowie ein Casein der Fa. Ardex GmbH, Witten.

Als Beschleuniger wurden Calciumformiat (Fa. Perstorp Specialty Chemicals AB, Perstorp) und amorphes Al_2O_3 (Gezedral® BZ 111 (BE), der Fa. BK Giuliani, Ludwigshafen) getestet. Als Wasserretentionsmittel kam Methylcellulose (MHEC, Tylose® 149 MHB 10000 P2) der Fa. SE Tylose GmbH & Co KG, Wiesbaden zum Einsatz. Alle angegebenen Zusatzmitteldosierungen beziehen sich auf den Zementanteil in der Mischung.

2.3 Zementleimuntersuchungen

Alle Zementleime wurden mit einem Wasser/Zement – Wert (w/z – Wert) von 0,55 angemischt, was beim frischen Zement ein Ausbreitmass von 18 cm ergibt. Die Zusatzmittel wurden generell im Anmachwasser gelöst, außer Methylcellulose, welche trocken in den Zement einge-mischt wurde.

Die Oberflächenladung der Leime aus frischem bzw. vorhydratisiertem Zement wurde mittels Zeta – Potential-messung (DT 1200 der Fa. Dispersion Technology INC.,



The accelerators tested were calcium formate (Perstorp Speciality Chemicals AB, Perstorp) and amorphous Al_2O_3 (Gezedral® BZ 111 (BE) from BK Giulini, Ludwigshaven). Methyl cellulose (MHEC, Tylose® 149 MHB 10000 P2) from SE Tylose GmbH & Co KG, Wiesbaden, was used as the water-retention agent. All the specified dosages are relative to the cement fraction in the mixture.

2.3 Cement paste investigations

All the cement pastes were mixed with a water/cement ratio (w/c ratio) of 0.55, which gives a flow table spread for the fresh cement of 18 cm. Apart from methyl cellulose, which was mixed into the cement in a dry state, the additives were dissolved in the mixing water.

In each case the surface charges on the pastes made from fresh and pre-hydrated cements were determined by zeta potential measurement (DT 1200 from Dispersion Technology Inc., Bedford Hills, USA) in distilled water after 4 and 20 minutes' hydration. The corresponding ionic background was recorded before each measurement.

The dispersive ability of the superplasticizers was tested as specified in the modified DIN EN 1015-3 test with the aid of a "mini-slump" test using a Vicat ring (height: 2.5 cm, internal diameter: 1.3 cm) [8]. The effectiveness of the methyl cellulose was determined as specified in EN 495-2 using the filter paper test [9]. In all cases the measured water retention values are relative to the quantity of mixing water. The influence of the accelerators on the setting behaviour of the aged cement samples was determined by heat flow calorimetry (equipment from TAM Air Thermometric, Järfälla, Sweden). The measurements were performed up to 45 h. The cement samples were mixed outside the calorimeter so it was not possible to measure the initial peak.

3 Results

3.1 Sorption behaviour of the cement

Figure 1 shows appearance of cement samples that have been exposed to moisture. Agglomeration and slight lump formation occurs after only 1 day's storage in moist air. Large flakes that no longer exhibit any free-

Bedford Hills, USA) in destilliertem Wasser nach jeweils 4 bzw. 20 Minuten Hydratation ermittelt. Vor jeder Messung wurde der entsprechende Ionenhintergrund aufgenommen.

Die Prüfung der Dispergierwirkung der Fließmittel erfolgte nach modifizierter DIN EN 1015-3 mit Hilfe eines „Mini-Slump“ Tests unter Verwendung eines Vicat-Rings (Höhe: 2.5 cm, Innendurchmesser: 1,3 cm) [8]. Die Wirksamkeit der Methylcellulose wurde nach EN 495-2 anhand des Papiertuchtests bestimmt [9]. Die dabei ermittelten Wasserretentionswerte beziehen sich stets auf die Menge an Anmachwasser. Der Einfluss der Beschleuniger auf das Abbindeverhalten der gealterten Zementproben wurde wärmeflusskalorimetrisch verfolgt (Gerät der Fa. TAM Air Thermometric, Järfälla, Schweden). Die Messdauer betrug 45 h. Da die Zementproben außerhalb des Kalorimeters angemischt wurden, konnte der Initialpeak nicht erfasst werden.

3 Ergebnisse

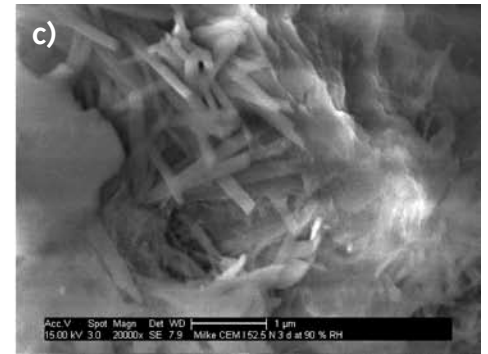
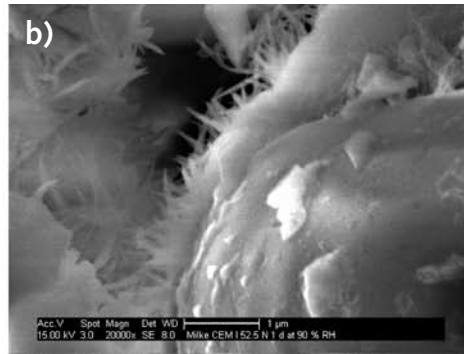
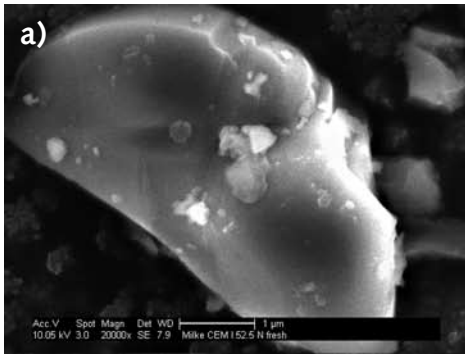
3.1 Sorptionsverhalten des Zements

Bild 1 zeigt das Erscheinungsbild der feuchteexponierten Zementproben. Bereits nach 1 d Lagerung an feuchter Luft tritt Agglomeration und leichte Klumpenbildung ein. Nach 3tägiger Exposition sind aus dem Zementpulver großflächige Schuppen entstanden, die keinerlei Rieselfähigkeit mehr aufweisen – ein deutlicher Hinweis auf beträchtliche Wasseraufnahme. Die vorhydratisierten Zemente wurden vor den weiteren Untersuchungen in einem Achatmörser wieder auf die ursprüngliche Mahlfeinheit gebracht.

Bild 2 zeigt rasterelektronenmikroskopische Aufnahmen der Oberfläche des frischen und vorhydratisierten Zements. Die Aufnahmen belegen, dass die Oberfläche des frischen Zements keinerlei Hydratationsprodukte ausweist. Nach einem Tag Vorhydratation bei 90% rel. Feuchte ist die Oberfläche jedoch bereits mit ersten Hydratationsprodukten (feinen Ettringitnadeln) bedeckt. Dadurch erhöht sich die spezifische Oberfläche des Zements von $0,33 \text{ m}^2/\text{g}$ auf $0,49 \text{ m}^2/\text{g}$ (Blaine). Nach drei Tagen Lagerung sind wesentlich zahlreichere, mehrere μm lange Ettringitkristalle auf der Zementkornoberfläche erkennbar. Die BET-Oberfläche des Zements steigt

1 Appearance of the cement samples that had been exposed to moisture after storage for a) 1 day and b) 3 days

Erscheinungsbild der feuchteexponierten Zementproben a) nach 1 Tag und b) nach 3 Tagen Lagerung



2 Scanning electron microscope photomicrographs of the CEM I 52,5 N cement a) in the fresh state, and after exposure to moisture for b) 1 day and c) 3 days

Rasterelektronenmikroskopische Aufnahmen des Zements CEM I 52,5 N a) in frischem Zustand; b) nach 1 Tag und c) nach 3 Tagen Feuchteexposition

flowing properties – a clear indication of substantial water sorption – were produced from the cement powder after 3 days' exposure. Before any further investigations the pre-hydrated cements were brought back to their original fineness in an agate mortar.

Figure 2 shows scanning electron photomicrographs of the surface of the fresh and pre-hydrated cements. The photographs confirm that the surface of the fresh cement does not exhibit any hydration products. However, after one day's pre-hydration at 90% relative humidity the surface is covered with initial hydration products (fine ettringite needles). This raises the specific surface area of the cement from 0.33 m²/g to 0.49 m²/g (Blaine). Substantially more numerous ettringite crystals that are several µm long can be seen on the surface of the cement particles after three days' storage. The BET surface area of the cement rises from 1.4 m²/g in the fresh state to 2.3 m²/g after 1 day's exposure to moisture, and after 3 days' storage it reaches a value of 4.1 m²/g.

Figure 3 shows sections from the FTIR-ATR spectra of the fresh and pre-hydrated cements in the ranges 4000–2700 cm⁻¹ and 1780–1210 cm⁻¹. The fresh cement exhibits only a weak water peak at 3400 cm⁻¹, which is attributable to the content of gypsum and hemihydrate. However, the intensity of the water peak has increased significantly with cement that has been stored in moist conditions. Significant carbonation of the cement, which can be seen from the peak at 1420 cm⁻¹, was also observed. On the other hand the fresh cement contains only a small quantity of carbonates.

The sorption of water vapour and CO₂ on the cement can be quantified by thermogravimetry (Fig. 4). The fresh cement exhibits only a slight loss in weight totalling 2 mass%, which is attributable mainly to the decomposition of CaCO₃ in the temperature range from 650 to 720 °C. The pre-hydrated samples exhibit substantially higher weight losses of 6.5 mass% (1 day's

von 1,4 m²/g in frischem Zustand auf 2,3 m²/g nach 1 d Feuchteexposition und erreicht nach 3 Tagen Lagerung einen Wert von 4,1 m²/g.

Bild 3 zeigt Ausschnitte aus den FTIR-ATR-Spektren des frischen und vorhydratisierten Zements in den Bereichen 4000–2700 cm⁻¹ und 1780–1210 cm⁻¹. Der frische Zement weist nur eine schwache Wasserbande bei 3400 cm⁻¹ auf, die auf den Gehalt an Gips und Halbhydrat zurückzuführen ist. Beim feuchtegelagerten Zement dagegen hat die Intensität der Wasserbande deutlich zugenommen. Außerdem war eine beachtliche Carbonatisierung des Zements, sichtbar an der Bande um 1420 cm⁻¹, zu beobachten. Der frische Zement enthält dagegen nur eine geringe Menge an Carbonaten.

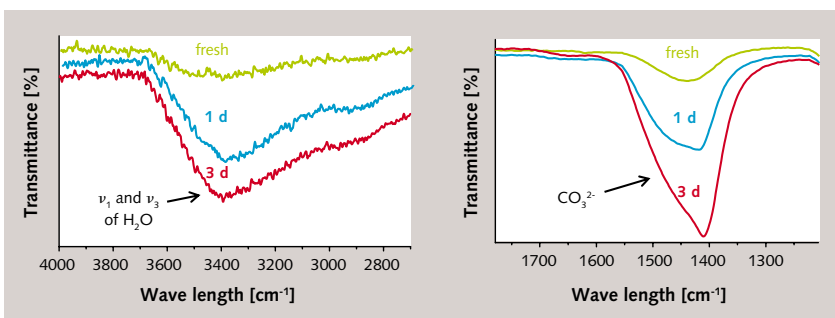
Die Wasserdampf- und CO₂-Sorption am Zement lässt sich mit Hilfe von Thermogravimetrie quantifizieren (Bild 4). Der frische Zement weist einen nur geringen Massenverlust von insgesamt 2 Gew. % auf, der hauptsächlich auf Zersetzung von CaCO₃ im Temperaturbereich von 650 bis 720 °C zurückzuführen ist. Die vorhydratisierten Proben zeigen wesentlich höhere Gewichtsverluste von 6,5 Gew. % (1 d Lagerung) bzw. 11,5 Gew. % (3 d Lagerung). Diese sind im unteren Temperaturbereich auf Wasserabgabe sowie zwischen 650 und 720 °C auf die Freisetzung von CO₂ aus Carbonatisierungsprodukten zurückzuführen.

Bild 5 zeigt den Hydratationswärmefluss für frischen und vorhydratisierten Zement über einen Zeitraum von 2 Tagen. Der feuchtegelagerte Zement weist im Vergleich zur frischen Probe eine deutlich geringere Hydratationswärme auf – ein Indiz dafür, dass ein Teil der Hydratation bei der Lagerung bereits vorweggenommen wurde. Der Peak der Haupthydratation tritt deutlich später auf. Somit zeigt ein feuchtegelagerter Zement ein signifikant verzögertes Abbindeverhalten.

Die Bildung von Hydratphasen auf der Zementkornoberfläche als Folge der Feuchteexposition bedingt eine Änderung der Oberflächenladung, was durch Messung des Zeta-Potentials der Proben vor und nach Alterung nachgewiesen wurde (Bild 6). Generell waren die Oberflächenladungen der feuchteexponierten Zementproben weniger negativ oder gar positiv, verglichen mit frischem Zement. Der Trend ist 20 Minuten nach dem Anmischen des Zements mit Wasser noch deutlicher ausgeprägt als 4 Minuten nach dem Anmischen. Der Effekt ist auf die Ettringitbildung während der Vorhydratation zurückzuführen. Aus früheren Untersuchungen ist bekannt, dass Ettringit ein positives Zeta-Potential von 4,2 mV aufweist [10].

3 FTIR-ATR spectra of fresh (black) and pre-hydrated CEM I 52,5 N cement (blue: exposure time 1 d; red: 3 d)

FTIR-ATR Spektren des frischen (schwarz) und vorhydratisierten CEM I 52,5 N (blau: Expositionszeit 1 d; rot: 3 d)



storage) and 11.5 mass% (3 days' storage). These are attributable to the loss of water in the lower temperature range and the release of CO₂ from the carbonation products between 650 and 720 °C.

Figure 5 shows the flow of heat of hydration for fresh and pre-hydrated cement over a period of 2 days. Cement stored in moist conditions exhibits a significantly lower heat of hydration than the fresh sample – an indication that part of the hydration has already taken place during the storage. The peak in the main hydration occurs significantly later. Cement that has been stored in moist conditions therefore exhibits significantly retarded setting behaviour.

The formation of hydrate phases on the surface of the cement particles as a consequence of the exposure to moisture causes a change in the surface charge, which can be shown by measuring the zeta potential of the sample before and after ageing (Fig. 6). In general the surface charges of the moisture-exposed cement samples were less negative, or even positive, when compared with the fresh cement. This trend is even more significant 20 minutes after the cement has been mixed with water than 4 minutes after the mixing. The effect can be attributed to the formation of ettringite during the pre-hydration. It is known from earlier investigations that ettringite has a positive zeta potential of 4.2 mV [10].

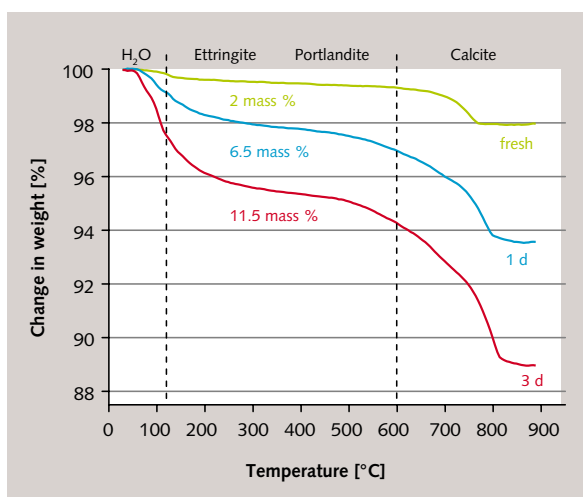
3.2 Action of the superplasticizers

The dispersing action of superplasticizers with cements that have been exposed to moisture is examined below. The effectiveness of the superplasticizers was assessed by the flow-table spread in the mini-slump test. The dosage of the additives was chosen so that a flow-table spread of 26 cm was achieved with fresh cement with a w/c value of 0.55.

Figure 7 summarizes the results for fresh cement and cement that has been stored under moist conditions with and without superplasticizers. The flow behaviour of the pre-hydrated cements differs significantly from that of the fresh cement. The plain cement (without superplasticizer) shows a steady decrease in flowability with increasing moist storage. This causes a rising water demand due, among other things, to the increased specific surface area. The decrease in flowability after 1 day's storage turns out to be significantly lower when the superplasticizer is added. The plasticizing effect after the addition of casein is fully retained even after 1 day's moisture absorption. This distinguishes this superplasticizer from polycarboxylate and NSF resin, which exhibit a drop in the plasticizing action with aged cement (NSF drops more sharply than PCE). After 3 days' storage none of the superplasticizers investigated were still able to plasticize these cements; the same values were obtained as for cement without superplasticizer.

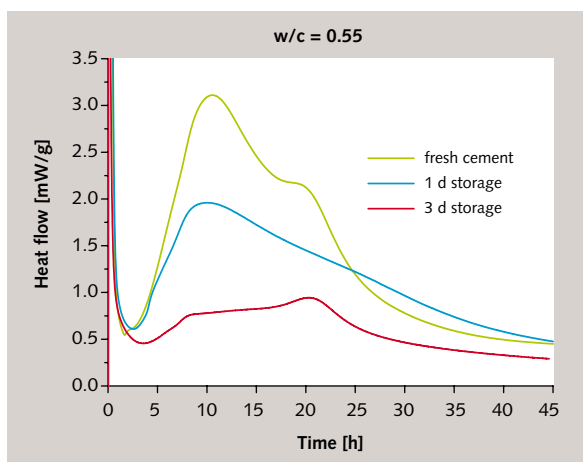
3.3 Action of the water-retention agent

Water-retention agents are mainly used in machine-applied plasters, tile adhesives and cement-based sealants. The most important water-retention agents are based on methyl cellulose (MHPC for plasters and MHEC



4 Thermogravimetric analysis of fresh CEM I 52,5 N cement (green) and of cement stored in moist conditions (blue: storage time 1 d; red: 3 d)

Thermogravimetrische Analyse des frischen (grün) und des feuchtegelagerten Zements CEM I 52,5 N (blau: Lagerzeit 1 d; rot: 3 d)



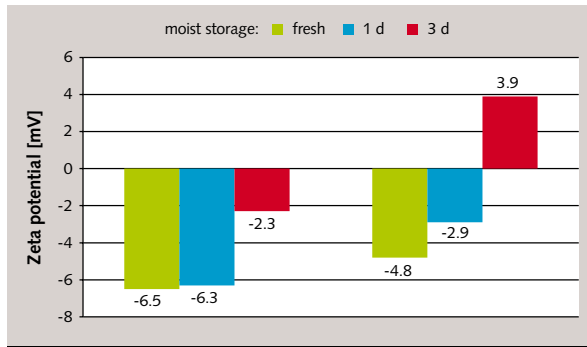
5 Hydration behaviour of fresh CEM I 52,5 N cement (green) and of cement that has been exposed to moisture (blue: storage time 1 d; red: 3 d), determined by thermocalorimetry

Wärmekalorimetrisch verfolgter Hydrationsverlauf des frischen (grün) und feuchteexponierten Zements CEM I 52,5 N (blau: Lagerzeit 1 d; rot: 3 d)

3.2 Wirkung der Fließmittel

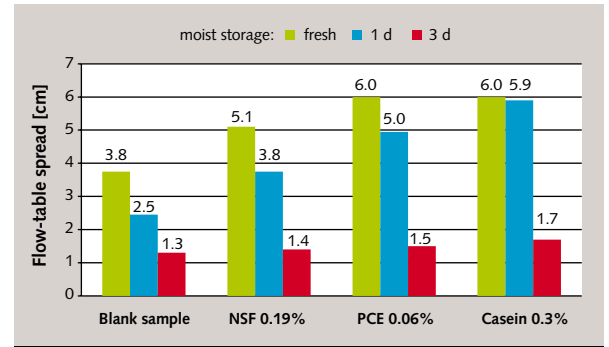
Im Folgenden wurde die Dispergierwirkung von Fließmitteln mit feuchteexponiertem Zement untersucht. Die Wirksamkeit der Fließmittel wurde anhand des Ausbreitmass im „Mini-Slump“ Test beurteilt. Die Wahl der Zusatzmittel-Dosierung erfolgte so, dass mit frischem Zement bei einem w/z-Wert von 0,55 ein Ausbreitmass von 26 cm erzielt wurde.

Bild 7 gibt einen Überblick über die Ergebnisse für frischen und feuchtegelagerten Zement ohne und mit Fließmittel. Das Fließverhalten der vorhydratisierten Zemente weicht deutlich von dem des frischen Zements ab. Der reine Zement (ohne Fließmittel) zeigt mit zunehmender Feuchte Lagerung eine stetige Abnahme der Fließfähigkeit. Dies hat einen steigenden Wasseranspruch u. a. infolge der erhöhten spezifischen Oberfläche zur Folge. Bei Zugabe von Fließmitteln fällt der Abfall der Fließfähigkeit nach 1 Tag Lagerung deutlich geringer aus. Insbesondere nach Zugabe von Casein bleibt die Fließwirkung auch nach 1-tägiger Feuchteaufnahme vollständig erhalten. Dies zeichnet dieses Fließmittel gegenüber Polycarboxylat und NSF-Harz aus, welche einen Rückgang der Fließwirkung mit gealtertem Zement verzeichnen (NSF fällt stärker ab als PCE). Nach 3-tägiger Lagerung ist keines der untersuchten Fließmittel mehr in der Lage, diesen Zement zu verflüssigen; es werden die gleichen Werte wie für den Zement ohne Zusatzmittel erhalten.



6 Zeta potential of cement pastes ($w/c = 0.55$) made from fresh (green) and pre-hydrated CEM I 52,5 N cement (blue: storage time 1 d; red: 3 d)

Zeta-Potential von Zementleimen ($w/z = 0,55$) aus frischem (grün) und vorhydratisiertem Zement CEM I 52,5 N (blau: Lagerzeit 1 d; rot: 3 d)



7 Flow table spread of cement pastes ($w/c = 0.55$) made from fresh (green) and pre-hydrated CEM I 52,5 N cement (blue: storage time 1 d; red: 3 d) with and without superplasticizer

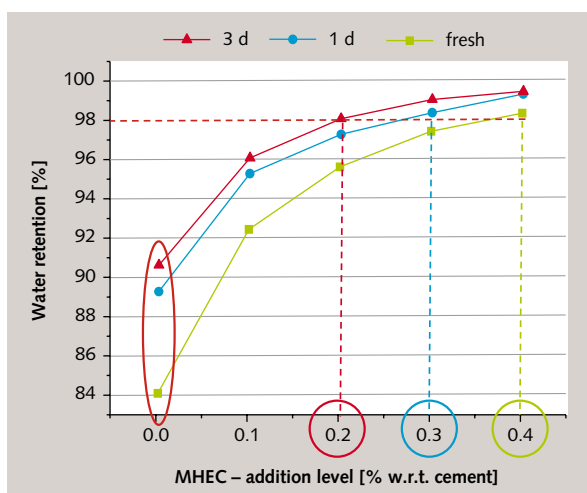
Ausbreitmaß von Zementleimen ($w/z = 0,55$) aus frischem (grün) und vorhydratisiertem CEM I 52,5 N (blau: Lagerzeit 1 d; rot: 3 d) bei An- und Abwesenheit von Fließmitteln

for tile adhesives). This study examined the effectiveness of methyl hydroxyethyl cellulose with cement that has been stored under moist conditions, for which the target was a water retention of 98% or higher.

Figure 8 shows the water retention of the pastes made from fresh and pre-hydrated cements containing different levels of MHEC. The pre-hydrated cement generally shows significantly better water retention than the fresh cement. This effect is explained by the finer surface structure of cement that has been stored under moist conditions, which results in smaller pores that lose less water. 0.4 mass % MHEC is required to achieve a water retention of > 98% for unaged cement. With pre-hydrated cement this value can be reached with significantly lower addition levels. Only 0.2 mass % MHEC is needed to achieve 98% water retention with cement aged for 3 days. At the same time the viscosity of the paste rises steeply after the cement has been exposed to moisture in spite of the lower MHEC addition level (Fig. 9). The workability decreases significantly because of the crumbly consistency and has to be corrected by increased addition of water when the plaster is mixed. The tests confirm that cement that has been exposed to water always leads to significantly better water retention values and at the same time a higher water demand.

8 Water retention of pastes made from fresh (green) and pre-hydrated cement on addition of different levels of MHEC (blue: storage time 1 d; red: 3 d)

Wasserretention von Leimen aus frischem (grün) und vorhydratisiertem Zement bei Zusatz unterschiedlicher Dosierungen von MHEC (blau: Lagerzeit 1 d; rot: 3 d)



3.3 Wirkung des Wasserretentionsmittels

Wasserretentionsmittel werden vor allem in Maschinenputzen, Fliesenklebern und Dichtschlämmen eingesetzt. Die wichtigsten Wasserretentionsmittel basieren auf Methylcellulose (MHPC für Putze und MHEC für Fliesenkleber). In dieser Studie wurde die Wirksamkeit einer Methylhydroxyethylcellulose mit feuchtegelagertem Zement untersucht, wobei eine Wasserretention von 98% oder höher angestrebt wurde.

Bild 8 zeigt die Wasserretention von Leimen aus frischem und vorhydratisiertem Zement bei unterschiedlichen MHEC-Dosierungen. Der vorhydratisierte Zement zeigt generell eine deutlich bessere Wasserretention als der frische Zement. Dieser Effekt erklärt sich durch die feinere Oberflächenstruktur von feuchtegelagertem Zement, wodurch kleinere Poren entstehen, die weniger Wasser abgeben. Um eine Wasserretention von > 98% zu erhalten, werden 0,4 M.-% an MHEC für den ungealterten Zement benötigt. Beim vorhydratisiertem Zement kann dieser Wert mit deutlich geringeren Dosierungen erreicht werden. So genügen lediglich 0,2 M.-% MHEC, um 98 % Wasserretention mit 3 Tage gealtertem Zement zu erhalten. Gleichzeitig steigt die Viskosität des Leims nach der Feuchteexposition des Zements stark an, trotz niedrigerer MHEC-Dosierung (Bild 9). Die Verarbeitbarkeit nimmt aufgrund der krümeligen Konsistenz deutlich ab und muss durch erhöhte Wasserzugabe beim Anmischen des Putzes korrigiert werden. Die Versuche belegen, dass feuchteexponierter Zement stets zu signifikant besseren Wasserrückhaltewerten führt und gleichzeitig einen höheren Wasseranspruch zeigt.

3.4 Wirkung von Beschleunigern

Bild 10 zeigt den Einfluss der Vorhydratation auf die Wirkung zweier Beschleuniger, ermittelt anhand wärmekalorimetrischer Untersuchungen. Als Beschleuniger wurden Ca-Formiat und amorphes Al_2O_3 geprüft. Ihre Dosierungen wurden so gewählt, dass das Maximum des Haupthydrationspeaks bei Zusatz der Beschleuniger nach gleicher Hydrationszeit (~ 9 Stunden) wie beim frischen Zement eintrat. Wie bereits im Bild 5 dargestellt, zeigt feuchtegelagerter Zement eine deutlich verzögerte Wärmefreisetzung, insbesondere nach 3 Tagen Exposition.

3.4 Action of accelerators

Figure 10 shows the effect of pre-hydration on the action of two accelerators, determined with the aid of calorimetric investigations. The accelerators tested were Ca formate and amorphous Al_2O_3 . Their addition levels were chosen so that the maximum of the main hydration peak on addition of the accelerator occurs after the same hydration time (≈ 9 hours) as with fresh cement. As already shown Fig. 5, the cement stored under moist conditions exhibits a significantly retarded release of heat, especially after 3 days' exposure.

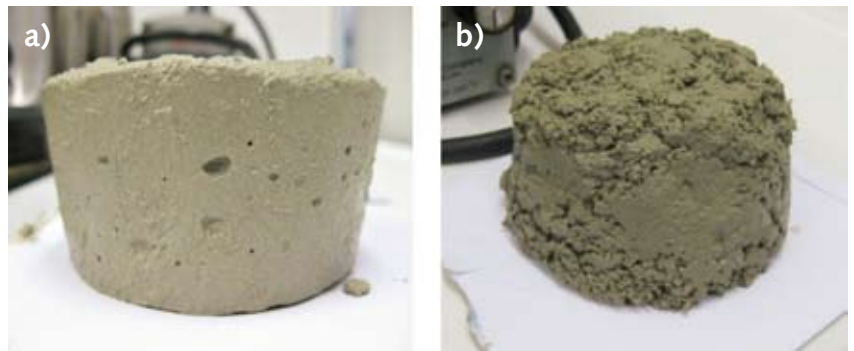
The results indicate that the accelerating action of the additives is significantly reduced in cement that has been exposed to moisture for 1 day. The accelerating action is completely lost in cement that has been pre-hydrated for 3 days. The effect is somewhat stronger with calcium formate than with Al_2O_3 . Cement that has been stored under moist conditions for 3 days is even retarded by the two "accelerators".

4 Conclusions

Cement can exhibit altered properties during extended storage in moist atmospheres. It is assumed that these effects are attributable to the take-up of atmospheric humidity and to carbonation at the surface of the cement particles. As part of a project supported by the Nanocem Research Association a commercial Portland cement (CEM I 52,5 N) was exposed to atmospheric humidity under controlled conditions (35 °C, 90% relative humidity, storage time 1 and 3 days). Its interaction with different additives (superplasticizers, water-retention agents and accelerators) was then investigated.

The results presented here show that that the take-up of moisture and the carbonation can cause a significant change in the flow, water-retention and setting behaviour patterns. Both the specific surface area and the surface charge of a cement are changed as a result of the surface hydration, which has a substantial effect on the interaction with admixtures, such as superplasticizers, water-retention agents and accelerators. The following relationships were found:

- » In cement that has been exposed to moisture the action of superplasticizers in pre-hydrated cement is generally less than in fresh cement. The dispersing power of the biopolymer-based superplasticizer



Die Ergebnisse lassen erkennen, dass die beschleunigende Wirkung der Zusatzmittel in Zement, der 1 Tag Feuchte ausgesetzt wurde, deutlich reduziert ist. In 3 Tage vorhydratisiertem Zement ist die beschleunigende Wirkung gänzlich verlorengegangen. Der Effekt ist bei Calciumformiat etwas stärker als beim Al_2O_3 . Der 3 Tage feuchtegelagerte Zement wird von beiden „Beschleunigern“ sogar verzögert.

9 Appearance of the cement paste after the water retention test; left: cement pre-hydrated for 1 day containing 0.3 mass % MHEC; right: cement pre-hydrated for 3 days containing 0.2 mass % MHEC

Erscheinungsbild des Zementleims nach dem Wasserretentionstest; links: mit 1 Tag vorhydratisiertem Zement und 0,3 M.-% MHEC; rechts: mit 3 Tage vorhydratisiertem Zement und 0,2 M.-% MHEC

4 Schlussfolgerungen

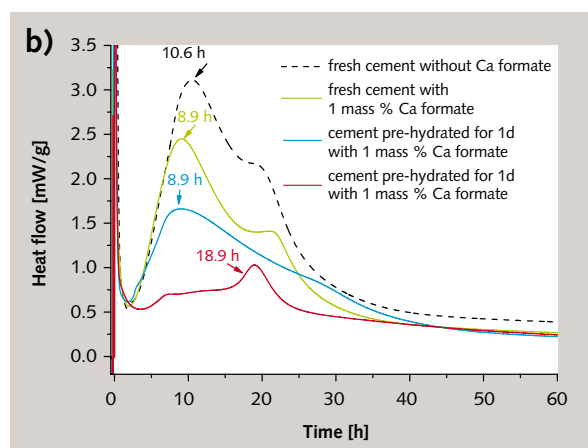
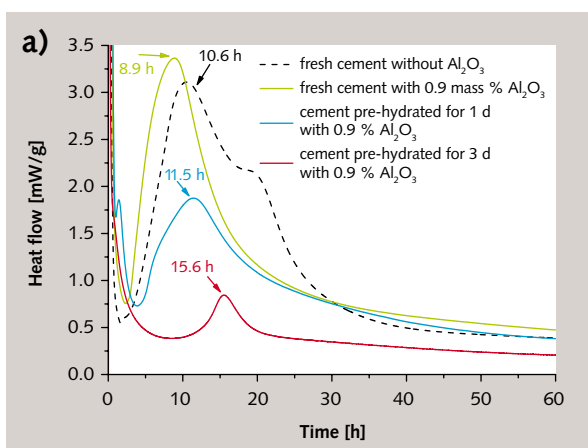
Zement kann während längerer Lagerung in feuchter Atmosphäre veränderte Eigenschaften zeigen. Es wird angenommen, dass diese Effekte auf die Aufnahme von Luftfeuchtigkeit sowie Carbonatisierung an der Zementkornoberfläche zurückzuführen sind. Im Rahmen des vom Forschungsverbund Nanocem geförderten Projekts wurde ein kommerzieller Portland-Zement (CEM I 52,5 N) unter kontrollierten Bedingungen Luftfeuchtigkeit ausgesetzt (35 °C, 90% rel. Feuchte, Lagerzeit 1 bzw. 3 Tage). Anschließend wurde seine Wechselwirkung mit verschiedenen Zusatzmitteln (Fließmittel, Wasserretentionsmittel sowie Beschleuniger) untersucht.

Die vorgestellten Ergebnisse zeigen, dass Feuchteaufnahme und Carbonatisierung das Fließ-, Wasserretentions- und Abbindeverhalten von Zementen deutlich verändern können. Infolge Oberflächenhydratation verändern sich sowohl die spezifische Oberfläche als auch die Oberflächenladung eines Zements, was die Wechselwirkung mit Zusatzmitteln wie z. B. Fließmitteln, Wasserretentionsmitteln oder Beschleunigern erheblich beeinflusst. Folgende Zusammenhänge wurden gefunden:

- » In feuchteexponiertem Zement ist die Wirkung von Fließmitteln im vorhydratisierten Zement generell geringer als in frischem Zement. Die Dispergierkraft des

10 Setting behaviour of cement pastes made from fresh (green) and pre-hydrated CEM I 52,5 N cement (blue: storage time 1 d; red: 3 d) in the presence of 0.9 mass % Al_2O_3 -based accelerator (left) and 1 mass % calcium formate (right)

Abbindeverhalten von Zementleimen aus frischem (grün) und vorhydratisiertem CEM I 52,5 N (blau: Lagerzeit 1 d; rot: 3 d) in Anwesenheit von 0.9 M.-% Al_2O_3 -basiertem Beschleuniger (links) und 1 M.-% Calciumformiat (rechts)



- casein is least strongly affected by moist storage, while the polycarboxylate is more strongly affected and the NSF resin is particularly strongly affected.
- » Cement that has been stored under moist conditions exhibits a significantly improved water retention capacity with, at the same time, a higher water demand to achieve the workability required in practice. This cement therefore requires lower addition levels of methylcellulose to reach a high water retention.
 - » In pre-hydrated cement there is a significant decrease in the accelerating action of setting accelerators based on Ca formate and amorphous Al_2O_3 . In cement with long exposure to moisture (3 d) they can sometimes turn into retarders.
- Biofließmittels Casein wird von der Feuchtelagerung am wenigsten, die von Polycarboxylat jedoch stärker und von NSF-Harz besonders stark beeinträchtigt.
- » Feuchtegelagerter Zement zeigt ein signifikant verbessertes Wasserrückhaltevermögen bei gleichzeitig höherem Wasseranspruch zur Einstellung einer praxisgerechten Verarbeitbarkeit. Deshalb reichen für diesen Zement geringere Methylcellulose-Dosierungen zur Erreichung einer hohen Wasserretention aus.
 - » In vorhydratisiertem Zement nimmt die beschleunigende Wirkung von Abbindebeschleunigern auf Basis Ca-formiat und amorphem Al_2O_3 deutlich ab. In Zement mit langer Feuchteexposition (3 d) können sie z. T. in Verzögerer umschlagen.

The results confirm that exposure to moisture and take-up of CO_2 can in some cases have a very strong effect on the storage stability and the functionality of dry pre-mixed mortars. Portland cement that is exposed for an extended time to moist air can exhibit significantly changed behavior with additives. The effects of this surface hydration can be both positive and negative with respect to the action of superplasticizers, although the detrimental effects are predominant.

Die Ergebnisse belegen, dass Feuchteexposition und CO_2 -Aufnahme die Lagerstabilität und Funktionsfähigkeit von Trockenmörtelmischungen z.T. sehr stark beeinflussen können. Ein Portlandzement, der längere Zeit feuchter Luft ausgesetzt war, kann ein signifikant verändertes Verhalten mit Zusatzmitteln zeigen. Die Effekte dieser Oberflächenhydratation können sowohl positiv als auch negativ bezüglich der Wirkung der Zusatzmittel sein, wobei die schädlichen Auswirkungen überwiegen.

Acknowledgement

The authors would like to thank the EU Nanocem network for financial support of the investigations into cement as part of Core Project No. 7.

Danksagung

Die Autoren danken dem EU-Netzwerk Nanocem für finanzielle Förderung der Untersuchungen zum reinen Zement im Rahmen des Core Project # 7.

REFERENCES

- [1] Richartz, W., Eick, H. (1973): "Effect of storage conditions on the properties of cement", ZKG INTERNATIONAL, No. 2, pp. 67–74
- [2] Sprung, S. (1978): "Effect of storage conditions on the properties of cement", ZKG INTERNATIONAL, No. 6, pp. 305–309
- [3] Barbic, L., Tinta, V., Lozar, B., Marinkovic, V. (1991): "Effect of Storage Time on the Rheological Behavior of Oil Well Cement Slurries", J. Am. Ceram. Soc., 74, No. 5, pp. 945–949
- [4] Schmidt, G., Bier, T. A., Wutz, K., Maier, M. (2007): "Characterization of the ageing behaviour of premixed dry mortars and its effect on their workability properties", ZKG INTERNATIONAL 60, No. 6, pp. 94–103
- [5] Al-Mutawa F.; Whittaker M.; Arkless L.; Dubina E.; Plank J.; Black L.: "The Effects of Prehydration at Moderate Humidities on the Engineering Properties of Portland Cement", C. H. Fentiman, R. J. Mangabhai (Eds.), Cement and Concrete Science, London, 2011, 12–13 September, conference proceedings
- [6] Dubina, E., Wadsö, L., Plank, J. (2011): "A sorption balance study of water vapour sorption on anhydrous cement minerals and cement constituents", Cement and Concrete Research 41, pp. 1196–1204
- [7] Winnefeld, F. (2008): "Influence of cement ageing and addition time on the performance of superplasticizer", ZKG INTERNATIONAL 61, No. 11, pp. 68–77
- [8] German Institute for Standardization: DIN EN 1015-3 Methods of test for mortar for masonry – Part 3: Determination of consistence of fresh mortar (by flow table); German version, Berlin, Beuth Verlag, 2007
- [9] EN 459-2, Building lime – Part 2: Test methods, European Committee for Standardization, 2010
- [10] Plank, J., Hirsch, Ch. (2007): "Impact of zeta potential of early cement hydration phases on superplasticizer adsorption", Cement and Concrete Research 37, pp. 537–542

Paper 7

Investigation of the long-term stability during storage of drymix mortars, Part 2. Influence of Moisture Exposure on the Performance of Self-levelling mortars (SLUs)

E. Dubina, J. Plank

INTERNATIONAL ANALYTICAL REVIEW “ALITINFORM”, 4 – 5 (26), (2012), 86 – 99.

Abstract

It is well established that the shelf-life of dry mix mortars can be severely impacted by improper storage conditions. Especially fast-setting formulations based on a ternary binder system (OPC/CAC/CaSO₄) are known to be very sensitive. In this study, the behaviour of a SLU formulation when exposed to atmospheric moisture and CO₂ was studied. The SLU formulation was stored in moist air for 1 and 3 days at 35 °C and 90 % RH. The consequences of this ageing were analysed by FTIR-ATR, SEM, *in-situ* XRD technique and isothermal calorimetry. XRD, FTIR and SEM investigations revealed that the surfaces of the SLU powder exposed to moisture were covered with abundant ettringite crystals. Also, the performance of tartrate and citrate retarders with the aged SLU powder was tested. In the fresh self-levelling mortar, tartrate provided ~ 3 hours of workability time while citrate achieved only ~ 0.5 hours. In the aged SLU, the retarding performance of tartrate decreased significantly (~ 70 %) while that of citrate improved. Dispersing ability of casein superplasticizer was also severely impacted, as a consequence of ageing. After only 1 day of storage in moist air, the SLU containing casein no longer was fluidized, and after 3 days of storage, a foul odor occurred which indicated substantial decomposition of the biopolymer. Ageing also caused a higher water demand to achieve sufficient flowability, thus leading to poor early compressive strength. The study demonstrates that the shelf-life of SLU mortars can be severely impacted if stored under inappropriate conditions. High quality packaging is recommended to avoid performance failures.

Key words: *Ageing; self-levelling underlayment (SLU); tartrate retarder; citric retarder; casein; polycarboxylate;*

1. Introduction

Self-levelling underlayments (SLUs) are commonly applied on floor screeds or other foundations in order to level uneven, rough surfaces [1-3]. The mortar levels itself under the influence of gravity and produces a smooth surface. For commercial SLUs, the binder system is based on OPC. However, when fast setting and high early strength development are required, a rapid hardening mortar containing OPC, CAC and calcium sulphate as binders is used [4, 5]. The principle reaction causing the exceptionally fast strength development is rapid and massive ettringite formation from CAC (especially the mayenite phase, $C_{12}A_7$ contained therein) and anhydrite. This reaction is often referred to as “chemical drying”, because of the huge uptake of water by ettringite which incorporates 48.9 wt. % of water in its crystal structure. Another advantage of this ternary binder system is reduced shrinkage, compared to Portland cement-based mortars. Again, this effect is a result of massive ettringite formation which leads to expansion as a consequence of water uptake in the ettringite crystals. In order to obtain a mortar with sufficiently long workability (at least 1 hour), hydration retarders based on the salts of α -hydroxycarboxylic acids, such as e.g. tartrate or citrate, are commonly used.

Applicators are well aware that the performance of drymix mortars can change after a prolonged period of storage, particularly in humid atmosphere [6]. Also, researchers have described the effects of ageing on the properties of dry mortars [7]. The principal consequences of this ageing phenomenon, often referred to as “prehydration”, include rapid loss of workability, acceleration or retardation of setting, and reduced strength [8]. It is also established that cement prehydration caused by improper storage can be one of the reasons for poor response of admixtures in specific formulations [9].

This article presents the second part of a study on the effects of atmospheric moisture and CO_2 on cements and mortar formulations. In the first part, the physicochemical effects of water sorption on the surfaces of pure clinker phases as well as different sulphates (gypsum, hemihydrate and anhydrite) and free lime were investigated [10]. By using a water vapour balance instrument it was possible to determine for all cement constituents the relative humidity (“threshold values”) at which their water sorption commences. There it was shown that sorbed water can be bound physically, chemically or in both ways. Chemical sorption leads to the formation of a thin (only several nm thick) layer of hydration products on the

surfaces of these phases. Consequently, the specific surface area and surface charge of a cement change upon prehydration, which can greatly impact its interaction with admixtures. In this second part of the study, the impact of prehydration on the performance of retarders and of casein superplasticizer in a SLU formulation based on a ternary binder system containing OPC, CAC and calcium sulphate was studied. This system was chosen as an example representing other drymix mortar formulations. In the experiments, a basic SLU formulation without retarder was exposed at 35 °C to moist air (relative humidity, RH 90 %) for 1 and 3 days. The aged powder was characterised by XRD, FTIR-ATR and SEM techniques to identify the types and amounts of prehydration products. Afterwards, the aged SLU mortar was formulated with tartrate or citrate retarders and their effectiveness in such prehydrated formulation was studied. In another experiment, a SLU formulation containing casein as superplasticizer was exposed to moist air, and the effects of this ageing on the flow properties of the mortar were investigated. From the results it was hoped to gain insight into the mechanisms underlying the decreased performance of admixtures in aged drymix mortars.

2. Experimental

2.1 Materials

2.1.1 SLU formulation

A basic SLU formulation was used in this study. Its composition is shown in **Table 1**. The formulation is based on a ternary binder system containing CEM I 52.5 N (HeidelbergCement AG, Geseke plant, Germany), grey calcium aluminate cement (CAC) with approx. 40 wt. % Al₂O₃ (Fondu® from Kerneos S.A., Neuilly Sur Seine, France) and calcium sulphate (anhydrite from Solvay Chemicals, Bad Wimpfen, Germany). The water-to-binder ratio of the fresh mortar was 0.25 and for the aged drymix was 0.5 respectively. The physical properties of the binders used in this formulation are presented in **Table 2**.

The SLU mortar was prepared by dry-blending the components (except the retarders) in an overhead shaker (Fa. Heidolph Reax 20, Schwabach, Germany) for 20 min to achieve a homogeneous mix. The tartrate and citrate retarders were added later to the aged, moisture exposed formulation in order to determine the impact of prehydration on their retarding effectiveness.

The effect of ageing on casein was tested by exposing a fully formulated SLU (including casein) to moist air for 1 day and 3 days respectively. For both storage conditions, the flowability of the SLU was determined using a “mini slump test”, and the results were compared with those from the fresh, unaged SLU.

Table 1: Basic SLU formulation used in the study

Component	Function	wt. %
Ordinary Portland cement (CEM I 52.5 N)	Binder	47.3
Calcium aluminate cement (approx. 40 % Al ₂ O ₃)	Binder	32.8
CaSO ₄ (synthetic anhydrite)	Binder	19.1
Li ₂ CO ₃ (particle size < 40 μm)	Accelerator	0.3
Polycarboxylate (PCE)	Superplasticizer	0.4
Sodium potassium tartrate (KNaC ₄ H ₄ O ₆ · 4 H ₂ O) or Trisodium citrate (Na ₃ C ₆ H ₅ O ₇ · 2 H ₂ O)	Retarder	0.4
Water (for 100 wt.% of dry blend)		25 (fresh system) 50 (aged system)

Table 2: Physical properties of the binder components used in the SLU formulation

Property	CEM I 52.5 N	grey CAC	CaSO₄
d ₅₀ value / μm	10.3	10.8	3.1
density / g/cm ³	3.3	3.2	3.0
specific surface area (Blaine) / cm ² /g	3300	3250	6000

2.1.2 Superplasticizer and retarder samples

As superplasticizer, a commercial sample of a polycarboxylate (Melflux® 2651 F from BASF, Germany) was used.

Commercial sodium potassium (2R, 3R)-tartrate (Seignette salt, made from naturally occurring L-tartaric acid, Merck, Darmstadt, Germany) and trisodium citrate dihydrate (Sigma-Aldrich, Taufkirchen, Germany) were used as retarders to achieve sufficient workability time for the SLU formulation. In the tests with SLU holding casein, the polycarboxylate was replaced by 0.12 g (0.12 % by weight of binders) of an industrial bovine casein obtained from ARDEX GmbH, Witten, Germany.

2.2 Aging of samples in moist air

The dry SLU formulations (without retarder) were spread out on 60 x 135 cm plexiglas plates in a thin layer of about 1 mm thickness and placed in a climate chamber containing moist air of 90 % RH at 35 °C. Storage periods were 1 and 3 days respectively. The experimental set-up is displayed in **Figure 1**.

For the XRD and SEM investigations, sample holders from these instruments which held the dry SLU formulations were stored and aged in the climate chamber. This method allows to analyse the prehydrated dry mortar as is, without impact from the preparation on the sample holder.



Fig. 1. Experimental set-up for ageing of the SLU in moist air: climate chamber (**left**) and thin layer of SLU powder on the plexiglas plate (**right**)

2.3 Sample analysis

All fresh and aged samples were analysed by X-ray diffraction (D8 Advance instrument from Bruker AXS, Karlsruhe, Germany, equipped with Cu K α X-ray source) and IR spectroscopy (FTIR-ATR, Vertex 70 instrument from Bruker Optics, Karlsruhe, Germany). Scanning electron microscopic (SEM) images were taken from uncoated samples before and after exposure to humidity using a FEI XL 30 FEG microscope (FEI, Eindhoven, Netherlands).

Hydration behaviour of the fresh and prehydrated SLU formulations was studied by using isothermal conduction calorimetry. There, 4 g of SLU powder were filled into 10 mL tubular glass ampoules, mixed with deionised water (w/b = 0.5) at 21 °C, shaken for 1 min in a wobbler and then placed in an isothermal conduction calorimeter (TAM air instrument from

Thermometric, Järfälla, Sweden) to monitor the heat flow of the reaction over a period of 7 days.

With the help of *in-situ* XRD (range of measurement between 8 - 44° 2 θ), the time-dependent course of hydration of the SLU formulations was tracked. Again, the pastes were prepared by mixing 4 g of the SLU formulation with 2 mL of DI water. During the first 12 h, complete scans were taken every 30 min.

Flowability over time was measured utilizing the “mini slump test” according to EN 12706 [11]. A slump cone with an inner diameter of 30 mm and a height of 50 mm was used. The paste was filled to the brim of the cone and levelled before the mould was vertically lifted from the surface of the glass plate. The resulting spread of the paste was measured twice, the second measurement being perpendicular to the first. The final spread value was taken as the average of the two measured ones.

Finally, early age (1 day) compressive strengths of hardened SLU formulations were determined according to DIN EN 196-1 [12].

3. Results and Discussion

3.1 Characterization of aged SLU

Figure 2 shows the XRD patterns of the fresh and aged SLU formulations. In the diagram of the prehydrated SLU formulation, the intensities of the reflections from anhydrite are lower than in the fresh sample which signifies consumption of sulphate during ageing. At the same time, diffraction signals characteristic for ettringite appear. Their intensity increases with ageing time, as more and more ettringite is formed.

FTIR-ATR investigations revealed that the SLU formulations also undergo carbonation (**Figure 3**). In addition to increasingly intense water bands at ~ 3400 cm⁻¹ and 1600 cm⁻¹ which signify the sorption of water, also the band characteristic for carbonate at 1412 cm⁻¹ became stronger as a result of CO₂ uptake. The band at 1125 cm⁻¹ which originates from SO₄²⁻ contained in CaSO₄ undergoes a shift to 1108 cm⁻¹ due to ettringite formation. Furthermore, consumption of anhydrite and CAC over time can be observed from the IR spectra.

Figure 4 shows SEM images of the fresh and aged SLU formulations. The surfaces of the particles from the fresh SLU formulation appear smooth and free of hydration products (**Figure 4 a**), while in the samples aged for 1 and 3 days (**Figures 4 b and c**) abundant hydration products, especially ettringite crystals, occupy the surfaces of the binders. After 3 days of ageing, some of the ettringite needles have grown to a size of 5 μm .

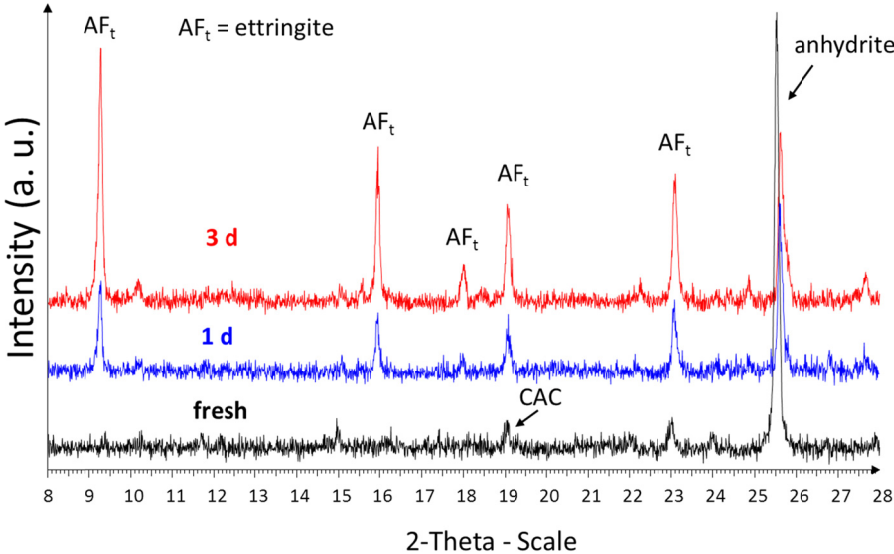


Fig. 2. XRD patterns of fresh (black) and aged (1 d: blue; 3 d: red) SLU formulations, shown in the range of 8 – 28 ° 2 θ

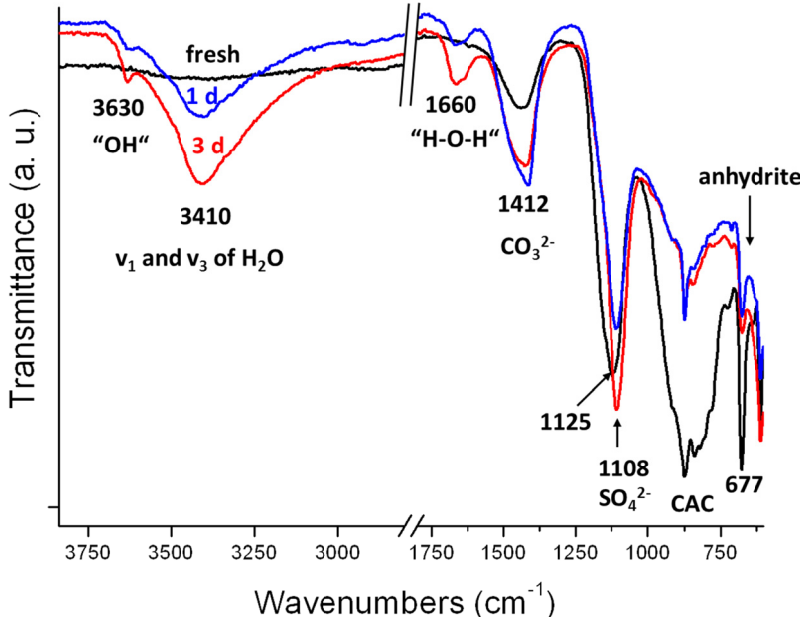


Fig. 3. FTIR-ATR spectra of fresh (black) and aged (1 d: blue; 3 d: red) SLU formulations

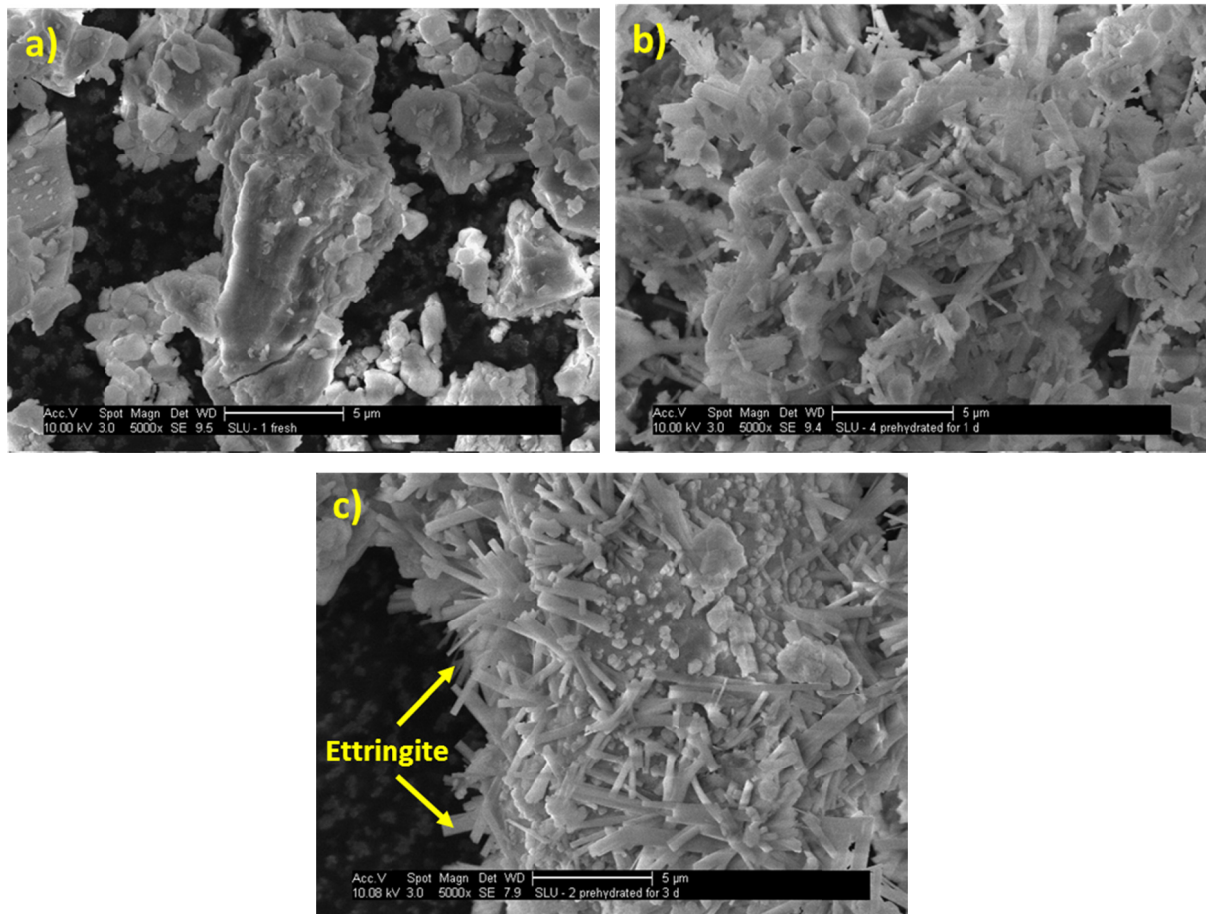


Fig. 4. SEM images of SLU blend fresh **(a)** and aged at 35 °C and 90 % RH for 1 day **(b)** and 3 days **(c)**

3.2 Flow Behaviour of SLU

3.2.1 Fresh SLU

At first, the flow behaviour of the fresh SLU formulation containing either tartrate or citrate as retarder was investigated. Measurement of the mortar spread over time following DIN EN 12706 revealed that this particular formulation functions only with tartrate as retarder (**Figure 5**). For this combination, a total workability period of 3.5 hours was found which is excellent. While in the presence of citrate, the workability period was reduced to 0.5 hour only.

These differences in retarder effectiveness can be explained by isothermal calorimetry: in the presence of citrate, hydration of the SLU already begins only 30 minutes after mixing with water while in the presence of tartrate, hydration commences only after ~ 9 hours (**Figure 6**).

In-situ XRD revealed that when citrate was present as retarder, ettringite formation started already within the first 40 minutes of hydration, thus signifying that citrate does not retard hydration of this SLU formulation sufficiently (**Figure 7 a**). Such behaviour is quite common for SLUs containing a combination of polycarboxylate-based superplasticizer and citrate. When citrate is present, most PCEs cannot achieve long-lasting flowability. This effect is owed to competitive adsorption between PCE and citrate [13]. Highly anionic PCE products are required to overcome this negative effect of citrate on PCE. Whereas lowering the dosage of citrate from initial 0.4 wt. % to 0.2 wt. % does not improve the length of the workability period of the system.

In comparison, tartrate which provided a prolonged workability period for the fresh SLU system retarded ettringite formation for ~ 7 hours (**Figure 7 b**), similar as to what has been observed in heat flow calorimetry (**Figure 6**).

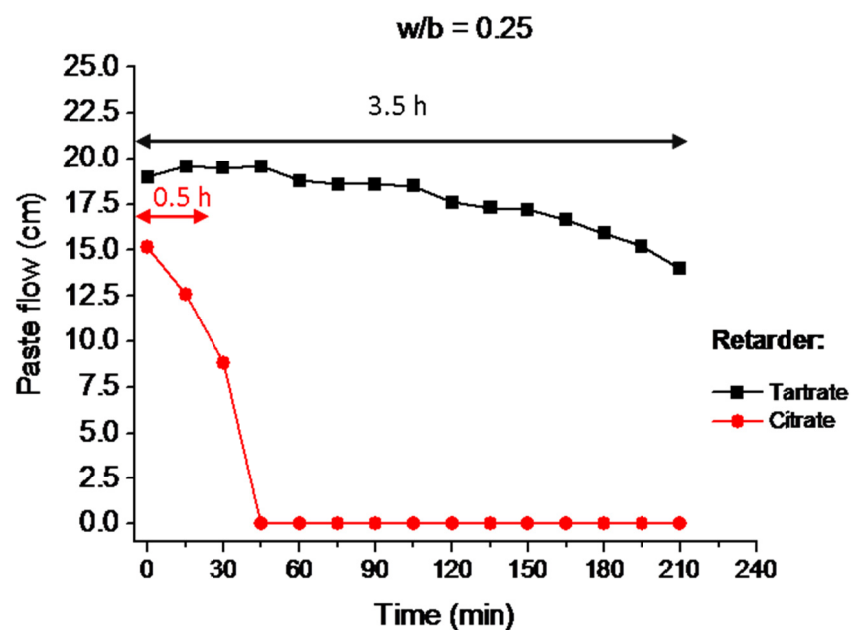


Fig. 5. Flowability over time for fresh, unaged SLU paste ($w/b = 0.25$) containing different retarders (tartrate or citrate; dosage: 0.4 % by weight of binders).

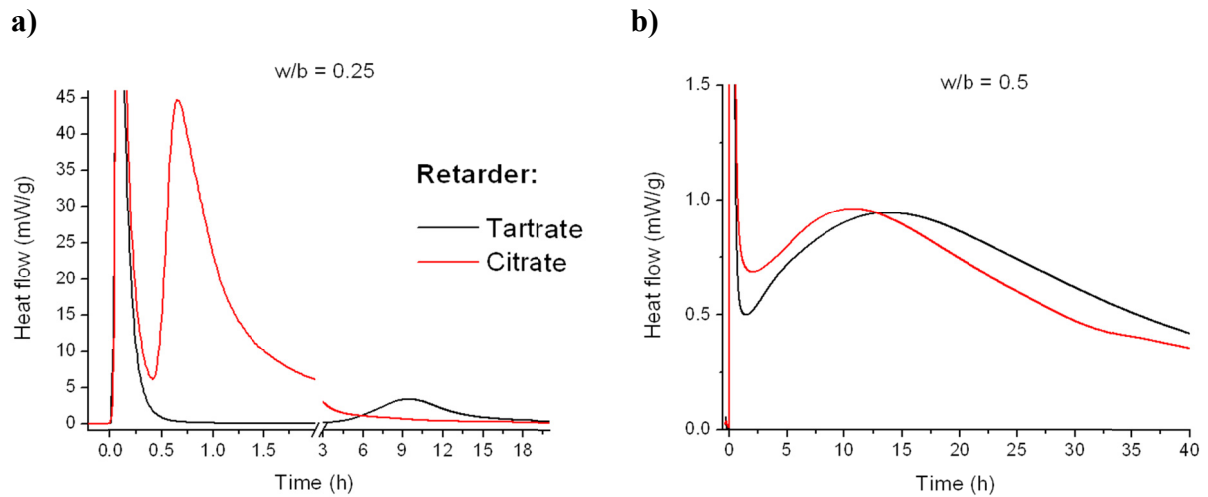


Fig. 6. Isothermal heat flow calorimetry of SLU pastes containing tartrate or citrate as retarders; **a)** fresh SLU (w/b ratio 0.25) and **b)** SLU aged for 1 day (w/b ratio 0.5).

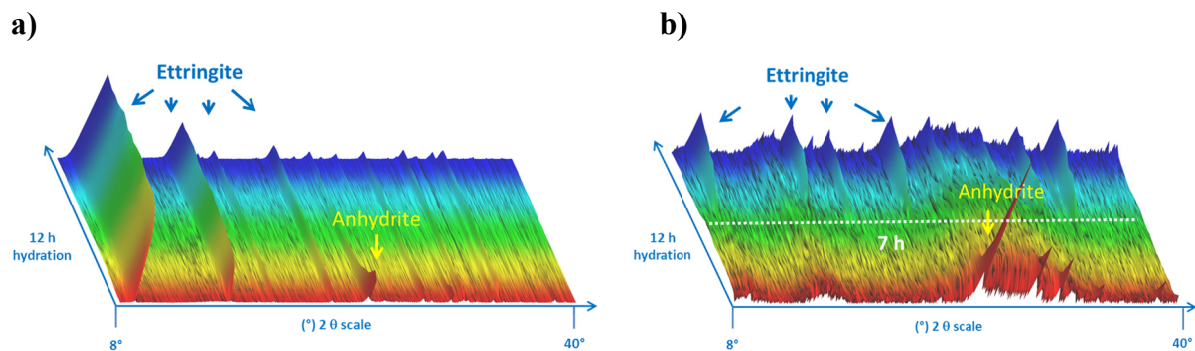


Fig. 7. *In-situ* XRD of fresh unaged SLU pastes (w/b = 0.25) hydrated over 12 h containing citrate **(a)** and tartrate **(b)** as retarders

3.2.2 Aged SLU

After exposure to humidity, the water demand of the SLU formulation increased drastically. The initial water/binder ratio of 0.25 which produced a very liquid paste for the fresh SLU could not fluidize the aged system, as is shown in **Figure 8**. Instead, a non-slump mixture with barely wetted binder particles, especially in the presence of citrate retarder, was attained. During exposure to moisture, an abundance of ettringite crystals was formed on the surfaces of the binders. This effect leads to an increase in water demand to wet these surfaces, and additionally, the ettringite crystals tangle with each other and thus reduce the mobility of

individual particles in the paste. **Figure 9** schematically illustrates these phenomena: In the fresh system, the surfaces of the binder particles are free to react with water, while in the prehydrated system, the layer of ettringite needles existing on the surface hinders the access of water to the bulk material.

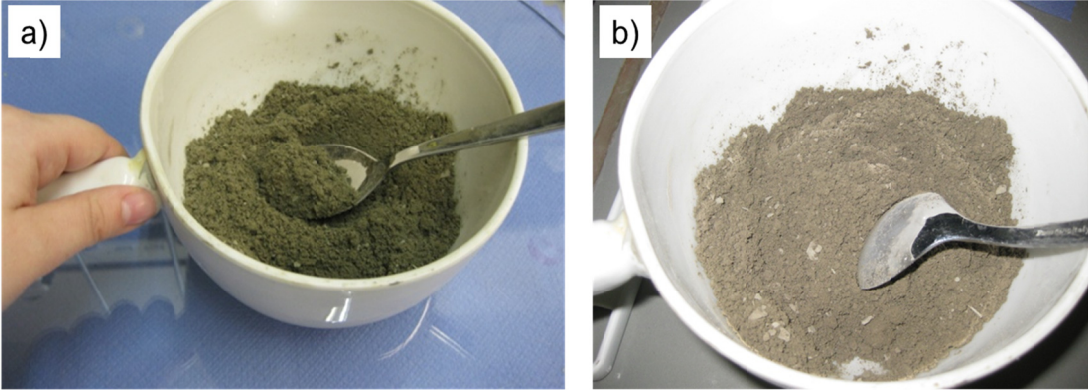


Fig. 8 Consistency of the SLU formulation ($w/b = 0.25$) aged for 1 day at $35\text{ }^\circ\text{C}/90\text{ \% RH}$ containing (a) tartrate and (b) citrate as retarder

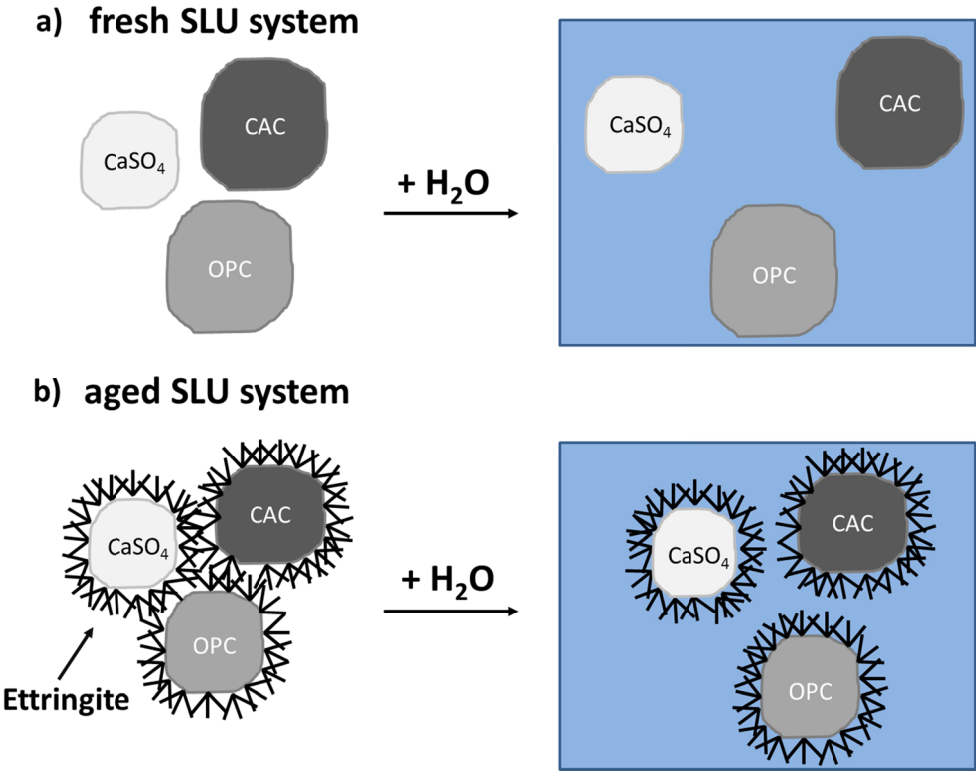


Fig. 9 Schematic illustration of effects influencing the flow behaviour and water demand of fresh (a) and aged (b) SLU formulations mixed with water

Thus, in all further experiments using the aged SLU the water/binder ratio was increased to 0.5 to obtain a free-flowing paste. At this w/b ratio, a free flowing and self-levelling paste was obtained.

Next, hydration of the SLU aged for 1 day and then blended with tartrate or citrate as retarders was monitored by heat flow calorimetry. The results are presented in **Figure 6 b**. For both retarders, very similar heat flow curves were found. This is opposite to the behaviour in the fresh systems where both retarders produced completely different curves. There, citrate had only little retarding effect while tartrate acted as strong retarder (**Figure 6 a**). In the aged system, however, citrate performed as a strong retarder and became almost comparable to tartrate.

Flowability over time of the prehydrated SLU containing tartrate as retarder is displayed in **Figure 10**. After only 1 day of exposure, a huge decrease in fluidity (~ 40 %) of the aged SLU was observed. After 3 days of moist storage, fluidity decreased even further and was only ~ 70 % of the initial value. This result signifies that ageing of the SLU affects the performance of tartrate particularly strong. Opposite to this, the citrate retarder appears to benefit from prehydration of the SLU. After 1 day of ageing, flowability of the SLU decreased but remained constant over ~ 3 hours. In fact, flowability of the citrate-based SLU was superior over that formulated with tartrate (**Figure 11**). After 3 days of ageing, the SLU paste containing citrate behaved even more unusual: after mixing with water, the system showed no flowability for ~ 30 min, as displayed in **Figure 11**. This was followed by a period of ~ 2 hours with reasonable fluidity until the paste started to set and stiffen. Such unusual behaviour has been reported from jobsites where workers became quite confused because of this time-dependent change in mortar workability.

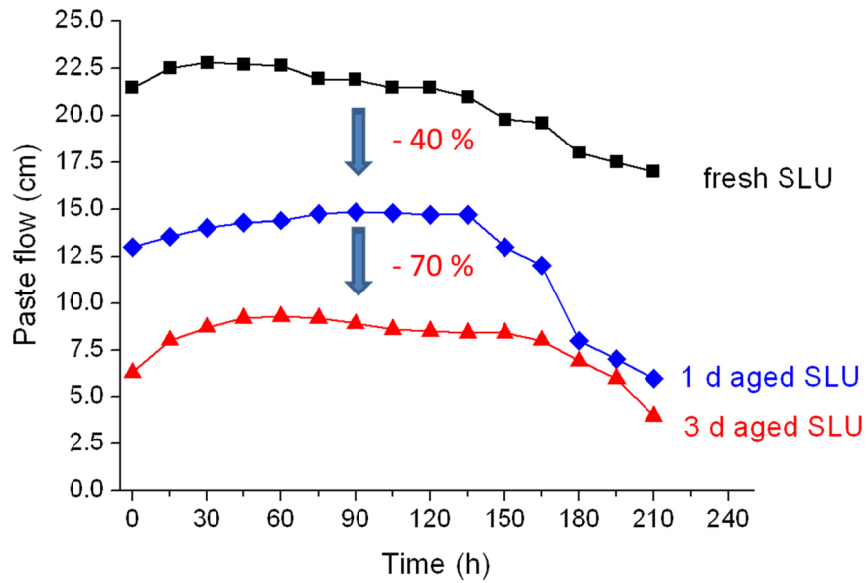


Fig. 10 Flowability over time of fresh and aged self-levelling mortars ($w/b = 0.5$) containing tartrate as retarder (dosage: 0.4 % by weight of binders)

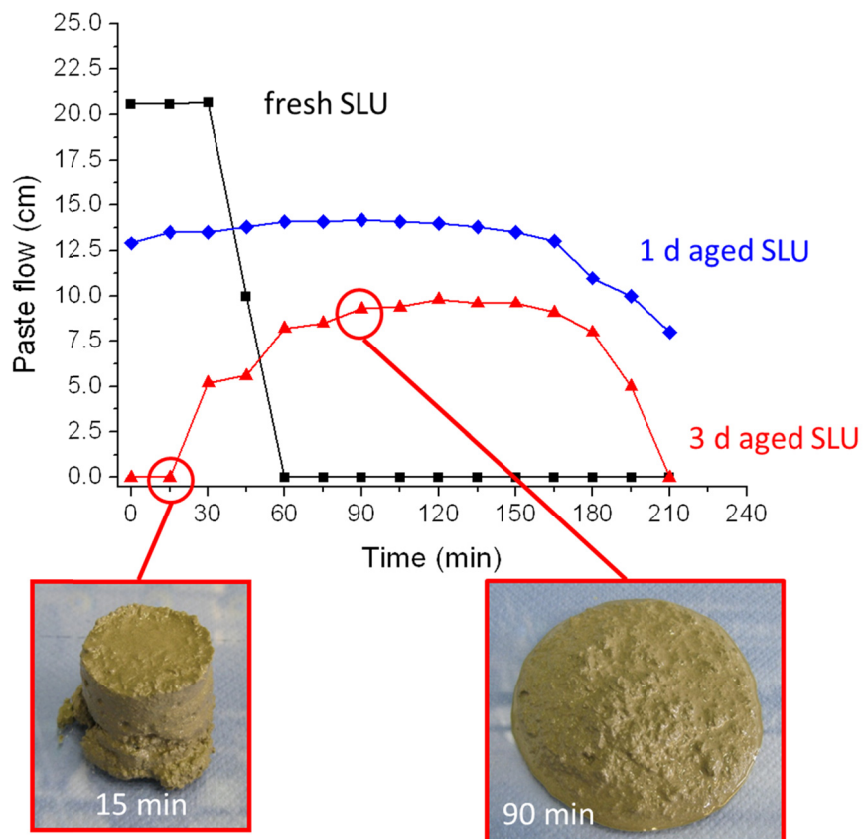


Fig. 11 Flowability over time of fresh and aged self-levelling mortars ($w/b = 0.5$) containing citrate as retarder (dosage: 0.4 % by weight of binders)

Additionally, the effect of prehydration on the dispersing ability of casein, a common superplasticizer used in commercial SLU formulations, was studied. In these experiments, the polycarboxylate superplasticizer was replaced in the formulation as shown in **Table 1** (w/b = 0.5; retarder: tartrate) with 0.12 % bwob of an industrial bovine casein sample obtained from a dry mortar producer. When fresh, this SLU produced a flow value of ~ 18 cm which was retained for ~ 1 hour. However, after moisture exposure for 1 day only at 35 °C, this SLU powder no longer became fluid after mixing with water. After 3 days of ageing, a foul odor was noticed from the SLU mixture which now was even more stiff and developed gas bubbles when mixed with water. These effects clearly indicate that under moist conditions and slightly elevated temperature, the biopolymer which is composed of three different proteins [14] undergoes fermentation and hydrolysis. This decomposition leads to a loss of dispersing ability. Comparative testing employing a polycarboxylate superplasticizer revealed that this type of admixture does not decompose under the conditions studied here, but also experiences a loss in dispersing performance which is owed to massive ettringite formation.

The uptake of moisture and CO₂ during aging also impacts the strength development of the SLU. **Figure 12** shows a comparison of two specimens prepared from fresh or aged SLU formulation. In the sample made from the aged SLU blend, numerous anhydrous CAC and CaSO₄ particles were observed, thus indicating that here, hydration was not homogeneous throughout the matrix. This effect negatively impacts the compressive strength development of the SLU mortar. For the SLU aged for 1 day and containing citrate as retarder, the 1 day compressive strength was reduced by as much as 40 % of the initial value which was $78.8 \pm 2 \text{ N/mm}^2$ for the unaged system. Similar results were obtained for the tartrate based SLU system aged for a period over 1 day.

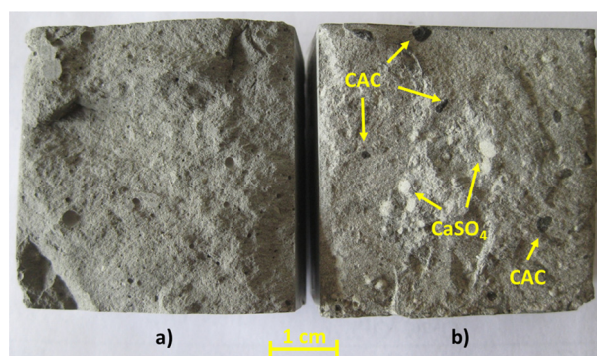


Fig. 12 Fracture surfaces of 24 h hardened specimens (40 mm x 40 mm) prepared from fresh **(a)** and 1 day aged **(b)** SLU formulations containing citrate as retarder

4. Conclusions

The experiments signify that when exposed to moist air, SLU formulations undergo significant ageing which negatively impacts their shelf-life stability. In wet atmosphere, especially CAC and anhydrite react to form abundant ettringite crystals which cover the surfaces of the binders. This massive formation of ettringite causes three major effects:

- (1) Modification of the chemical composition and electrical charge of the binder particles
- (2) Imbalance of sulphate in the system, due to premature consumption of anhydrite
- (3) Incomplete or delayed hydration of some binder particles, as a result of hindered access of water to these surfaces

Also, the performance of chemical admixtures can be severely impacted by moisture exposure of the dry mortar. Here, it was found that effectiveness of tartrate as retarder is reduced while citrate gains from partial surface hydration of the SLU powder. Another admixture, casein superplasticizer, undergoes chemical decomposition and quickly loses its dispersing ability. These findings demonstrate the diversity of effects of ageing on the performances of admixtures.

Apart from these chemical effects, prehydration of a SLU blend was found to also negatively impact mechanical properties such as flow behaviour or compressive strength development.

This study demonstrates that proper storage of drymix mortars which excludes the potential of moisture uptake is essential for their shelf-life stability. However, considering the harsh environments of actual construction sites one has to acknowledge that storage conditions there are not always ideal. Therefore, dry mortar producers are recommended to use high quality packaging, e.g. with moisture barriers such as PE or aluminium foils, to bag their products.

References

1. *Bayer, R., Lutz, H., Dry Mortars, Ullmann's Encyclopedia of Industrial Chemistry // 6th ed., Vol. 11, Wiley-VCH, Weinheim (2003), p. 83–108.*
2. *Plank, J., Technology Trends in the European Dry Mix Mortar Industry // Proceedings of 1st Conference on Research and Application of Commercial Mortar, Shanghai/China, Nov. 10-11 (2005), p. 26–40, ISBN 7-111-17818-1/TU.853.*
3. *Winter, Ch., Plank, J., The European Dry-Mix Mortar Industry (Part 1), Zement-Kalk-Gips International (2007), No. 60, 6. p. 62–69.*
4. *Harbron, R., A general description of flow-applied floor screeds - an important application for complex formulations based on CAC // Proceedings of the International Conference on Aluminate Cement (CAC), Edinburgh, 16-19 July (2001), p. 597–604.*
5. *Amathieu, L., Bier, T.A., Scrivener, K.L., Mechanisms of set acceleration of Portland cement through CAC addition // Proceedings of the International Conference on Aluminate Cement (CAC), Edinburgh, 16-19 July (2001), p. 303–317.*
6. *Zurbriggen, R., Götz-Neunhoeffler, F. Mechanism and resulting damages of prolonged retardation in aged dry mixes: A case study of mixed-binders containing tartaric acid // GDCh-Monographie 37 (Tagung Bauchemie 2007), p. 111–118.*
7. *Schmid, G., Bier, T.A., Wutz, K., Maier, M., Characterization of the ageing behaviour of premixed dry mortars and its effect on their workability properties // Zement-Kalk-Gips International (2007), No. 60, 6. p. 94–103.*
8. *Al-Mutawa, F., Whittaker, M., Arkless, L., Dubina, E., Plank, J., Black, L., The Effects of Prehydration at Moderate Humidities on the Engineering Properties of Portland Cement // C. H. Fentiman, R. J. Mangabhai (Eds.), Cement and Concrete Science, London, 2010, 12-13 September, conference proceedings.*
9. *Winnefeld, F., Influence of cement ageing and addition time on the performance of superplasticizer // Zement-Kalk-Gips International (2008), No. 61, 11. p. 68 – 77.*

10. Dubina, E., Plank, J., Wadsö, L., Black, L., König, H., Investigation of the long-term stability during storage of cement in drymix mortars Part 1. Prehydration of clinker phases, free lime and sulfate phases under different relative humidities (RH) // ALITinform 3 (20) (2011), p. 38–45.
11. DIN EN 12706, Adhesives-test methods for hydraulic setting floor smoothing and/or leveling compounds – determination of flow characteristics, 1999 from <http://www2.din.de/>.
12. DIN EN 196-1, Methods of testing cement – Part 1: Determination of strength, 2005 from <http://www2.din.de/>.
13. Plank J., Winter Ch., Competitive adsorption between superplasticizer and retarder molecules on mineral binder surface // Cem. Concr. Res. 38 (2008), p. 599–605.
14. Plank, J., Bian, H., Method to assess the quality of casein used as superplasticizer in self-leveling compounds // Cem. Concr. Res. 40 (5) (2010), p. 710–715.